Nitric oxide reactivity of Copper(II), Manganese(II) and Iron(III) complexes with N-donor and O-donor ligands

A Dissertation submitted to the
Indian Institute of Technology Guwahati as
Partial fulfillment for the Degree of
Doctor of Philosophy in Chemistry

Submitted by

Aswini Kalita
(Roll No. 09612203)

Supervisor

Dr. Biplab Mondal

Department of Chemistry
Indian Institute of Technology Guwahati
January, 2015

भारतीय प्रौद्योगिकी संस्थान गुवाहाटी
INDIAN INSTITUTE OF TECHNOLOGY GUWAHATI
North Guwahati, Assam – 781039, India

Dr. Biplab Mondal
Associate Professor
Department of Chemistry

Phone : + 91-361-258-2317
Fax: + 91-361-258-2349
E-mail: biplab@iitg.ernet.in

Certificate

This is to certify that Mr. Aswini Kalita has been working under my supervision since July, 2009 as a regular Ph. D. student in the Department of Chemistry, Indian Institute of Technology Guwahati. I am forwarding his thesis "**Nitric oxide reactivity of Copper(II), Manganese(II) and Iron(III) complexes with N-donor and O-donor ligands**" being submitted for the Ph. D. degree.

I certify that he has fulfilled all the requirements according to the rules of this Institute regarding the investigations embodied in his thesis and this work has not been submitted elsewhere for a degree.

January, 2015 **Biplab Mondal**

Statement

I hereby declare that this thesis entitled "**Nitric oxide reactivity of Copper(II), Manganese(II) and Iron(III) complexes with N-donor and O-donor ligands**" is the outcome of research work carried out by me under the supervision of Dr. Biplab Mondal, in the Department of Chemistry, Indian Institute of Technology Guwahati, India.

In keeping with the general practice of reporting scientific observations, due acknowledgements have been made whenever work described here has been based on the findings of other investigators.

January, 2015 **Aswini Kalita**

Acknowledgements

This work would not have been possible without many people. In particular, I would like to express my deepest gratitude to:

First and foremost, I feel it as a great privilege in expressing my deepest and most sincere gratitude to my supervisor Dr. Biplab Mondal, for providing me the opportunity to conduct research in his group and giving me freedom in defining and carrying out my Ph.D; for his patience in correcting and reviewing my muddled drafts and helping me to improve my writing skills. My heartfelt thanks to you sir for the unlimited support and patience shown to me. He has also created an indispensable environment for me to conduct my project work.

I am also thankful to my doctoral committee Chairman and members Prof. Gopal Das, Dr. Chivukula V. Sastri and Dr. Perumal Alagarsamy for sparing their precious time to evaluate the progress of my work. I would also like to thank to other faculty members for their kind help in carrying out this work. I am also grateful to all the technical staff of the department without whose help I could not have completed this thesis.

I would like to acknowledge CSIR, India for financial support and IIT Guwahati for all the facilities that were made available to me. I thank CIF, IIT Guwahati for providing the facility of X-ray single crystal, LC-MS, X-band EPR and NMR facility.

I would like to acknowledge Prof. Ramesh C. Deka, Department of Chemistry, Tezpur University, India for helping me by carrying out theoretical studies in my research.

It is an immense pleasure to thank my present lab mates Vikash, Kanhu, Somnath, Hemanta, Kuldeep, Soumen and Baishakhi for their support and help as well as for making a pleasant environment in the laboratory to work. Thanks once again all of you for making my leisure time interesting and joyful. Also my sincere thanks to my lab seniors, Dr. Amardeep Singh, Dr.

Moushumi Sarma, Dr. Pankaj Kumar; friend Dr. Apurba Kalita for their enormous help and support in my PhD life. I thank all the masters and summer research fellows of my lab, Tulika, Pritam, Ivy, Narayani, Najmul, Soham, Sayantani, Arpan, Hemrupa, Tarali, Ayushree, Nimisha, Samarjit, Bhagyasmeeta, Arnab, Rini, Munmi, Dikshita, Banashree and Shyamalee to whom I have the opportunity to work.

My special thanks to my friends of IIT Guwahati, Paramartha, Subrata, Bhaskar, Jiban, Jayanta, Nabajit, Bhanita, Subrata, Suraj, Abhijit, Somnath, Rosy, Minakshi, Shilpi, Pranjal, Rakesh for their help and support during this long time of my research.

My special thanks to chemistry teacher, Dr. Diganta Choudhury, B. Borooah College for his life-long encouragement in my life. Thanks to my close friends Kishor, Rishipad, Diganta, Ajit, Bikash and Murakan for their support and help. At the last, but not the least, to my parents, my sisters, sister-in-laws, nephew and niece, near and dear friend Sangita for their endless moral support, encouragement and motivation at difficult times. My PhD endeavors would not have been completed without their blessings and support. I express my sincere gratitude to them. I would like to thank all others who are associated with my work directly or indirectly at IIT Guwahati for their help.

Aswini Kalita

Contents

Synopsis

The thesis entitled, "**Nitric oxide reactivity of Copper(II), Manganese(II) and Iron(III) complexes with N-donor and O-donor ligands.**" is divided into five chapters.

Chapter 1: Introduction

Nitric oxide (NO) is known to play key roles in various physiological activities including blood pressure control, neurotransmission, immune response etc.[1,2] Since most of these activities of NO is ultimately defined by its reactivity with the metallo-proteins, activation of NO by transition metal ions has attracted a considerable research interest.[3,4] In this regard iron-nitrosyls have been studied extensively in enzyme and model systems.[5]

NO is known to induce reduction of Cu(II) centers in laccase, cytochrome c. There are several reported examples of the reduction of Cu(II) center in various Cu(II)-complexes by NO. The reduction proceeds either through a de-protonation mechanism or the [Cu^{II}-NO] intermediate formation as observed in case of ferriheme systems.[6-8] Ligand frameworks have a considerable effect in controlling the mechanism of the reduction of a Cu(II) center by NO.[9] Apparently, the stability of the [Cu^{II}–NO] intermediate depends on the chelate ring size and substitution present in the ligand frameworks though has not been studied extensively.[10]

On the other hand, Mn(II)-nitrosyls with porphyrin, phthalocyanins have been synthesized and characterized structurally.[11] A few Mn(II) complexes of N-donor ligands having amide group have been reported to react with NO in acetonitrile solution to afford stable

Mn(II)-nitrosyl complex.[12] The reduction of Mn center in *bis*-μ-oxo complex by NO leading to the reductive nitrosylation of the metal ion was exemplified by Mascharak et al.[13] Mn-nitrosyl complexes, though a limited number, have been shown to be useful for photodynamic therapy.[14]

This thesis has been focused on the reactivity studies of Cu(II)-, Mn(II)- and Fe(III)-complexes with NO. Second and third chapters describe the formation and reactivity of Cu(II)-nitrosyls leading to N-nitrosation and C-nitrosation of the ligand frameworks. Fourth chapter describes the reactivity of a Mn(II) complex with NO resulting in corresponding Mn-nitrosyl. In the last chapter, the reductive nitrosylation of non-heme iron complex leading to the formation of Fe(II)-nitrosyls has been discussed.

Chapter 2: Nitric oxide reactivity of copper(II) complexes of bidentate amine ligands

The stability and formation of [Cu^{II}-NO] intermediate are reported to depend on the chelate ring size and substitution present in the ligand frameworks.[10] In continuation to that, Cu(II) complexes of 1,3-diaminopropane (**L_1**) and N-isopropylpropane-1,3-diamine (**L_2**) were prepared to study their reactivity with NO. The complexes, **2.1** and **2.2** were characterized by spectroscopic studies and X-ray crystal structure determination (figure 1).

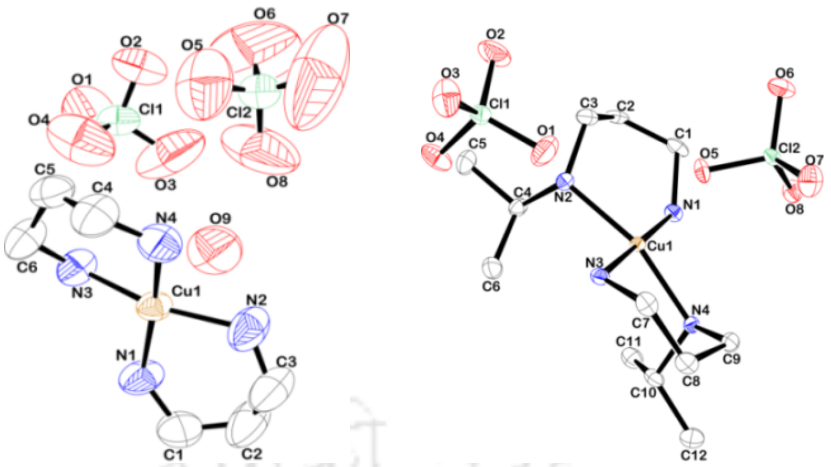

(a) **(b)**

Figure 1 ORTEP diagram of complexes **2.1** (a) and **2.2** (b) (50% thermal ellipsoid plots, H-atoms are omitted for clarity).

In acetonitrile solution, complexes **2.1** and **2.2** displayed *d-d* bands with λ_{max} at 570 nm (ε, 152 M^{-1} cm^{-1}) and 579 nm (ε, 156 M^{-1} cm^{-1}), respectively. Both the complexes displayed one electron paramagnetism and characteristic signals in X-band EPR spectroscopy (Figure 2). For complex **2.1**, $g_{\parallel}$, $g_{\perp}$ and $A_{\parallel}$ values are 2.334, 2.013 and 203×10^{-4} cm^{-1}; whereas for complex **2.2** the values are 2.302, 2.010 and 198×10^{-4} cm^{-1}, respectively. Magnetic moment of the complexes **2.1** and **2.2** are 1.60 and 1.67 BM, respectively.

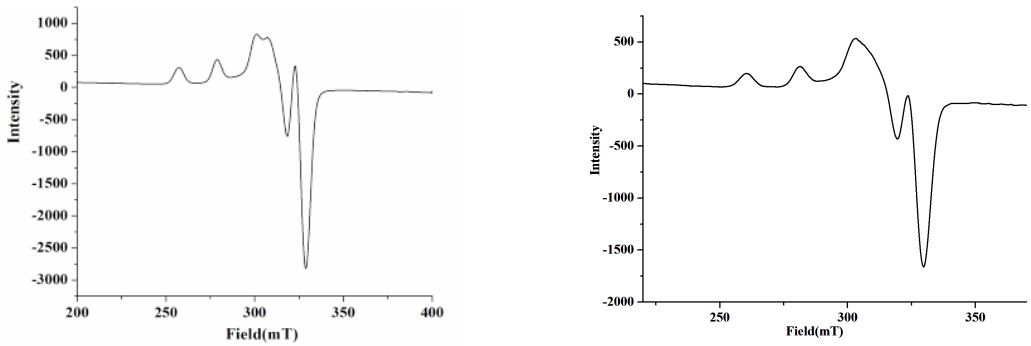

(a) **(b)**

Figure 2 X-band EPR spectra of complexes **2.1** (a) and **2.2** (b) at 77 K in acetonitrile.

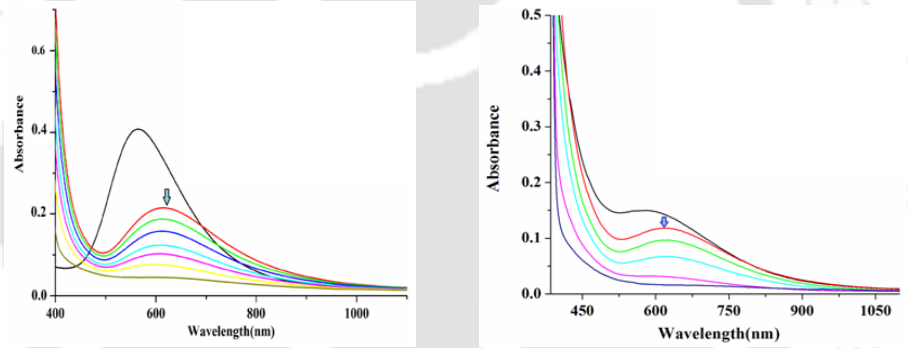

(a) **(b)**

Figure 3 UV-visible spectra of complexes **2.1** (a) and **2.2** (b) before (black trace) and after purging NO showing the formation and decay of [Cu^{II}-NO] intermediates in acetonitrile.

In degassed acetonitrile solution of the complexes, addition of NO was found to result in

unstable [Cu^{II}-NO] intermediate prior to the reduction of Cu(II) to Cu(I). This was evidenced by UV-visible and solution FT-IR spectroscopy (Figures 3 and 4, respectively).

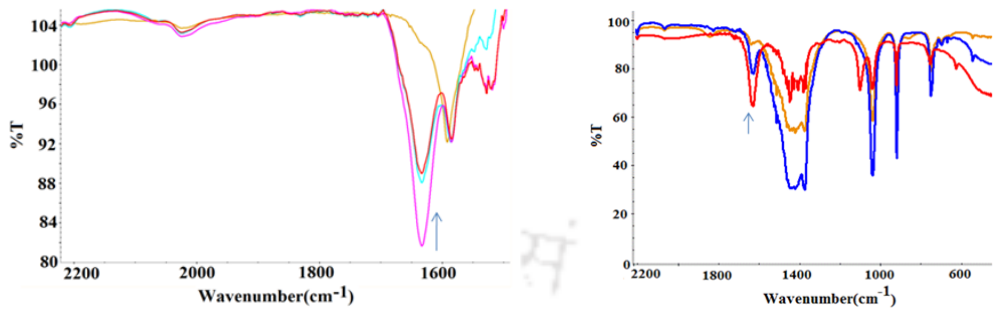

(a) **(b)**

Figure 4 Solution FT-IR spectra of complexes **2.1** (a) and **2.2** (b) after purging NO showing the formation of unstable [Cu^{II}-NO] intermediates in acetonitrile.

In case of complex **2.1**, the reduction of the Cu(II) center by NO afforded ligand transformation through diazotization at the primary amine site of ligand $\mathbf{L_1}$.

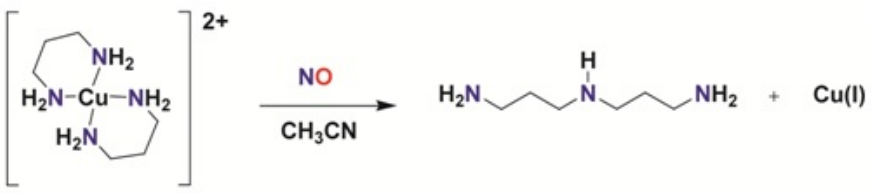

Scheme 1

However, selective N-nitrosation at the secondary amine site of ligand $\mathbf{L_2}$ was observed in case of **2.2** (Scheme 1). This is perhaps because of higher nucleophilicity of secondary amine N- compared to the primary one. The modified ligands, $\mathbf{L_1}'$ and $\mathbf{L_2}'$ were isolated and characterized.

It has been found that in methanol and water solution, complexes **2.1** and **2.2** do not react with NO.

Chapter 3: C-nitrosation of a *β*-diketiminate ligand in copper(II) complex

In this chapter, Cu(II) complex of electron rich *β*-diketiminate ligand has been utilized to study its reactivity with NO. The Cu(II) complex, **3.1** was prepared by stirring the free ligand ($\mathbf{L_3}$) with equivalent amount of Cu(II) acetate, dihydrate in acetonitrile at room temperature. Complex **3.1** was characterized by spectroscopic techniques as well as by single crystal structure determination. The ORTEP diagram of complex **3.1** is shown in figure 3.1. The crystal structure reveals the mononuclear metal center with a distorted square planar geometry where the anionic *β*-diketiminate and acetate act as bidentate

ligands. The bite angle of the diketiminate ligand is 96.30°; whereas for acetate, this is 64.22°. Complex **3.1** in acetonitrile solution absorbs at 772 nm and 559 nm in the visible spectrum (Figure 5) along with intra-ligand transitions in UV-region.

L_3 in complex **3.1** in acetonitrile solution was found to undergo oxidative degradation to the corresponding ketone di-imine, **L_3'** when heated to 50 °C for 2 h under aerobic condition. The modified ketone di-imine ligand, **L_3'** was isolated quantitatively after removal of Cu(II) ion using aqueous Na_2S. When the crude reaction mixture was kept at room temperature, dark green crystals of complex **3.2** appeared. The ORTEP diagram of complex **3.2** is shown in figure 5. The crystal structure reveals the presence of heptanuclear Cu(II) unit with diol di-imine of **L_3** which actually dehydrates while demetallated to afford the ketone di-imine.

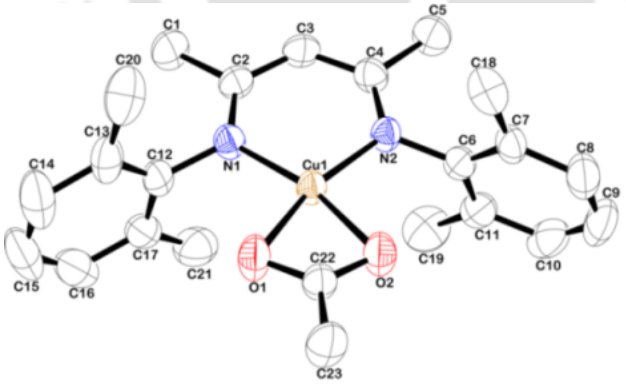

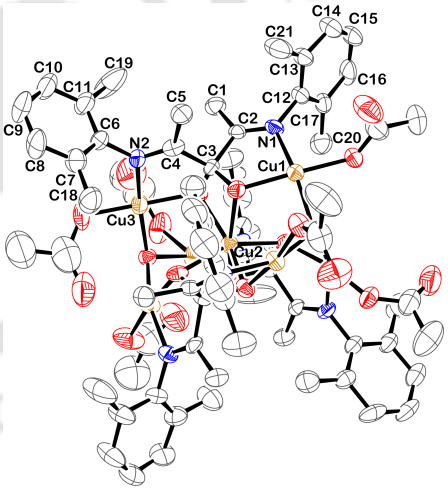

(a) **(b)**

Figure 5 ORTEP diagram of complexes **3.1** (**a**) and **3.2** (**b**) (50% thermal ellipsoid plot; H-atoms are removed for clarity).

In comparison, addition of NO to the degassed acetonitrile solution of complex **3.1** resulted in color change from brown to deep green through a transient intermediate step. The absorptions at 559 and 772 nm were diminished and a new band at 580 nm appeared (Figure 6) for a short while suggesting the formation of the transient intermediate. This is presumably due to the formation of Cu(II)-nitrosyl intermediate. The decay of 580 nm absorption band was associated with the appearance of another band at 640 nm (Figure 6) which is attributed to the *d-d* transition of Cu(II) complex of modified oxime di-imine ligand, $\mathbf{L_3}^{//}$. Complex **3.3** was isolated as solid and characterized. Removal of Cu(II) ion from the solution of complex **3.3** afforded the corresponding modified oxime di-imine ligand, $\mathbf{L_3}^{//}$. The formation of $\mathbf{L_3}^{//}$ was confirmed by various spectral analyses as well as by X-ray single crystal structure determination (Figure 6). Presumably, NO first binds to the metal center to form Cu(II)-nitrosyl intermediate as indicated by UV-visible and EPR studies. In the next step, nucleophillic attack to N-atom of NO by the diketiminate ligand takes place with successive loss of proton resulting to the oxime di-imine moiety.

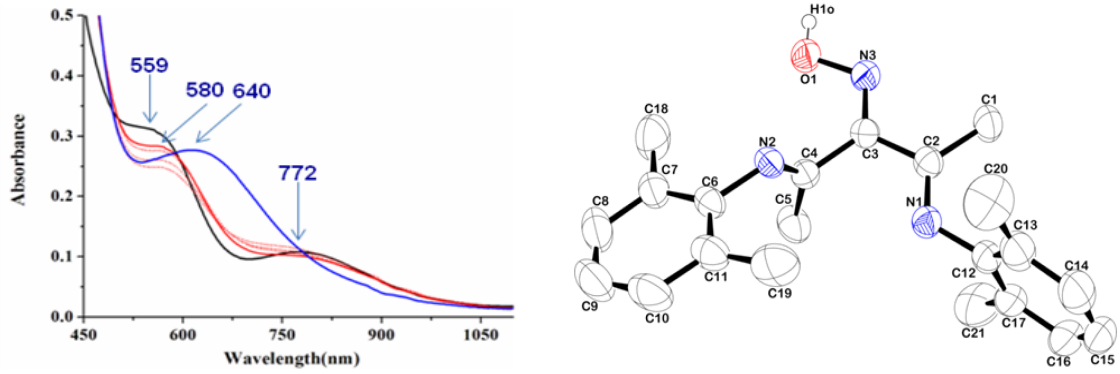

(a) **(b)**

Figure 6 (a) UV-visible spectra of complex **3.1** before (black trace) and after (red trace) purging NO in acetonitrile. Blue represents the final compound (complex **3.3**), (b) ORTEP diagram of oxime di-imine, $\mathbf{L_3}^{//}$ (50% thermal ellipsoid plot; H-atoms and solvent molecules are removed for clarity).

Chapter 4: Nitric oxide reactivity of a manganese(II) complex leading to the nitrosation of the ligand

In our laboratory, we have been studying the reactivity of NO with Cu(II) complexes and found the reduction of metal ion by NO leads to the diazotization and N-nitrosation at the primary and secondary amine centers of ligand frameworks, respectively. The N-nitrosation, in cases of Cu(II) complexes, may not necessarily proceeds always through a Cu(II)-nitrosyl formation. Depending upon the ligand denticity and geometry of the complex, it may proceeds through a deprotonation mechanism in presence of base. For example, in case of tetradentate tripodal ligand (Scheme 2), the N-nitrosation takes place through a Cu(II)-nitrosyl intermediate. In case of tetradentate macrocyclic ligand (Scheme

3), it proceeds through a deprotonation of the N-H group. This diversity of the mechanistic pathway actually prompted us to study the NO reactivity of Mn(II) complexes.

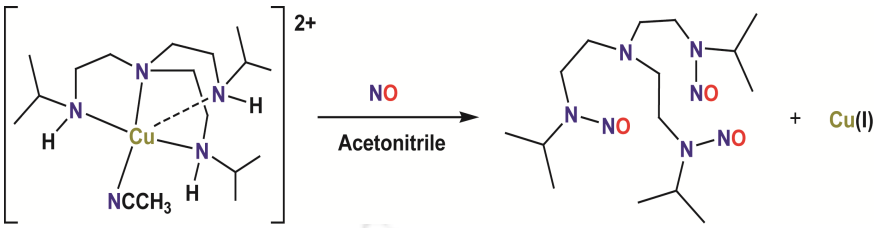

Scheme 2

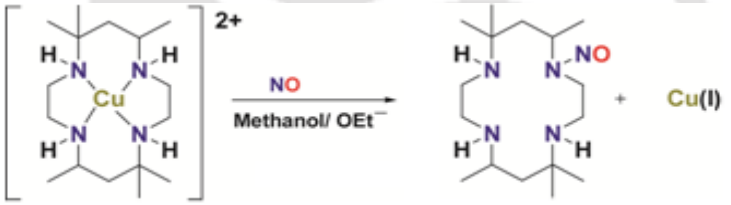

Scheme 3

In this chapter, a tetradentate N-donor ligand, **L_4** [N, N/-bis((pyridin-2-yl)methyl)ethane-1,2-diamine] having two pyridine nitrogen and two aliphatic secondary amine nitrogen has been chosen. Earlier, NO reactivity of Cu(II)

complex of the same ligand was reported from our laboratory. So the present study also demonstrates the difference of reactivity towards NO while moving from Cu(II) to Mn(II).

Complex **4.1** was synthesized by dissolving ligand, $\mathbf{L_4}$ with $MnCl_2.4H_2O$. The complex **4.1** was characterized by spectroscopic techniques as well as X-ray single crystal structure determination (Figure 7).

Addition of NO gas in dry and degassed acetonitrile solution of complex **4.1** was not found to result in any change. This is perhaps because of strong coordination of chloride ion with Mn(II).

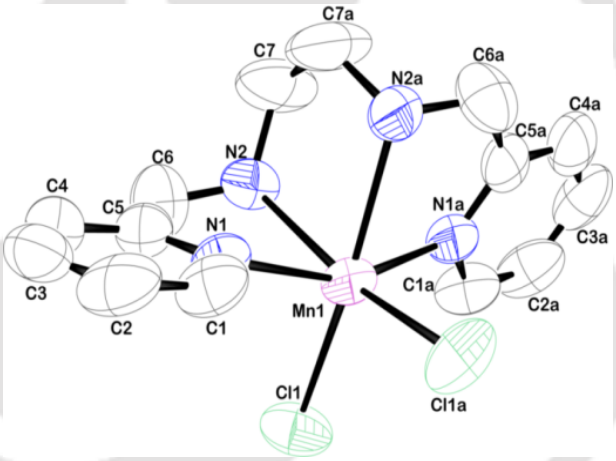

Figure 7 ORTEP diagram of complex **4.1** (50% thermal ellipsoid plot; H-atoms are removed for clarity).

To study further, the chloride ions in complex **4.1** were replaced by water to afford complex **4.2**. This was done by treating the acetonitrile solution of complex **4.1** with aqueous silver nitrate followed by addition of saturated aqueous sodium perchlorate solution. The complex **4.2** can also be prepared by stirring a mixture of manganese(II) perchlorate, hexahydrate with equivalent amount of ligand, $\mathbf{L_4}$ in acetonitrile under argon atmosphere (Scheme 4). The complex **4.2** exhibited a broad *d-d* band with λ_{max} at 644 nm (ε, 201 M^{-1} cm^{-1}).

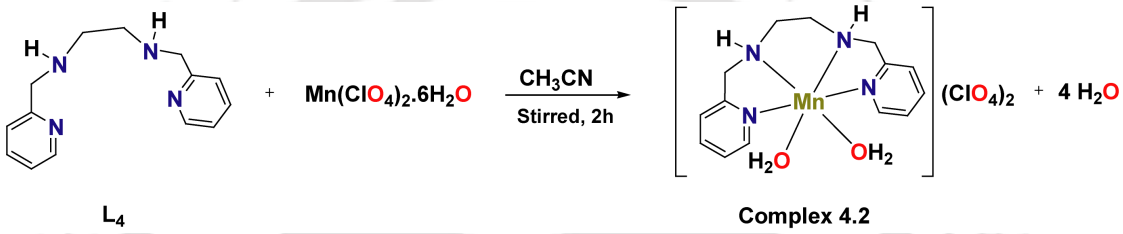

Scheme 4

Addition of NO gas into the degassed acetonitrile solution of complex **4.2** resulted in the appearance of a new band at 415 nm (Figure 8). The intensity of this newly appeared band was found to decay with time and finally diminished indicating the unstable nature of the intermediate. In solution FT-IR study, the addition of NO to the acetonitrile solution of complex **4.2** displayed a new strong stretching frequency at 1718 cm^{-1} (Figure 8) corresponding to the unstable [Mn^{II}-NO] complex.

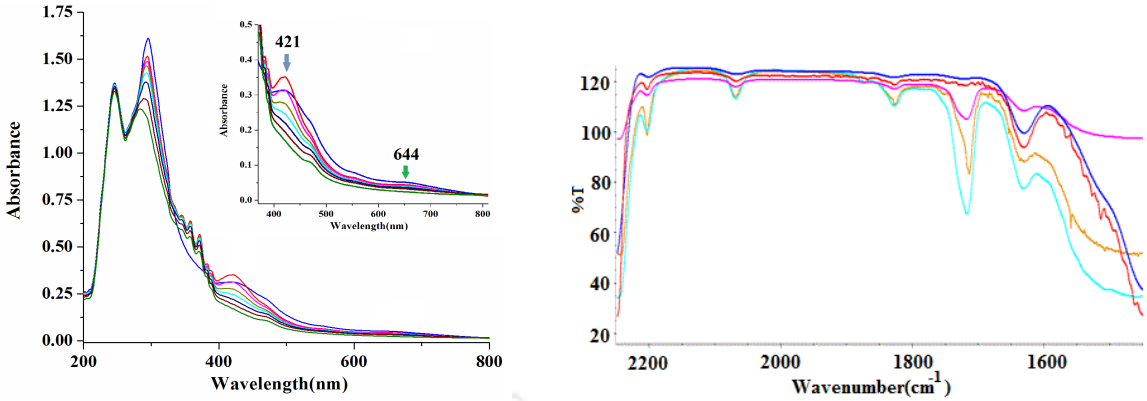

(a) **(b)**

Figure 8 (a) UV-visible spectra of complex **4.2** (blue trace), after purging NO (red trace) and gradual decay of intensity of peaks at 421nm and 644 nm with time in acetonitrile; (b) FT-IR spectra of complex **4.2** after purging NO (green trace) and gradual decay of the peak at 1718 cm^{-1} in acetonitrile.

The frozen intermediate was found to be silent in X-band EPR (Figure 9a) as expected. The unstable nature of the intermediate did not allow its isolation of further characterization. The decomposition of the [Mn^{II}-NO] intermediate is resulted in the reduction of Mn(I) and NO^{+}. The broad ^{1}H-NMR signals of the complex **4.2** became sharp and well resolved after its reaction with NO (Figure 9b) as a result of the reduction of paramagnetic Mn(II) to diamagnetic Mn(I).

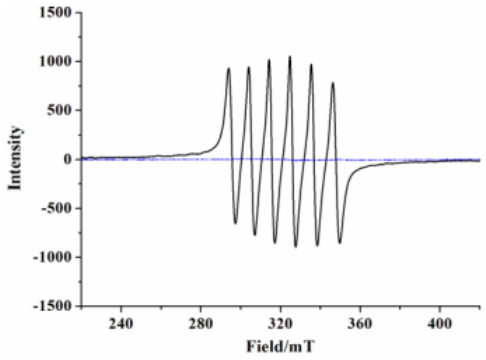

(a)

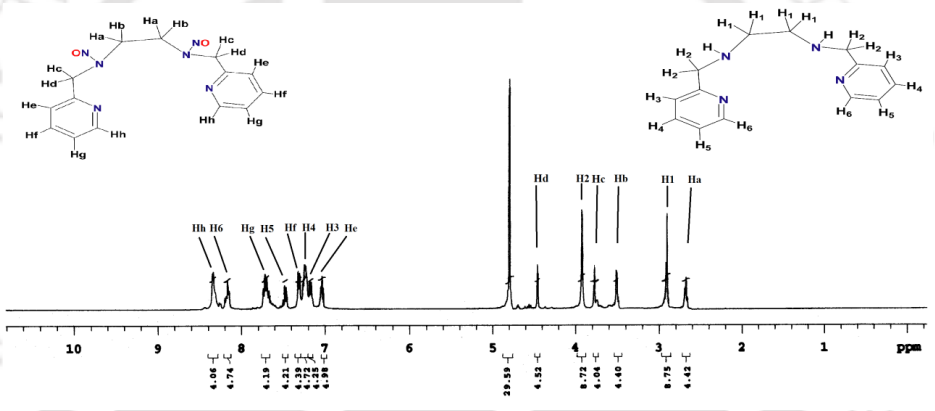

(b)

Figure 9 (a) X-band EPR spectra of complex **4.2** before (black trace) and after (blue dotted trace) addition of NO in acetonitrile; (b) ^{1}H-NMR spectrum of complex **4.2** after purging NO at argon atmosphere in CD_3CN.

Although, there is no direct evidence of formation of NO^+ in the reaction mixture, it was supported by N-nitrosation of the ligand. Nitrosation product, $\mathbf{L_4}'$ was isolated from the reaction mixture and characterized using spectroscopic analyses as well as single crystal X-ray structure determination. The ORTEP diagram of $\mathbf{L_4}'$ is shown in figure 10.

It should be noted that the Cu(II) complex of $\mathbf{L_4}$ did not undergo reduction in presence of NO itself. However, addition of base NaOEt to the solution of the complex followed by NO resulted in the reduction of Cu(II) center along with N-nitrosation. It was found to follow a deprotonation pathway.

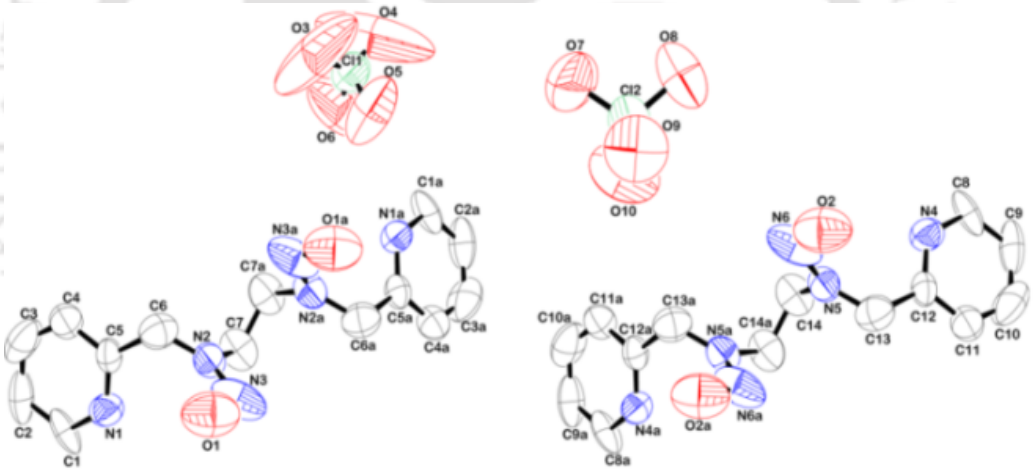

Figure 10 ORTEP diagram of perchlorate salt of $\mathbf{L_4}'$ (50% thermal ellipsoid plot; H-atoms are removed for clarity).

Chapter 5: Reductive nitrosylation of iron(III) complexes of tetradentate ligands

Complexes **5.1** and **5.2** were synthesized by the reaction of ligands $\mathbf{L_5}$ [N,N'-bis(2-hydroxybenzyl)-1,2-phenylenediamine] and $\mathbf{L_6}$ [N,N'-bis(2-hydroxybenzyl)-1,2-ethylenediamine], respectively with stoichiometric amount of iron(III) chloride, hexahydrate in methanol. The complexes **5.1** and **5.2** exhibited a broad *d-d* band with λ_{max} at 532 nm (ε, 236 M^{-1} cm^{-1}) and at 539 nm (ε, 159 M^{-1} cm^{-1}), respectively in methanol. Even after several attempts, we could not grow the X-ray quality crystals of the complexes. Complexes **5.1** and **5.2** were fully optimized using PBE functional and DNP basis set in the presence of solvent methanol. The optimized structures are shown in figure 11 and their selected geometric parameters are given in table 1. The calculated metric parameters of the complexes are in good agreement with the experimental data of similar complexes.

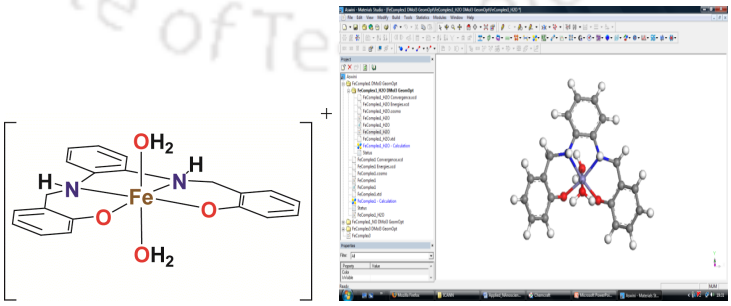

(a)

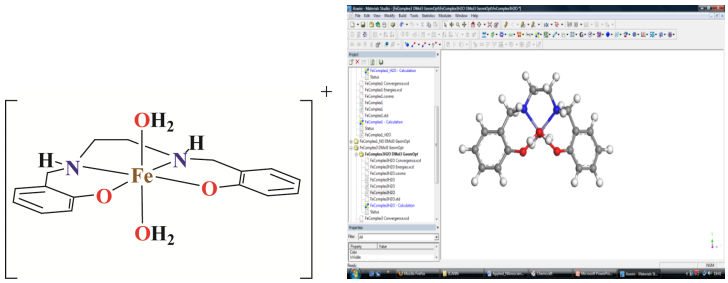

(b)

Figure 11 Optimized structures of complexes **5.1** (a) and **5.2** (b).

Addition of NO gas into the dry and degassed methanol solution of complexes **5.1** and **5.2** resulted in the complexes **5.3** and **5.4**, respectively. The reaction was monitored by UV-visible spectroscopy (Figure 12).

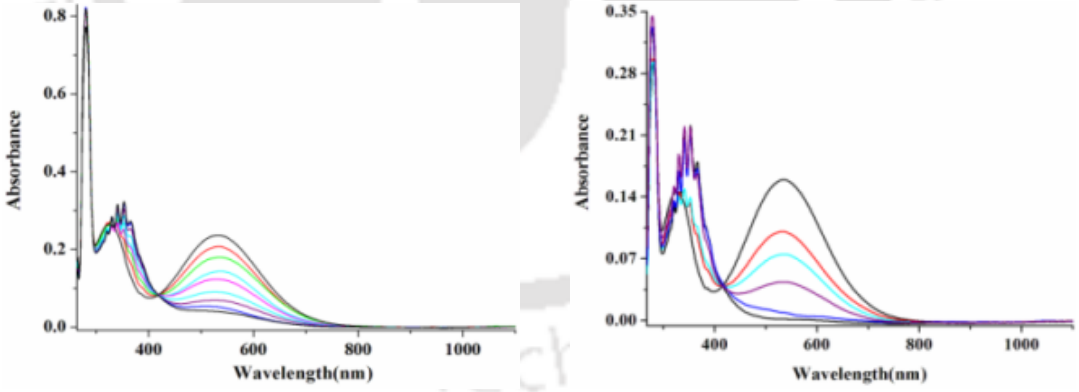

(a) **(b)**

Figure 12 UV-visible spectra of complexes **5.1** (a) and **5.2** (b) before (black trace) and after addition of NO in methanol.

The complexes **5.3** and **5.4** were isolated and characterized using various spectroscopic techniques. In FT-IR study, complexes **5.3** and **5.4** displayed strong stretching frequency at 1648 cm^{-1} and 1657 cm^{-1}, respectively (Figure 13) which are attributed to the corresponding [Fe^{II}-NO] moiety.

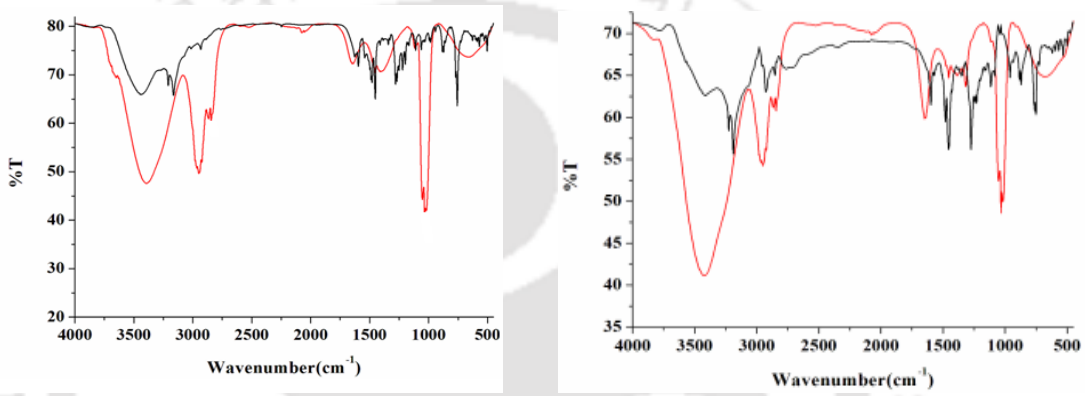

(a) **(b)**

Figure 13 FT-IR spectra of complexes **5.3** (a) and **5.4** (b), shown by red traces in KBr pellet.

The structures of complexes **5.3** and **5.4** were also fully optimized using PBE functional and DNP basis set in the presence of solvent methanol.

Table 1 Selected metric parameters of the complexes optimized at PBE/DNP level of calculation.

	Complex **5.1**	Complex **5.2**	Complex **5.3**	Complex **5. 4**
Fe1-O1	2.031	2.038	2.352	2.294
Fe1-O2	1.894	1.899	1.938	1.953
Fe1-O3	1.890	1.899	1.919	1.934
Fe1-O5	2.047	2.039	-	-
Fe1-N1	2.066	2.021	2.026	2.025
Fe1-N2	2.069	2.033	2.035	2.024
Fe1-N3	-	-	1.710	1.713
N3-O4	-	-	1.199	1.199

The optimized structures of the complexes are shown in figure 14 and their selected geometric parameters are given in table 1. These are in good agreement with the experimental data of similar complexes.

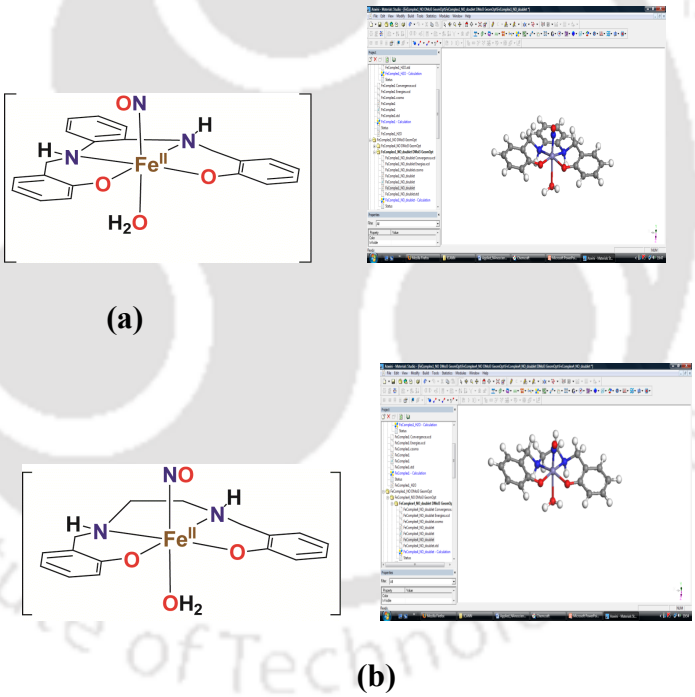

Figure 14 Optimized structures of complexes **5.3** (a) and **5.4** (b).

References

1. Ignarro, L. J. (Ed.). *Nitric Oxide: Biology and Pathobiology*, Academic Press, San Diego, 2000.

2. Fang, F. C. (Ed.). *Nitric Oxide and Infection*, Kluwer Academic/Plenum, New York, 1999.

3. (a) Moncada, S., Palmer, R. M. J., Higgs, E. A. *Pharmacol. Rev*. **199**1, *43*, 109; (b) Butler, A. R., Williams, D. L. *Chem. Soc. Rev*. **1993**, *22*, 233.

4. Jia, L., Bonaventura, C., Bonaventura, J., Stamler, J. S. *Nature*. **1996**, *380*, 221.

5. (a) Meininger, D. J.; Jonathan, D. C.; Hadi, D. A.; Zachary, J. T. *Inorg. Chem*. **2013**, *52*, 12468. (b) Michael D. P.; Lippard, S. J. *Chem. Commun.,* **2012**, *48*, 11981.

6. Tran, D.; Ford, P. C. *Inorg. Chem*. **1996**, *35*, 2411.

7. Tsuge, K.; DeRosa, F.; Lim, M. D.; Ford, P. C. *J. Am. Chem. Soc.* **2004**, *126*, 7846.

8. Sarma, M.; Kalita, A.; Kumar, P.; Singh, A.; Mondal, B. *J. Am. Chem. Soc.* **2010**, *132*, 7846.

9. Kumar, P.; Kalita, A.; Mondal, B. *Dalton Trans*. **2013**, *42*, 5731.

10. Sarma, M.; Kumar, V.; Kalita, A.; Deka, R. C.; Mondal, B. *Dalton Trans*. **2012**, *41*, 9543.

11. Goldner, M.; Geniffke, B.; Franken, A.; Murray, K. S.; Homborg, H. Z. *Anorg. Allg. Chem*. **2001**, *627*, 935.

12. Hoffman-Luca, C. G.; Eroy-Reveles, A. A.; Alvarenga, J.; Mascharak, P. K. *Inorg. Chem.* **2009**, *48*, 9104.

13. Ghosh, K., Eroy-Reveles, A. A., Olmstead, M. M., Mascharak, P. K. *Inorg. Chem*. **2005**, *44*, 8469.

14.(a) Ghosh, K., Eroy-Reveles, A. A., Avila, B., Holman, T. H., Olmstead, M. M., Mascharak, P. K. *Inorg. Chem.* **2004,** *43*, 2988; (b) Merkle, A. C., Fry, N. L., Mascharak, P. K., Lehnert, N. *Inorg. Chem*. **2011**, *50*, 12192.

Chapter 1

Introduction

1.1 General aspects of nitric oxide

Nitric oxide (NO) is an omnipresent intercellular messenger in all vertebrates which modulates blood pressure, neurotransmission and immune response. The biological role for NO as the endothelium derived relaxation factor (EDRF) was identified nearly 30 years ago.[1] Furchgott, Ignarro and Murad got Nobel Prize in 1998 due to their discovery of multiple roles that NO plays in physiological and pathological functions in human body.[2] NO easily diffuses through the plasma membranes to reach target proteins within the cell due to its lipophilic nature. Being a free radical, NO reacts rapidly with other free radicals; for example, the reaction with superoxide ion O_2^- to form peroxynitrite ion $ONOO^-$ (equation 1.1) occurs with a nearly diffusion-limited rate constant ($k_2 \sim 1010\ M^{-1}\ s^{-1}$).[3]

---------- (eq. 1.1)

Some of its activities are attributed to the formation of nitrosyl complexes of metallo-proteins primarily, iron and copper proteins.[4] The best characterized examples include its reactivity with ferroheme enzyme, soluble guanylyl cyclase (sGC).[5] In sGC, the formation of the nitrosyl complex with Fe(II) leads to labilization of a *trans* axial (proximal) histidine ligand in the protein backbone, and the resulting change in the protein conformation is believed to activate

the enzyme for catalytic formation of the secondary messenger cyclic-guanylyl monophosphate (cGMP) from guanylyl triphosphate (GTP). The enzymatic formation of cGMP results into the relaxation of smooth muscle tissue of blood vessels, hence lowering blood pressure.[5]

The interaction of NO with metal centers has been of interest because of its flexibility to act either as an electron donor or acceptor during metal-NO binding.[6] NO reacts with the oxygen adduct of ferrous heme proteins (*e.g.* oxyhaemoglobin) to generate nitrate and ferri-heme; this reaction is responsible for the majority of NO metabolism in the vasculature. NO can also interact with iron-sulphur enzymes (e.g. aconitase, NADH dehydrogenase).[7] The reduction of Cu(II) centers in some proteins, such as cytochrome *c* oxidase (cCO) and laccase, to Cu^{I} on exposure to NO has been known since long back.[8,15] In cCO, the NO reduction of Cu(II) to Cu(I) is believed to play the role in regulating the electron transport activity of this protein.[8] NO is also known to involve in the generation of powerful secondary nitrating and/or oxidizing agents, like NO_2 and peroxynitrite.[9]

1.2 Metal-nitrosyl bonding

Since the biological roles of NO are ultimately defined by its reactivity with metallo-proteins, the interaction of NO with transition metal ions has been a subject of interest for chemists and biochemists. The formation of nitrosyls of metallo-proteins are believed to be the key step for most of the biochemical activities of NO in mammalian biology.[10-14] The molecular orbital (MO) diagram of NO is shown in figure 1.1. It has a $^2\Pi$ ground state.[15] From the molecular

orbital theory, its bond order is 2.5, consistent with its bond length (1.154 Å) between those of N_2 (1.06 Å) and O_2 (1.18 Å). The singly occupied MO is a π^* orbital, but polarized toward nitrogen in a manner opposing the polarization of the lower energy bonding π orbitals resulting in a relatively nonpolar diatomic molecule. Consequently, NO shows stretching frequency at 1875 cm^{-1} with low intensity in the infrared absorption spectrum.

The highest occupied molecular orbital (HOMO) possesses only nitrogen character as greater electronegativity of the O-atom lowers the energy of O-atom. Hence, NO prefers to bind to the metal *via* N-atom. It can bind to metal by the loss of one electron forming NO^+, nitrosonium cation or by gaining one electron forming nitroxyl anion (NO^-).

The NO^+ is isoelectronic with carbon monoxide (CO), and it behaves as a two-electron donor to the metal and accepts electrons from the metal *via* back-bonding.

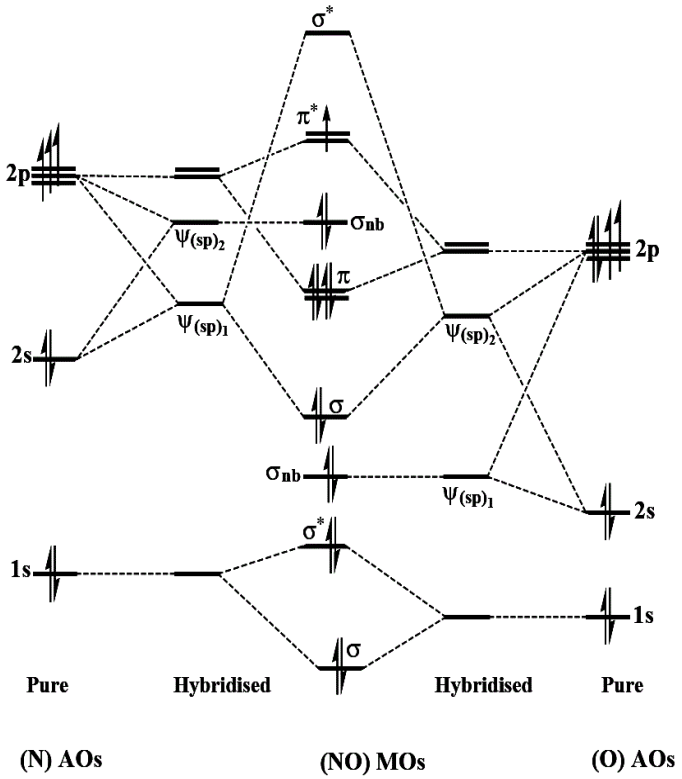

Figure 1.1 Molecular orbital diagram of nitric oxide (NO).

Trends in structure and bonding of metal-nitrosyls are usually described by using the Enemark-Feltham approach.[16]

Based on the literature, the binding modes of NO to metal ion can be of three types: (i) linear end on, (ii) bent end on and (iii) side-on.

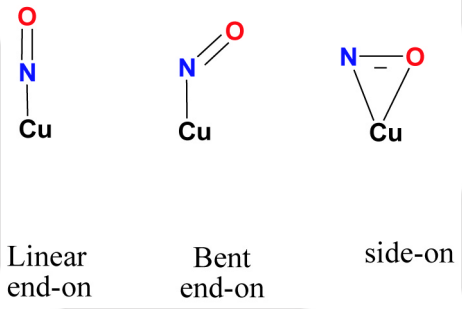

Figure 1.2 Different binding modes of NO to metal centers.

Linear and bent NO ligands can be distinguished using infrared spectroscopy. In case of linear, ν_{NO} appears in the range of 1650–1900 cm^{-1}, whereas for bent nitrosyls the range is 1525–1690 cm^{-1}.

1.3 Objective of the present work

For metal ion, the ability to form a stable nitrosyl complex and the structure of that depends strongly on the oxidation state of the metal ion. In this regard, the iron-nitrosyls, both in protein and synthetic model systems have been studied extensively. NO has been shown to interact reversibly with iron complexes to form iron-nitrosyls. The binding in these complexes is similar to the coordination of dioxygen to such metal centers, although the nitrosyl products are comparatively more stable and easy to characterize than their superoxo analogues. The nitroprusside anion, $[Fe(CN)_5(NO)]^{2-}$ is, perhaps, the earliest discovered nitrosyl complex, and it remains the subject of intense research efforts.[17] A series of trigonal bipyramidal $\{Fe{-}NO\}^7$ complexes has been reported by Borovik and co-workers.[18] These complexes were synthesized with tripodal ligands derived from *tris*-(carbamoylmethyl) amine by reaction of $[Fe^{II}(OAc)_2]$ with the *tri*-potassium salt of the ligand. Magnetic moment, Mossbauer, and ESR data are all consistent with an electronic configuration of $[Fe^{III}\text{-}\overline{NO}]$.[19] $\{Fe\text{-}NO\}^7$coordination complexes such as [Fe(NO)(EDTA)] and $[Fe(L)(NO)(N_3)_2]$ (L = triazacyclononane and derivatives) have been studied in great detail by Solomon and co workers using diverse spectroscopic and analytical techniques. These studies have shown the $\{Fe\text{-}NO\}^7$complexes to be best described as a high-spin ferric ion (S = 5/2) antiferromagnetically coupled to $\overline{NO}$ (S = 1).[20-23] Mossbauer spectroscopic studies on these complexes also found to be in agreement with this description .[24] The iron nitrosyl complexes $[Fe(NO)X(CH_2CH_2SC_6H_4\text{-}o\text{-}S)_2]$ (X = NR, S) have also been cited as models for the active sites in nitrogenase enzymes. Lippard and co-workers have

described the diiron dinitrosyl complex $[Fe_2(\mu\text{-Et-HPTB})(\mu\text{-}O_2CPh)(NO)_2][BF_4]_2.3MeCN$ (Et-HPTB = N,N,N/,N/-*tetrakis*(N-ethyl-2 benzimidazolylmethyl)-2-hydroxy-1,3-diaminopropane) as a model for the binding of O_2 to non-heme iron proteins .[25]

Other reports describe roles of NO as an inhibitor for metalloenzymes such as cytochrome P_{450}, cytochrome oxidase,[26] nitrile hydratase,[27] and catalase,[28] as a substrate for mammalian peroxidases, and as the vasodilator carried by a salivary ferri-heme protein of blood-sucking insects.[29] Heme centers are also involved in the *in vivo* generation of NO by oxidation of arginine catalyzed by nitric oxide synthase (NOS) enzymes. [30] Ferri-heme proteins are known to undergo reduction to ferroheme in aqueous solution on exposure to NO. These reactions proceed through two distinct steps: (i) formation of iron(III)-nitrosyl adduct; (ii) followed by the pH dependent reduction of Fe(III) to Fe(II) with a simultaneous attack of hydroxide ion to the activated nitrosonium group [Fe^{III}–NO ↔ Fe^{II}–NO^+] leading to the formation of nitrate (NO_3^-).

Recently, the reactivity of several iron(III) porphyrinates containing silanethiolate ligands with NO is reported by Tonzetich group.[31] In the complex [Fe(OMe)(TPP)] and $[Fe(OH)(H_2O)(TMP)]$ (TPP = dianion of mesotetraphenylporphine; TMP = dianion of meso-tetramesitylporphine), Fe(III) centre undergoes reductive nitrosylation to afford the Fe^{II}-NO complex when treated with NO (Scheme 1.1).

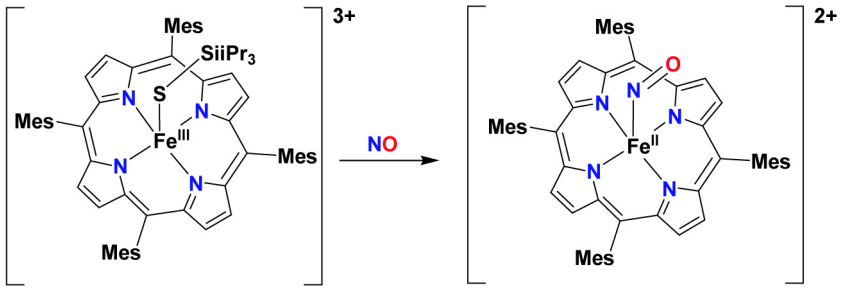

Scheme 1.1

It is reported that NO binds reversibly to the Fe(III) complex of a *tetra*-amido macrocyclic ligand.[32] Upon reaction with NO, the corresponding iron(III) complex results in Fe(II)-nitrosyl which is labile and dissociates readily upon purging N_2 (Scheme 1.2).

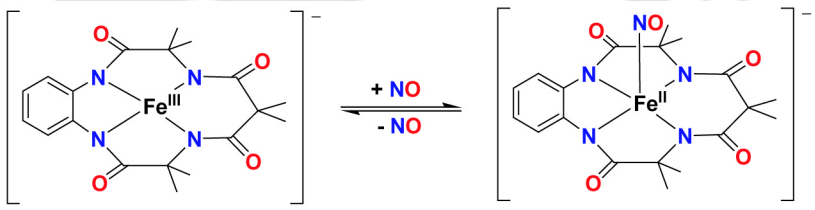

Scheme 1.2

Reduction of Cu(II) centers by NO have been demonstrated in cytochrome *c* oxidase and laccase.[6,8,15] Tran et al has reported the reaction of NO with the Cu(II) complex, $[Cu(dmp)_2(X)]^{2+}$ (dmp = 2,9-dimethyl-1,10-phenanthroline, X= solvent) in methanol that leads to formation of a tetra-coordinated $[Cu^{I}(dmp)_2]$ complex along with methyl nitrite and H_2O (equation 1.2). This reaction was proposed to proceed through the formation of $[Cu^{II}$-NO] species.[33]

$$[Cu(dmp)_2(X)]^{2+} + NO + CH_3OH \longrightarrow [Cu(dmp)_2]^{+} + H_2O + CH_3ONO + H^{+}$$

------- (eq.1.2)

The detailed mechanism of this reaction was studied by Ford et al. In methanol, the product of the $[Cu(dmp)_2(H_2O)]^{2+}$ oxidation of NO is CH_3ONO; in water, it is NO_2^-.The reaction did not occur in CH_2Cl_2 unless methanol was added, and in such solutions the reaction rate was linearly dependent on the concentration of alcohol added.[34]

In recent years there are number of examples from our group which demonstrated the reduction of Cu(II) center by NO which proceed through the $[Cu^{II}$-NO] intermediate and afforded N-nitrosation in the ligand frameworks. For example:

Cu(II) complex of *tris*-(2-isopropyl aminoethyl)amine on reaction with NO affords reduction of Cu(II) centre with simultaneous *tri*-nitrosation of the ligand (Scheme 1.3).[35]

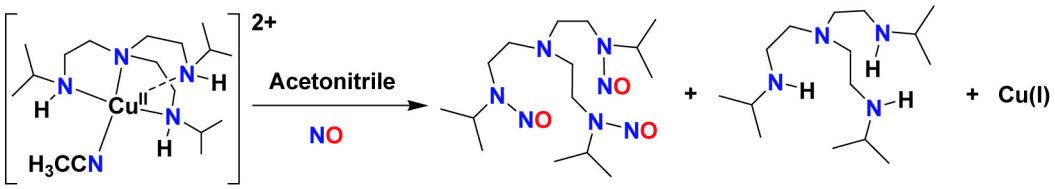

Scheme 1.3

Cu(II) complexes of ethylenediamine and its substituted derivatives react with NO to result in the reduction of Cu(II) and mono- and di -nitrosation of the ligand (Scheme 1.4).[36]

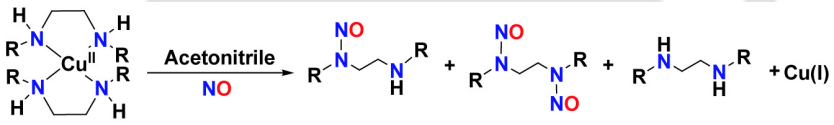

R = Methyl, ethyl and *iso*-butyl

Scheme 1.4

NO reactivity of Cu(II) complexes of bidentate and tridentate amine ligands, lead to the reduction of Cu(II) centers and nitrosation and diazotization of the ligands (Scheme 1.5).[37]

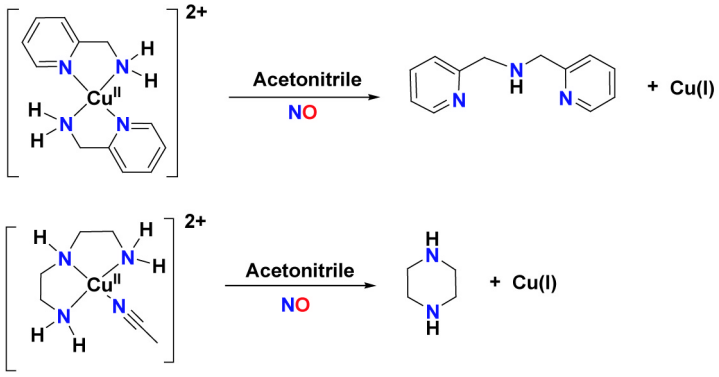

Scheme 1.5

NO reactivity of Cu(II) complexes of bidentate amine ligands having aliphatic and aromatic N-donor sites lead to the reduction of Cu(II) centers and concomitant nitrosation of the ligand (Scheme 1.6).[38]

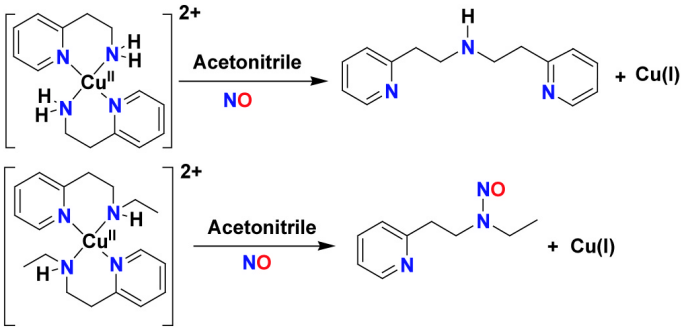

Scheme 1.6

In an other example, Ford et al reported the reduction of Cu(II) center in $[Cu(DAC)]^{+}$ (DAC = 1,8-bis(9-anthracylmethyl)cyclam) by NO with simultaneous N-nitrosation of the ligand.[39] The reduction was found to take place in presence of a base and a mechanistic pathway involving the deprotonation of the ligand was proposed.

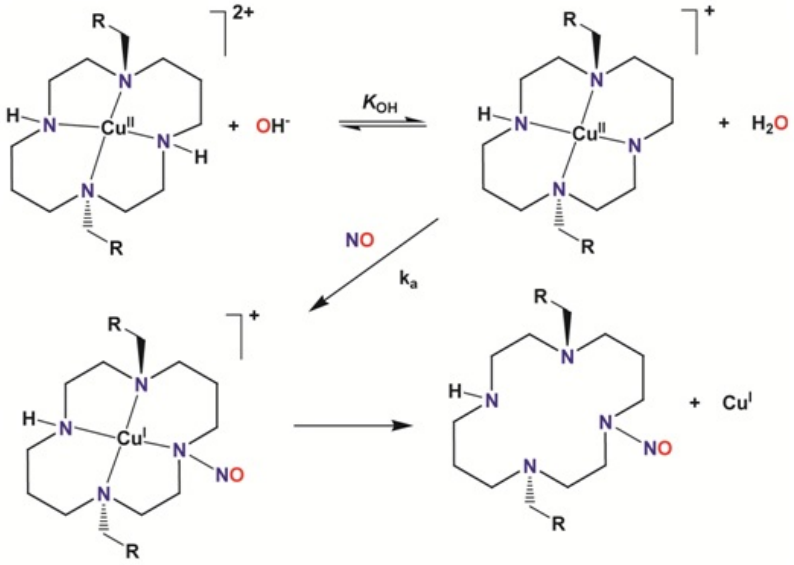

R= anthracene

Scheme 1.7

Although the free ligand is strongly fluorescent, the analogous solution of $[Cu(DAC)]^{2+}$ displays no luminescence at room temperature, because of paramagnetic quenching by the

Cu(II) center. Addition of NO to the methanol solution of $[Cu(DAC)]^{2+}$ displays anthracene-type fluorescence (Scheme 1.7).[40,41]

Similarly, in case of tetra dentate macrocyclic ligand (Scheme 1.8), the reduction of Cu(II) center was found to proceed through a deprotonation of the N-H group.[42]

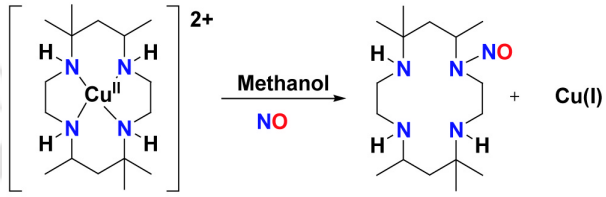

Scheme 1.8

However, in Cu(II)-complexes of tetradentate non-macrocyclic ligands (Scheme 1.9), the reduction of Cu(II) centers were found to proceed through a deprotonation of the N-H group.[43]

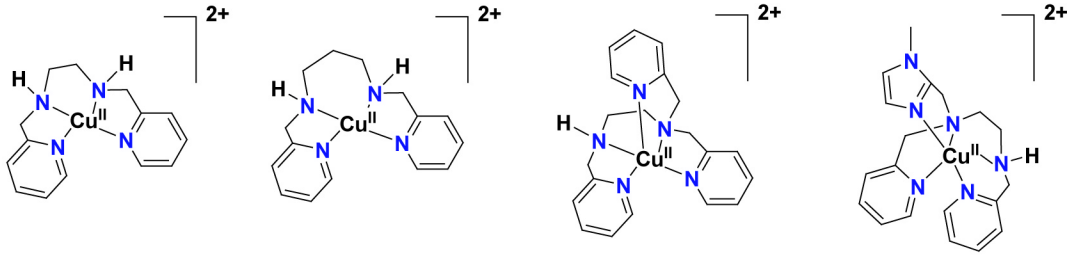

Scheme 1.9

On the basis of these observations, two pathways have been proposed in the context of the mechanism of the reduction of Cu(II) centre by NO.[40] In one case, NO initially reacts with the Cu(II) to form a [Cu^{II}-NO] (or Cu^{I}-NO^{+}) intermediate complex. Alternatively, the initial step involves a reversible deprotonation of the coordinated secondary amine followed by addition of NO at the amide site with concomitant electron transfer to reduce the Cu(II) center.[40]

Mn-nitrosyl complexes have not been studied extensively compared to iron or copper nitrosyls. Stable Mn-nitrosyls are reported with porphyrin[44], phthalocyanine[45] ligands.

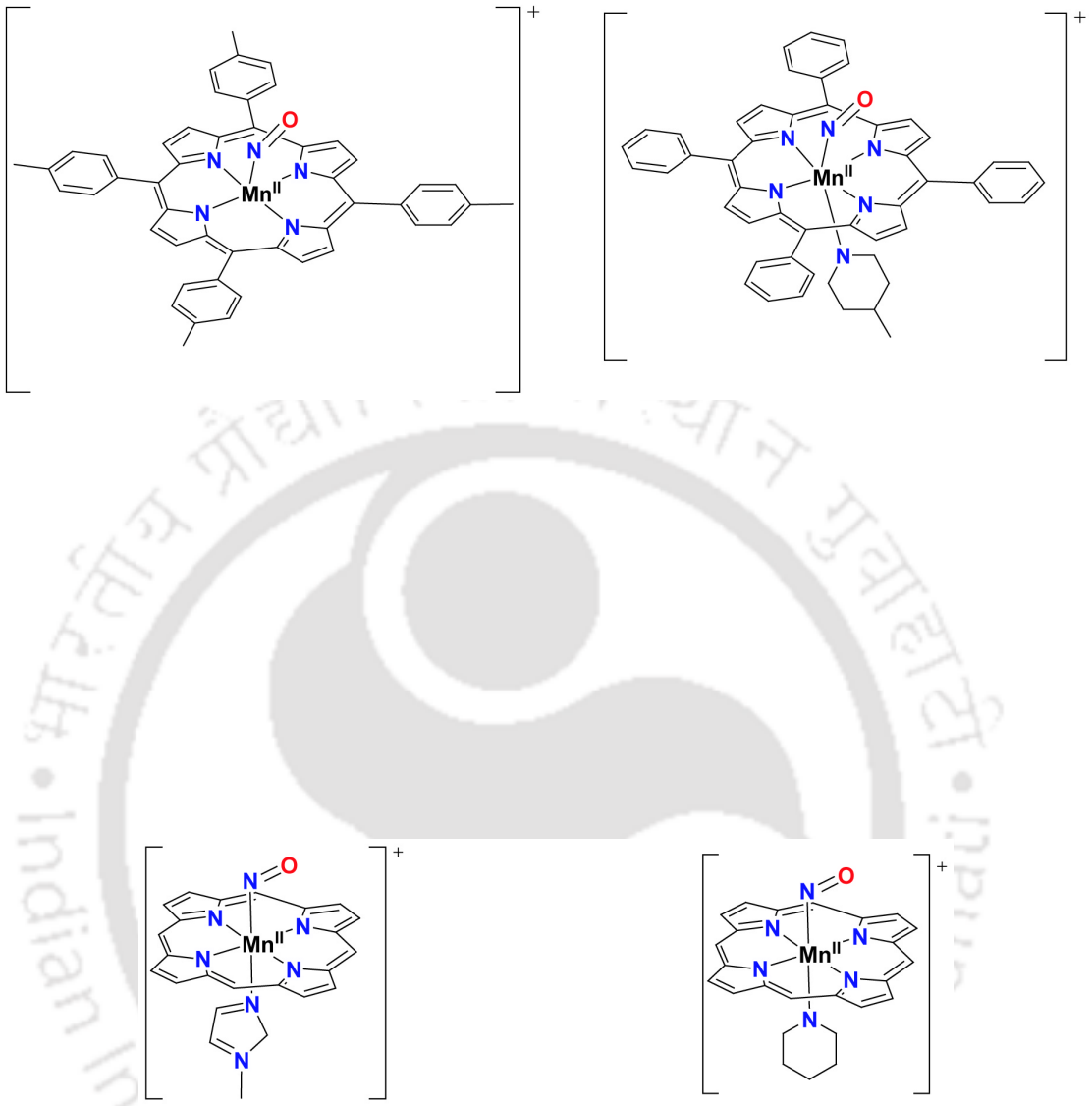

Figure 1.3 Some Mn-nitrosyl complexes containing porphyrin moiety.

A few examples of Mn-nitrosyls with pentadentate ligand *N*, *N*-bis(2-pyridylmethyl)amine-*N*-ethyl-2-pyridine-2-carboxamide ($PaPy_3H$; H is the dissociable carboxamide hydrogen), namely, $[Mn(PaPy_3)(H_2O)]ClO_4$ and $[Mn(PaPy_3)(Cl)]ClO_4$, with bound carboxamido nitrogen are reported in connection to the photo dynamic therapy.[46]

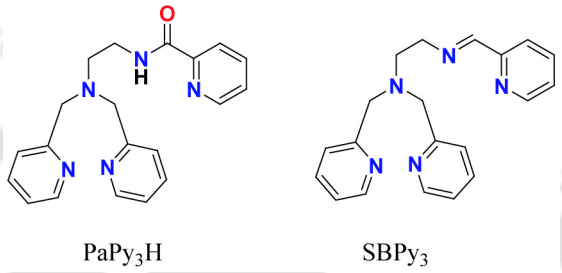

$PaPy_3H$ $SBPy_3$

Figure 1.4 Pentadentate amido and imine ligands

$[Mn(PaPy_3)(H_2O)]ClO_4$ upon reaction with NO affords the diamagnetic $\{Mn\text{-}NO\}^6$, $[Mn(PaPy_3)(NO)]ClO_4$ (Scheme 1.10). It should be noted that complexes with non-bonded carboxamido nitrogen such as $[Mn(SBPy_3)Cl]ClO_4$ and $[Mn(PaPy_3H)(Cl)_2]$, do not react with NO. Collectively, these reactions indicate that NO reacts only with the Mn(II) center ligated to at least one carboxamido nitrogen.

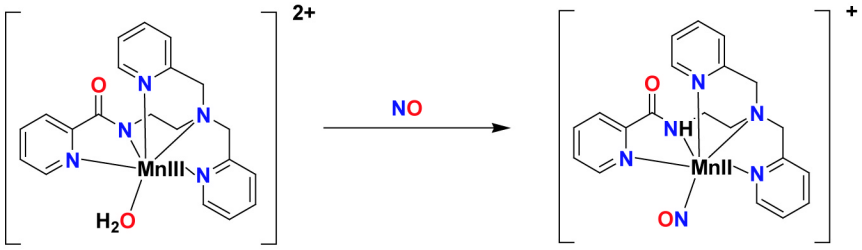

Scheme 1.10

Dimanganese(III) (μ-oxo) complex $[(Mn(PaPy_3))_2(\mu\text{-}O)](ClO_4)_2$ upon reaction with NO in acetonitrile produces the $\{Mn\text{-}NO\}^6$, $[Mn(PaPy_3)\text{-}(NO)](ClO_4)$ *via* reductive nitrosylation (Scheme 1.11).[47]

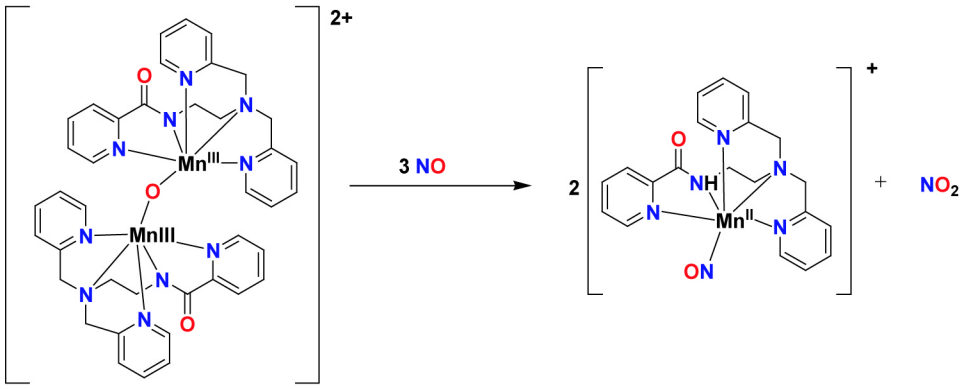

Scheme 1.11

The diamagnetic {Mn-NO}^{6}, [Mn(PaPy$_3$)(NO)]ClO$_4$ was characterized structurally and exhibits the photolability of NO.

All these examples actually instigate us to study the NO reactivity of various transition metal complexes in solution.

This thesis has been focused on the formation of Cu(II), Mn(II) and Fe(III)-nitrosyls and their reactivity studies. Second and third chapters describe the formation and reactivity of Cu(II)-nitrosyls leading to N-nitrosation and C-nitrosation of the ligand frameworks. Fourth

chapter describes the reactivity of a Mn(II) complex with NO resulting in corresponding Mn-nitrosyl. In the last chapter, the formation of non-heme iron-nitrosyls by the reaction of NO with Fe(III)-complexes of salen type of ligands has been described.

(a) Chapter 2: Nitric oxide reactivity of copper(II) complexes of bidentate amine ligand: Two Cu(II) complexes of 1,3-diaminopropane ($\mathbf{L_1}$) and N-isopropylpropane-1,3-diamine ($\mathbf{L_2}$) were prepared to study their reactivity with NO. The complexes, **2.1** and **2.2** were characterized by spectroscopic techniques as well as X-ray single crystal structure determination. The reduction of the Cu(II)-centers in both the complexes by NO leads to the modification of the ligands. Complexes **2.1** and **2.2** do not react with NO in methanol and water medium.

b) Chapter 3: C-nitrosation of a β-diketiminate ligand in copper(II) complex: A Cu(II) complex, **3.1** of a *β*-diketiminate ligand {$\mathbf{L_3}$ = (4-(2,6-dimethylphenylimino)pentane-2-ylidene)-2,6-dimethylbenzeneamine} has been synthesized and characterized. In acetonitrile solution of the complex, the *β*-diketiminate ligand undergoes oxidative degradation to the corresponding ketone di-imine under aerobic condition. Addition of NO to the acetonitrile solution of complex **3.1** affords the corresponding oxime di-imine ligand. All the modified ligands have been isolated and characterized.

c) Chapter 4: Nitric oxide reactivity of a manganese(II) complex leading to nitrosation of the ligand: Mn(II) complex, **4.2**, in acetonitrile solution was found to react with NO to afford unstable Mn(II)-nitrosyl intermediate. Subsequently, Mn(II) center in complex **4.2** was found to

undergo reduction to Mn(I) with a simultaneous N-nitrosation of the ligand. The N-nitrosated ligand was isolated and characterized. The corresponding Cu(II) complex of the same ligand in presence of NO was not found to yield Cu(II)-nitrosyl.

d) Chapter 5: Reductive nitrosylation of iron(III) complexes of tetradentate ligands: In this chapter, we have synthesized two Fe(III) complexes with salen type of tetradentate ligands, having O-donor and N-donor sites (**L_5** and **L_6**) and characterized by spectroscopic techniques. The NO reactivity of those complexes have been studied in methanol medium. The reductive nitrosylation of the Fe(III) centers was observed to form the Fe(II)-nitrosyl complexes. It was monitored by UV-visible, FT-IR and EPR spectroscopic studies. Geometries of all the complexes have been optimized by DFT calculations.

1.4 References

1. (a) Ignarro, L. J.; Buga, G. M.; Wood, K. S.; Byrns, R. E.; Chaudhuri, G. *Proc. Natl. Acad. Sci. U.S.A.* **1987**, *84*, 9265; (b) Rapoport, R. M.; Draznin, M. B.; Murad, F. *Nature*. **1983**, *306*, 174.

2. (a) Murrad, F. *Angew. Chem., Int. Ed. Engl.* **1999**, *38*, 1856; (b) Ignaro, L. J. *Angew. Chem., Int. Ed. Engl.* **1999**, *38*, 1882; (c) Furchgott, R. F. *Angew. Chem., Int. Ed. Engl.* **1999**, *38*, 1870; (d) Wang, P. G.; Xian, M.; Tang, X.; Wu, X.; Wen, Z.; Cai, T.; Janczuk, A. J. *Chem. Rev.* **2002**, *102*, 1091.

3. Kissner, R.; Nauser, T.; Bougnon, P.; Lye, P. G.; Koppenol, W. H. *Chem. Res. Toxicol.* **1997***, 10*, 1285.

4. (a) Traylor, T. G.; Sharma, V. S. *Biochemistry.* **1992**, *31*, 2847; (b) Radi, R. *Chem. Res. Toxicol.* **1996**, *9***,** 828.

5. (a) Kim, S.; Deinum, G.; Gardner, M. T.; Marletta, M. A.; Babcock, G. T. *J. Am. Chem. Soc.* **1996**, *118*, 8769; (b) Burstyn, J. N.; Yu, A. E.; Dierks, E. A.; Hawkins, B. K.; Dawson, B. K. *Biochemistry*. **1995**, *34*, 5896.

6. (a) Ford, P. C.; Fernandez, B. O.; Lim, M. D.; *Chem. Rev*. **2005**, *105*, 2439; (b) Torres, J.; Cooper, C. E.; Wilson, M. T. *J. Biol. Chem*. **1998**, *273*, 8756.

7. Cooper, C. E. *Biochimica et Biophysica Acta.* **1999**, *1411*, 290.

8. Cooper, C. E.; Torres, J.; Sharpe, M. A.; Wilson, M. T. *FEBS Lett.* **1997**, *414*, 281.

9. (a) Schopfer, M. P.; Mondal, B.; Lee, D.-H.; Sarjeant, A. A. N.; Karlin, K. D. *J. Am. Chem. Soc*. **2009**, *131*, 11304; (b) Maiti, D.; Lee, D.-H.; Sarjeant, A. A. N.; Pau, M. Y. M.; Solomon, E. I.; Gaoutchenova, K.; Sundermeyer, J.; Karlin, K. D. *J. Am. Chem. Soc*. **2008**, *130*, 6700; (c) Park, G. A.; Deepalatha, S.; Simona, C. P.; Lee, D.-H.; Mondal, B.; Sarjeant, A. A. N.; Rio, D. Del.; Pau, M. Y. M.; Solomon, E. I.; Karlin, K. D. *J. Biol. Inorg. Chem.* **2009**, *14*, 1301; (d) Kumar, V.; Kalita, A.; Mondal, B. *Dalton Trans*. **2013**, *42*, 16264.

10. Butler, A. R.; Williams, D. L. *Chem. Soc. Rev*. **1993**, 233.

11.(a) Feelisch, M.; Stamler, J. S. *Methods in Nitric Oxide Research*; John Wiley and Sons; Chichester, England, **1996**; (b) Jia, L.; Bonaventura, C.; Bonaventura, J.; Stamler, J. S.

Nature. **1996**, *380*, 221; (c) Galdwin, M. T.; Lancaster Jr., J. R.; Freeman, B. A.; Schechter, A. N. *Nat. Med*. **2003**, *9*, 496.

12. Ye, R. W.; Toro-Suarez, I.; Tiedje, J. M.; Averill, B. A. *J. Biol. Chem.* **1991**, *266*, 12848.

13. (a) Godden, J. W.; Turley, S.; Teller, D. C.; Adman, E. T.; Liu, M.Y.; Payne, W. J.; LeGall, J. *Science*. **1991**, *153*, 438; (b) Adman, E. T.; Turley, S.; in *Bioinorganic Chemistry of Copper;* Karlin, K. D.; Tyekllr, Z.; Eds., Chapman & Hall, Inc.: New York, **1993**; pp 397; (c) Ferguson, S. J. *Curr. Opin. Chem. Biol.* **1998**, *2*, 182.

14. (a) Richardson, D. J.; Watmough, N. J.; *Curr. Opin. Chem. Biol.* **1999**, *3*, 207; (b) I. Moura, I.; Moura, J. J. G. *Curr. Opin. Chem. Biol.* **2001**, *5*, 168; (c) Tocheva, E. I.; Rosell, F. I.; Mauk, A. G.; Murphy, M. E. P. *Biochem.* **2007**, *46*, 12366; (d) Torres, J.; Cooper, C. E.; Wilson, M. *J. Biol. Chem.*, **1998**, *273*, 8756; (e) Zhou, X.; Espey, M. G.; Chen, J. X.; Hofseth, L. J.; Miranda, K. M.; Hussain, S. P.; Winks, D. A.; Harris, C. C. *J. Biol. Chem.*, **2000**, *275*, 21241.

15. Greenwood, N. N. Earnshaw. *Chemistry of the Elements*; Pergamon Press: Oxford, **1993**; p 508.

16. Enemark, J. H.; Feltham, R. D. *Coord. Chem. Rev.* **1974**, *13*, 339.

17. (a) Haskin, C. J.; Ravi, N.; Lynch, J. B.; Munck, E.; Que, L., Jr. *Biochemistry* **1995**, *34*, 11090; (b) Go´mez, J. A.; Guenzburger, D. *Chem. Phys.* **2000**, *253*, 73.

18. Ray, M.; Golombek, A. P.; Hendrich, M. P.; Yap, G. P. A.; Liable- Sands, L. M.; Rheingold, A. L.; Borovik, A. S. *Inorg. Chem.* **1999**, *38*, 3110.

19. Hammes, B. S.; Ramos-Maldonado, D.; Yap, G. P. A.; Liable- Sands, L.; Rheingold, A. L.; Young, V. G.; Borovik, A. S. *Inorg. Chem.* **1997**, *36*, 3210.

20. Brown, C. A.; Pavlosky, M. A.; Westre, T. E.; Zhang, Y.; Hedman, B.; Hodgson, K. O.; Solomon, E. I. *J. Am. Chem. Soc.* **1995**, *117*, 715.

21. Westre, T. E.; Dicicco, A.; Filipponi, A.; Natoli, C. R.; Hedman, B.; Solomon, E. I.; Hodgson, K. O. *J. Am. Chem. Soc.* **1994**, *116*, 6757.

22. Zhang, Y.; Pavlosky, M. A.; Brown, C. A.; Westre, T. E.; Hedman, B.; Hodgson, K. O.; Solomon, E. I. *J. Am. Chem. Soc.* **1992**, *114*, 9189.

23. Farrar, J. A.; Grinter, R.; Pountney, D. L.; Thomson, A. J. *Dalton Trans.* **1993**, 2703.

24. Hauser, C.; Glaser, T.; Bill, E.; Weyhermuller, T.; Wieghardt, K. *J. Am. Chem. Soc.* **2000**, *122*, 4352.

25. Feig, A. L.; Bautista, M. T.; Lippard, S. J. *Inorg. Chem.* **1996**, *35*, 6892.

26. Cleeter, M. W. J.; Cooper, J. M.; Darley-Usmar, V. M.; Moncada, S.; Scapira, A. H. V. *FEBS Lett.* **1994**, *345*, 50.

27. (a) Noguchi, T.; Hoshino, M.; Tsujimura, M.; Odaka, M.; Inoue, Y.; Endo, I. *Biochemistry.* **1996**, *35,* 16777; (b) Odaka, M.; Fujii, K.; Hoshino, M.; Noguchi, T.; Tsujimura, M.; Nagashima, S.; Yohda, M.; Nagamune, T.; Inoue, Y.; Endo, I. *J. Am. Chem. Soc.* **1997**, *119,* 3785.

28. Brown, G. C. *Eur. J. Biochem.* **1995**, *232*, 188.

29. (a) Ribiero, J. M. C.; Hazzard, J. M. H.; Nussenzveig, R. H.; Champagne, D. E.; Walker, F. A. *Science.* **1993**, *260*, 539; (b) Ding, X. D.; Weichsel, A.; Balfour, C.; Shokhireva, T. Kh.; Pierik, A.; Averill, B. A.; Montfort, W. R.; Walker, F. A. *J. Am. Chem. Soc*. **1999**, *121*, 128.

30. (a) Abu-Soud, H. M.; Ichimori, K.; Nakazawa, H.; Stuehr, D. J. *Biochemistry.* **2001**, *40*, 6876; (b) Stuehr, D.; Pou, S.; Rosen, G. M. *J. Biol. Chem.* **2001**, *276*, 14533; (c) Ford, P. C. *Pure Appl. Chem.* **2004**, *76*, 335.

31. Meininger, D. J.; Caranto, J. D.; Arman, H. D.; Tonzetich, Z. J. *Inorg. Chem*. **2013**, *52*, 12468.

32. Pluthz, M. D.; Lippard, S. J. *Chem. Commun.* **2012**, *48*, 11981.

33. Tran, D.; Ford, P. C. *Inorg. Chem*. **1996**, *35*, 2411.

34. Tran, D.; Skelton, B. W.; White, A. H.; Laverman, L. E.; Ford, P. C. *Inorg. Chem*. **1998**, *37*, 2505.

35. Sarma, M.; Kalita, A.; Kumar, P.; Singh, A.; Mondal, B. *J. Am. Chem. Soc*. **2010**, *132*, 7846.

36. Sarma, M.; Mondal, B. *Dalton Trans*. **2012**, *41*, 2927.

37. Sarma, M.; Mondal, B. *Inorg. Chem*. **2011**, *50*, 3206.

38. Sarma, M.; Kumar, V.; Kalita, A.; Deka, R. C.; Mondal, B. *Dalton Trans*., **2012**, *41*, 2927.

39. Fernandez, B. O.; Lim, M. D.; Ford, P. C. *Chem. Rev.* **2005**, *105*, 2439.

40. Tsuge, K.; DeRosa, F.; Lim, M. D.; Ford, P. C. *J. Am. Chem. Soc.* **2004**, *126*, 6564.

41. Franz, K. J.; Singh, N.; Lippard, S. J. *Angew. Chem., Int. Ed.* **2000**, *39*, 2120.

42. Kalita, A.; Kumar, P.; Deka, R. C.; Mondal, B. *Inorg. Chem*. **2011**, *50*, 11868.

43. Kumar, P.; Kalita, A.; Mondal, B. *Dalton Trans*., **2013**, *42*, 5731.

44. (a) Piciulo, P. L.; Rupprecht, G.; Scheidt, W. R. *J. Am. Chem. Soc*. **1974**, *96*, 5293; (b) Scheidt, W. R.; Hatano, K.; Rupprecht, G. A.; Piciulo, P. L. *Inorg. Chem*. **1979**, *18*, 292; (c) Wayland, B. B.; Olson, L. W. *Inorg. Chim. Acta.* **1974**, *11*, L23; (d) Wayland, B. B.; Olson, L. W.; Siddiqui, Z. U. *J. Am. Chem. Soc*. **1976**, *98*, 94.

45. Goldner, M.; Geniffke, B.; Franken, A.; Murray, K. S.; Homborg, H. *Z. Anorg. Allg. Chem*. **2001**, *627*, 935.

46. (a) Ghosh, K.; Eroy-Reveles, A. A.; Avila, B.; Holman, T. H.; Olmstead, M. M.; Mascharak, P. K. *Inorg. Chem.* **2004,** *43*, 2988; (b) Merkle, A. C.; Fry, N. L.; Mascharak, P. K.; Lehnert, N. *Inorg. Chem*. **2011**, *50*, 12192.

47. (a) Ghosh, K.; Eroy-Reveles, A. A.; Olmstead, M. M.; Mascharak, P. K. *Inorg. Chem*. **2005**, *44*, 8469; (b) Hoffman-Luca, C. G.; Eroy-Reveles, A. A.; Alvarenga, J.; Mascharak, P. K. *Inorg. Chem.* **2009**, *48*, 9104.

Chapter 2

Abstract

Two Cu(II) complexes, **2.1** and **2.2** with $\mathbf{L_1}$ and $\mathbf{L_2}$ [$\mathbf{L_1}$ = propane-1, 3-diamine ; $\mathbf{L_2}$ = N-isopropylpropane-1,3-diamine], respectively, were synthesized and characterized structurally. In acetonitrile solution of the complexes, the Cu(II) center was found to reduce in presence of NO gas. The formation of [Cu^{II}-NO] intermediate prior to the reduction of Cu(II) center was evidenced by UV-visible, solution FT-IR, X-band EPR studies. This reduction led to the ligand transformation through diazotization at primary amine site in complex **2.1**; whereas, N-nitrosation at the secondary amine site of the ligand was observed in **2.2**. The final organic products were isolated and characterized by spectroscopic studies.

2.1 Introduction

Activation of nitric oxide (NO) by transition metal ions has been a subject of interest since the discovery of its bioregulatory roles in mammalian biology.[1-6] Much of these activities are attributed to the interactions of NO with metal ions leading to the formation of nitrosyl complexes of metallo-proteins.[1-3] In this context, iron-nitrosyls have been studied extensively.[7-13] The reduction of Cu(II) centers in cytochrome *c* oxidase and laccase by NO is known for a long time.[14-17] A number of Cu(II) complexes have been utilized recently to exemplify the reduction of Cu(II) by NO. For example, in $[Cu(dmp)_2(X)]^{2+}$ (dmp = 2,9-dimethyl-1,10-phenanthroline, X = solvent) and analogous complexes, Cu(II) undergoes reduction by NO. Detailed mechanistic study revealed that the reduction proceeds through an inner-sphere pathway.[18, 19] The reduction was resulted in the nitrosation of the solvent resulting into methylnitrite or NO_2^- in case of methanol or water, respectively (equation 2.1).[18, 19]

$$[Cu(dmp)_2(X)]^{2+} + NO + CH_3OH \longrightarrow [Cu(dmp)_2]^{+} + H_2O + CH_3ONO + H^+$$

-----(2.1)

In contrast, in methanol solution, $[Cu^{II}(DAC)]^{2+}$ {DAC = 1,8-bis(9-anthracylmethyl) derivative of the macrocyclic tetraamine cyclam (1,4,8,11-tetraazacyclotetradecane)} in presence of NaOEt was found to react with NO leading to the reduction of Cu(II) center with a

simultaneous nitrosation of the ligand.[20] From detail quantitative and theoretical studies, a pathway analogous to the inner-sphere mechanism for electron transfer was suggested where NO is the reductant, Cu(II), the oxidant and the coordinated amido anion behaves as the bridging ligand (Scheme 1.7, Chapter 1).

The reaction of $[Ru(NH_3)_6]^{3+}$ with NO in alkaline solution resulting in the Ru(II)-dinitrogen complex, $[Ru(NH_3)_5(N_2)]^{2+}$ was reported to proceed through a similar pathway.[21] Nitrosation of a coordinated amide ligand with simultaneous reduction of Ru(III) to Ru(II) results into a coordinated nitroso amine, which upon subsequent dehydration afforded the coordinated dinitrogen complex. A mechanism, more close to that of ferriheme reduction, involving the initial NO coordination to the Cu(II) center to form $[Cu^{II}\text{-}NO \leftrightarrow Cu^{I}\text{-}NO^{+}]$ was suggested by Wayland.[22] Subsequent amine deprotonation and migration of NO^+ to the coordinated amide would result into the nitrosoamine.

Recently, with $[Cu^{II}(tren)(CH_3CN)]^{2+}$, $[Cu^{II}(taea)(CH_3CN)]^{2+}$, $[Cu^{II}(tiaea)(CH_3CN)]^{2+}$, $[Cu(pymea)_2]^{2+}$ and $[Cu(baea)(CH_3CN)]^{2+}$ [tren = *tris*-(2-aminoethyl)amine; taea = *tris*-(2-ethylaminoethyl)amine; tiaea = *tris*-(2-isopropylaminoethyl)amine; pymea = pyridine-2-methylamine and baea = *bis*-(2-aminoethyl)amine], the reduction of Cu(II) center by NO was found to proceed through the formation of a thermally unstable $[Cu^{II}\text{-}NO]$ intermediate.[23] However, in the reaction of Cu(II) complexes of ppmea and mimpea [ppmea, 2-(pyridin-2-yl)-N-((pyridin-2-yl)methyl)ethaneamine; mimpea,

N-((methyl-1H-imidazol-2-yl)methyl)-2-(pyridine-2-yl)ethanamine], with NO, the formation of an [Cu^{II}–NO] complex has not been observed prior to the reduction.[24] This is attributed to the much lower values of the equilibrium constants, K_{NO} (equation 2.2) as reported earlier in case of $[Cu(dmp)_2(X)]^{2+}$.[19]

$$[(L)_2Cu^{II}]^{2+} + NO \underset{}{\overset{K_{NO}}{\rightleftharpoons}} [(L)_2Cu^{II}(NO)]^{2+} \quad \text{--------- (2.2)}$$

In addition, in case of $[Cu(mtad)]^{2+}$ [mtad = 5,5,7,12,12,14-hexamethyl-1,4,8,11-tetraazacyclotetradecane], the reduction takes place in methanol medium in presence of NaOMe through a deprotonation pathway as reported earlier in case of $[Cu(DAC)]^{2+}$.[25] However, $[Cu(tmd)_2]^{2+}$, tmd = 5,5,7-trimethyl-[1,4]-diazepane], facile reduction was observed in dry acetonitrile through a [Cu^{II}-NO] intermediate. Hence, the ligand frameworks definitely have a significant role in controlling the mechanistic pathway for the reduction of Cu(II) by NO. In this context, two Cu(II) complexes with ligands $\mathbf{L_1}$ and $\mathbf{L_2}$ [$\mathbf{L_1}$ = propane-1,3-diamine ; $\mathbf{L_2}$ = N-isopropylpropane-1,3-diamine] (Figure 2.1) have been prepared and their interactions with NO have been studied.

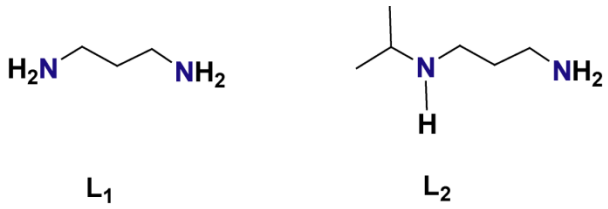

Figure 2.1 Ligands used for the present study.

2.2 Experimental Section

2.2.1 General

All reagents and solvents of reagent grade were purchased from commercial sources and used as received except specified. Acetonitrile was distilled from calcium hydride. Deoxygenation of the solvent and solutions was effected by repeated vacuum/purge cycles or bubbling with nitrogen for 30 minutes. NO gas was purified by passing it through a KOH and P_2O_5 column. UV-visible spectra were recorded on a Perkin Elmer Lambda 25 UV-visible spectrophotometer. FT-IR spectra of the solid samples were taken on a Perkin Elmer spectrophotometer with samples either prepared as KBr pellets or in solution in sodium chloride cell. Solution electrical conductivity was measured using a Systronic 305 conductivity bridge. ^{1}H-NMR spectra were recorded in a 400 MHz Varian FT spectrometer. Chemical shifts (ppm) were referenced either with an internal standard (Me_4Si) or to the residual solvent peaks. The X-band Electron Paramagnetic Resonance (EPR) spectra were recorded on a JES-FA200 ESR spectrometer, at room temperature and 77 K with microwave power, 0.998 mW; microwave frequency, 9.14

GHz and modulation amplitude, 2. Elemental analyses were obtained from a Perkin Elmer Series II Analyzer. The magnetic moment of complexes was measured on a Cambridge Magnetic Balance. Single crystals were grown by slow diffusion followed by slow evaporation technique. The intensity data were collected using a Bruker SMART APEX-II CCD Difractometer, equipped with a fine focus 1.75 kW sealed tube MoK_{α} radiation (λ = 0.71073 Å) at 273(3) K, with increasing ω (width of 0.3° per frame) at a scan speed of 3 s/frame. The SMART software was used for data acquisition. Data integration and reduction were undertaken with SAINT and XPREP software.[26] Multi-scan empirical absorption corrections were applied to the data using the program SADABS.[27] Structures were solved by direct methods using SHELXS-97 and refined with full-matrix least squares on F^2 using SHELXL-97.[28] All non-hydrogen atoms were refined anisotropically. Structural illustrations have been drawn with ORTEP-3 for Windows.[29]

2.2.2 Synthesis of L_1

Propane-1, 3-diamine (**L_1**) was purchased from commercial source.

2.2.3 Synthesis of L_2

Propane-1, 3-diamine (740 mg) was allowed to react with acetone (580 mg) at - 40 °C for 5 h and then temperature was elevated to room temperature to result in the formation of

corresponding imine. It was then reduced by using 2.1 equivalent of $NaBH_4$ in methanol (Scheme 2.1). Yield: 986 mg (~85%). Elemental analyses: calcd. (%): C, 62.01; H, 13.88; N, 24.11; found (%): C, 62.11; H, 13.78; N, 24.14. FT-IR (in KBr): 3420, 2829, 1648, 1568, 1474, 1325 and 1037 cm^{-1}. ^{1}H-NMR: (400 MHz, $CDCl_3$): δ_{ppm}: 2.59-2.52 (3H, m), 2.45 (2H, t), 1.81 (2H, s), 1.44 (2H, m) and 0.85 (6H, d). ^{13}C-NMR: (100 MHz, $CDCl_3$) δ_{ppm}: 48.6, 45.0, 40.2, 33.7 and 22.6. Mass ($M+H^+$)/z: calcd: 117.1313; found: 117.1445.

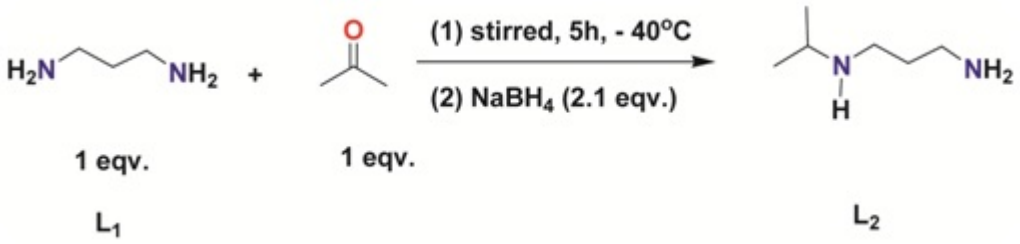

Scheme 2.1

2.2.4 Synthesis of complex 2.1

To a stirring solution of copper(II) perchlorate, hexahydrate; $Cu(ClO_4)_2 \cdot 6H_2O$ (0.741 g, 2 mmol) in 15 ml methanol, solution of ligand **L_1** (0.296 g, 4 mmol) in 10 ml methanol was added drop wise. The reaction mixture was allowed to stir for 2 h at room temperature. The blue solid precipitate of complex **2.1** was filtered and dried in vacuum. Yield: 0.660 g (~80%).

UV-vis. (methanol): λ_{max}, 552 nm (ε, 245 M^{-1} cm^{-1}), (acetonitrile): λ_{max}, 570 nm (ε, 152 M^{-1} cm^{-1}). FT-IR (KBr pellet): 3211, 1587, 1141, 1112, 1087 and 496 cm^{-1}. EPR data (in acetonitrile at 77 K): $g_{\|}$, 2.334, $g_{\perp}$, 2.013 and $A_{\|}$, 203×10^{-4} cm^{-1}. The complex **2.1** behaves as 1:2 electrolyte in methanol solution [Λ_M (S cm^{-1}), 270]. The observed magnetic moment is 1.64 BM.

2.2.5 Synthesis of complex 2.2

To a stirred solution of $Cu(ClO_4)_2{\cdot}6H_2O$ (0.741 g, 2 mmol) in 15 ml methanol was added a solution of ligand $\mathbf{L_2}$ (0.464 g, 4 mmol) in 10 ml methanol. The reaction mixture was allowed to stirr for 2 h at room temperature. Complex **2.2** appears as a shining blue solid precipitate after which it was filtered and dried. Yield: 0.690 g (~70%). UV-vis. (methanol): λ_{max}, 598 nm (ε, 248 M^{-1} cm^{-1}), (acetonitrile): λ_{max}, 579 nm (ε, 156 M^{-1} cm^{-1}). FT-IR (KBr pellet): 3307, 3263, 1590, 1092, 1045, 1014 and 623 cm^{-1}. EPR data (in acetonitrile at 77 K): $g_{\|}$, 2.302, $g_{\perp}$, 2.010 and $A_{\|}$, 198×10^{-4} cm^{-1} The complex **2.2** behaves as 1:2 electrolyte in methanol solution [Λ_M (S cm^{-1}), 265]. The observed magnetic moment is found to be 1.60 BM.

2.2.6 Isolation of modified ligand L_1'

To 30 ml of degassed acetonitrile solution of complex **2.1** (410 mg), freshly prepared NO was bubbled. The blue color of the solution turned green and finally becomes colorless. The reaction mixture was opened to air and stirred for 2 h. The volume was reduced to 5 ml and a saturated solution of Na_2S was added to ensure complete precipitation of copper ions. The precipitate was filtered and 50 ml of water was added. The organic part was extracted using chloroform (25 ml × 3 portions). The collected organic solution was dried over vacuum and subjected to column chromatography using silica gel to get the pure $\mathbf{L_1}'$. Yield: 70 mg (~55%). Elemental analyses: calcd. (%) C, 54.92; H, 13.06; N, 32.02; found (%): C, 54.91; H, 13.09; N, 32.07. FT-IR (in KBr pellet): 3427, 2943, 1641, 1493, 1492 and 694 cm^{-1}. ^{1}H-NMR: (400 MHz, $CDCl_3$): δ_{ppm}: 4.26 (4H, b s), 2.54-2.51 (4H, t), 2.45-2.42 (4H, t), 1.45-1.38 (4H, m) and 0.914 (1H, b s). ^{13}C-NMR: (100 MHz, $CDCl_3$): δ_{ppm}: 47.6, 40.1 and 33.4. Mass $(M+H^+)/z$: calcd: 132.1422, found: 132.0756.

2.2.7 Isolation of modified ligand $\mathbf{L_2}'$

Complex **2.2** (495 mg) was dissolved in degassed acetonitrile (20 ml). To this NO gas was purged till the blue color of the solution changed to colorless through an intermediate green color. The solution was allowed to stand for ½ h. The excess NO was removed by applying vacuum and purging argon. The volume of the solution was reduced to ~ 2 ml. To this saturated aqueous solution of Na_2S was added and the mixture was stirred for ½ h. The black precipitate thus appeared was filtered out. To the filtrate 20 ml of water was added. Few drops of acetic

acid were added to neutralize the solution and then the organic part was extracted with chloroform (3 portions × 25 ml). Extracted organic portion was dried under vacuum and purified by column chromatography to obtain pure $\mathbf{L_2}'$. Yield: 95 mg (~80%). Elemental analyses: calcd. (%) C, 49.63; H, 10.41; N, 28.94; found (%): C, 49.61; H, 10.39; N, 28.95. FT-IR (in KBr pellet): 3418, 2930, 1564, 1386, 910 and 734 cm^{-1}. ^{1}H-NMR: (400 MHz, $CDCl_3$): δ_{ppm}: 4.63-4.58 (1H, m), 3.56-3.53 (2H, t), 2.67-2.64 (2H, t), 2.12 (2H, b s), 1.66-1.59 (2H, m) and 1.44-1.42 (6H, d). ^{13}C-NMR: (100 MHz, $CDCl_3$): δ_{ppm}: 55.5, 40.3, 39.6, 30.3 and 21.7. Mass $(M+H^+)/z$: calcd: 146.1215, found: 146.1279.

2.3 Results and discussion

Ligand $\mathbf{L_1}$ was procured from Sigma Aldrich and used as received. $\mathbf{L_2}$ was synthesized from the reaction of $\mathbf{L_1}$ with acetone followed by the reduction with $NaBH_4$ (experimental section). The elemental analyses of $\mathbf{L_2}$ showed good agreement with the calculated values (experimental section). It was further characterized by ^{1}H-NMR, ^{13}C-NMR, Mass spectroscopy (experimental section). Complexes **2.1** and **2.2** were synthesized by the reaction of copper(II) perchlorate hexahydrate with the respective ligands in 1:2 ratio (experimental section and scheme 2.2). Both the complexes were isolated as solid. They displayed satisfactory elemental analyses (experimental section). Further characterization of the complexes has been done using various spectroscopic methods (experimental section and appendix I). The formation of the complexes is authenticated by their X-ray single crystal structure determination. Perspective

ORTEP views are shown in figure 2.2. Crystallographic data, important bond angles and distances are listed in tables 2.1, 2.2 and 2.3, respectively.

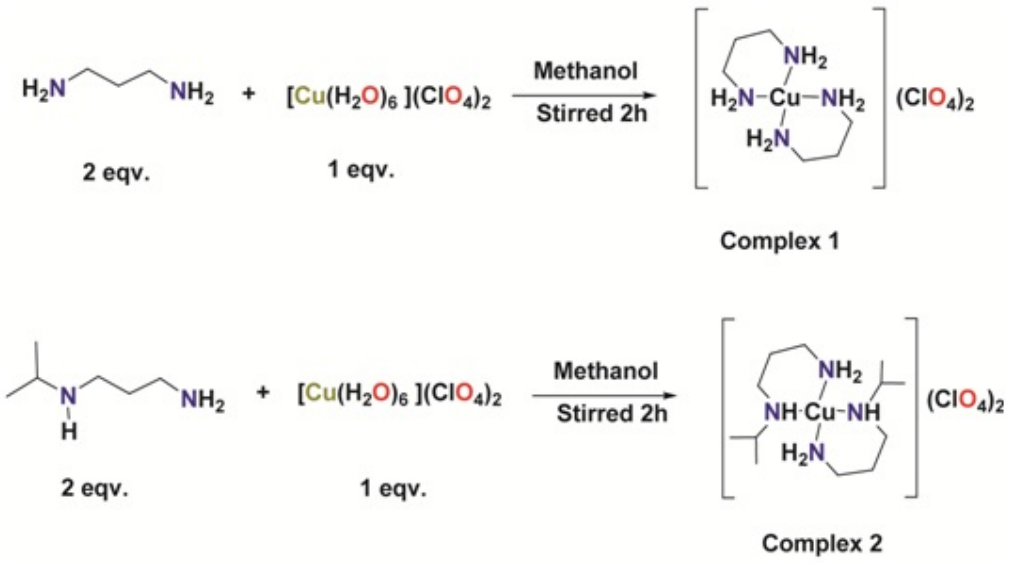

Scheme 2.2

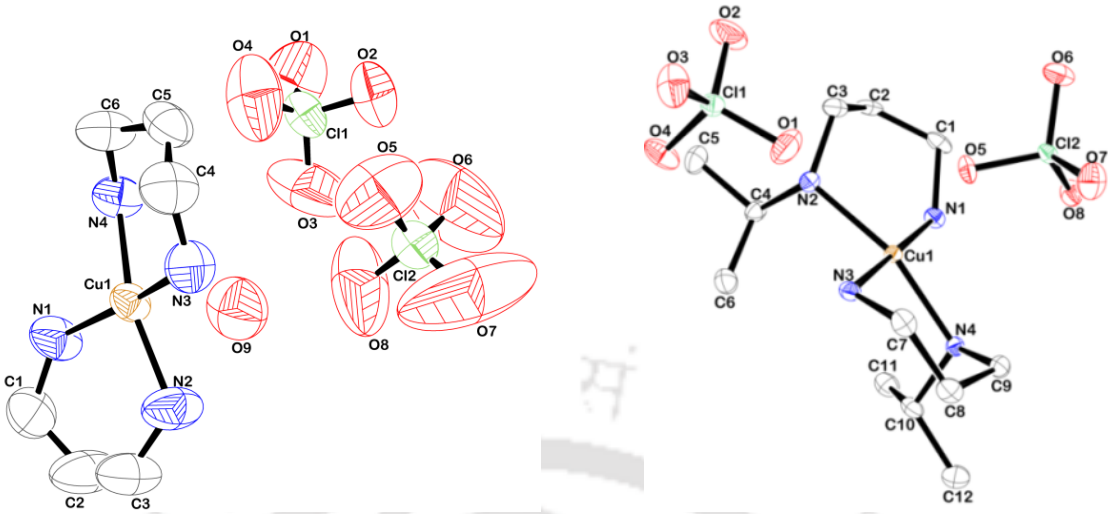

(a) **(b)**

Figure 2.2 ORTEP diagram of complexes (a) **2.1** and (b) **2.2** (50% thermal ellipsoid plot, hydrogen atoms are omitted for clarity).

Table 2.1 Crystallographic data for complexes **2.1** and **2.2**

	Complex **2.1**	Complex **2.2**
Formulae	$C_6 H_{22} Cl_2 Cu N_4 O_9$	$C_{12} H_{32} Cl_2 Cu N_4 O_8$
Mol. wt.	428.72	494.86
Crystal system	Monoclinic	Monoclinic
Space group	P2(1)/c	P2(1)/c
Temperature /K	296(2)	296(2)

Wavelength /Å	0.71073	0.71073
a /Å	7.8579(5)	11.0304(4)
b /Å	14.3068(8)	15.0381(6)
c /Å	14.8942(9)	12.5819(6)
α/°	90.00	90.00
β/°	99.841(3)	104.402(5)
γ/°	90.00	90.00
V/ Å^3	1649.79(17)	2021.45(15)
Z	4	4
Density/Mgm^{-3}	1.726	1.626
Abs. co-eff. /mm^{-1}	1.695	1.392
Abs. correction	none	multi-scan
F(000)	884	1036
Total no. of reflections	2840	3550
Reflections, $I > 2\sigma(I)$	2114	2983
Max. 2θ/°	25.00	24.99
Ranges (h, k, l)	-8≤h ≤8 -17≤ k ≤16 -17≤ l ≤ 17	-13≤h ≤10 -16≤ k ≤17 -12≤ l ≤ 14
Complete to 2θ (%)	97.7	99.9
Refinement method	Full-matrix least-squares on F^2	Full-matrix least-squares on F^2
Goof (F^2)	1.097	0.667
R indices [$I > 2\sigma(I)$]	0.0798	0.0335
R indices (all data)	0.0936	0.0439

Table 2.2 Selected bond length (Å) of complexes **2.1** and **2.2**

Complex **2.1**	Bond length (Å)	Complex **2.2**	Bond length (Å)
Cu1 - N3	2.020(6)	Cu1 - O1	2.398(2)
Cu1 - N1	1.995(6)	Cu1 - N1	2.036(3)
Cu1 - N2	2.020(5)	Cu1 - N3	2.047(2)
Cu1 - N4	2.005(7)	Cu1 - N4	2.052(2)
Cu1 - O9	2.576(8)	Cu1 - N2	2.050(2)
Cu1 - O4	2.640(1)	N1 - C1	1.491(4)
N3 - C4	1.410(1)	N3 - C7	1.491(5)
N1 - C1	1.497(9)	N4 - C10	1.503(4)
N2 - C3	1.484(8)	N4 - C9	1.504(5)
C2 - C1	1.460(1)	N2 - C4	1.506(4)
C2 - C3	1.490(1)	N2 - C3	1.496(4)

C4 - C5	1.440(1)	C4 - C6	1.523(4)
C6 - C5	1.460(1)	C4 - C5	1.521(5)
C6 - N4	1.430(1)	C8 - C7	1.515(4)

Table 2.3 Selected bond angles (°) of complexes **2.1** and **2.2**

Complex **2.1**	Bond angle (°)	Complex **2.2**	Bond angle (°)
N3 - Cu1 - N1	88.4(3)	O1- Cu1-N1	84.8(1)
N3 - Cu1 - N2	161.9(3)	O1- Cu1-N3	93.37(9)
N3 - Cu1 - N4	92.5(3)	O1- Cu1-N4	93.50(9)
N3 - Cu1 - O9	77.3(3)	O1- Cu1-N2	103.99(9)
N3 - Cu1 - O4	106.5(4)	N1- Cu1-N3	178.1(1)
N1 - Cu1 - N2	92.7(2)	N1- Cu1-N4	90.4(1)
N1 - Cu1 - N4	167.3(3)	N1- Cu1-N2	89.3(1)
N1 - Cu1 - O9	98.7(3)	N3- Cu1-N4	89.6(1)
N1 - Cu1 - O4	84.9(4)	N3- Cu1-N2	91.2(1)
N2 - Cu1 - N4	90.4(2)	N4- Cu1-N2	162.4(1)
N2 - Cu1 - O9	84.7(2)	O2- Cl1-O3	109.0(1)
N4 - Cu1 - O4	82.7(4)	Cu1-N1- C1	119.3(2)
O9 - Cu1 - O4	174.9(4)	Cu1-N4-C10	111.3(2)
Cu1 - N4 - C6	124.1(5)	Cu1-N4-C9	112.9(2)
N2 - Cu1 - O4	91.6(4)	Cu1-N2-C4	111.9(2)
N4 - Cu1 - O9	93.8(3)	Cu1-N2- C3	113.5(2)

In both the complexes, Cu(II) center is surrounded by four N-atoms, two from each of the ligand unit in an overall distorted square planar geometry. The Cu-$O_{(perchlorate)}$ distances are 2.642 Å and 2.398 Å, respectively for complexes **2.1** and **2.2**; which are little more than the bonding distances.[23, 30] Average Cu-N distances in complexes **2.1** and **2.2** are 2.020 Å and 2.050 Å, respectively. These are within the range in other reported complexes. [23, 30]

In acetonitrile solution, complexes **2.1** and **2.2** displayed absorption at 570 nm and 579 nm in the visible region which are attributed to the *d-d* transitions. The small shift in λ_{max} in case of

complex **2.2** compared to **2.1** is attributed to the increasing covalent character of σ-bond on moving from H to isopropyl group at N-substitution.[31] Both the complexes exhibited axial EPR spectra at 77 K corresponding to the square planar Cu(II) complexes with (experimental section and appendix I).[32]

2.3.1 Nitric oxide reactivity

To a dry and degassed acetonitrile solution of complex **2.1**, addition of NO gas resulted in a green intermediate. In UV-visible study, a shift of λ_{max} of the *d-d* transition from 570 nm to 615 nm was observed immediately after purging NO in acetonitrile solution of complex **2.1** (Figure 2.3). This new band is assigned as the *d-d* band of corresponding [Cu^{II}-NO] intermediate complex. In acetonitrile solution, [Cu^{II}-NO] intermediate of $[Cu(tiaea)(CH_3CN)]^{2+}$ and $[Cu(teaea)(CH_3CN)]^{2+}$ [tiaea = *tris*(2-isopropylaminoethyl)amine and teaea = *tris*(2-ethylaminoethyl)amine], displayed *d-d* transition at 640 nm and 605 nm, respectively.[23] In cases of $[Cu(amepy)_2]^{2+}$ and $[Cu(aeta)_2]^{2+}$ [amepy = 2-aminomethyl pyridine; aeta = *bis*-(2-aminoethyl)amine], the *d-d* band appeared at 660 nm and 595 nm, respectively.[23] The intensity of this absorption band diminished with time suggesting the reduction of Cu(II) center to Cu(I) following pseudo-first order kinetics (Figure 2.3, inset). The rate constant was calculated to be 1.028×10^{-2} s^{-1}at 298 K. The λ_{max} of the *d-d* transition of complex **2.2** was shifted from 579 nm to 608 nm in presence of NO in acetonitrile solvent

suggesting the formation of [Cu^{II}-NO] intermediate (Figure 2.4). The rate constant for the reduction of Cu(II) to Cu(I) in this case was 1.099×10^{-3} s^{-1}at 298 K (Figure 2.4, inset).

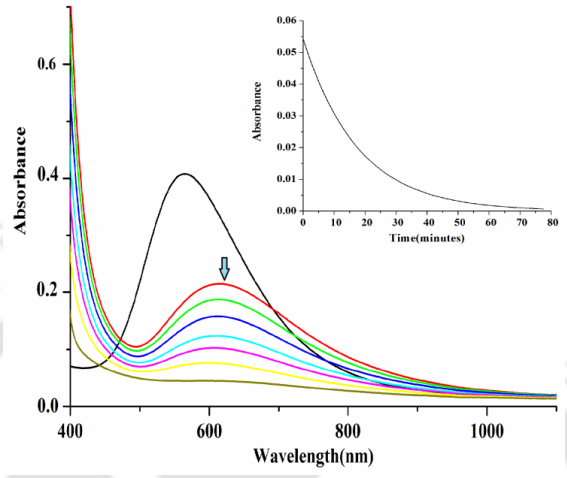

Figure 2.3 UV-visible spectra of complex **2.1** before (black trace) and after purging NO in acetonitrile.

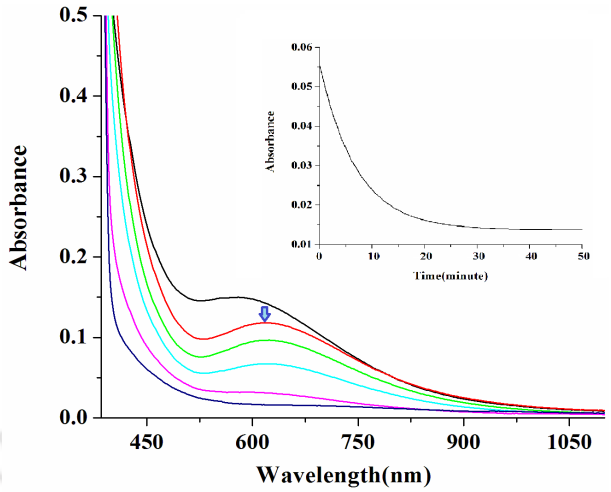

Figure 2.4 UV-visible spectra of complex **2.2** before (black trace) and after purging NO in acetonitrile.

The faster rate of decomposition of the intermediate in case of complex **2.2** compared to **2.1** is attributed to the presence of electron donating isopropyl group in $\mathbf{L_2}$. In case of $[Cu(tiaea)(CH_3CN)]^{2+}$ and $[Cu(teaea)(CH_3CN)]^{2+}$, the order of rate constants was

$[Cu(tiaea)(CH_3CN)]^{2+}$ > $[Cu(teaea)(CH_3CN)]^{2+}$ at 298 K indicating the effect of bulk of N-alkyl group on the ligand framework.[23]

The *d-d* transition for corresponding $[Cu^{II}\text{-NO}]$ intermediate in case of $[Cu(amepy)_2]^{2+}$, $[Cu(aeta)_2]^{2+}$, $[Cu(tiaea)\text{-}(CH_3CN)]^{2+}$ and $[Cu(teaea)(CH_3CN)]^{2+}$ appeared at 660, 595, 640 and 605 nm.[23] The difference in absorption band in the visible region of $[Cu^{II}\text{-NO}]$ for complexes **2.1** and **2.2** compared to $[Cu(amepy)_2]^{2+}$ is, presumably, because of the greater chelate ring size.

Although complexes **2.1** and **2.2** exhibit characteristic EPR signals in acetonitrile solvent; the respective intermediates formed in their reaction with NO were EPR silent at 298 K owing to the anti-ferromagnetic coupling of the paramagnetic Cu(II) center with NO (Figure 2.5 and appendix I). Further, complete reduction of Cu(II) center by NO also results in EPR silent Cu(I) solution; however, the presence of the *d-d* band of the intermediate complexes indicates the existence of $[Cu^{II}\text{-NO}]$ rather than Cu(I). It should be noted that structurally characterized $[Cu(CH_3NO_2)_5(NO)][PF_6]_2$ complex was reported as EPR silent.[33]

Further support of the formation of the $[Cu^{II}\text{-NO}]$ intermediate came from the solution FT-IR studies. Complexes **2.1** and **2.2** in acetonitrile solution displayed the formation of new stretching bands at ~1638 and 1635 cm^{-1}, respectively, after their reaction with NO (Figure 2.6 and appendix I). These are attributed to the stretching frequencies of NO coordinated to Cu(II)

centers. The intensity of these bands diminished with time indicating unstable nature of the intermediates. For $[Cu(tren)(CH_3CN)]^{2+}$ [tren = N,N-*bis*(2-aminoethyl)ethane-1,2-diamine],

ν_{NO} stretching appeared at 1650 cm^{-1} in acetonitrile.[23] On the other hand, the ν_{NO} frequency appears at 1642 and 1635 cm^{-1} in cases of $[Cu(amepy)_2]^{2+}$ and $[Cu(aeta)_2]^{2+}$, respectively, in acetonitrile.[23]

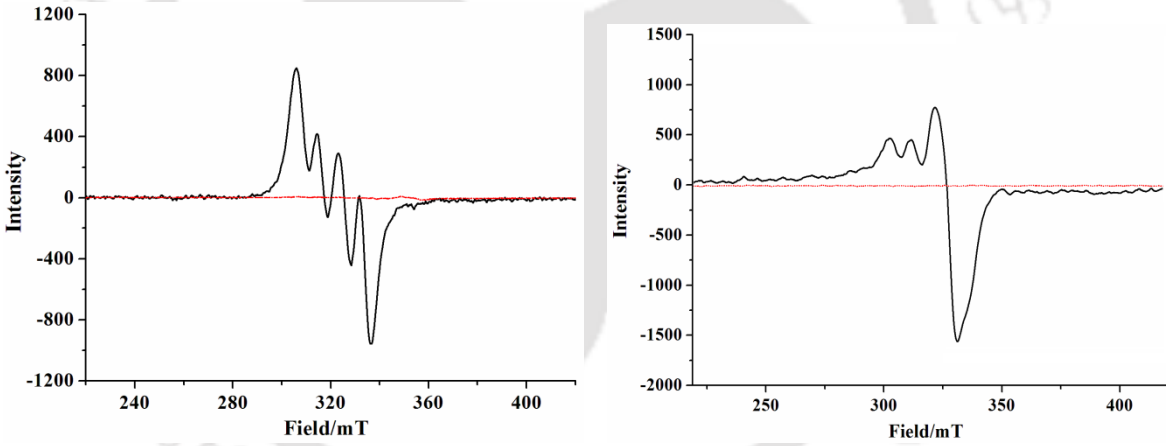

(a) **(b)**

Figure 2.5 X-Band EPR spectra of complexes **2.1** (a) and **2.2** (b) before (black trace) and after purging NO (red trace) in acetonitrile at room temperature.

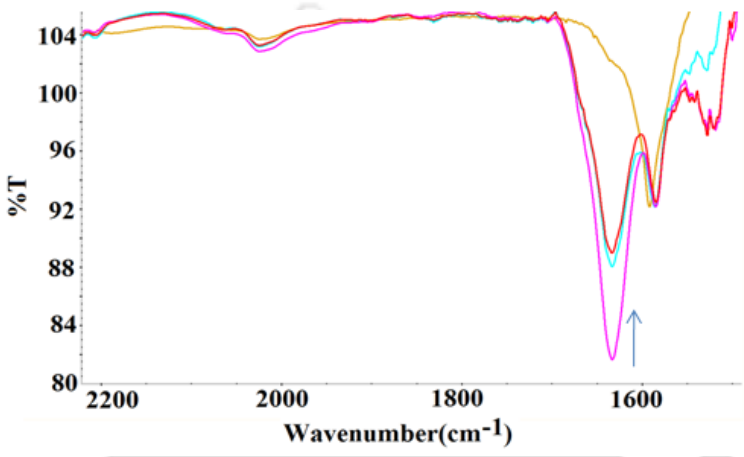

Figure 2.6 FT-IR spectra of complex **2.1** after purging NO (pink trace) and gradual decay of the intensity of the peak at 1638 cm^{-1} in acetonitrile at room temperature.

For $[Cu(CH_3NO_2)_5(NO)][PF_6]_2$, it appear at 1933 cm^{-1} in nujol mull. This higher ν_{NO} frequency in case of $[Cu(CH_3NO_2)_5(NO)][PF_6]_2$ can be attribute to the combined effect of

nature of ancillary ligands attached to the metal center and bent geometry [Cu1-N1-O1 ~ 121.0(3)°] of the nitrosyl ligand at an equatorial site.[33]

The reduction of Cu(II) center by NO in complex **2.1** was associated with concomitant diazotization of the primary amine center of the ligand which resulted into the formation of $\mathbf{L_1}'$ (Scheme 2.3). The diazotization of primary amines during the reduction of Cu(II) by NO was observed earlier also.[23, 30]

However, N-nitrosation at the ligand framework was observed in case of complex **2** under similar reaction condition (Scheme 2.4). This is attributed to the better nucleophilic character of secondary amine compared to the primary one.

(2.1)

Scheme 2.3

(2.2)

Scheme 2.4

The organic products were isolated and characterized by the regular spectroscopic studies.

2.4 Conclusion

In conclusion, the reactivity of NO with two Cu(II) complexes in acetonitrile has been studied. The formation of unstable [Cu^{II}-NO] intermediate prior to the reduction of Cu(II) was observed upon addition of NO in acetonitrile solution of the complexes. The stability of the [Cu^{II}-NO] intermediate formed depends on the chelate ring size and substitution present in the ligand frameworks. The reduction resulted into modification of the ligand through diazotization or N-nitrosation of the ligand frame works.

2.5 Reference

1. *Nitric Oxide: Biology and Pathobiology*, Ignarro, L. J. Ed.; Academic Press; San Diego, 2000.

2. (a) Moncada, S.; Palmer, R. M. J.; Higgs, E. A. *Pharmacol. Rev*. **1991**, *43*, 109. (b) Butler, A. R.; Williams, D. L. *Chem. Soc. Rev*. **1993**, 233. (c) *Methods in Nitric Oxide Research*; Feelisch, M.; Stamler, J. S. Eds.; John Wiley and Sons; Chichester, England, 1996.

3. (a) Jia, L.; Bonaventura, C.; Bonaventura, J.; Stamler, J. S. *Nature*, **1996**, *380*, 221. (b) Galdwin, M. T.; Lancaster Jr., J. R.; Freeman, B. A.; Schechter, A. N. *Nat. Med*. **2003**, *9*, 496.

4. (a) Ye, R. W.; Toro-Suarez, I.; Tiedje, J. M.; Averill, B. A. *J. Biol. Chem.* **1991**, *266*, 12848. (b) Hulse, C. L.; Averill, B. A.; Tiedje, J. M. *J. Am. Chem. Soc.* **1989**, *111*, 2322. (c) Jackson, M. A.; Tiedje, J. M.; Averill, B. A. *FEBS Lett.* **1991**, *291*, 41.

5. (a) Godden, J. W.; Turley, S.; Teller, D. C.; Adman, E. T.; Liu, M.Y.; Payne, W. J.; LeGall, J. *Science* **1991**, *153*, 438. (b) Adman, E. T.; Turley, S. in *Bioinorganic Chemistry of Copper;* Karlin, K. D.; Tyekllr, Z.; Eds., Chapman & Hall, Inc.: New York, 1993; pp 397. (c) Ferguson, S. J. *Curr. Opin. Chem. Biol.* **1998**, *2*, 182.

6. (a) Richardson, D. J.; Watmough, N. J. *Curr. Opin. Chem. Biol.* **1999**, *3*, 207. (b) Moura, I.; Moura, J. J. G. *Curr. Opin. Chem. Biol.* **2001**, *5*, 168. (c) Tocheva, E. I.; Rosell, F. I.; Mauk, A. G.; Murphy, M. E. P. *Biochem.* **2007**, *46*, 12366. (d) Zhou, X.; Espey, M. G.; Chen, J. X.; Hofseth, L. J.; Miranda, K. M.; Hussain, S. P.; Winks, D. A.; Harris, C. C. *J. Biol. Chem.* **2000**, *275*, 21241.

7. (a) Chien, J. C. W. *J. Am. Chem. Soc.* **1969**, *91*, 2166. (b) Wayland, B. B.; Olson, L. W. *J. Am. Chem. Soc.* **1974**, *96*, 6037. (c) Trofimova, N. S.; Safronov, A. Y.; Ikeda, O. *Inorg. Chem.* **2003**, *42*, 1945.

8. (a) Walker, F. A. *J. Inorg. Biochem.* **2005**, *99*, 216. (b) Rousseau, D. L.; Li, D.; Couture, M.; Yeh, S. R. *J. Inorg. Biochem.* **2005**, *99*, 306. (c) George, S. J.; Allen, J. W. A.; Ferguson, S. J.; Thorneley, R. N. F. *J. Biol. Chem.* **2000**, *275*, 33231.

9. (a) Pinakoulaki, E.; Gemeinhardt, S.; Saraste, M.; Varotsis, C. *J. Biol. Chem.* **2002**, *277*, 23407. (b) Praneeth, V. K. K.; Paulat, F.; Berto, T. C.; DeBeer George, S.; Nather, C.; Sulok, C.; Lehnert, N. *J. Am. Chem. Soc.* **2008**, *130*, 15288.

10. (a) Soldatova, A. V.; Ibrahim, M.; Olson, J. S.; Czernuszewicz, R. S.; Spiro, T. G. *J. Am. Chem. Soc.* **2010**, *132*, 4614. (b) Wasser, I. M.; de Vries, S.; Moe¨nne-Loccoz, P.; Schro¨der, I.; Karlin, K. D. *Chem. Rev.* **2002**, *102*, 1201.

11. (a) Hoshino, M.; Maeda, M.; Konishi, R.; Seki, H.; Ford, P. C. *J. Am. Chem. Soc.* **1996**, *118*, 5702. (b) Fernandez, B. O.; Lorkovic, I. M.; Ford, P. C. *Inorg. Chem.* **2004**, *43*, 5393. (c) Lehnert, N.; Praneeth, V. K. K.; Paulat, F. *J. Comput. Chem.* **2006**, *27*, 1338.

12. (a) Ellison, M. K.; Scheidt, W. R. *J. Am. Chem. Soc.* **1999**, *121*, 5210. (b) Linder, D. P.; Rodgers, K. R.; Banister, J.; Wyllie, G. R. A.; Ellison, M. K.; Scheidt, W. R. *J. Am. Chem. Soc.* **2004**, *126*, 14136.

13. (a) Lim, M. D.; Lorkovic, I. M.; Ford, P. C. *J. Inorg. Biochem.* **2005**, *99*, 151. (b) Shamir, D.; Zilbermann, I.; Maimon, E.; Gellerman, G.; Cohen, H.; Meyerstein, D. *Eur. J. Inorg. Chem.* **2007**, 5029.

14. (a) Torres, J.; Svistunenko, D.; Karlsson, B.; Cooper, C. E.; Wilson, M. T. *J. Am. Chem. Soc*. **2002**, *124*, 963. (b) Torres, J.; Cooper, C. E.; Wilson, M. T. *J. Biol. Chem*. **1998**, *273*, 8756. (c) Martin, C. T.; Morse, R. H.; Kanne, R. M.; Gray, H. B.; Malmstrom, B. G.; Chan, S. I. *Biochemistry*. **1981**, *20*, 5147.

15. Gorren, A. C. F.; Boer, de E.; Wever, R. *Biochem. Biophys. Acta.* **1987**, *916*, 38.

16. Tran, D.; Ford, P. C. *Inorg. Chem.* **1996**, *35,* 2411.

17. (a) Brown, G. C. *Biochim. Biophys. Acta.* **2001**, *1504*, 46. (b) Torres, J.; Sharpe, M. A.; Rosquist, A.; Cooper, C. E.; Wilson, M. T. *FEBS Lett.* **2000**, *475*, 263. (c) Wijma, H. J.; Canters, G. W.; Vries, de S.; Verbeet, M. P. *Biochem.* **2004**, *43*, 10467.

18. Tran, D.; Skelton, B. W.; White, A. H.; Laverman, L. E.; Ford, P. C. *Inorg. Chem*. **1998**, *37*, 2505.

19. Lim, M. D.; Capps, K. B.; Karpishin, T. B.; Ford, P. C. *Nitric Oxide, Biol. Chem.* **2005**, *12*, 244.

20. (a) Tsuge, K.; DeRosa, F.; Lim, M. D.; Ford, P. C. *J. Am. Chem. Soc*. **2004**, *126*, 6564. (b) Khin, C.; Lim, M. D.; Tsuge, K.; Iretskii, A.; Wu, G.; Ford, P. C. *Inorg. Chem.* **2007**, *46*, 9323.

21. Pell, S. D.; Armor, J. N. *J. Am. Chem. Soc.* **1973**, *95*, 7625.

22. (a) Wayland, B. B.; Olson, L. W. *Chem. Commun.* **1973**, 897. (b) Choi, I.-K.; Liu, Y.; Wei, Z.; Ryan, M. D. *Inorg. Chem.* **1997**, *36*, 3113.

23. (a) Sarma, M.; Singh, A.; Gupta, S. G.; Das, G.; Mondal, B. *Inorg. Chim. Acta*, **2010**, *363*, 63. (b) Sarma, M.; Kalita, A.; Kumar, P.; Singh, A.; Mondal, B. *J. Am. Chem. Soc.* **2010**, *132*, 7846. (c) Sarma, M.; Mondal, B. *Inorg. Chem*. **2011**, *50*, 3206.

24. Kumar, P.; Kalita, A.; Mondal, B. *Dalton Trans.* **2011**, *40*, 8656.

25. Kalita, A.; Kumar, P.; Deka, R. C.; Mondal, B. *Inorg. Chem.* **2011**, *50*, 11868.

26. SMART, SAINT and XPREP, Siemens Analytical X-ray Instruments Inc., Madison, Wisconsin, USA, 1995.

27. Sheldrick, G. M. SHELXS-97, University of Gottingen, Germany, 1997.

28. Farrugia, L. J. *J. Appl. Crystallogr.* **1997**, *30*, 565.

29. (a) Andzelm, J.; Koelmel, C.; Klamt, A. *J. Chem. Phys*, **1995**, *103*, 9312. (b) Delly, B. *J. Chem. Phys*. **1990**, *92*, 508.

30. (a) Sarma, M.; Mondal, B. *Dalton Trans.* **2012**, *41*, 2927. (b) Sarma, M.; Kumar, V.; Kalita, A.; Deka, R. C.; Mondal, B. *Dalton Trans.* **2012**, *41*, 9543.

31. Hiroshi, Y.; Taro, I. *Bull. Chem. Soc. Jap.* **1969**, *42*, 2187.

32. (a) Hathaway, B. J.; Tomlinson, A. A. G. *Coord. Chem. Rev.* **1970**, *5*, 1. (b) Hathway, B. J.; Billing, D. E.; Nicols, P.; Procter, I. M. *J. Chem. Soc. A*. **1969**, 312. (c) Hathway, B. J. in *Comprehensive Coordination Chemistry* eds. Wilkinson, G.; Gillard, R. D.; McCleverty, J. A. Pergamon, Oxford, 1987, Vol 5, pp 533-594. (d) Patra, A. K.; Ray, M.; Mukherjee, R. *Dalton Trans*. **1999**, 2461.

33. Wright, A. M.; Wu, G.; Hayton, T. W. *J. Am. Chem. Soc*. **2010**, *132*, 14336.

Chapter 3

Abstract

A Cu(II) complex, **3.1** of a *β*-diketiminate ligand, **L_3** {**L_3** = (4-(2,6-dimethylphenylimino)pentane-2ylidene)-2,6-dimethylbenzeneamine} has been synthesized and characterized. Single crystal X-ray structure reveals the presence of mononuclear Cu(II) unit with a distorted square planar geometry. In acetonitrile solution of the complex, the *β*-diketiminate ligand undergoes oxidative degradation to form the corresponding ketone di-imine under aerobic condition. Addition of NO to the acetonitrile solution of complex **3.1** affords the corresponding oxime di-imine ligand. All the modified ligands have been isolated and characterized.

3.1 Introduction

β-diketiminate derivatives with bulky aromatic group as N-substituents have attracted considerable research interest from coordination chemists.[1-3] These mono-anionic bidentate ligands are isoelectronic to cyclopentadienyl anions; their steric and electronic properties can easily be altered by switching to appropriate amine and diketone derivatives for synthesis.[4,5] They afford coordinatively unsaturated and stable mono-/ binuclear complexes of transition and lanthanide metal ions.[6,7] These complexes find extensive applications as catalysts as well as models for active sites of metallo-enzymes.[8-10]

In general, β-diketiminate frameworks, obtained from the reaction of acetylacetone with appropriate aniline derivative, are stable and allow the synthesis and characterization of a wide range of metal complexes.[11] However, examples of ligand modification during catalysis reactions are also known in some cases.[12-13] Itoh and coworkers demonstrated that *β*-diketiminate ligand with mesityl substituents at N-atom in Cu(II) complex in methanol solution undergoes easy oxidative transformation to the corresponding keto-diimine under aerobic condition.[14] When the reaction mixture was allowed to stand for few days, the crystals of Cu(II) complex of the corresponding hemiacetal derivative of the ketone diimine were obtained. However, the demetallation of this complex was reported to afford the corresponding ketone diimine. The similar reaction was reported with complexes of Zn(II), also.[15] In anaerobic condition, the reaction does not occur. The labelling experiment with $^{18}O_2$

confirmed the involvement of molecular oxygen. The reaction was proposed to proceed through the formation of bridged peroxo intermediate.[14] In spite, there has not been much study on the degradation of β-diketiminate ligand frameworks in presence of metal ions.

This reaction instigates to study the reactivity of Cu(II) complex of a β-diketiminate ligand, (**L_3**), with molecular oxygen and NO (Figure 3.1). The ligand undergoes oxidative degradation to the corresponding ketone di-imine, **$L_3^{/}$** in case of reaction with molecular oxygen and C-nitrosation during reaction with NO to afford corresponding oxime di-imine, **$L_3^{//}$**.

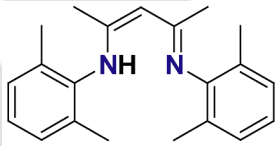

Figure 3.1 Ligand, **L_3**, used for the present study.

3.2 Experimental Section

3.2.1 General:

All reagents and solvents were purchased from commercial sources and were of reagent grade. Acetonitrile was distilled from calcium hydride. Deoxygenation of the solvent and solutions were effected by repeated vacuum/purge cycles or bubbling with Ar for 30 minutes. NO gas was purified by passing through KOH and P_2O_5 column. UV-visible spectra were recorded on a Perkin Elmer lamda 25 UV-visible spectrophotometer. FT-IR spectra were taken on a Perkin

Elmer spectrophotometer with either sample prepared as KBr pellets or in solution in a sodium chloride cell. Solution electrical conductivity was checked using a Systronic 305 conductivity bridge. ^{1}H-NMR spectra were obtained with a 400 MHz Varian FT- spectrometer. Chemical shifts (ppm) were referenced either with an internal standard (Me_4Si) for organic compounds or to the residual solvent peaks. The X-band Electron Paramagnetic Resonance (EPR) spectra of the complexes and of the reaction mixtures were recorded on a JES-FA200 ESR spectrometer. Elemental analyses were obtained from a Perkin Elmer Series II Analyzer. The magnetic moment of complexes are measured on a Cambridge Magnetic Balance.

Single crystals were grown by slow diffusion followed by slow evaporation technique. The intensity data were collected using a Bruker SMART APEX-II CCD diffractometer, equipped with a fine focus 1.75 kW sealed tube MoKα radiation (λ = 0.71073 Å) at 273(3) K, with increasing ω(width of 0.3° per frame) at a scan speed of 3 s/frame. The SMART software was used for data acquisition. Data integration and reduction were undertaken with SAINT and XPREP software.[15] Multi-scan empirical absorption corrections were applied to the data using the program SADABS.[16] Structures were solved by direct methods using SHELXS-97 and refined with full-matrix least squares on F^2 using SHELXL-97.[17] All non-hydrogen atoms were refined anisotropically. Structural illustrations have been drawn with ORTEP-3 for Windows.[18]

3.2.2 Synthesis of ligand L_3

The ligand **L_3** was synthesized by a reported procedure.[19] A mixture of 20.3 ml 2, 6-dimethylaniline (20 g, 0.17 mol), 8.5 ml 2, 4-pentanedione (8.25 g, 0.08 mol) and 14.2 g p-toluenesulphonic acid in 250 ml of dry toluene was refluxed for 24 h. The toluene was decanted, and to the solid residue, 200 ml diethyl ether, 150 ml water and 36 g $Na_2CO_3.10$ H_2O was added. After stirring for 25 min, the ether layer was separated, dried with $MgSO_4$, and the solvent was removed in vacuum. The residue was dried in vacuum at 100 °C for 6 h to remove any remaining free 2, 6-dimethylaniline, giving crystalline solid of **L_3**. Yield: 18.8 g (~74%). FT-IR (KBr pellet): 3009, 2918, 2852, 1625, 1551, 1487, 1465, 1432, 1376, 1278, 1181, 1090, 1024 and 767 cm^{-1}. ^{1}H-NMR: (600 MHz, $CDCl_3$): δ_{ppm}: 1.80 (6H, s), 2.28 (12H, s), 4.99 (1H, s), 7.04-7.06 (2H, t), 7.13-7.15 (4H, d) and 12.32 (1H, s). ^{13}C-NMR: (150 MHz, $CDCl_3$): δ_{ppm}: 18.5, 20.4, 93.6, 124.4, 127.9, 132.2, 143.9 and 160.9.

3.2.3 Synthesis of complex 3.1

Copper(II) acetate, dihydrate (0.997 g, 5 mmol) was dissolved in 10 ml of acetonitrile. To this chloroform solution (10 ml) of **L_3** (1.53 g, 5 mmol) was added slowly with constant stirring. The color of the solution turned into brown from green. The stirring was continued for 2 h at room temperature. The solution was dried in rotary evaporator to obtain a brown solid. The solid was then washed with distilled water and dried to get crystalline solid of complex **3.1**. Yield: 2.02 g (~80%). UV-vis. (acetonitrile): λ_{max}, 772 nm (ε, 55 M^{-1} cm^{-1}). X-band EPR (in

acetonitrile at 77 K): $g_{||}$, 2.189; $g_{\square}$, 2.056 and $A_{\|}$, 128×10^{-4} cm^{-1}. FT-IR (KBr pellet): 3016, 2975, 2919, 1556, 1529, 1470, 1393, 1261, 1182, 1024, 945, 859, 761, 692 and 609 cm^{-1}. Complex **3.1** behaves as non-electrolyte in acetonitrile solution. The calculated magnetic moment is found to be 1.57 BM.

3.2.4 Synthesis of complex 3.2

Complex **3.1** (100 mg) was dissolved in 20 ml acetonitrile in a round bottom flask. The solution was heated to 50 °C with constant stirring for 2 h under aerobic condition while the color of the solution changed to dark green. The reaction mixture was then cooled to room temperature and allowed to stand for 24 h to obtain green crystals of complex **3.2**. The crystals were filtered out and characterized. Yield, 53 mg (~80%). UV-vis. (acetonitrile): λ_{max}, 725 nm (ε, 158 M^{-1} cm^{-1}). FT-IR (KBr pellet): 3419, 2921, 1647, 1590, 1469, 1440, 1092, 1036 and 766 cm^{-1}.

3.2.5 Synthesis of complex 3.3

To a degassed acetonitrile (10 ml) solution of complex **3.1** (100 mg), NO was purged till the color of the solution changed to deep green from light brown. The solution was allowed to stand at room temperature for ½ h. The excess NO was removed by applying several cycles of vacuum followed by purging Ar. The volume of the solution was reduced to 2 ml and benzene (10 ml) was added to make a layer and kept in freezer for overnight. The complex **3.3** was obtained as green precipitate. It was filtered off and washed with diethylether. Yield, 80 mg

(~74%). UV-vis. (acetonitrile): λ_{max}, 640 nm (ε, 189 M^{-1} cm^{-1}). FT-IR (KBr pellet): 3444, 2921, 1627, 1566, 1470, 1439, 1335, 1198, 1094 and 768 cm^{-1}.

3.2.6 Isolation of ligand $L_3^{/}$

Complex **3.1** (300 mg) was dissolved in 20 ml acetonitrile in a round bottom flask. The solution was heated to 50 °C with constant stirring for 2 h under aerobic condition while the color of the solution changed to dark green. After cooling down to room temperature, the volume of the solution was reduced to 2 ml. To this, 5 ml saturated aqueous solution of Na_2S was added with constant stirring for ½ h. The black precipitate thus appeared was filtered off and the filtrate was diluted with 25 ml water. Then the organic part was extracted with chloroform (3 portions × 20 ml). The combined chloroform layer was dried and subjected to column chromatography to get $\mathbf{L_3^{/}}$. Yield, 135 mg (~60%). FT-IR (KBr pellet): 3419, 2922, 1705, 1675, 1593, 1471, 1440, 1366, 1208, 110, 1092 and 764 cm^{-1}. ^{1}H-NMR: (400 MHz, $CDCl_3$): δ_{ppm}: 1.94 (6H, s), 2.02 (12H, s), 5.00 (1H, s), 6.92-6.95 (2H, t) and 7.01-7.05 (4H, d). ESI-Mass $(M+H^+)/z$: calcd: 321.1889; found: 321.1934.

3.2.7 Isolation of modified ligand, $L_3^{//}$

Complex **3.1** (300 mg) was dissolved in acetonitrile (10 ml). To this, NO gas was purged till the color of the solution changed to deep green. The solution was allowed to stand for ½ h. The

excess NO was removed by applying vacuum and purging argon. The volume of the solution was reduced to ~ 1 ml. To this saturated aqueous solution of Na_2S was added and the mixture was stirred for ½ h. The black precipitate thus appeared was filtered out. To the filtrate 20 ml of water was added. Few drops of acetic acid were added to neutralize the solution and then the organic part was extracted with chloroform (3 portions × 25 ml). Extracted organic portion was dried under vacuum and pure $\mathbf{L_3}^{//}$ was obtained. Yield, 52 mg (~ 65%). FT-IR (KBr pellet): 3144, 3017, 2852, 1666, 1625, 1591, 1470, 1368, 1337, 1206, 1092, 1069, 1001, 830, 817, 771 and 764 cm^{-1}. ^{1}H-NMR: (600 MHz, $CDCl_3$): δ_{ppm}: 1.92 (3H, s), 1.96 (3H, s), 2.01(6H, s), 2.13 (6H, s), 6.90-6.95 (2H, m), 7.02-7.04 (4H, t) and 10.93 (1H, s). ^{13}C-NMR: (150 MHz, $CDCl_3$): δ_{ppm}: 16.2, 18.1, 18.5, 20.7, 123.3, 124.1, 125.2, 128.0 and 164.6. The X-ray quality single crystals were grown from the chloroform solution of the modified ligand, $\mathbf{L_3}^{//}$.

3.3 Results and discussion

The ligand $\mathbf{L_3}$ has been prepared by reacting acetylacetone with 2, 6-dimethyl aniline using a reported procedure.[19] The Cu(II) complex, **3.1** used for the present study has been prepared by stirring the free ligand with equivalent amount of Cu(II) acetate, dihydrate in acetonitrile at room temperature. Complex **3.1** was characterized by various spectroscopic techniques as well as by single crystal structure determination. The ORTEP diagram is shown in figure 3.2. The crystal structure reveals the mononuclear metal center with a distorted square planar geometry where the anionic *β*-diketiminate and acetate act as bidentate ligands. The crystallographic data,

important bond angles and distances are listed in tables 3.1, 3.2 and 3.3, respectively. The average Cu-N distance is 1.900 Å. C-N and C-C distances of the diketiminate framework are 1.340 Å and 1.387 Å, respectively. Average Cu-$O_{acetate}$ distance is 2.018 Å. In acetate, the C-O distance is 1.255 Å. The bite angle of the diketiminate ligand is 96.30°; whereas for acetate, this is 64.22°. For Cu(II) complex of the *β*-diketiminate ligand having mesityl substituents at N atom, the average Cu-N and Cu-O distances are 1.915 and 2.028 Å, respectively.[18]

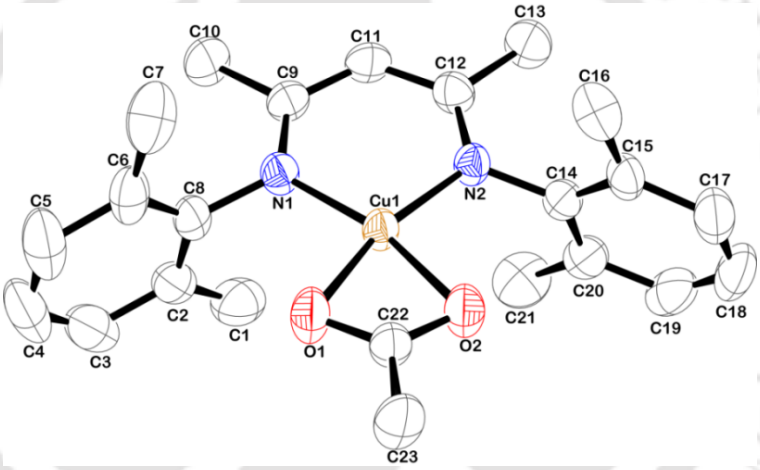

Figure 3.2 ORTEP diagram of complex **3.1** (50% thermal ellipsoid plot; H-atoms are removed for clarity).

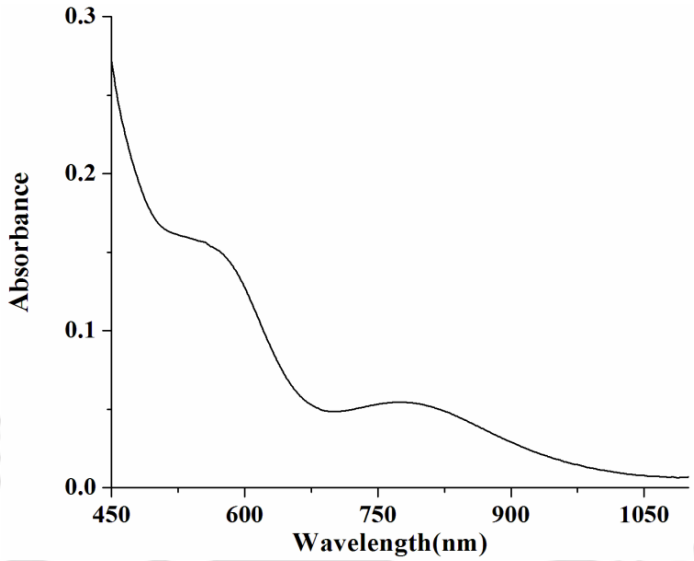

Figure 3.3 UV-visible spectrum of complex **3.1** in acetonitrile.

Complex **3.1** in acetonitrile solution absorbs at 772 nm and 559 nm in the visible spectrum (Figure 3.3) along with intra-ligand transitions in UV-range. In X-band EPR spectra, complex **3.1** displays four line spectrum characteristics to the square planar Cu(II) complexes with ground state (Figure 3.4).[20]

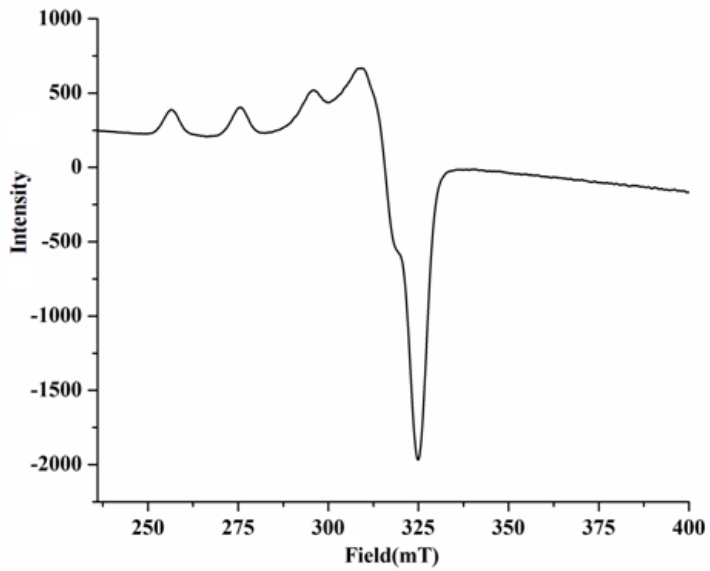

Figure 3.4 X-band EPR spectrum of complex **3.1** in acetonitrile at 77 K.

Complex **3.1** in acetonitrile solution when heated to 50 °C for 2 h under aerobic condition, the color of the solution changes to green from brown. The modified ketone di-imine ligand, $\mathbf{L_3}'$ was isolated quantitatively from the reaction mixture after removal of Cu(II) ion using aqueous

Na_2S (experimental section). $\mathbf{L_3}^{/}$ was characterized using various spectral analyses. We could not grow the X-ray quality crystals of it. However, when the crude reaction mixture was kept at room temperature, dark green crystals of complex **3.2** appeared. The ORTEP diagram of complex **3.2** is shown in figure 3.5. The crystal data and bond angles and distances are shown in tables 3.1, 3.2 and 3.3, respectively. The crystal structure reveals the heptanuclear structure of complex **3.2** and the formation of corresponding diol di-imine which actually dehydrates while demetallated to afford the ketone di-imine. PLATON/SQUEEZE was performed to refine the framework for complex **3.2** along with the water molecules in the crystal by excluding the disordered solvent electron densities.[21] These calculations amount to 601 electrons may be attributed to the water molecules.

Table 3.1 Crystallographic data for complexes **3.1**, **3.2** and $\mathbf{L_3}^{//}$.

	Complex **3.1**	Complex **3.2**	$\mathbf{L_3}^{//}$
formulas	$C_{23}H_{28}Cu_1N_2O_2$	$C_{77}H_{129}Cu_7N_7O_{38}$	$C_{21}H_{25}N_3O_1$
mol. wt.	428.01	2205.65	335.44
crystal system	Triclinic	Cubic	Mononclinic
space group	*P-1*	*P 21 3*	*I2/c*
temperature/K	296(2)	296(2)	296(2)
wavelength /Å	0.71073	0.71073	0.71073
a/Å	7.0615(3)	22.7589(3)	21.2119(14)
b/Å	12.4388(6)	22.7589(3)	7.8518(4)
c/Å	13.4851(8)	22.7589(3)	23.5414(15)
α/°	70.511(5)	90.00	90.00
β/°	83.469(4)	90.00	95.420(6)
γ/°	76.344(4)	90.00	90.00
V/Å^3	1084.26(10)	11788.3(2)	3903.3(4)
Z	2	4	8
density/Mg m^{-3}	1.311	1.243	1.142

abs. coeff /mm^{-1}	1.027	1.310	0.071
abs. correction	multi-scan	multi-scan	none
F(000)	450	4588	1440
total no. of reflections	3822	6992	3442
reflections, $I > 2\sigma(I)$	3330	5668	2194
Max. 2θ/deg	25.00	25.24	25.00
ranges (h, k, l)	$-8 \le h \le 8$ $-14 \le k \le 8$ $-16 \le l \le 15$	$-14 \le h \le 21$ $-10 \le k \le 27$ $-18 \le l \le 22$	$-24 \le h \le 25$ $-9 \le k \le 9$ $-27 \le l \le 27$
Complete to 2θ (%)	99.9	99.7	99.8
refinement method	full-matrix least-squares on F^2	full-matrix least-squares on F^2	full-matrix least-squares on F^2
GoF (F^2)	0.966	1.065	1.011
R indices [$I > 2\sigma(I)$]	0.0478	0.0648	0.0573
R indices (all data)	0.1357	0.1303	0.1615
Flack parameter	-	-0.010(19)	-

Table 3.2 Selected bond length (Å) of complexes **3.1**, **3.2** and $\mathbf{L_3^{//}}$.

Complex **3.1**	Bond length (Å)	Complex **3.2**	Bond length (Å)	$\mathbf{L_3^{//}}$	Bond length (Å)
Cu1-O2	2.015(2)	Cu2-O5	2.102(3)	O1-H1	0.819(2)
Cu1-O1	2.022(2)	Cu2-O6	2.108(4)	O1-N3	1.381(3)
Cu1-N1	1.899(3)	Cu1-O5	1.937(3)	N1-C9	1.267(3)
Cu1-N2	1.910(3)	Cu1-N1	2.001(4)	N1-C8	1.442(3)
O2-C22	1.254(5)	Cu1-O4	2.009(2)	N2-C12	1.281(3)
O1-C22	1.257(4)	Cu1-O2	1.964(4)	N2-C14	1.426(3)
N1-C8	1.443(5)	Cu1-O3	2.326(4)	N3-C11	1.279(3)
N1-C9	1.340(4)	Cu3-O6	1.945(3)	C9-C11	1.502(3)
N2-C14	1.434(3)	Cu3-N2	1.993(4)	C9-C10	1.492(4)
N2-C12	1.336(4)	Cu3-O7	1.977(2)	C11-C12	1.477(3)
C11-C12	1.394(5)	Cu3-O8	2.345(6)	C12-C13	1.495(4)

Table 3.3 Selected bond angles (°) of complexes **3.1**, **3.2** and $\mathbf{L_3^{//}}$.

Complex **3.1**	Bond angles (°)	Complex **3.2**	Bond angles (°)	$L_3^{//}$	Bond angles (°)
O2- Cu1-O1	64.2(1)	O6- Cu2-O5	154.6(1)	H1-O1-N3	109.5(2)
O2- Cu1-N1	164.0(1)	O5- Cu2-O6	65.8(1)	C9-N1-C8	120.6(2)
O2- Cu1-N2	99.7(1)	O5- Cu1-N1	82.7(2)	C12-N2-C14	120.3(2)
O1- Cu1-N1	99.7(1)	O5- Cu1-O4	92.1(1)	O1-N3-C11	112.4(2)
O1- Cu1-N2	163.8(1)	O5- Cu1-O2	170.1(2)	N1-C9-C11	117.1(2)
N1- Cu1-N2	96.3(1)	O5- Cu1-O3	94.6(2)	N1-C9-C10	126.7(2)
Cu1-O2-C22	89.3(2)	N1- Cu1-O4	158.7(1)	N3-C11-C9	124.4(2)
Cu1-O1-C22	89.0(2)	N1- Cu1-O2	93.0(2)	N3-C11-C12	117.2(2)
Cu1-N1-C8	116.7(2)	N1- Cu1-O3	103.0(2)	N2-C12-C11	115.4(2)
Cu1-N1-C9	123.8(2)	O4- Cu1-O2	88.8(1)	N2-C12-C13	125.8(2)
C8-N1-C9	119.5(3)	O4- Cu1-O3	98.0(1)	N1-C8-C6	121.4(2)
Cu1-N2-C14	116.9(2)	O2- Cu1-O3	95.0(2)	N1-C8-C2	116.8(2)
Cu1-N2-C12	123.4(2)	Cu2-O6- Cu3	108.8(2)	N2-C14-C20	119.7(2)
C14-N2-C12	119.7(2)	Cu2-O5- Cu1	110.3(2)	N2-C14-C15	118.6(2)

This oxidative transformation is similar to what Itoh et al was reported earlier with mesityl substuted β-diketiminate. The crystal structure of the Cu(II) complex with intermediate hemiacetal of the corresponding diketiminate was reported from methanol solution. Demetallation of this complex using aqueous ammonia afforded the ketone diimine. A similar ligand oxygenation reaction was reported in Co(II) complexes of tetraaza macrocyclic dibenzotetramethyltetraaza-[14]annulene dianion.[22]

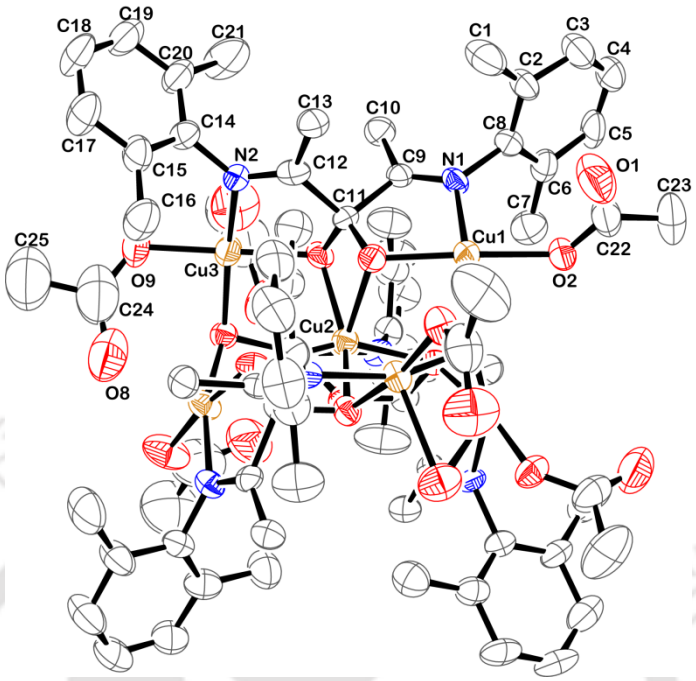

Figure 3.5 ORTEP diagram of complex **3.2** (50% thermal ellipsoid plot; H-atoms and solvent molecules are removed for clarity).

Addition of NO to the degassed acetonitrile solution of complex **3.1** resulted in color change

from brown to deep green through a transient intermediate step. The absorptions 559 nm and 772 nm are diminished and a new band at 580 nm appeared (Figure 3.6) for a short while suggesting the formation of the transient intermediate. This is presumably due to the formation of [Cu^{II}-NO] intermediate. The frozen reaction mixture appeared silent in X-band EPR as expected for a [Cu^{II}-NO] intermediate. FT-IR spectrum of the intermediate could not be recorded owing to its very less stability. The 580 nm absorption band diminished within few seconds and resulted in the appearance of an absorption band at 640 nm (Figure 3.6) which is attributed to the *d-d* transition of Cu(II) complex of modified oxime di-imine ligand, $\mathbf{L_3}^{//}$.

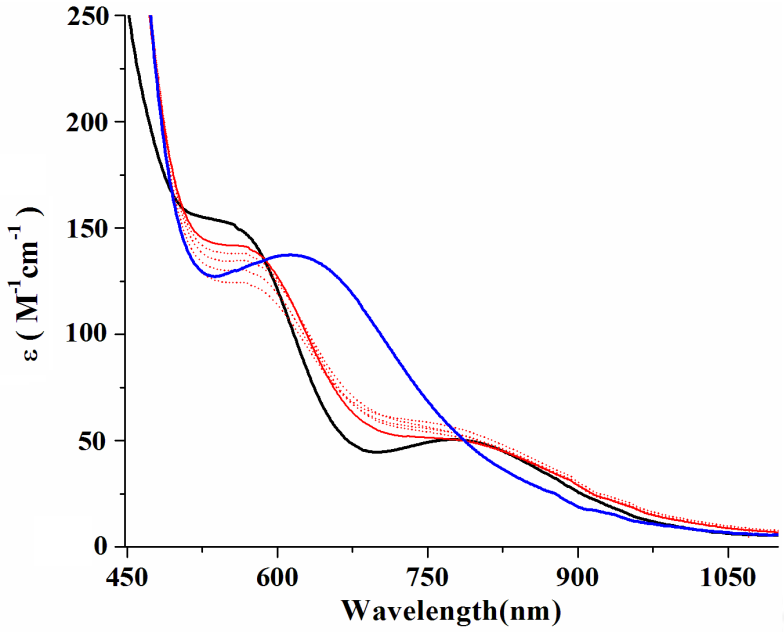

Figure 3.6 UV-visible spectra of complex **3.1** before (black trace) and after (red trace) purging NO in acetonitrile. Blue trace represents the final compound (complex **3.3**).

Complex **3.3** has been isolated as solid and characterized (experimental section and appendix II).

In FT-IR spectroscopy, complex **3.3** exhibits new stretching frequency at 1627 cm^{-1}. This band is assigned as the coordinated oxime stretching frequency (appendix II).[23]

Removal of Cu(II) ion from the solution of complex **3.3** afforded the corresponding modified oxime diimine ligand, $\mathbf{L_3}^{//}$. The formation of $\mathbf{L_3}^{//}$ has been confirmed by various spectral analyses as well as by X-ray single crystal structure determination. The ORTEP diagram of $\mathbf{L_3}^{//}$ is shown in figure 3.7. Crystallographic data, important bond distances and angles are listed in tables 3.1, 3.2 and 3.3, respectively. The $C\text{-}N_{imine}$ distances are 1.267 and 1.281 Å. $C\text{-}N_{oxime}$ distance is 1.279 Å and $N\text{-}O_{oxime}$ is 1.381 Å.

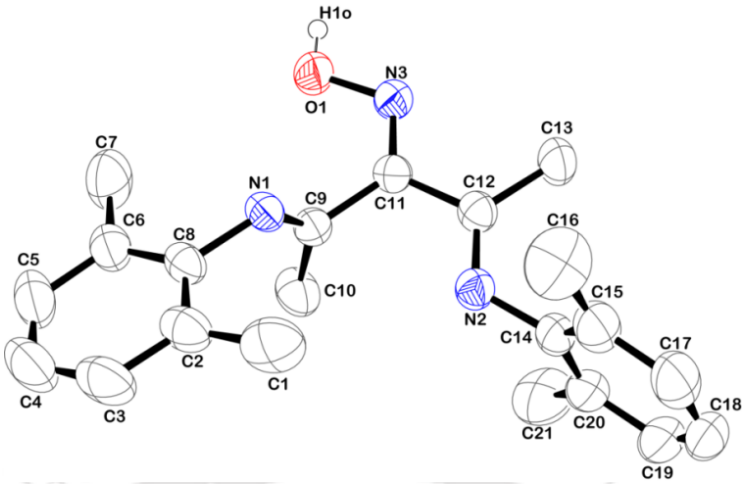

Figure 3.7 ORTEP diagram of the oxime di-imine, $\mathbf{L_3}^{//}$ (50% thermal ellipsoid plot; H-atoms are removed for clarity).

It should be noted that C-nitrosation does not occur while NO is purged to the acetonitrile solution of the free ligand. Though the detail mechanism of the C-nitrosation in the present case is not yet fully understood, presumably NO first binds to the metal center to form [Cu^{II}-NO] intermediate as indicated by UV-visible and EPR studies. In the next step, nucleophillic attack to N-atom of NO by the diketiminate ligand takes place with successive loss of proton resulting to the oxime di-imine moiety (Scheme 3.1).

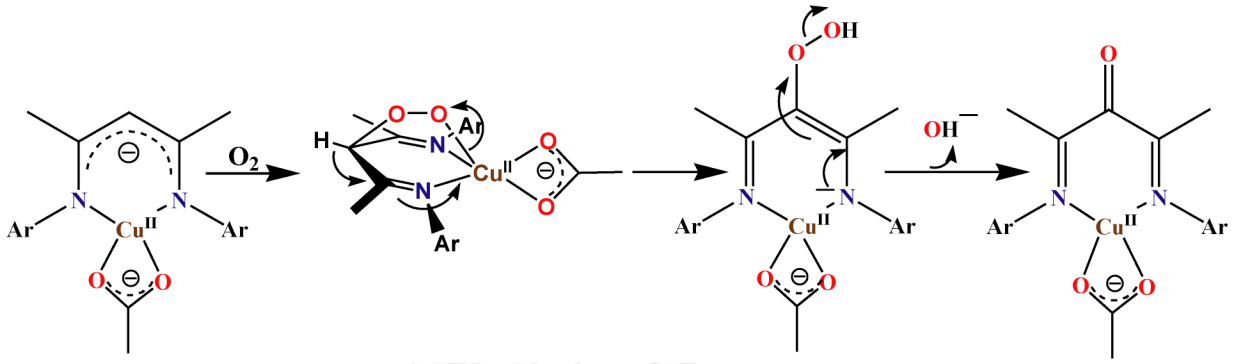

Scheme 3.1

3.4 Conclusion

In the Cu(II) complex, the *β*-diketiminate ligand, **L_3** undergoes oxidative degradation in acetonitrile solution under aerobic condition to afford corresponding ketone di-imine. The reaction possibly proceeds through a peroxo intermediate. On the other hand, addition of NO to the acetonitrile solution of complex **3.1** results in the C-nitrosation of the ligand framework and affords corresponding oxime di-imine. The modified ligands are isolated and characterized. The formation of the oxime di-imine is further supported by X-ray singe crystal structure determination. The reaction, presumably, proceeds through the formation of [Cu^{II}-NO] intermediate.

3.5 References

1. (a) Radzewich, C. E.; Coles, M. P. ; Jordan, R. F. *J. Am. Chem. Soc*. **1998**, *120*, 9384. (b) Radzewich, C. E.; Guzei, I. A.; Jordan, R. F. *J. Am. Chem. Soc*. **1999**, *121*, 8673. (c) Qian, B.; Scanlon, IV, W. J.; Smith, III, M. R. ; Motry, D. H. *Organometallics* **1999**, *18*, 1693.
2. (a) Kakaliou, L.; Scanlon, IV, W. J.; Qian, B.; Baek, S. W.; Smith, III, M. R.; Motry, D. H. *Inorg. Chem*. **1999**, *38*, 5964. (b) Gibson, V. C.; Segal, J. A.; White, A. J. P.; Williams, D. J. *J. Am. Chem. Soc.* **2000**, *122*, 7120. (c) Ding, Y.; Roesky, H. W.; Noltemeyer, M.; Schmidt, H. G.; Power, P. P. *Organometallics* **2001**, *20*, 1190.
3. (a) Gibson, V. C.; Maddox, P. J.; Newton, C.; Redshaw, C.; Solan, G. A.; White, A. J. P.; Williams, D. J. *Chem. Commun.* **1998**, 1651. (b) Vollmerhaus, R.; Rahim, M.; Tomaszewski, R.; Xin, S.; Taylor, N. J.; Collins, S. *Organometallics* **2000**, *19*, 2161. (c) Dove, A. P.; Gibson, V. C.; Marshall, E. L.; White, A. J. P.; Williams, D. J. *Chem. Commun.* **2001**, 283.
4. (a) Chamberlain, B. M.; Cheng, M.; Moore, D. R.; Ovitt, T. M.; Lobkovsky, E. B.; Coates, G. W. *J. Am. Chem. Soc.* **2001**, *123*, 3229. (b) Cheng, M.; Attygalle, A. B.; Lobkovsky, E. B.; Coates, G. W. *J. Am. Chem. Soc.* **1999**, *121*, 11583. (c) Cheng, M.; Lobkovsky, E. B.; Coates, G. W. *J. Am. Chem. Soc.* **1998**, *120*, 11018. (d) Ayers, A. E.; Klapotke, T. M.; Dias, H. V. R. *Inorg. Chem.* **2001**, *40*, 1000.
5. (a) Parks, J. E.; Holm, R. H. *Inorg. Chem*. **1968**, *7*, 1408. (b) Bailey, P. J.; Coxall, R. A.; Dick, C. M.; Fabre, S.; Parsons, S. *Organometallics.* **2001**, *20*, 798. (c) Prust, J.; Stasch,

A.; Zheng, W.; Roesky, H. W.; Alexopoulos, E.; Uson, I.; Bohler, D.; Schuchardt, T. *Organometallics*. **2001**, *20*, 3825.

6. Cheng, M.; Moore, D. R.; Reczek, J. J.; Chamberlain, B. M.; Lobkovsky, E. B.; Coates, G. W. *J. Am. Chem. Soc.* **2001**, *123*, 8738.
7. Stender, M.; Eichler, B. E.; Hardman, N. J.; Power, P. P.; Prust, J.; Noltemeyer, M.; Roesky, H. W. *Inorg. Chem.* **2001**, *40*, 2794.
8. (a) Holland, P. L.; Tolman, W. B. *J. Am. Chem. Soc*. **1999**, *121*, 7270. (b) Holland, P. L.; Tolman, W. B. *J. Am. Chem. Soc*. **2000**, *122*, 6331.
9. Dai, X.; Warren, T. H. *Chem. Commun*. **2001**, 1998.
10. Smith, J. M.; Lachicotte, R. J.; Pittard, K. A.; Cundari, T. R.; Lukat-Rodgers, G.; Rodgers, K. R.; Holland, P. L. *J. Am. Chem. Soc*. **2001**, *123*, 9222.
11. (a) Yokota, S.; Tachi, Y.; Nishiwaki, N.; Ariga, M.; Itoh, S. *Inorg. Chem*. **2001**, *40*, 5316. (b) Jazdzewski, B. A.; Holland, P. L.; Pink, M.; Young, Jr., V. G.; Spencer, D. J. E.; Tolman, W. B. *Inorg. Chem*. **2001**, *40*, 6097. (c) Budzelaar, P. H. M.; van Oort, A. B.; Orpen, A. G. *Eur. J. Inorg. Chem*. **1998**, 1485.
12. Radzewich, C. E.; Coles, M. P.; Jordan, R. F. *J. Am. Chem. Soc*. **1998**, *120*, 9384.
13. Fekl, U.; Kaminsky, W.; Goldberg, K. I. *J. Am. Chem. Soc*. **2001**, *123*, 6423.
14. Yokota, S.; Tachi, Y.; Itoh, S. *Inorg. Chem*. **2002**, *41*, 1342.
15. SMART, SAINT and XPREP, Siemens Analytical X-ray Instruments Inc., Madison, Wisconsin, USA, 1995.

16. Sheldrick, G. M. SADABS: software for Empirical Absorption Correction, University of Gottingen, Institut fur Anorganische Chemieder Universitat, Tammanstrasse 4, D-3400 Gottingen, Germany, 1999–2003.

17. Sheldrick, G. M. SHELXS-97, University of Gottingen, Germany, **1997**.

18. Farrugia, L. J. *J. Appl. Crystallogr.* **1997**, *30*, 565.

19. Gelder, de, R.; Gal, A. W.; Budzelaar, P. H. M. *Organometallics*. **1998**, *17*, 4121.

20. Kalita, A.; Kumar, P.; Deka, R. C.; Mondal, B. *Inorg. Chem.* **2011**, *50*, 11868.

21. Van der Sluis, P.; Spek, A.L. *Acta Crystallogr.* **1990**, *A46*, 194.

22. Weis, M. C.; Goedken, V. L. *J. Am. Chem. Soc*. **1976**, *98*, 3389.

23. Das, O.; Paria, S.; Zangrando, E.; Paine, T. K. *Inorg. Chem*. **2011**, *50*, 11375.

Chapter 4

Abstract

Manganese(II) complexes, $[Mn(L_4)Cl_2]$, **4.1** and $[Mn(L_4)(H_2O)_2](ClO_4)_2$, **4.2** { $\mathbf{L_4}$ = *N*^{1},*N*^{2}-*bis* ((pyridine-2-yl)methyl)ethane-1,2-diamine} were prepared and characterized. In acetonitrile solution, complex **4.1** did not react with nitric oxide. However, addition of nitric oxide gas to the acetonitrile solution of complex **4.2** results an unstable Mn(II)-nitrosyl intermediate. The formation of nitrosyl intermediate was evidenced by UV-visible, solution FT-IR, ^{1}H-NMR spectral studies. Subsequently, Mn(II) center in the complex **4.2** undergoes reduction to Mn(I) with a simultaneous N-nitrosation of the ligand. The N-nitrosated ligand was isolated and characterized. In contrast, the corresponding Cu(II) complex of the same ligand in presence of nitric oxide was not found to yield Cu(II)-nitrosyl.

4.1 Introduction

The reactions of nitric oxide (NO) with transition metal ions and formation of metal-nitrosyls have long been of interest because of their relevance and importance in biological systems.[1,2] Many of the physiological events of NO are attributed to the formation of nitrosyls of metalloproteins.[3] For instance, metal-nitrosyl adducts are believed to play important roles in nitrosation reactions of various thiols to result in S-nitrosothiols which are proposed as carriers of NO equivalents in cellular systems.[4] On the other hand, the reduction of metal ion by NO has been known for a long time. For example, ferriheme proteins are known to undergo reduction to ferroheme in presence of NO through Fe(III)-nitrosyl intermediate. In this direction, iron-nitrosyls, both in protein and synthetic model systems have been studied extensively.[5-8] The reduction of Cu(II) centers in some proteins, such as cytochrome *c* oxidase and laccase, by NO is known for a long time.[9,10] In recent years this has been exemplified by a number of model Cu(II) complexes.[11,12]

On the other hand, though the examples of manganese-nitrosyls in organometallic, porphyrin and thalocyanine complexes are reported, the detail reactivity of manganese complexes with NO has not been studied to that extent.[13,14] A few Mn(II)-nitrosyls have been reported recently with an aim to develop NO releasing material for photo dynamic therapy.[15] Other than those, Mascharak et. al. have reported the reaction of a μ-oxo bridged Mn(III) complex with

NO resulting in the reductive nitrosylation of the metal ion and it leads to the formation of Mn(II)-nitrosyl complex in presence of excess NO.[16]

In our laboratory, we have been studying the reactivity of NO with Cu(II) complexes and found the reduction of metal ion by NO which leads to the N-nitrosation and diazotization at the secondary and primary amine centers, respectively, of ligand frameworks.[12] Interestingly, the N-nitrosation, in cases of Cu(II) complexes, may not necessarily always proceeds through Cu(II)-nitrosyl formation. Depending upon the ligand denticity and geometry of the complex, it may proceeds through a deprotonation mechanism in presence of base. For example, in case of tetradentate tripodal ligand, the N-nitrosation takes place through a Cu(II)-nitrosyl intermediate.[17] In case of tetradentate macrocyclic ligand, it proceeds through a deprotonation of the N-H group.[18] This diversity of the mechanistic pathway actually prompted us to study the NO reactivity of Mn(II) complexes.

For the present study, a tetradentate N-donor ligand, $\mathbf{L_4}$ {$\mathbf{L_4}$ = *N*^{1}, *N*^{2}-*bis* ((pyridine-2-yl)methyl)ethane-1,2-diamine} having two pyridine nitrogen and two aliphatic amine nitrogen is chosen (Figure 4.1). Earlier, the NO reactivity of Cu(II) complex of the same ligand has been reported from our laboratory. So the present study will also demonstrate the difference of reactivity towards NO while moving from Cu(II) to Mn(II).

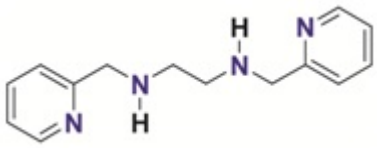

Figure 4.1 Ligand ($\mathbf{L_4}$) used for the present study.

4.2 Experimental Section

4.2.1 General

All reagents and solvents of reagent grade were purchased from commercial sources and used as received except specified. Acetonitrile was distilled from calcium hydride. Deoxygenation of the solvent and solutions was effected by repeated vacuum/purge cycles or bubbling with argon for 30 minutes. NO gas was purified by passing it through a KOH and P_2O_5 column. UV-visible spectra were recorded on a Perkin-Elmer Lambda 25 UV-visible spectrophotometer. FT-IR spectra of samples were taken on a Perkin Elmer spectrophotometer either with samples prepared as KBr pellets or in solution in a NaCl cell. Solution electrical conductivity was measured using a Systronic 305 conductivity bridge. ^{1}H-NMR spectra were recorded in a 400 MHz Varian FT spectrometer. Chemical shifts (ppm) were referenced either with an internal standard (Me_4Si) or to the residual solvent peaks. The X-band Electron Paramagnetic Resonance (EPR) spectra were recorded on a JES-FA200 ESR spectrometer, at room temperature and 77 K with microwave power, 0.998 mW; microwave frequency, 9.14 GHz and

modulation amplitude, 2. Elemental analyses were obtained from a Perkin Elmer Series II Analyzer. The magnetic moment of complex was measured on a Cambridge Magnetic Balance.

Single crystals were grown by slow diffusion followed by slow evaporation technique. The intensity data were collected using a Bruker SMART APEX-II CCD diffractometer, equipped with a fine focus 1.75 kW sealed tube MoK_α radiation (λ = 0.71073 Å) at 273(3) K, with increasing ω (width of 0.3° per frame) at a scan speed of 3 s/frame. The SMART software was used for data acquisition.[19] Data integration and reduction were undertaken with SAINT and XPREP software.[20] Structures were solved by direct methods using SHELXS-97 and refined with full-matrix least squares on F^2 using SHELXL-97.[21] Structural illustrations have been drawn with ORTEP-3 for Windows.[22]

4.2.2 Synthesis of L_4

The ligand **L_4** was prepared by a reported procedure.[23] To a solution of pyridine-2-carboxaldehyde (2.14 g, 20 mmol) in 20 ml methanol, ethylenediamine (0.60 g, 10 mmol) was added into a 50 ml round bottom flask equipped with a stirring bar. The solution was refluxed for 5 h. The resulting reddish-yellow solution was then reduced by $NaBH_4$ (1.52 g, 40 mmol). Removal of the solvent under reduced pressure affords a crude mass. It was dissolved in water (50 ml) and extracted with chloroform (4 portions × 50 ml). The organic part was dried under reduced pressure and the reddish yellow oil thus obtained was subjected to chromatographic purification using a silica gel column to yield the pure ligand, **L_4** as yellow

oil. Yield: 1.96 g (~ 80%). FT-IR in KBr: 2791, 1591, 1475, 1431 and 767 cm^{-1}. ^{1}H-NMR (400 MHz, $CDCl_3$): δ_{ppm}: 2.81 (s, 4H), 3.91 (s, 4H), 7.12-7.15 (t, 2H), 7.30 (d, 4H), 7.60-7.64 (t, 2H) and 8.52-8.53 (d, 2H). ^{13}C-NMR (100 MHz, $CDCl_3$) δ_{ppm}: 46.9, 53.1, 120.5, 120.8, 134.4, 147.5 and 157.8. ESI-Mass (m + 1)/z, calcd 243.32; found: 243.04.

4.2.3 Synthesis of complex 4.1

Manganese chloride, tetrahydrate (0.989 g, 5 mmol) was dissolved in 10 ml of distilled methanol. To this solution, **L_4** (1.21 g, 5 mmol), dissolved in distilled methanol, was added slowly with constant stirring. The color of the solution turned into pale-yellow. The stirring was continued for 2 h at room temperature. The volume of the solution was then reduced to ~ 2 ml. To this, diethyl ether (10 ml) was added to layer on it and kept overnight in a freezer. This resulted into yellow colored precipitate of complex **4.1**. Yield: 1.58 g (~ 85%) and UV-vis. (acetonitrile): λ_{max}, , 474 nm (ε, 380 M^{-1} cm^{-1}), 595 nm (ε, 201 M^{-1} cm^{-1}). X-band EPR (in acetonitrile at RT) g_{av}, 2.025. FT-IR (KBr pellet): 3429, 3270, 3232, 2884, 1604, 1569, 1481, 1431, 1264, 1095, 1008, 775 and 637 cm^{-1}. ^{1}H-NMR (400 MHz, CD_3OD) δ_{ppm}: 1.33 (s, 4H), 2.52 (s, 4H), 8.67 (s, 4H), 9.10 (s, 2H) and 9.86 (s, 2H). μ_{obs}, 5.82 BM.

4.2.4 Synthesis of complex 4.2

Complex **4.1** (0.736 g, 2 mmol) was dissolved in minimum volume of acetonitrile. To this, aqueous solution of silver nitrate (0.680 g, 4 mmol; 2 ml) was added with constant stirring. The precipitate of AgCl was removed by filtration through a frit. To the filtrate, aqueous solution of sodium perchlorate (20%, 2 ml) was added dropwise and the mixture was kept in freezer for 12 h which afforded the precipitate of complex **4.2**. Yield, 595 mg (~ 60%).

The complex **4.2** can also be prepared from manganese(II) perchlorate, hexahydrate. $Mn(ClO_4)_2.6H_2O$ (1.81 g, 5 mmol) was dissolved in 10 ml of distilled acetonitrile. To this solution, $\mathbf{L_4}$ (1.21 g, 5 mmol) was added slowly with constant stirring. The color of the solution turned into brown from colorless. The stirring was continued for 2 h at room temperature. The volume of the solution was then reduced to 2 ml. To this, benzene (5 ml) was added to layer on it and kept overnight in a freezer. This resulted in dark brown colored precipitate of complex **4.2**. Yield: 2.44 g (~82%) and UV-vis. (acetonitrile): λ_{max}, 246 nm (ε, 7108 M^{-1} cm^{-1}), 296 nm (ε, 8345 M^{-1} cm^{-1}), 421 nm (ε, 1620 M^{-1} cm^{-1}), 644 nm (ε, 210 M^{-1} cm^{-1}). X-band EPR (in acetonitrile at RT): g_{av}, 2.02155. FT-IR (KBr pellet): 3314, 3234, 2885, 1612, 1440, 1314, 1148, 1091, 930, 770 and 626 cm^{-1}. ^{1}H-NMR (400 MHz, CD_3CN) δ_{ppm}: 0.65(s, 4H), 4.43 (s, 4H), 7.35 (d, 4H) and 4.92 (s, 4H). Molar conductivity in acetonitrile, Λ_M (S cm^{-1}), 224. μ_{obs}, 5.76 BM. ESI Mass $[Mn(L_4)(H_2O)_2]^{2+}$, calcd: 166.5561; found: 166.5469.

4.2.5 Isolation of modified ligand L_4'

Complex **4.2** (0.992 g, 2.0 mmol) was dissolved in 10 ml of distilled and degassed acetonitrile. To this solution NO gas was purged for 1 minute. After removing the excess NO by several cycles of vacuum purge, the resulting yellowish solution was allowed to stand at room temperature for 1 h. A light pink colored precipitate was formed which was then separated by filtration under argon and the filtrate was dried over vacuum. The crude mixture was then purified by column chromatography to get pure ligand $\mathbf{L_4}$ as yellow oil and $\mathbf{L_4}^{/}$-perchlorate as light yellow solid. Yield: $\mathbf{L_4}$: 95 mg (30%) and $\mathbf{L_4}^{/}$-perchlorate: 146 mg (40%). FT-IR (KBr pellet): 3408, 2928, 1668, 1592, 1571, 1457, 1436, 1355, 1151, 1118, 1093, 998, 758 and 614 cm^{-1}. ESI-Mass (m+1)/z, calcd. 301.1335; found: 301.1287. ^{1}H-NMR (400 MHz, $CDCl_3$) δ_{ppm}: 4.19-4.21 (t, 1H), 4.56-4.58 (t, 1H), 5.00 (s, 2H), 5.05 (s, 1H), 5.14 (s, 2H), 5.82 (s, 1H), 7.81–7.83 (d, 1H), 7.91-7.98 (m, 3H), 8.47-8.51 (m, 3H) and 8.73–8.75 (d, 1H). ^{13}C-NMR (100 MHz, $CDCl_3$) δ_{ppm}: 46.0, 50.5, 124.9, 125.4, 142.3, 145.7 and 156.1.

4.3 Results and discussion

The ligand, $\mathbf{L_4}$ was prepared using a reported protocol from the reaction of ethylenediamine with two equivalents of pyridine-2-carboxaldehyde followed by reduction of the corresponding imine using $NaBH_4$ (experimental section).[23] The ligand was characterized by various spectroscopic techniques (experimental section). Complex **4.1** was prepared from the reaction

of manganese(II) chloride, tetrahydrate with equivalent amount of ligand, $\mathbf{L_4}$ in methanol (Scheme 4.1).

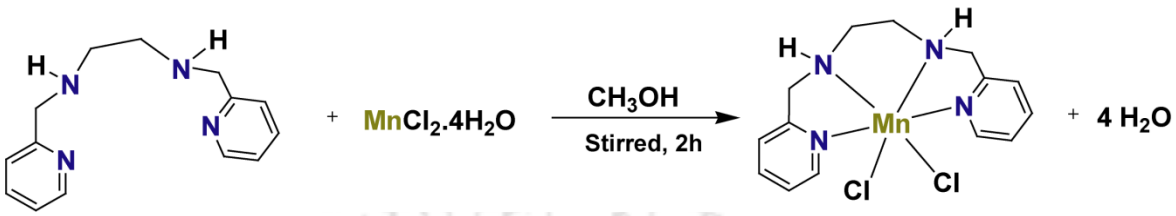

Scheme 4.1

The complex was characterized by various spectroscopic methods as well as single crystal X-ray structure determination. The ORTEP view of complex **4.1** is shown in figure 4.2. Crystallographic data, important bond angles and distances are listed in tables 4.1, 4.2 and 4.3, respectively. The crystal structure reveals a distorted octahedral geometry around the central metal ion. Four nitrogen atoms from the ligand and two chlorine atoms are coordinated to the Mn(II) center. The Cl atoms are coordinated in *cis*-geometry. The Mn-N_{py} and Mn-N_{amine} distances are 2.271 and 2.328 Å respectively. The average Mn-Cl distance is 2.471 Å. These are within the range of reported complexes.[15] Complex **4.1** displays characteristic signal in X-band EPR spectroscopy (Appendix III).

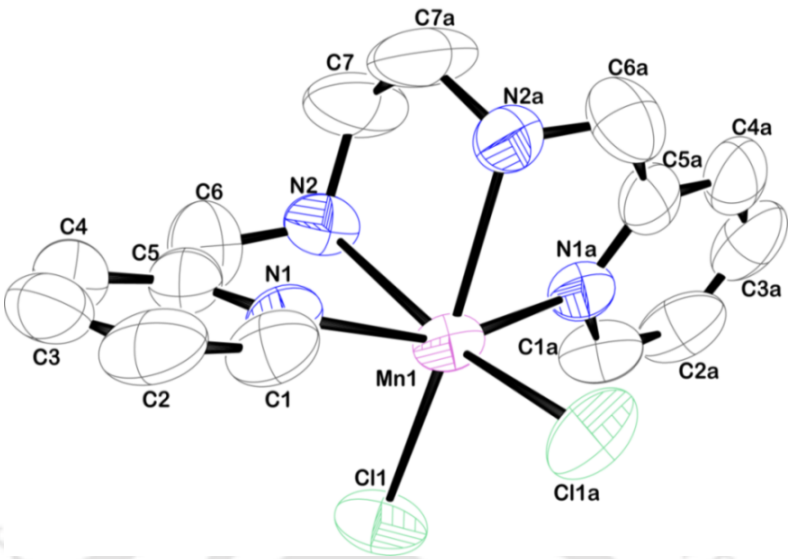

Figure 4.2 ORTEP diagram of complex **4.1** (50% thermal ellipsoid plot; H-atoms are removed for clarity).

In acetonitrile solution, it shows *d-d* transition at 595 nm along with intra ligand transitions in UV-region (Appendix III).

Table 4.1 Crystallographic data for complex **4.1**

	Complex **4.1**
formulas	$C_{14}H_{16}Mn_1N_4Cl_2$
mol. wt.	366.15
crystal system	Orthorhombic
space group	*Aba2*
temperature/K	296(2)
wavelength /Å	0.71073
a/Å	15.6763(17)
b/Å	12.2746(12)

c/Å	8.5407(12)
α/°	90.00
β/°	90.00
γ/°	90.00
V/Å^3	1643.4(3)
Z	4
density/Mg m^{-3}	1.480
abs. coeff /mm^{-1}	1.126
abs. correction	none
F(000)	748
total no. of reflections	1122
reflections, $I > 2\sigma(I)$	934
Max. 2θ/deg	25.24
ranges (*h*, *k*, *l*)	$-18 \leq h \leq 17$ $-14 \leq k \leq 13$ $-10 \leq l \leq 5$
Complete to 2θ (%)	98.7
refinement method	full-matrix least-squares on F^2
GoF (F^2)	0.999
R indices [$I > 2\sigma(I)$]	0.0354
R indices (all data)	0.1014

Table 4.2 Selected bond lengths (Å) of complex **4.1**

	Bond length (Å)		Bond length (Å)
Mn1-Cl1	2.471(2)	N2-C7	1.441(9)
Mn1-N1	2.271(5)	C1-C2	1.384(9)
Mn1-N2	2.328(4)	C2-C3	1.37(1)
N1-C1	1.338(7)	C3-C4	1.37(1)
N1-C5	1.339(7)	C4-C5	1.370(9)
N2-C6	1.455(8)	C5-C6	1.529(8)

Table 4.3 Selected bond angles (°) of complex **4.1**

	Bond angle (˚)		Bond angle (˚)
Cl1- Mn1-N1	96.1(1)	Mn1-N1-C1	124.3(3)

Cl1- Mn1-N2	91.3(1)	Mn1-N1-C5	117.2(3)
N1- Mn1-N2	73.2(1)	C1-N1-C5	118.2(4)
N1- Mn1- Cl1	96.1(1)	Mn1-N2- C6	110.6(3)
N2- Mn1- Cl1	91.3(1)	Mn1-N2- C7	108.3(4)

Addition of NO gas in dry and degassed acetonitrile solution of complex **4.1** did not result in any change. It has been monitored by UV-visible spectroscopy (Figure 4.3). This is perhaps because of strong coordination of chloride ion with Mn(II).

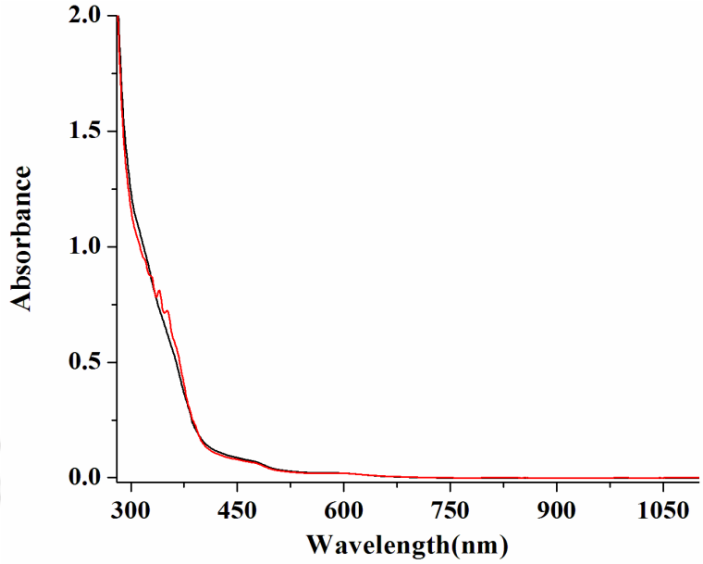

Figure 4.3 UV-visible spectra of complex **4.1** (black trace), after purging NO (red trace) in acetonitrile.

To study further, the chloride ions in complex **4.1** are replaced by water to afford complex **4.2**. It has been done by treating the acetonitrile solution of complex **4.1** with aqueous silver nitrate followed by addition of saturated aqueous sodium perchlorate solution (experimental section). The complex **4.2** can also be prepared by stirring a mixture of manganese(II) perchlorate,

hexahydrate with equivalent amount of ligand in acetonitrile under argon atmosphere (experimental section). It was characterized by spectral analyses and microanalysis (experimental section). Even after several attempts, an X-ray quality single crystal of the complex has not been grown. Complex **4.2** in acetonitrile solution absorbs at 644 nm in the UV-visible spectrum (Figure 4.4). Addition of NO gas into the degassed acetonitrile solution of complex **4.2** resulted in the appearance of a new band at 421 nm (Figure 4.4). The intensity of this newly appeared band was found to decay with time and finally diminished indicating the unstable nature of the intermediate. The decay was found to follow a pseudo first order kinetics with a rate constant 4.3×10^{-3} s^{-1} at 298 K.

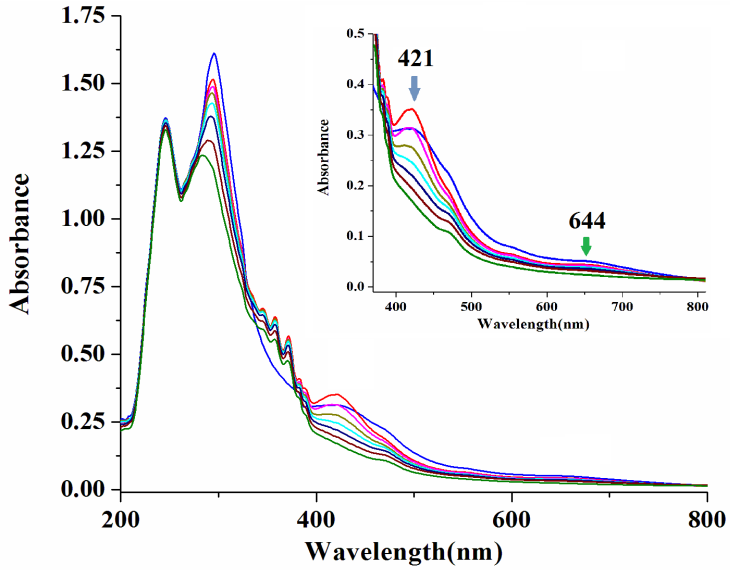

Figure 4.4 UV-visible spectrum of complex **4.2** before (blue trace) and after (red trace) purging NO. Inset shows the decay of the intensity of peaks at 421 nm and 644 nm with time in acetonitrile.

In solution FT-IR study, the addition of NO gas to the acetonitrile solution of complex **4.2** displayed a new strong stretching frequency at ~1718 cm^{-1}(Figure 4.5). The intensity of this

band was found to diminish with time suggesting this stretching from an unstable intermediate. This has been assigned as the coordinated nitrosyl stretching. In EPR study, the intermediate was found to be silent (Figure 4.6). Thus, intermediate is presumably Mn(II)-mononitrosyl. This has been further supported from the ESI mass spectrum of the intermediate. The peak at 327.112 corresponds to Mn(II)-mononitrosyl (Appendix III). The unstable nature of the intermediate did not allow its isolation for further characterization. It should be noted that the correct assignment of the formal oxidation states of the metal in metal nitrosyls is difficult because of non-innocent nature of NO ligands. NO can exist as NO^+, NO (radical) or NO^- in metal nitrosyl complexes. The observed intermediate is diamagnetic complex of Mn(II) with NO having $\{MnNO\}^6$ configuration according to Enemark-Feltham notation. Thus, it may have Mn(I)-NO^+, Mn(II)-NO or Mn(III)-NO^- configuration. Since the crystal structure is not available, direct comparison of the metric parameters with other reported results to assign the configuration is not possible. On the other hand, the nitrosyl stretching frequency in the intermediate complex appears at 1718 cm^{-1} in solution FT-IR spectroscopy. This is comparable with the other reported Mn(II)-nitrosyls having Mn(I)-NO^+ configuration.[24]

The decomposition of the [Mn^{II}-NO] intermediate is resulted in the reduction of Mn(I) and NO^+. The reduction was confirmed by the disappearance of the EPR signal of Mn(II) (Figure 4.6).

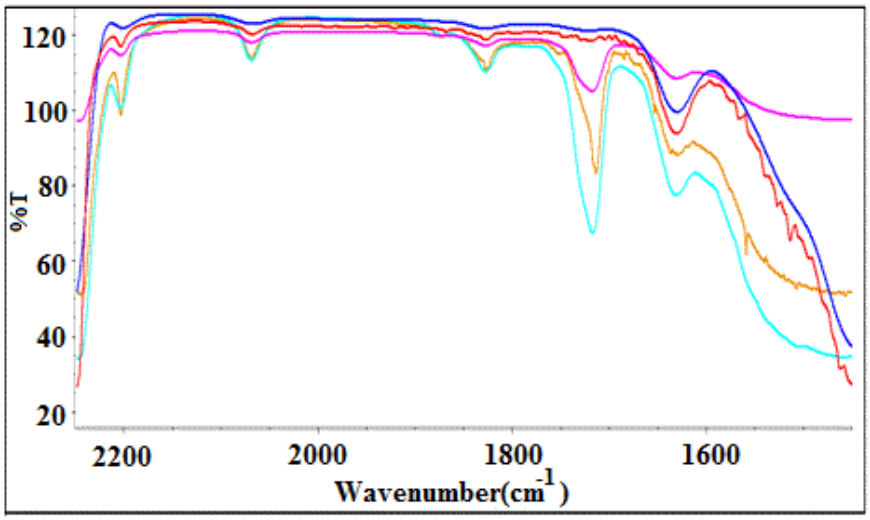

Figure 4.5 FT-IR spectra of complex **4.2** after purging NO (green trace) and gradual decay of the intensity of the peak at 1718 cm^{-1} in acetonitrile.

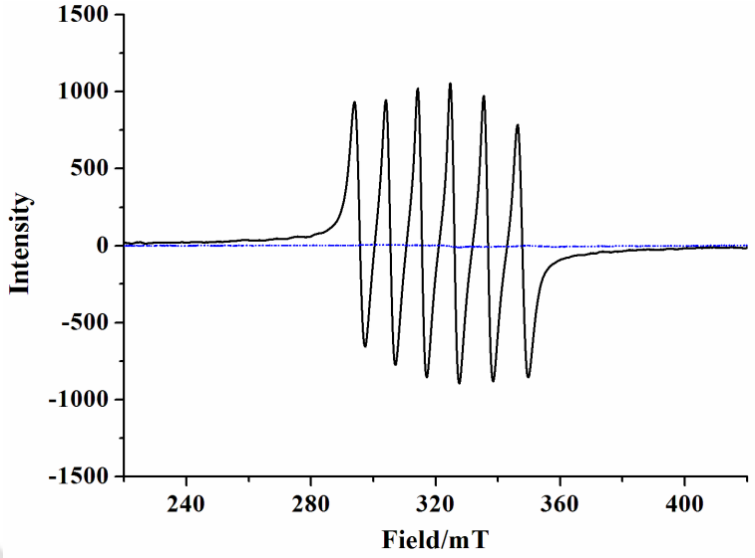

Figure 4.6 X-band EPR spectra of complex **4.2** before (black trace) and after (blue trace) the reaction with NO in acetonitrile at room temperature.

In addition, the broad ^{1}H-NMR signals of the complex **4.2** became sharp and well resolved after its reaction with NO (Figure 4.7**)**. This has been attributed to the reduction of paramagnetic Mn(II) to diamagnetic Mn(I) by NO (Scheme 4.2).

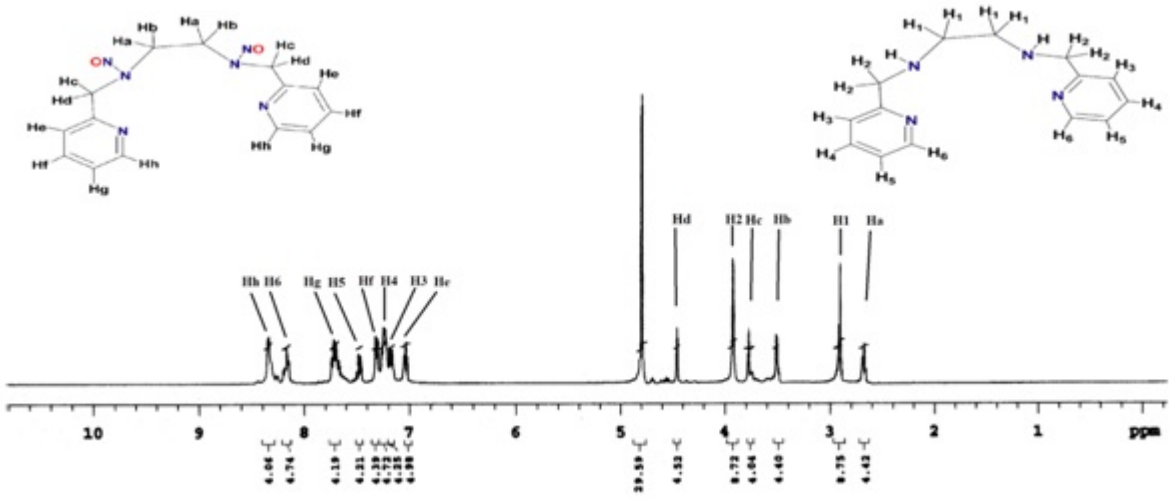

Figure 4.7 ^{1}H-NMR spectrum of complex **4.2** after the reaction of NO under argon atmosphere in CD_3CN showing the formation of $\mathbf{L_4}'$ along with $\mathbf{L_4}$.

Scheme 4.2

Although, there is no direct evidence of formation of NO^+ in the reaction mixture, this has been supported by N-nitrosation of the ligand. Nitrosation product, $\mathbf{L_4'(ClO_4)_2}$ was isolated from the reaction mixture (experimental section) and characterized using various spectroscopic analyses as well as single crystal X-ray structure determination. The ORTEP diagram of $\mathbf{L_4'(ClO_4)_2}$ is shown in figure 4.8. The crystallographic data, selected bond angles and distances are listed in tables 4.4, 4.5 and 4.6, respectively. In FT-IR spectrum the N-NO stretching frequency appeared at 1457 cm^{-1} which is in the range of other reported examples.[12]

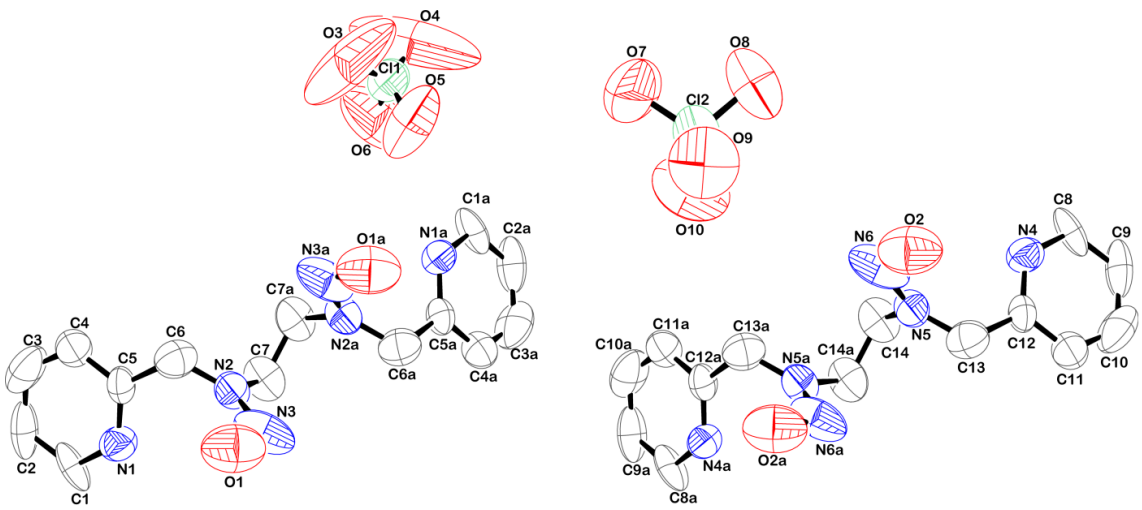

Figure 4.8 ORTEP diagram of $\mathbf{L_4'(ClO_4)_2}$ (50% thermal ellipsoid plot; H-atoms are removed for clarity).

It should be noted that in cases of Cu(II) complexes of various N-donor ligands, the addition of NO gas was found to result in [Cu^{II}-NO] intermediate prior to the reduction of metal center. This reduction resulted in the N-nitrosation of the ligand framework. It was observed that while more than one nitrosation sites are available, the nitrosation takes place to all the sites.

Table 4.4 Crystallographic data for modified ligand $\mathbf{L_4'(ClO_4)_2}$

	$\mathbf{L_4'(ClO_4)_2}$
formulas	$C_{14}\ H_{18}\ N_6\ O_{10}\ Cl_2$
mol. wt.	501.24
crystal system	Monoclinic
space group	*C2/c*
temperature/K	296(2)
wavelength /Å	0.71073
a/Å	22.837(6)
b/Å	14.466(6)
c/Å	13.121(4)
α/°	90.00
β/°	103.89(3)
γ/°	90.00
V/Å^3	4208(2)
Z	8
density/Mg m^{-3}	1.582
abs. coeff /mm^{-1}	0.375
abs. correction	none
F(000)	2064
total no. of reflections	1412
reflections, $I > 2\sigma(I)$	1119
Max. 2θ/deg	25.50
ranges (*h*, *k*, *l*)	$-127 \le h \le 26$ $-17 \le k \le 16$ $-15 \le l \le 15$
Complete to 2θ (%)	98.6
refinement method	full-matrix least-squares on F^2
GoF (F^2)	0.999
R indices [$I > 2\sigma(I)$]	0.1057
R indices (all data)	0.2977

Table 4.5 Selected bond lengths (Å) of $\mathbf{L_4'(ClO_4)_2}$

	Bond length (Å)		Bond length (Å)
Cl1-O5	1.42(1)	Cl2-O10	1.41(2)
Cl1-O4	1.40(1)	C6-N2	1.45(2)
Cl1-O3	1.40(1)	N2-N3	1.41(2)
Cl1-O6	1.42(2)	N2-C7	1.45(2)
Cl2-O9	1.14(2)	N3-O1	1.25(2)
Cl2-O8	1.36(2)	C13-N5	1.44(2)

Table 4.6 Selected bond angles (°) of $\mathbf{L_4'(ClO_4)_2}$

	Bond angles (°)		Bond angles (°)
O5- Cl1-O4	109.5(7)	O8- Cl2-O10	124(1)
O5- Cl1-O3	114.5(8)	O7- Cl2-O10	96(1)
O5- Cl1-O6	105.2(8)	C6- N2-N3	131(1)
O4- Cl1-O3	109.5(7)	C6- N2-C7	121(1)
O4- Cl1-O6	110.6(8)	N3- N2-C7	108(1)
O3- Cl1-O6	107.4(8)	N2-N3-O1	102(1)
O9- Cl2-O8	114(2)	N4- C12-C11	118(2)
O9- Cl2-O7	124(1)	N4- C12-C13	123(1)
O9- Cl2-O10	106(1)	O2-N6-N5	109(1)
O8- Cl2-O7	92(1)	N6-N5-C14	110(1)

Some Cu(II) complexes, depending upon the ligand framework, did not undergo reduction in presence of NO itself. However, addition of base NaOEt to the solution of those complexes followed by addition of NO resulted in the reduction of Cu(II) center along with N-nitrosation. In these cases, only mono-nitrosation was observed. For instance, the same ligand was used to prepare Cu(II) complex for NO reactivity study. Although the Cu(II) complexes did not react in degassed methanol solution, but in presence of sodium ethoxide as base the reduction was observed with simultaneous N-nitrosation.

Mn(II)-nitrosyls, having d^6 configuration according to Enemerk and Feltham notation, have been synthesized with porphyrin, thalocyanins. They were stable and structurally characterized. A series of Mn(II) complexes of N-donor ligands having amide group have been reported to react with NO in acetonitrile solution to afford stable Mn(II)-nitrosyl complexes. They were also characterized structurally. The reduction of Mn center in *bis*-μ-oxo complex by NO was exemplified earlier. This leads to the reductive nitrosylation of the metal ion. However, there is no example of reduction of Mn(II) by NO leading to simultaneous ligand nitrosation.

4.4 Conclusions

Mn(II) complex, **4.2**, in acetonitrile solution was found to react with NO to afford an unstable Mn(II)-nitrosyl intermediate. The formation of nitrosyl intermediate was evidenced by UV-visible, solution FT-IR, ^{1}H-NMR spectral studies. Subsequently, Mn(II) center in complex **4.2** was found to undergo reduction to Mn(I) with simultaneous N-nitrosation of the ligand. The N-nitrosated ligand was isolated and characterized. It should be noted that the corresponding Cu(II) complex of the same ligand in presence of NO was not found to yield Cu(II)-nitrosyl.

4.5 References

1. (a) Richter-Addo, G. B.; Legzdins, P. *Metal Nitrosyls*; Oxford University Press: New York, 1992. (b) Hayton, T. W.; Legzdins, P.; Sharp, W. B. *Chem. Rev.* **2002**, *102*, 935. (c) Feelisch, M.; Stamler, J. S. *Methods in Nitric Oxide Research*; Eds.; John Wiley and Sons; Chichester, England, 1996.

2. (a) Ford, P. C.; Lorkovic, I. M. *Chem. Rev.* **2002**, *102*, 993. (b) Mingos, D. M. P.; Sherman, D. J. *Adv. Inorg.Chem*. **1989,** *34*, 293. (c) Ghosh, A. *Acc. Chem. Res*. **2005**, *38*, 943. (d) Wang, P. G.; Xian, M.; Tang, X.; Wu, X.; Wen, Z.; Cai, T.; Janczuk, A. J. *Chem. Rev*. **2002**, *102*, 1091.(e) Butler, A. R.; Megson, I. L.; *Chem. Rev.* **2002**, *102*, 1155. (f) Williams, R. J. P. *Chem. Soc. Rev*. **1996**, 77.

3. (a) Ignarro, L. J. *Nitric Oxide: Biology and Pathobiology*; Ed.; Academic Press: San Diego, 2000. (b) Moncada, S.; Palmer, R. M. J.; Higgs, E. A. *Pharmacol. Rev*. **1991**, *43,* 109.(c) Butler, A. R.; Williams, D. L. *Chem. Soc. Rev*. **1993**, *233*. (d) Jia, L.; Bonaventura, C.; Bonaventura, J.; Stamler, J. S. *Nature*. **1996**, *380*, 221. (e) Galdwin, M. T.; Lancaster Jr., J. R.; Freeman, B. A.; Schechter, A. N. *Nat. Med*. **2003**, *9,* 496.

4. (a) Stamler, J. S.; Singel, D. J.; Loscalzo, J. *Science*. **1992**, *258*, 1898. (b) Stamler, J. S. *Cell*. **1994**, *78*, 931.(c) Feelisch, M. S.; Rassaf, T.; Mnaimneh, S.; Singh, N.; Byran, N. S.; Jourd'Heuil, D.; Kelm, M. *FASEB J.* **2002**, *16*, 1775. (d) Bryan, N. S.; Rassaf, T.; Maloney, R. E.; Rodriguez, C. M.; Saijo, F.; Rodriguez, J. R.; Feelisch, M. *Proc. Natl. Acad. Sci. U. S. A.* **2004**, *101,* 4308. (e) Luchsinger, B. P.; Rich, E. N.; Gow, A. J.; Williams, E. M.; Stamler, J. S.; Singel, D. J. *Proc. Natl. Acad. Sci. U. S. A.* **2003**, *100*, 461.

5. (a) Chien, J. C. W. *J. Am. Chem. Soc.* **1969**, *91*, 2166. (b) Wayland, B. B.; Olson, L. W. *J. Am. Chem. Soc.* **1974**, *96,* 6037. (c) Trofimova, N. S.; Safronov, A. Y.; Ikeda, O. *Inorg. Chem.* **2003**, *42,* 1945. (d) Walker, F. A. *J. Inorg. Biochem.* **2005**, *99,* 216. (e) Rousseau, D. L.; Li, D.; Couture, M.; Yeh, S. R. *J. Inorg. Biochem.* **2005**, *99*, 306.

6. (a) George, S. J.; Allen, J. W. A.; Ferguson, S. J.; Thorneley, R. N. F. *J. Biol. Chem.* **2000**, *275*, 33231. (b) Pinakoulaki, E.; Gemeinhardt, S.; Saraste, M.; Varotsis, C. *J. Biol. Chem.* **2002**, *277*, 23407. (c) Praneeth, V. K. K.; Paulat, F.; Berto, T. C.; George, S. D. B.; Nather, C.; Sulok, C.; Lehnert, N. *J. Am. Chem. Soc.* **2008**, *130*, 15288. (d) Soldatova, A. V.; Ibrahim, M.; Olson, J. S.; Czernuszewicz, R. S.; Spiro, T. G. *J. Am. Chem. Soc.* **2010,** *132*, 4614.

7. (a) Wasser, I. M.; Vries, de S.; Moe¨nne-Loccoz, P.; Schro¨der, I.; Karlin, K. D. *Chem. Rev.* **2002**, *102*, 1201. (b) Hoshino, M.; Maeda, M.; Konishi, R.; Seki, H.; Ford, P. C. *J. Am. Chem. Soc.* **1996**, *118*, 5702. (c) Fernandez, B. O.; Lorkovic, I. M.; Ford, P. C. *Inorg. Chem.* **2004**, *43*, 5393. (d) Lehnert, N.; Praneeth, V. K. K.; Paulat, F. *J. Comput. Chem.* **2006**, *27*, 1338.

8. (a) Ellison, M. K.; Scheidt, W. R. *J. Am. Chem. Soc.* **1999**, *121*, 5210. (b) Linder, D. P.; Rodgers, K. R.; Banister, J.; Wyllie, G. R. A.; Ellison, M. K.; Scheidt, W. R. *J. Am. Chem. Soc.* **2004**, *126*, 14136. (c) Lim, M. D.; Lorkovic, I. M.; Ford, P. C. *J. Inorg. Biochem.* **2005**, *99*, 151. (e) Shamir, D.; Zilbermann, I.; Maimon, E.; Gellerman, G.; Cohen, H.; Meyerstein, D. *Eur. J. Inorg. Chem.* **2007**, 5029.

9. (a) Torres, J.; Svistunenko, D.; Karlsson, B.; Cooper, C. E.; Wilson, M. T. *J. Am. Chem. Soc*. **2002**, *124*, 963. (b) Torres, J.; Cooper, C. E.; Wilson, M. T. *J. Biol. Chem*. **1998**, *273*, 8756. (c) Martin, C. T.; Morse, R. H.; Kanne, R. M.; Gray, H. B.; Malmstrom, B. G.; Chan, S. I. *Biochemistry*. **1981**, *20*, 5147.

10. (a) Gorren, A. C. F.; Boer, de E.; Wever, R. *Biochem. Biophys. Acta.* **1987**, *916*, 38. (b) Tran, D.; Ford, P. C. *Inorg. Chem.* **1996**, *35,* 2411. (c) Brown, G. C. *Biochim. Biophys.*

Acta. **2001**, *1504*, 46. (c) Torres, J.; Sharpe, M. A.; Rosquist, A.; Cooper, C. E.; Wilson, M. T. *FEBS Lett.* **2000**, *475*, 263. (d) Wijma, H. J.; Canters, G. W.; Vries, de S.; Verbeet, M. P. *Biochem.* **2004**, *43*, 10467.

11. (a) Tran, D.; Skelton, B. W.; White, A. H.; Laverman, L. E.; Ford, P. C. *Inorg. Chem*. **1998**, *37*, 2505. (b) Lim, M. D.; Capps, K. B.; Karpishin, T. B.; Ford, P. C. *Nitric Oxide, Biol. Chem.* **2005**, *12*, 244. (c) Khin, C.; Lim, M. D.; Tsuge, K.; Iretskii, A.; Wu, G.; Ford, P. C. *Inorg. Chem.* **2007**, *46*, 9323. (d) Pell, S. D.; Armor, J. N. *J. Am. Chem. Soc.* **1973**, *95*, 7625.

12. (a) Sarma, M.; Singh, A.; Gupta, S. G.; Das, G.; Mondal, B. *Inorg. Chim. Acta*. **2010**, *363*, 63. (b) Sarma, M.; Kalita, A.; Kumar, P.; Singh, A.; Mondal, B. *J. Am. Chem. Soc.* **2010**, *132*, 7846. (c) Sarma, M.; Mondal, B. *Inorg. Chem*. **2011**, *50*, 3206. (d) Sarma, M.; Mondal, B. *Dalton Trans.* **2012**, *41*, 2927. (e) Sarma, M.; Kumar, V.; Kalita, A.; Deka, R. C.; Mondal, B. *Dalton Trans*. **2012**, *41*, 9543.

13. (a) Yonetani, T.; Yamamoto, H.; Erman, J. E.; Leigh, J. J. S.; Reed, G. H. *J. Biol. Chem*. **1972**, *247*, 2447. (b) Dickinson, L. C.; Chien, J. C. W. *J. Biol. Chem.* **1977**, *252*, 6156. (c) Bender, A. T.; Kamada, Y.; Kleaveland, P. A.; Osawa, Y. *J. Inorg. Biochem.* **2002**, *91*, 625. (b) Spasojevic, I.; Batinic-Haberle, I.; Fridovich, I. *Nitric Oxide: Biol. Chem.* **2000**, *4*, 526.

14. (a) Ferrer-Sueta, Quijano, G.; Alvarez, B.; Radi, R. *Methods Enzymol.* **2002**, *349*, 23. (b) Shimanovich, R.; Hannah, S.; Lynch, V.; Gerasimchuk, N.; Mody, T. D.; Magda, D.; Sessler, J.; Groves, J. T. *J. Am. Chem. Soc.* **2001**, *123*, 3613. (c) Zahran, Z. N.; Lee, J.; Alguindigue, S. S.; Khan, M. A.; Richter-Addo, G. B. *Dalton Trans*. **2004**, 44. (d)

Christopher, A. J.; Kirsty, A. M.; Manuel, B.; Neil, C. G.; Nicholas, G. J.; Estefania, L.-R.; Guy, O. A.; Philip, R. H. *Dalton Trans*. **2004**, 683.

15. (a) Ghosh, K.; Eroy-Reveles, A. A.; Avila, B.; Holman, T. H.; Olmstead, M. M.; Mascharak, P. K. *Inorg. Chem.* **2004,** *43*, 2988. (b) Merkle, A. C.; Fry, N. L.; Mascharak, P. K.; Lehnert, N. *Inorg. Chem.* **2011**, *50*, 12192.
16. Ghosh, K.; Eroy-Reveles, A. A.; Olmstead, M. M.; Mascharak, P. K. *Inorg. Chem*. **2005**, *44*, 8469.
17. Sarma, M.; Kalita, A.; Kumar, P.; Singh, A.; Mondal, B. *J. Am. Chem. Soc.* **2010**, *132*, 7846.
18. Tsuge, K.; De Rosa, F.; Lim, M. D.; Ford, P. C. *J. Am. Chem. Soc.* **2004**, *126*, 6564.
19. SMART, SAINT and XPREP, *Siemens Analytical X-ray Instruments Inc*., Madison, Wisconsin, USA, 1995.
20. Sheldrick, G. M. *SADABS: Software for Empirical Absorption Correction;* University of Gottingen: Institut fur Anorganische Chemieder Universitat, Tammanstrasse 4, D-3400 Gottingen: Germany, 1999–2003.
21. Sheldrick, G. M. *SHELXS-97*; University of Gottingen: Germany, 1997.
22. Farrugia, L. J. *J. Appl. Crystallogr.* **1997**, *30*, 565.
23. Michelsen, K. *Acta Chem. Scand.* **1977**, *A31*, 429.
24. (a) Goodrich, L. E.; Paulat, F.; Praneeth, V. K. K.; Lehnert, N. *Inorg. Chem.* **2010**, *49*, 6293. (b) Enemark, J. H.; Feltham, R. D. *Coord. Chem. Rev.* **1974**, *13*, 339. (c) Scheidt, W. R.; Hatano, K.; Rupprecht, G.A.; Piciulo, P. L. *Inorg. Chem.* **1979**, *18*, 292. (d) Coleman, W. M.; Taylor, L. T. *J. Am. Chem. Soc.* **1978**, *100*, 1705. (e) Tangen, E.;

Conradie, J.; Franz, K.; Friedle, S.; Telser, J.; Lippard, S. J.; Ghosh, A. *Inorg. Chem.* **2010**, *49*, 2701.

Chapter 5

Abstract

Two iron(III) complexes, **5.1** and **5.2** with $\mathbf{L_5}$ and $\mathbf{L_6}$ [$\mathbf{L_5}$ = N,N'-bis(2-hydroxybenzyl)-1,2-diaminobenzene; $\mathbf{L_6}$ = N,N'-bis(2-hydroxybenzyl)ethylenediamine], respectively, were synthesized and characterized. In methanol solution of the complexes, the Fe(III) centre was found to reduce in presence of NO gas. The formation of [Fe^{III}-NO] intermediate prior to the reduction of Fe(III) center was evidenced by UV-visible, solution FT-IR, X-band EPR studies. The presence of excess NO gas leads to the reductive nitrosylation of the complexes leading to the formation of corresponding Fe(II)-nitrosyl complexes, **5.3** and **5.4**, respectively. The Fe(II)-nitrosyls were isolated as solid and characterized spectroscopically. DFT calculations were performed to optimize the structures of all the complexes.

5.1 Introduction

Nitric oxide (NO) is known to play significant roles in mammalian biology as an intracellular signaling agent and in cytotoxic immune response.[1] Under bioregulatory conditions, NO interacts with metal centers, primarily iron and copper.[2] The ferro-heme enzyme, sGC is the best-characterized example which becomes activated by the formation of iron(II) nitrosyl complex.[3] Concentrations of NO generated for bioregulation are low. For instance, submicromolar concentrations were reported in endothelium cells for blood pressure control.[4-5] In addition, catalase inhibition also apparently involves coordination of NO at a heme iron center.[4-5] The biological relevance of the formation and decay of metal-nitrosyls has become a subject of continuing research interest. In fact, the understanding of the interaction between NO and metal centers is very important to understand the biological activity of NO.

On the other hand, salen ligands are well known for their versatility with respect to steric and electronic modifications.[6] Many salen metal complexes have found important applications in homogeneous catalysis such as alkene epoxidation, ring-opening polymerization of epoxides with CO_2 etc.[7] Iron-based salen complexes have found to mimic for the active site in oxygenases for the oxidation of alkenes and alkanes with dioxygen.[8]

The reduced analogues, salan or tetrahydrosalen ligands, have received relatively less attention.[9] Perhaps, because of their less straight forward synthetic procedures. However, increased flexibility and stronger nitrogen donors make them attractive ligands.[10] Various iron complexes containing salan ligands were reported following the early works by Borer and co-workers.[11]

In the context of studying the reaction of NO with non-heme iron centers, the present set of salan ligands (Figure 5.1) has been chosen.

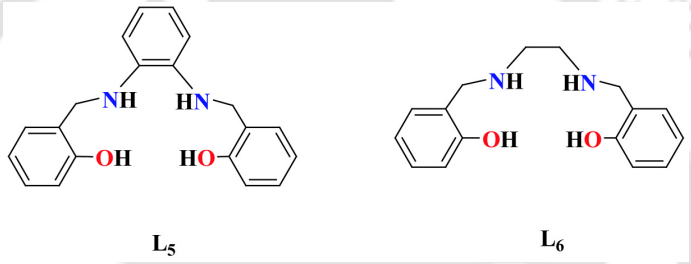

Figure 5.1 Ligands (**L_5** and **L_6**) used for the present study.

5.2 Experimental Section

5.2.1 General

All reagents and solvents of reagent grade were purchased from commercial sources and used as received except specified. Acetonitrile was distilled from calcium hydride. Deoxygenation of

the solvent and solutions was effected by repeated vacuum/purge cycles or bubbling with argon for 30 minutes. NO gas was purified by passing it through a KOH and P_2O_5 column. UV-visible spectra were recorded on a Perkin-Elmer LAMBDA 25 UV-visible spectrophotometer. FT-IR spectra were taken on a Perkin Elmer spectrophotometer with samples prepared either KBr pellets or in solution in sodium chloride cell. Solution electrical conductivity was measured using a Systronic 305 conductivity bridge. ^{1}H-NMR spectra were recorded in a 400 MHz Varian FT spectrometer. Chemical shifts (ppm) were referenced either with an internal standard (Me_4Si) or to the residual solvent peaks. The X-band Electron Paramagnetic Resonance (EPR) spectra were recorded on a JES-FA200 ESR spectrometer, at room temperature and 77 K with microwave power, 0.998 mW; microwave frequency, 9.14 GHz and modulation amplitude, 2. Elemental analyses were obtained from a Perkin Elmer Series II Analyzer. The magnetic moment of complex was measured on a Cambridge Magnetic Balance. DFT calculations were performed on complexes **5.1**, **5.2**, **5.3** and **5.4** from their available experimental data. All the complexes are fully optimized using PBE functional and DNP basis set in the presence of solvent water. The Conductor-like Screening Model (COSMO) as incorporated into the DMol^3 program with dielectric constant of 37.5 is adopted to study the solvent effect.[12]

5.2.2 Synthesis of L_{5a}

A mixture of 1, 2-diaminobenzene (2.16 g) and salicyldehyde (4.88 g) in 30 ml ethanol was stirred at room temperature for 4 hours. The resulting precipitate was filtered and washed with cold ethanol to yield the pure Schiff base, **L_{5a}**. (Yield: ~95%). C, H, N Analysis: calcd. C, 75.93%; H, 5.10%; N, 8.86%; found. C, 75.90%; H, 5.12%; N, 8.89%. FT-IR: 3446, 2851, 1613, 1480, 1276, 1192 and 760 cm^{-1}. ^{1}H-NMR: (400 MHz, $CDCl_3$): δ_{ppm}: 6.89-6.92(2H, d), 7.02-7.05 (2H, t), 7.21-7.234(2H, d), 7.24-7.37 (6H, m) and 8.62 (2H, s). ^{13}C-NMR: (100 MHz, $CDCl_3$): δ_{ppm}: 117.6, 119.1, 119.3, 119.8, 127.8, 132.5, 133.5, 142.6, 161.4 and 163.8.

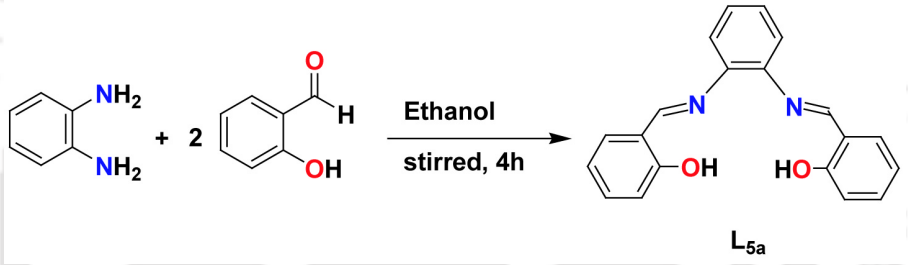

Scheme 5.1

5.2.3 Synthesis of L_5

The Schiff base $\mathbf{L_{5a}}$ was reduced to the corresponding ligand, $\mathbf{L_5}$, using 4 equivalent $NaBH_4$ in methanol solution. The solution was then dried and the crude mixture was dissolved in water, neutralised with acetic acid and the ligand $\mathbf{L_5}$ was extracted with chloroform. The volume of the resulting solution was then reduced in rotary-evaporator to obtain ligand $\mathbf{L_5}$. (Yield: ~90%). C, H, N Analysis: calcd. C, 74.98%; H, 6.29%; N, 8.74%; found C, 74.96%; H, 6.27%; N, 8.78%. FT-IR: 3421, 3289, 2851, 1602, 1506,1491,1454,1238 and 748 cm^{-1}. ^{1}H-NMR: (400 MHz, $CDCl_3$): δ_{ppm}: 4.35(4H, s), 6.80-6.93 (8H, m) and 7.16-7.20 (4H, m).^{13}C-NMR: (100 MHz, $CDCl_3$): δ_{ppm}: 47.7, 114.3, 116.4, 120.4, 121.5, 123.1, 129.4, 136.8 and 156.2.

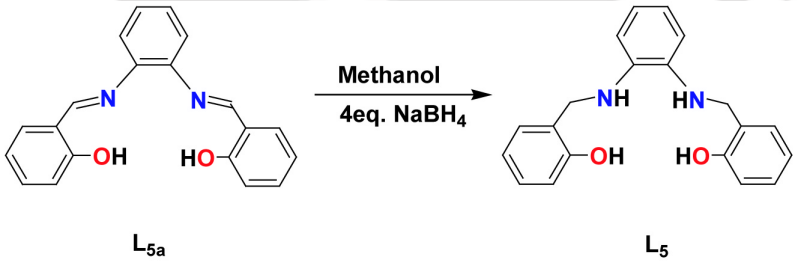

Scheme 5.2

5.2.4 Synthesis of L_{6a}

A mixture of ethylenediamine (1.20g) and salicyldehyde (4.88 g) in 30 ml ethanol was stirred at room temperature for 1 hour. The resulting precipitate was filtered and washed with cold ethanol to yield the pure Schiff base, **L_{6a}**. (Yield: ~95%). C, H, N Analysis: calcd. C, 72.13%; H, 5.30%; N, 10.56%; found C, 72.15%; H, 5.32%; N, 10.51%. FT-IR: 3451, 1636, 1577, 1497, 1283, 1149 and 749 cm^{-1}. ^{1}H-NMR: (400 MHz, $CDCl_3$): δ_{ppm}: 3.93(2H, s), 6.83-6.94 (4H, m), 7.21-7.30 (4H, m), 8.55 (2H, s) and 3.83 (2H, s). ^{13}C-NMR: (100 MHz, $CDCl_3$): δ_{ppm}: 59.8, 117.0, 118.8, 131.6, 132.5, 161.1 and 166.6.

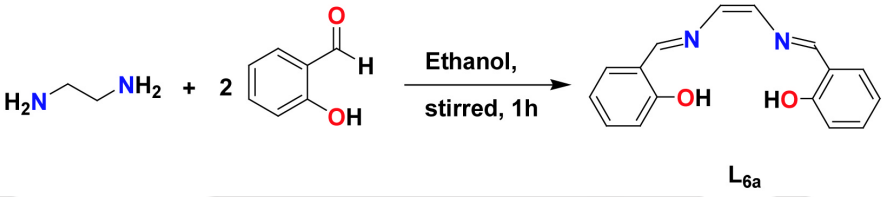

Scheme 5.3

5.2.5 Synthesis of L_6

The Schiff base **L_{6a}** was reduced to the corresponding ligand, **L_6**, using 4 equivalent $NaBH_4$ in methanol solution. The solution was then dried and the crude mixture was dissolved in water, neutralised with acetic acid and the ligand **L_6** was extracted with chloroform. The volume of the solution was then reduced in rotary-evaporator to obtain ligand **L_6**. (Yield: ~95%). C, H, N Analysis: calcd. C, 70.58%; H, 7.29%; N, 10.74%; found C, 70.56%; H, 7.28%; N, 10.77%.

FT-IR: 3463, 3276, 2861, 1615, 1590,1466,1413,1256 and 746 cm^{-1}. ^{1}H-NMR: (400 MHz, $CDCl_3$): δ_{ppm}: 2.81 (4H, s), 3.97(4H, s), 6.74-6.82 (4H, m), 6.94-6.96 (2H, d) and 7.13-7.17 (2H, d). ^{13}C-NMR: (100 MHz, $CDCl_3$): δ_{ppm}: 47.9, 52.6, 116.5, 119.3, 122.3, 128.6, 129.0 and 158.1.

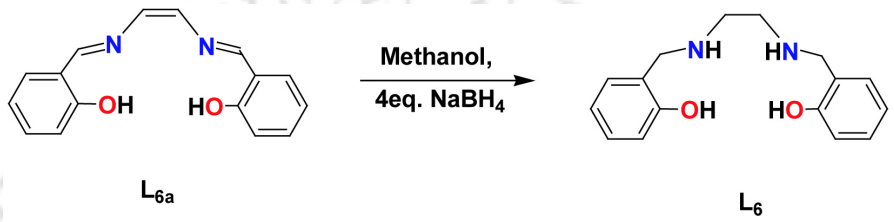

L_{6a} L_6

Scheme 5.4

5.2.6 Synthesis of complex 5.1

$FeCl_3.6H_2O$ (0.270 g, 1 mmol) was dissolved in 15 ml acetonitrile. To this solution, 0.320 g (1 mmol) of the ligand **L_5**, was added slowly with constant stirring. The color of the solution turned into dark pink from light brown. The stirring was continued for 4h at room temperature. The volume of the solution was then reduced to ~2 ml. This resulted into pink colored precipitate of complex **5.1**. Yield 0.525 g (90%). UV-vis. (methanol): λ_{max}, 532 nm (ε, 236 M^{-1} cm^{-1}).The X-Band EPR data (in methanol at RT): g_{av}, 2.007. FT-IR (KBr pellet): 3429, 3180, 2723, 1598, 1455, 1341, 1277, 1239, 1108 and 755 cm^{-1}. The complex **5.1** behaves as

1:1 electrolyte in methanol [Λ_M(Scm^{-1}), 88]. The calculated magnetic moment is found to be 5.77 BM. ESI-Mass (m+ 1), calcd 446.01; found: 445.95.

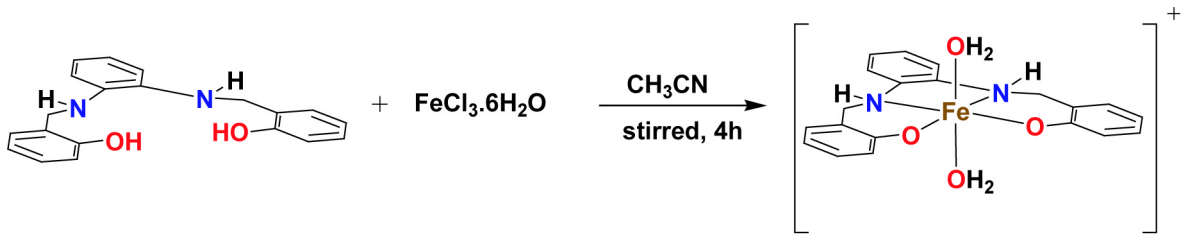

Complex 5.1

Scheme 5.5

5.2.7 Synthesis of complex 5.2

$FeCl_3.6H_2O$ (0.270 g, 1 mmol) was dissolved in 15 ml acetonitrile. To this solution, 0.272 g (1 mmol) of the ligand **L_6,** was added slowly with constant stirring. The color of the solution turned into deep red from light brown. The stirring was continued for 2 h at room temperature. The volume of the solution was then reduced to ~2 ml. This resulted into reddish colored precipitate of complex **5.2**. Yield: 0.504 g (93%). UV-vis. (methanol): λ_{max}, 539 nm (ε, 159 M^{-1} cm^{-1}).The X-Band EPR data (in methanol at RT): g_{av}, 2.006. FT-IR (KBr pellet): 3413,

3180, 2723, 1606, 1501, 1461, 1349, 1267, 1236, 1116 and 765 cm^{-1}. The complex **5.2** behaves as 1:1 electrolyte in methanol solution [$\Lambda_M(Scm^{-1})$, 85]. The calculated magnetic moment is found to be 5.87 BM. ESI-Mass (m+ 1), calcd 398.66; found: 398.98.

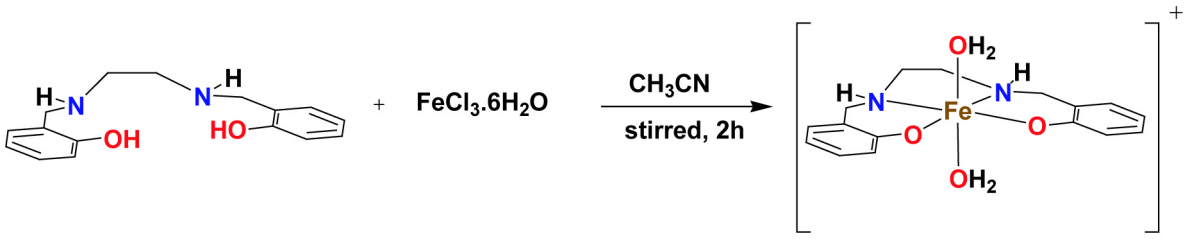

Complex 5.2

Scheme 5.6

5.2.8 Synthesis of complex 5.3

Complex **5.1** (0.820 g, 2.0 mmol) was dissolved in ~10 ml of dry and degassed methanol. To this solution NO gas was purged for 1 minute. After removing the excess NO by several cycles of vacuum purge, the resulting yellowish solution was allowed to stand at room temperature for 1 h. The volume of the solution was reduced under nitrogen atmosphere in a schlenk tube and layered with ~5 ml of ether. The solution was then kept overnight under freezer to obtain yellow colored precipitate. The precipitate was filtered off and dried to get solid complex **5.3**.

Yield: 0.550 g (66%). C, H, N Analysis: calcd. C, 56.89%; H, 4.77%; N, 9.95%; found C, 56.86%; H, 4.75%; N, 9.99%. FT-IR (KBr pellet): 3389, 2940, 2853, 1657, 1453, 1397, 1030 and 658 cm^{-1}. ESI-Mass (m+ 1), calcd 423.01; found: 422.99.

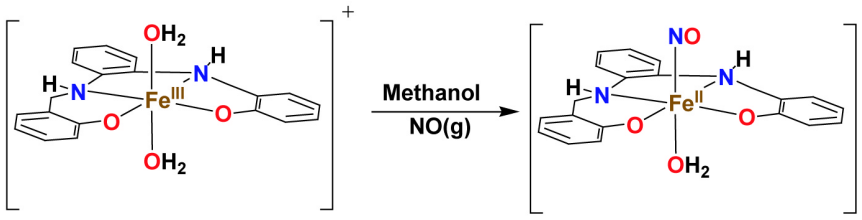

Complex 5.1 Complex 5.3

Scheme 5.7

5.2.9 Synthesis of complex 5.4

Similar procedure was followed for complex **5.4** as mentioned for complex **5.3**. For this, complex **5.2** (0.724 g, 2.0 mmol) was dissolved in ~10 ml of dry and degassed methanol. To this solution NO gas was purged for 1 minute. After removing the excess NO by several cycles of vacuum purge, the resulting light yellowish solution was allowed to stand at room temperature for 1 h. The volume of the solution was reduced under nitrogen atmosphere in a schlenk tube and layered with ~5 ml of ether. The solution was then kept overnight under freezer to obtain light yellow colored precipitate. The precipitate was filtered off and dried to get solid complex **5.4**. Yield: 0.525 g (71%). C, H, N Analysis: calcd. C, 51.36%; H, 5.39%; N,

11.23%; found C, 51.38%; H, 5.40%; N, 11.21%. FT-IR (KBr pellet): 3421, 2947, 2843, 1648, 1453, 1309, 1028 and 683 cm^{-1}. ESI-Mass (m + 1), calcd 375.11; found: 375.16.

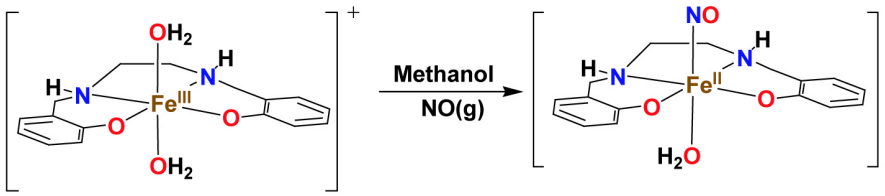

Complex 5.2 Complex 5.4

Scheme 5.8

5.3 Results and discussion

The salan ligands were prepared by reducing the corresponding salen analogues using sodium borohydride.[13] The microanalyses and spectral characterization confirmed the formulation of the ligands unambiguously (experimental section). The Fe(III) complexes, **5.1** and **5.2** were prepared by treating iron(III) chloride, hexahydrate with equivalent amount of the ligands $\mathbf{L_5}$ and $\mathbf{L_6}$, respectively, in acetonitrile (experimental section). The complexes were characterized by UV-visible, FT-IR, X-band EPR and ESI-mass spectroscopy (Appendix IV and figure 5.2). The micro analytical data of complexes **5.1** and **5.2** showed good agreement with the calculated values (experimental section). Even after several attempts, the X-ray quality crystals were not grown.

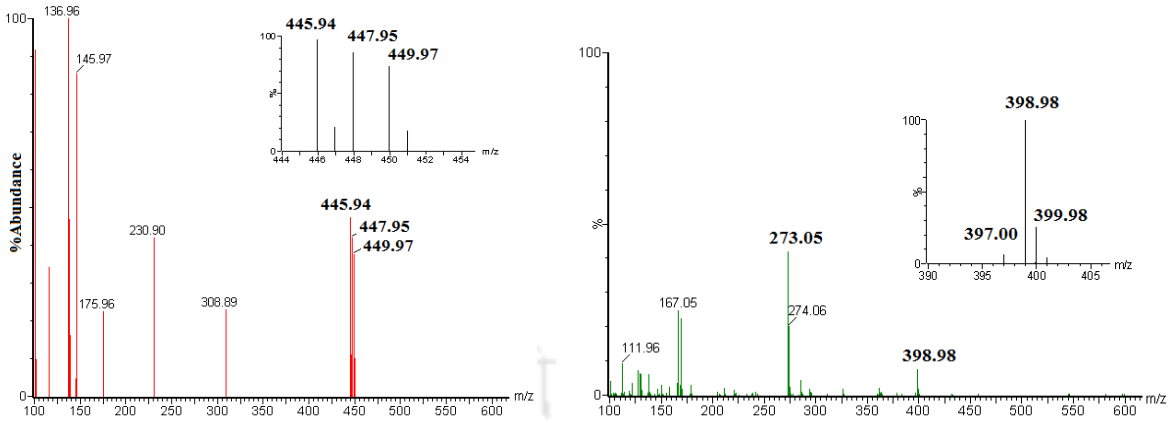

(a) **(b)**

Figure 5.2 ESI-mass spectra of complexes **5.1** (a) and **5.2** (b) in methanol.

5.3.1 Nitric oxide reactivity

Complex **5.1** in methanol solution shows absorption band centered at 532 nm with strong intra-ligand absorptions in the UV-region. Upon addition of NO to the dry and degassed methanol solution of complex **5.1**, the 532 nm band disappeared with a pseudo first order rate constant 1.2119×10^{-4} sec^{-1}(Figure 5.3 (a), inset).

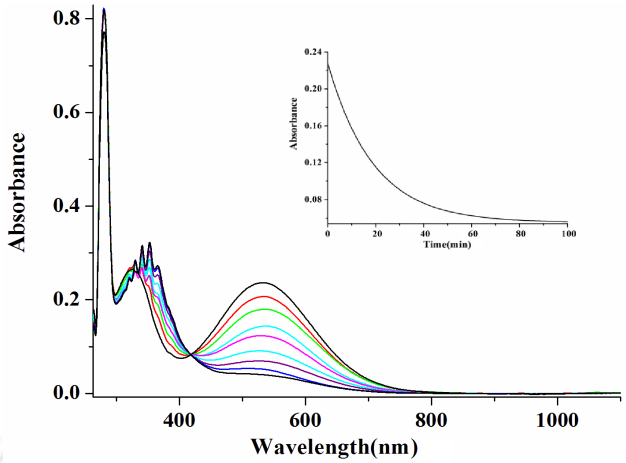

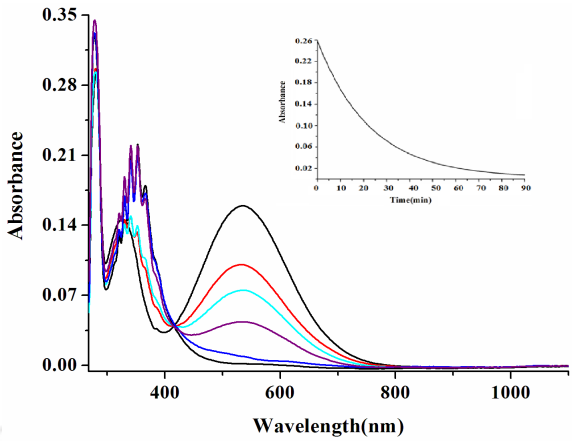

(a) **(b)**

Figure 5.3 UV-visible spectra of complex **5.1** (a) and **5.2** (b) before and after purging NO in methanol. [Inset: Time scan plot of (a) 532 nm and (b) 539 nm band after addition of NO].

In case of complex **5.2**, the absorption band at 539 nm was disappeared upon addition of excess NO following a pseudo first order rate constant, 7.302×10^{-4} sec^{-1}(Figure 5.3 (b), inset).

In solution FT IR studies, new stretching bands were appeared at 1657 and 1648 cm^{-1} on addition of excess NO to the dry and degassed methanol solution of complexes **5.1** and **5.2**, respectively (Figure 5.4). Addition of only one equivalent NO did not result in the formation of this new stretching frequency. However, the reduction of Fe(III) center was evidenced by UV-visible and EPR spectral studies. GC mass analyses of the reaction mixture displayed the presence of methyl nitrite suggesting the formation of NO^{+} during the reaction. With other heme and non-heme Fe(III) complexes it was found that the reaction with excess NO lead to the reductive nitrosylation resulting in corresponding Fe(II)-nitrosyls.[14] In the present case, the new stretching bands at 1657 and 1648 cm^{-1} were shifted upon labeling with ^{15}NO. Thus, these are attributed to the stretching frequency of υ_{NO} in Fe(II)-nitrosyls. In absence of moisture, these bands were found to be stable. For non-heme iron-nitrosyl complexes having $\{FeNO\}^{7}$ configuration, this frequency is quite lower compared to the other reported complexes.[15] However, this is consistent with the frequency of a iron-nitrosyl complex having $[Fe^{III}\text{-}NO^{-}]$ formulation with nitroxyl-like character.[16]

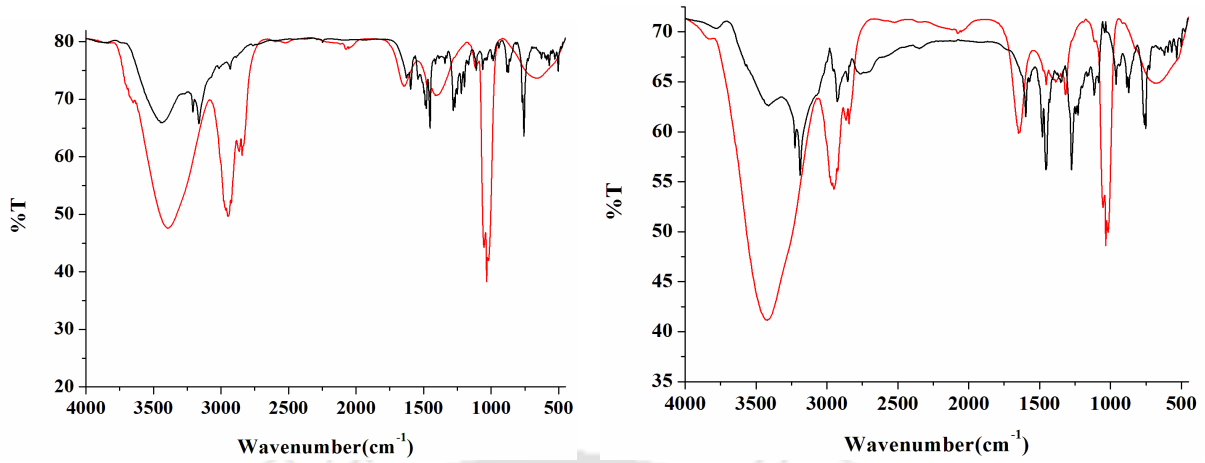

(a) **(b)**

Figure 5.4 IR spectra of complexes **5.1** (a) and **5.2** (b) before (black trace) and after (red trace) purging NO in methanol.

Thus, it is assumed that in the initial stage one equivalent of NO reacts with complexes **5.1** and **5.2** to afford the reduction of the Fe(III) centers in the respective complexes. In the subsequent steps, excess NO reacts with the corresponding Fe(II) centers to results in the Fe(II)-nitrosyls.

The Fe(II)-nitrosyl complexes were found to be stable and were isolated as solids. The spectral characterization of the complexes has been done (Figures 5.5 and appendix IV). Expected and observed fragmentation in mass spectroscopy is found satisfactory (Appendix IV). However, we could not grow the X-ray quality crystals of the complexes.

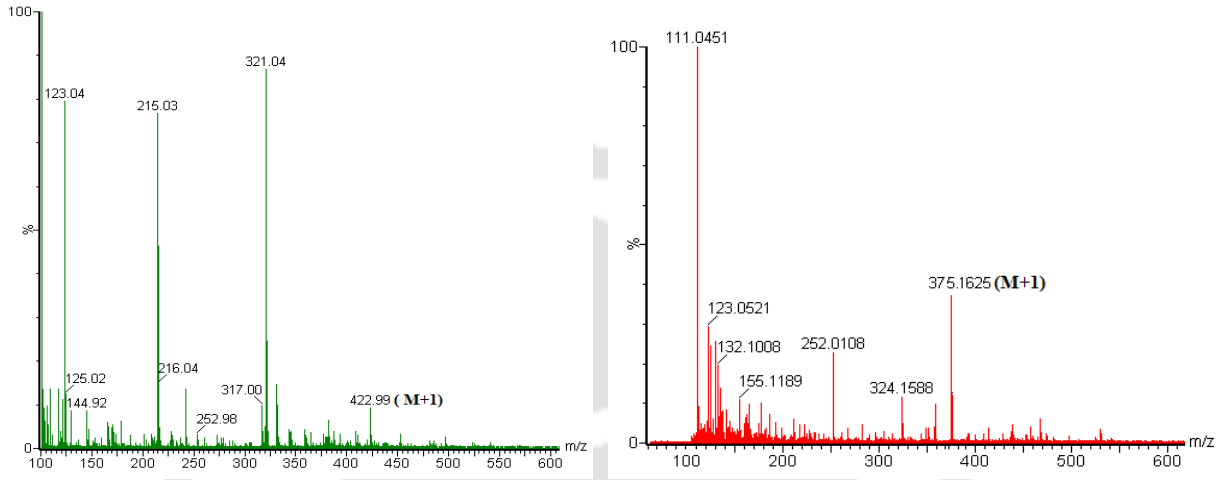

(a) **(b)**

Figure 5.5 ESI-mass spectra of complexes **5.3** (a) and **5.4** (b) in methanol.

It would be worth to mention here that Caulton and coworkers earlier demonstrated the role of NO as a reducing agent in reactions with metal salts.[17] $FeCl_2$ and $CoCl_2$ were found to react with NO in the presence of methanol and amines (base), to form metal nitrosyls and alkyl nitrite.[18] Other non-heme iron(III) complexes dithiocarbamate complexes, such as

(Fe^{III}(MGD)), iron(III) (dithiocarboxy)sarcosine (Fe^{III}(DTCS)), the antitumor agent iron(III) bleomycin (Fe^{III}(Blm)), $[Fe(bpb)(py)_2]ClO_4$ (H_2bpb) 1, 2-bis(picolinamido)benzene), and Fe(pyN_4) (pyN_4) 2, 6-$C_5H_3N[CMe(CH_2NH_2)_2]_2$ were reported to display similar reactivity.[19] However, in this regard, the most extensively studied non-heme iron(III) system is nitroprusside, $[Fe(CN)_5(NO)]^{2-}$.[18]

5.3.2 DFT analysis

Since, the crystal structures of the Fe(III) complexes and corresponding Fe(II)-nitrosyls were not grown, the DFT studies have been done on these complexes. The optimized structures of all the four complexes are shown in figures 5.6-5.11 and their selected geometric parameters are given in table 5.1. It is seen from figures 5.6-5.11 and table 5.1 that the structures of the complexes are in very good agreement with the experimental data of similar complexes. From the DFT calculations, it has been found that for complexes **5.3** and **5.4**, the calculated geometry is distorted octahedral with the NO group coordinated to the iron at an axial site. One solvent water molecule is coordinated to the metal center from other axial position. In the structurally characterized iron(II)–nitrosyl complexes, the NO group was reported to be coordinated to the iron centre at an axial site.[20] In the cases of complexes **5.3** and **5.4** the calculated geometry also suggests a bent geometry for NO coordination to the iron centre with an angle of 119.64°. The Fe–$N_{(NO)}$ and N–O distances are calculated to be 1.710 Å and 1.199 Å, respectively. These distances are little longer than the structurally reported one.[15,16] It would be interesting to note that the DFT analysis suggests that the Fe–NO bond is formed by the back donation from π*

orbital of NO ligand of the *d*-orbitals of Fe (Figures 5.10 and 5.11). The HOMO and LUMO energy values were also calculated in the presence of solvent. The HOMO orbital is mainly localized on the NO group and Fe atom whereas the LUMO orbital is localized mainly on NO group.

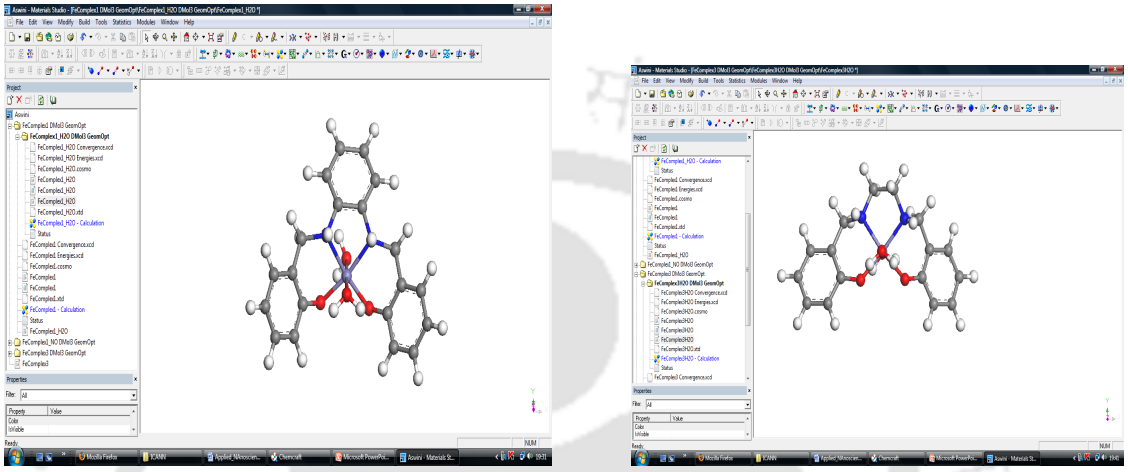

(a) **(b)**

Figure 5.6 Optimized structures of complexes **5.1** (a) and **5.2** (b).

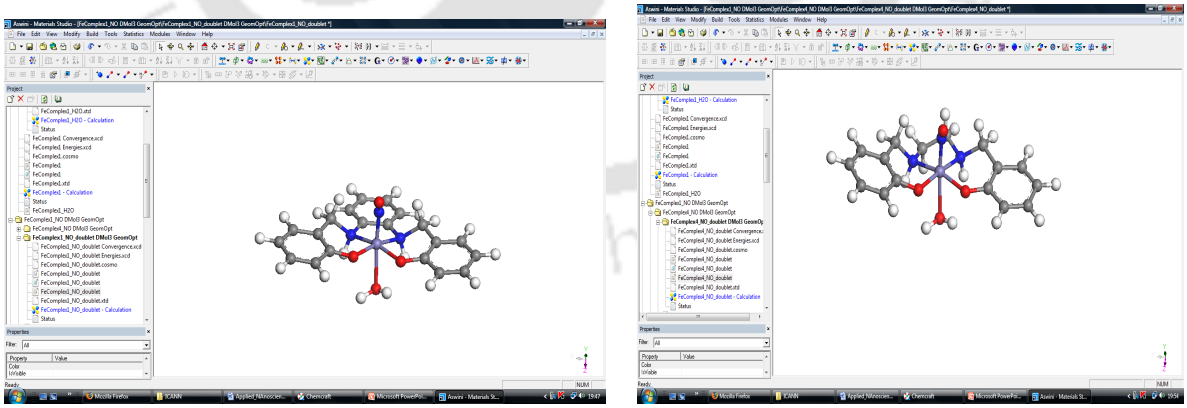

(a) **(b)**

Figure 5.7 Optimized structures of complexes **5.3** (a) and **5.4** (b).

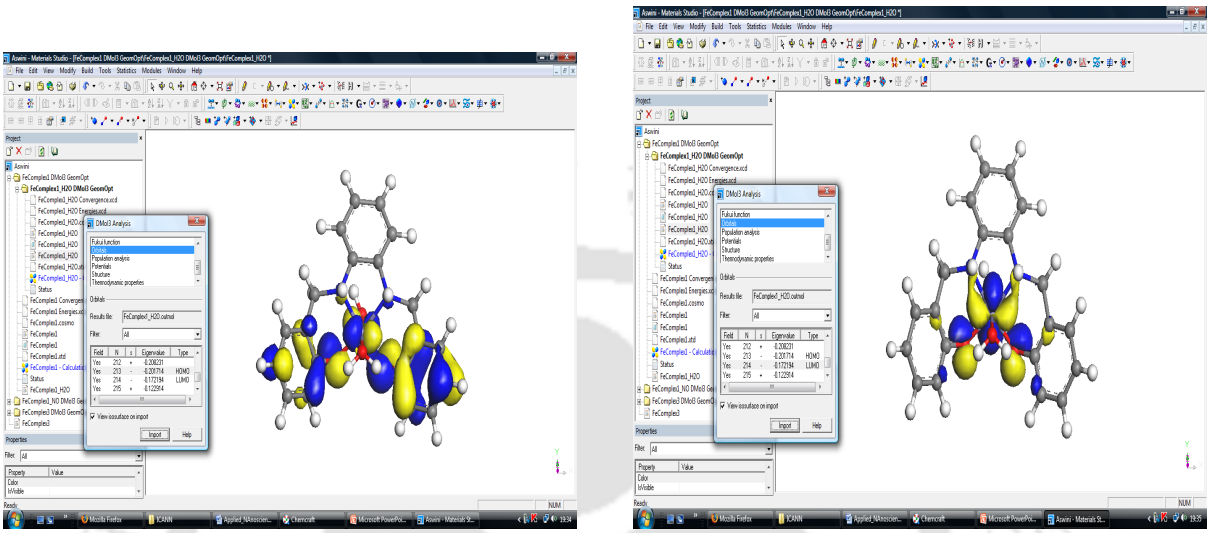

HOMO LUMO (d_{xy} and p_y orbitals of two oxygen)

Figure 5.8 HOMO-LUMO orbitals of the complex **5.1** showing the Fe-N bond.

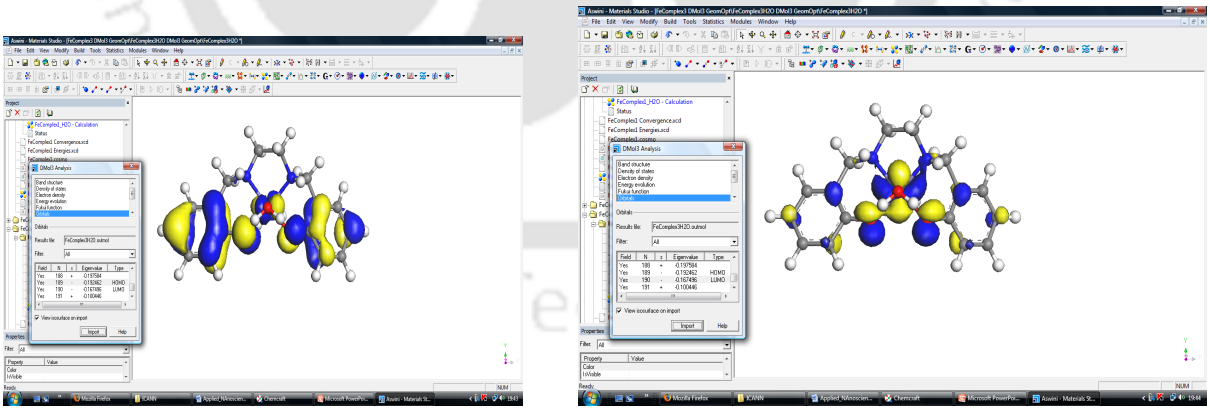

HOMO LUMO (d_{xy} and p_y orbitals of two oxygen)

Figure 5.9 HOMO-LUMO orbitals of the complex **5.2** showing the Fe-N bond.

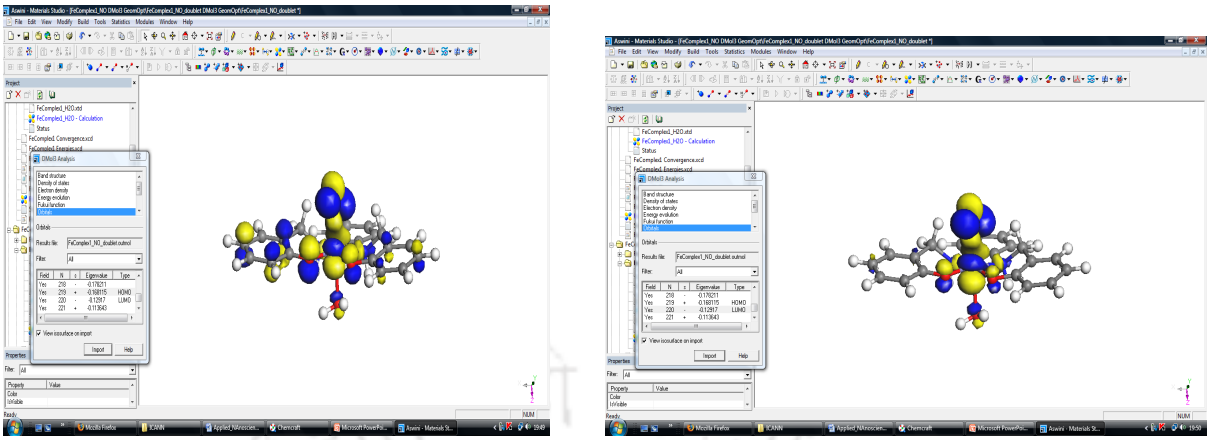

HOMO LUMO

Figure 5.10 HOMO-LUMO orbitals of the complex **5.3** showing the Fe-N bond.

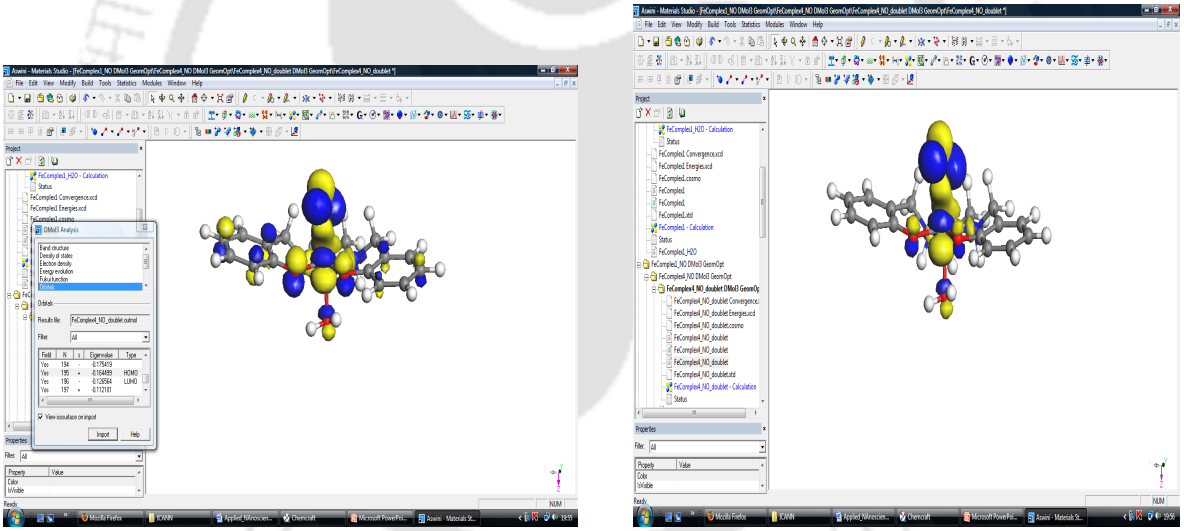

HOMO LUMO

Figure 5.11 HOMO-LUMO orbitals of the complex **5.4** showing the Fe-N bond.

Table 5.1 Selected metric parameters of the complexes optimized at PBE/DNP level of calculation.

	Complex **5.1**	Complex **5.2**	Complex **5.3**	Complex **5.4**
Fe1-O1	2.031	2.038	2.352	2.294
Fe1-O2	1.894	1.899	1.938	1.953
Fe1-O3	1.890	1.899	1.919	1.934
Fe1-O5	2.047	2.039	-	-
Fe1-N1	2.066	2.021	2.026	2.025
Fe1-N2	2.069	2.033	2.035	2.024
Fe1-N3	-	-	1.710	1.713
N3-O4	-	-	1.199	1.199

5.4 Conclusion

Two Fe(III) complexes, **5.1** and **5.2** of salan ligands, $\mathbf{L_5}$ and $\mathbf{L_6}$, respectively, were prepared and characterized. Addition of excess NO to the dry and degassed methanol solution of complexes **5.1** and **5.2** resulted in the reductive nitrosylation of the iron centers leading to the formation of corresponding Fe(II)-nitrosyl complexes, **5.3** and **5.4**, respectively. The Fe(II)-nitrosyls were isolated as solid and characterized. DFT calculations were performed to optimize the structures of the complexes.

5.5 Reference

1. (a) Nitric Oxide: Biology and Pathobiology; Ignarro, L., Ed.; Academic Press: San Diego, 2000. (b) Wink, D. A.; Mitchell, J. B. *Free Radical Biol. Med*. **1998**, *25*, 434.
2. (a) Martin, C. T.; Morse, R. H.; Kanne, R. M.; Gray, H. B.; Malmstrom, B. G.; Chan, S. I. *Biochemistry* **1981**, *20*, 5147. (b) Cooper, C. E.; Torres, J.; Sharpe, M. A.; Wilson, M. T. *FEBS Lett.* **1997**, *414*, 281. (c) Richter-Addo, G. B.; Legzdins, P. *Metal Nitrosyls*; Oxford University Press: New York, 1992. (d) Studbauer, G.; Giuffre, P.; Sarti, P. *J. Biol. Chem.* **1999**, *274*, 28128. (e) McCleverty, J. A. *Chem. Rev.* **2004**, *104*, 403.
3. (a) Kim, S.; Deinum, G.; Gardner, M. T.; Marletta, M. A.; Babcock, G. T. *J. Am. Chem. Soc.* **1996**, *118*, 8769. (b) Burstyn, J. N.; Yu, A. E.; Dierks, E. A.; Hawkins, B. K.; Dawson, B. K. *Biochemistry* **1995**, *34*, 5896.
4. (a) Moncada, S.; Palmer, R. M. J.; Higgs, E. A. *Pharmacol. Rev.* **1991**, *43*, 109. (b) Feldman, P. L.; Griffith, O. W.; Stuehr, D. J. *Chem. Eng. News* **1993**, *71*, 10. (c) Butler, A. R.; Williams, D. L. *Chem. Soc. Rev.* **1993**, 233.
5. (a) *Methods in Nitric Oxide Research*; Feelisch, M., Stamler, J. S., Eds.; John Wiley and Sons: Chichester, England, 1996 and references therein. (b) Wink, D. A.; Hanbauer, I.; Grisham, M. B.; Laval, F.; Nims, R. W.; Laval, J.; Cook, J.; Pacelli, R.; Liebmann, J.; Krishna, M.; Ford, P. C.; Mitchell, J. B. *Curr. Top. Cell. Regul.* **1996**, *34*, 159. (c) *Nitric*

Oxide and Infection; Fang, F. C., Ed.; Kluwer Academic/ Plenum Publishers: New York, 1999.

6. Cozzi, P. G. *Chem. Soc. Rev.* **2004**, *33*, 410.
7. (a) McGarrigle, E. M.; Gilheany, D. G. *Chem. Rev.* **2005**, *105*, 1563. (b) Darensbourg, D. J. *Chem. Rev*. **2007**, *107*, 2388. (c) Coates, G. W.; Moore, D. R. *Angew. Chem. Int. Ed.* **2004**, *43*, 6618.
8. (a) Fujii, H.; Funahashi, Y. *Angew. Chem. Int. Ed.* **2002**, *41*, 3638. (b) Kurahashi, T.; Oda, K.; Sugimoto, M.; Ogura, T.; Fujii, H. *Inorg. Chem*. **2006**, *45*, 7709. (c) Snyder, B. S.; Patterson, G. S.; Abrahamson, A. J.; Holm, R. H. *J. Am. Chem. Soc*. **1989**, *111*, 5214.
9. Whiteoak, C. J.; de Rosales, R. T. M.; White, A. J. P.; Britovsek, G. J. P. *Inorg. Chem.* **2010**, *49*, 11106.
10. Matsumoto, K.; Saito, B.; Katsuki, T. *Chem. Commun.* **2007**, 3619.
11. (a) Borer, L.; Thalken, L.; Ceccarelli, C.; Glick, M.; Zhang, J. H.; Reiff, W. M. *Inorg. Chem*. **1983**, *22*, 1719. (b) Borer, L.; Thalken, L.; Zhang, J. H.; Reiff, W. M. *Inorg. Chem*. **1983**, *22*, 3174.
12. (a) Andzelm, J.; Koelmel, C.; Klamt, A. *J. Chem. Phys.* **1995**, ***103,*** 9312. (b) Delly, B. *J. Chem. Phys*. **1990**, *92*, 508. (c) Frisch, M. J.; Trucks, G. W.; Schlegel, H. B.; Scuseria, G. E.; Robb, M. A.; Cheeseman, J. R.; Montgomery, J. A. Jr.; Vreven, T.; Kudin, K. N.; Burant, J. C.; Millam, J. M.; Iyengar, S. S.; Tomasi, J.; Barone, V.; Mennucci, B.; Cossi, M.; Scalmani, G.; Rega, N.; Petersson, G. A.; Nakatsuji, H.; Hada, M.; Ehara, M.; Toyota, K.; Fukuda, R.; Hasegawa, J.; Ishida, M.; Nakajima, T.; Honda, Y.; Kitao, O.; Nakai, H.; Klene, M.; Li, X.; Knox, J. E.; Hratchian, H. P.; Cross, J. B.; Bakken, V.; Adamo, C.;

Jaramillo, J.; Gomperts, R.; Stratmann, R. E.; Yazyev, O.; Austin, A. J.; Cammi, R.; Pomelli, C.; Ochterski, J. W.; Ayala, P. Y.; Morokuma, K.; Voth, G. A.; Salvador, P.; Dannenberg, J. J.; Zakrzewski, V. G.; Dapprich, S.; Daniels, A. D.; Strain, M. C.; Farkas, O.; Malick, D. K.; Rabuck, A. D.; Raghavachari, K.; Foresman, J. B.; Ortiz, J. V.; Cui, Q.; Baboul, A. G.; Clifford, S.; Cioslowski, J.; Stefanov, B. B.; Liu, G.; Liashenko, A.; Piskorz, P.; Komaromi, I.; Martin, R. L.; Fox, D. J.; Keith, T.; Al-Laham, M. A.; Peng, C. Y.; Nanayakkara, A.; Challacombe, M.; Gill, P. M. W.; Johnson, B.; Chen, W.; Wong, M. W.; Gonzalez, C.; Pople, J. A. *Gaussian 03*, revision A.1; Gaussian, Inc.: Pittsburgh PA, 2003.

13. (a) Song, F.; Wei, G.; Wang, L.; Jiao, J.; Cheng, Y.; Zhu, C. *J. Org. Chem.* **2012**, *77*, 4759. (b) Du, G.; Fanwick, P. E.; Abu-Omar, M. M. *Inorg. Chim. Acta*. **2008**, *361*, 3184.
14. (a) Fujii, S.; Kobayashi, K.; Tagawa, S.; Yoshimura, T. *Dalton Trans*. **2000**, *19*, 3310. (b) Vanin, A. F.; Liu, X.; Samouilov, A.; Stukan, R. A.; Zweier, J. L. *Biochim. Biophys. Acta*. **2000**, *1474*, 365.
15. (a) Berto, T. C.; Hoffman, M. B.; Murata, Y.; Landenberger, K. B.; Alp, E. E.; Zhao, J.; Lehnert, N. *J. Am. Chem. Soc.* **2011**, *133*, 16714. (b) Feig, A. L.; Bautista, M. T.; Lippard, S. J. *Inorg. Chem*. **1996**, *35*, 6892.
16. Jiang, Y.; Hayashi, T.; Matsumura, H.; Do, L. H.; Majumdar, A.; Lippard, S. J.; Moënne-Loccoz, P. *J. Am. Chem. Soc*. **2014**, *136*, 12524.
17. (a) Gwost, D.; Caulton, K. G. *J. Chem. Soc., Chem. Commun*. **1973**, *3*, 64. (b) Gwost, D.; Caulton, K. G. *Inorg. Chem.* **1973**, *12*, 2095.
18. Ford, P. C.; Fernandez, B. O.; Lim, M. D. *Chem. Rev*. **2005,** *105*, 2439.

19. (a) Fujii, S.; Yoshimura, T. *Coord. Chem. Rev*. **2000**, *198*, 89. (b) Chikira, M.; Iiyama, T.; Sakamoto, K.; Antholine, W. E.; Petering, D. H. *Inorg. Chem*. **2000**, *39*, 1779. (c) Iiyama, T.; Chikira, M.; Oyoshi, T.; Sugiyama, H. *J. Biol. Inorg. Chem.* **2003**, *8*, 135. (d) Patra, A. K.; Rose, M. J.; Olmstead, M. M.; Mascharak, P. K. *J. Am. Chem. Soc*. **2004**, *126*, 4780. (e) Lopez, J. P.; Heinemann, F. W.; Prakash, R.; Hess, B. A.; Horner, O.; Jeandey, C.; Oddou, J. L.; Latour, J.-M.; Grohmann, A. *Chem.-Eur. J.* **2002**, *8*, 5709.

20. (a) Lo, F-C.; Li, Ya-W.; Hsu, I.-J.; Chen, Chien-H.; Liaw, Wen-F. *Inorg. Chem.* **2014**, *53*, 10881. (b) Speelman, A. L.; Lehnert, N. *Acc. Chem. Res*. **2014**, *47*, 1106. (c) Majumdar, A.; Lippard, S. J. *Inorg. Chem*. **2013**, *52*, 13292. (d) Tonzetich, Z. J.; Heroguel, F.; Do, L. H.; Lippard, S. J. *Inorg. Chem*. **2011**, *50*, 1570.

Appendix I

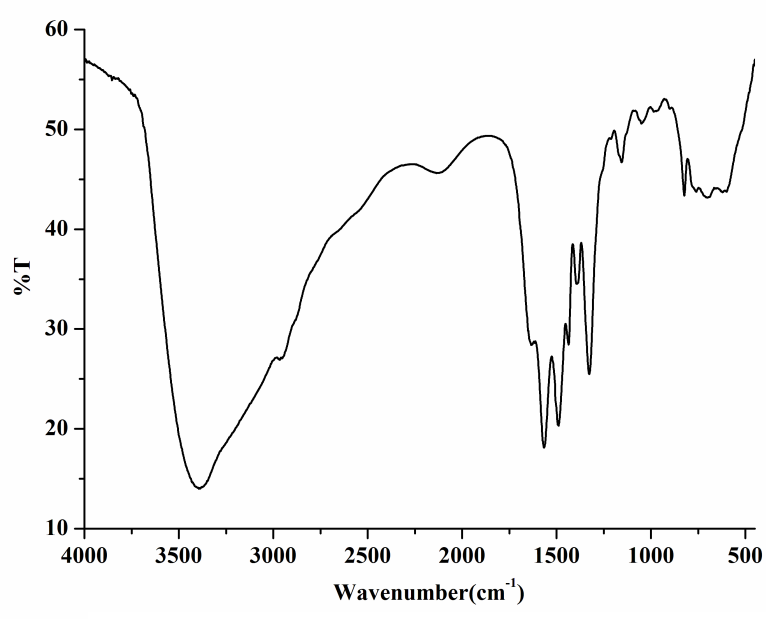

Figure A1.1 FT-IR spectrum of ligand $\mathbf{L_1}$ in KBr pellet.

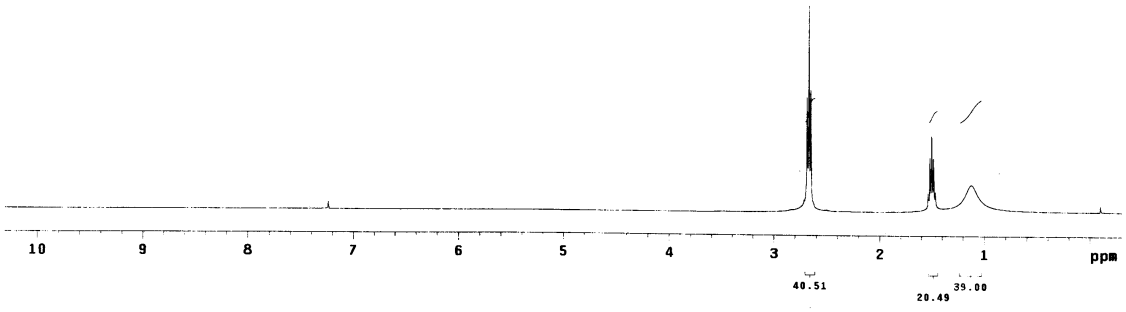

Figure A1.2 ^{1}H-NMR spectrum of ligand $\mathbf{L_1}$ in $CDCl_3$.

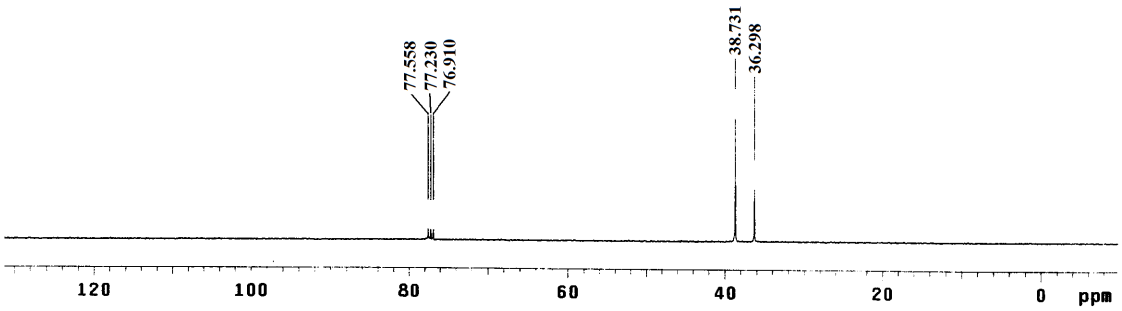

Figure A1.3 ^{13}C-NMR spectrum of ligand $\mathbf{L_1}$ in $CDCl_3$.

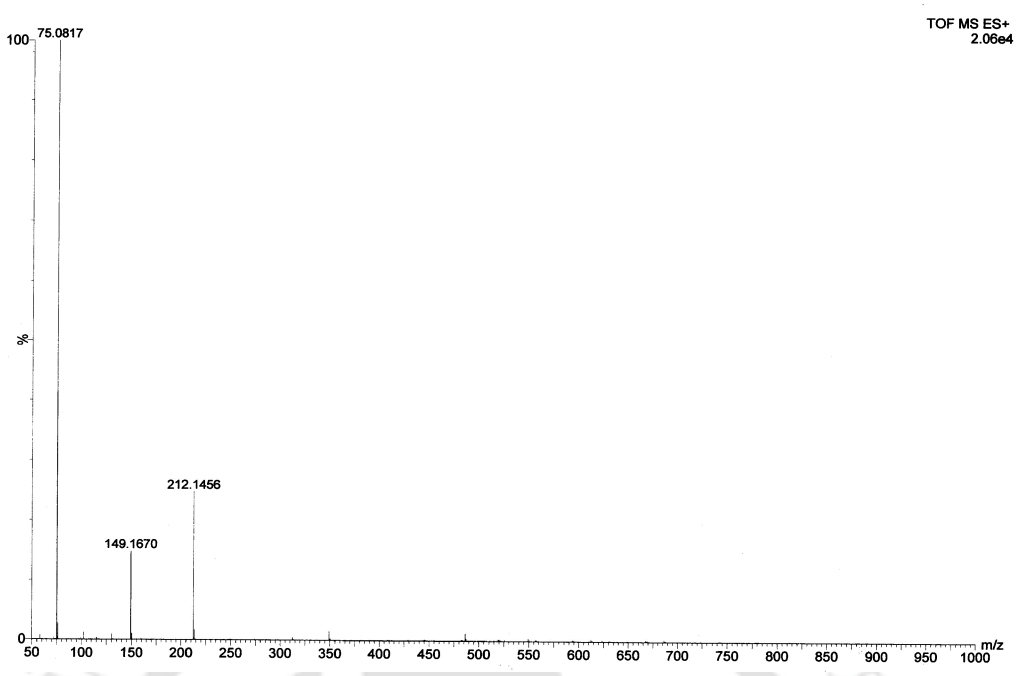

Figure A1.4 ESI mass spectrum of ligand $\mathbf{L_1}$ in methanol.

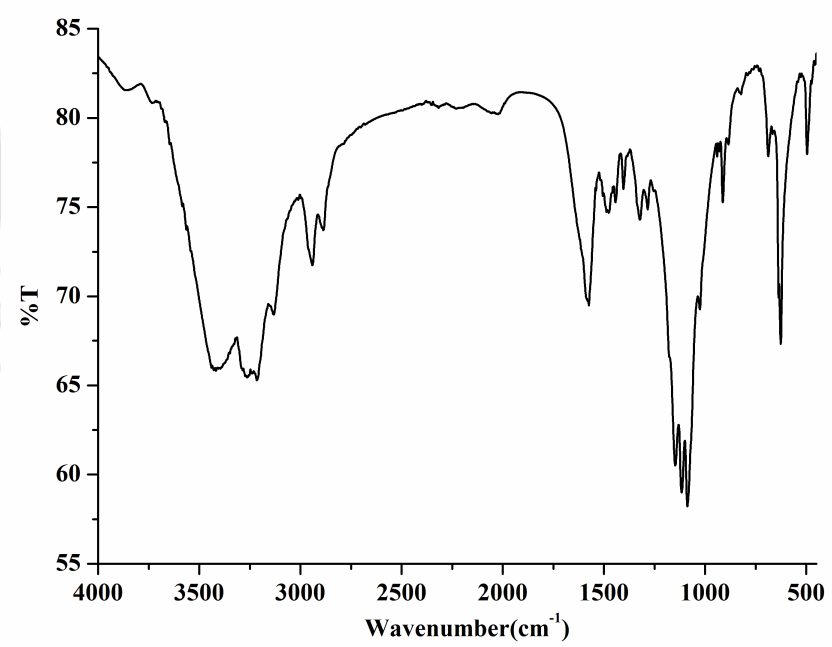

Figure A1.5 FT-IR spectrum of complex **2.1** in KBr pellet.

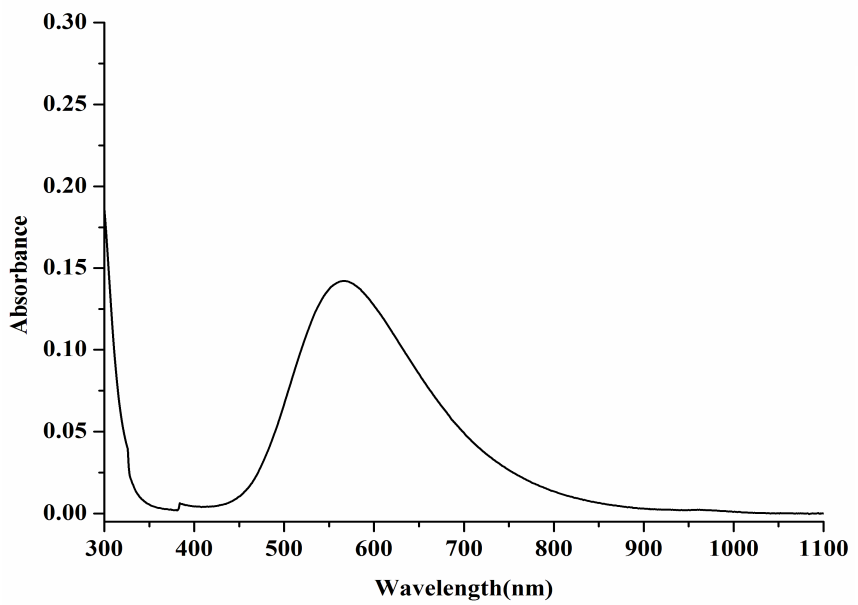

Figure A1.6 UV-visible spectrum of complex **2.1** in acetonitrile.

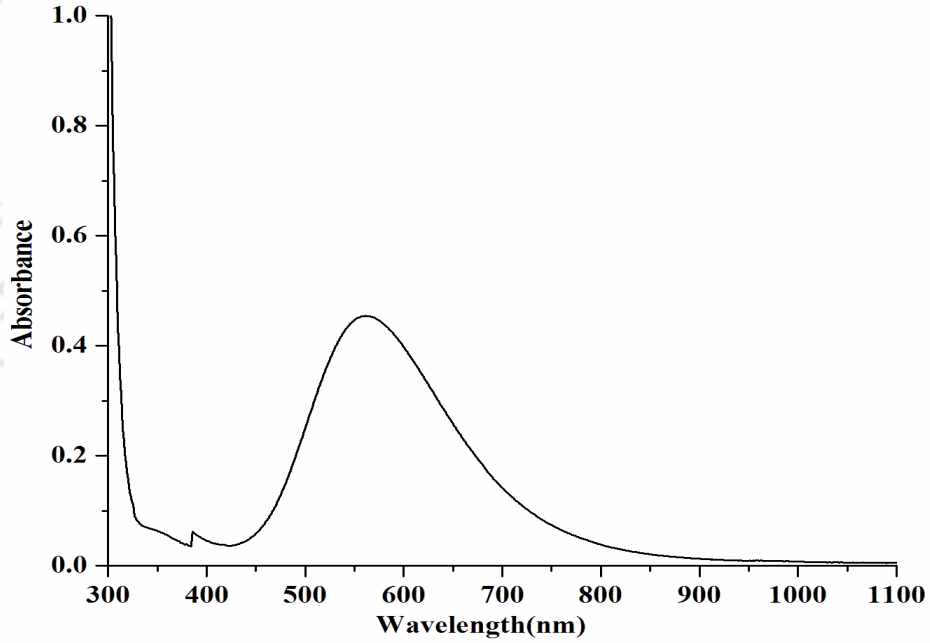

Figure A1.7 UV-visible spectrum of complex **2.1** in methanol.

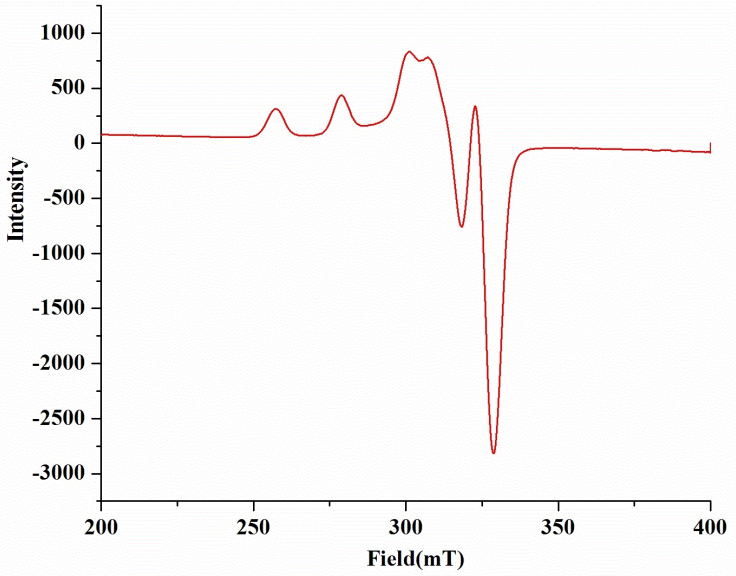

Figure A1.8 X-Band EPR spectrum of complex **2.1** in acetonitrile at 77 K.

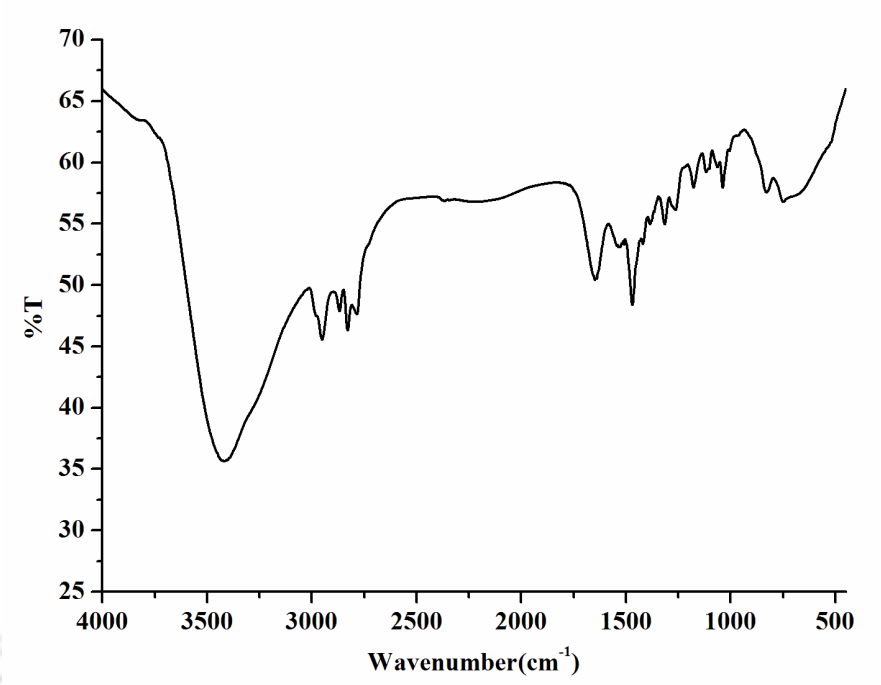

Figure A1.9 FT-IR spectrum of ligand $\mathbf{L_2}$ in KBr pellet.

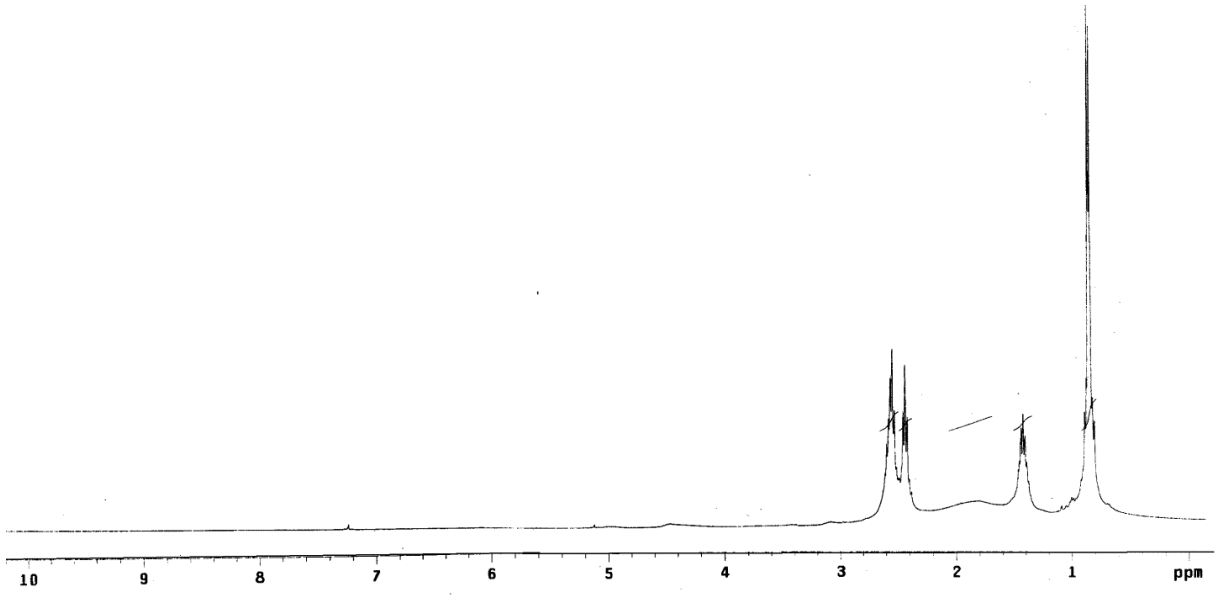

Figure A1.10 ^{1}H-NMR spectrum of ligand $\mathbf{L_2}$ in $CDCl_3$.

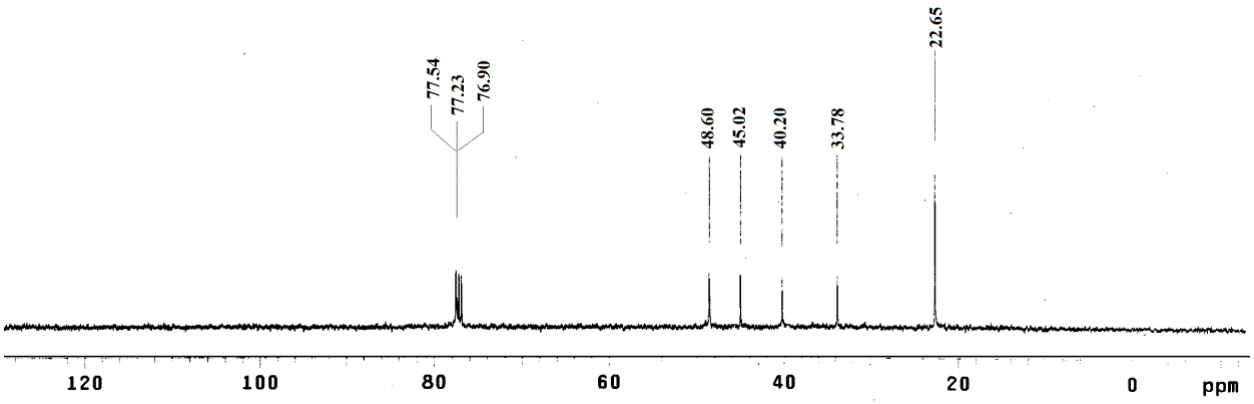

Figure A1.11 ^{13}C-NMR spectrum of ligand $\mathbf{L_2}$ in $CDCl_3$.

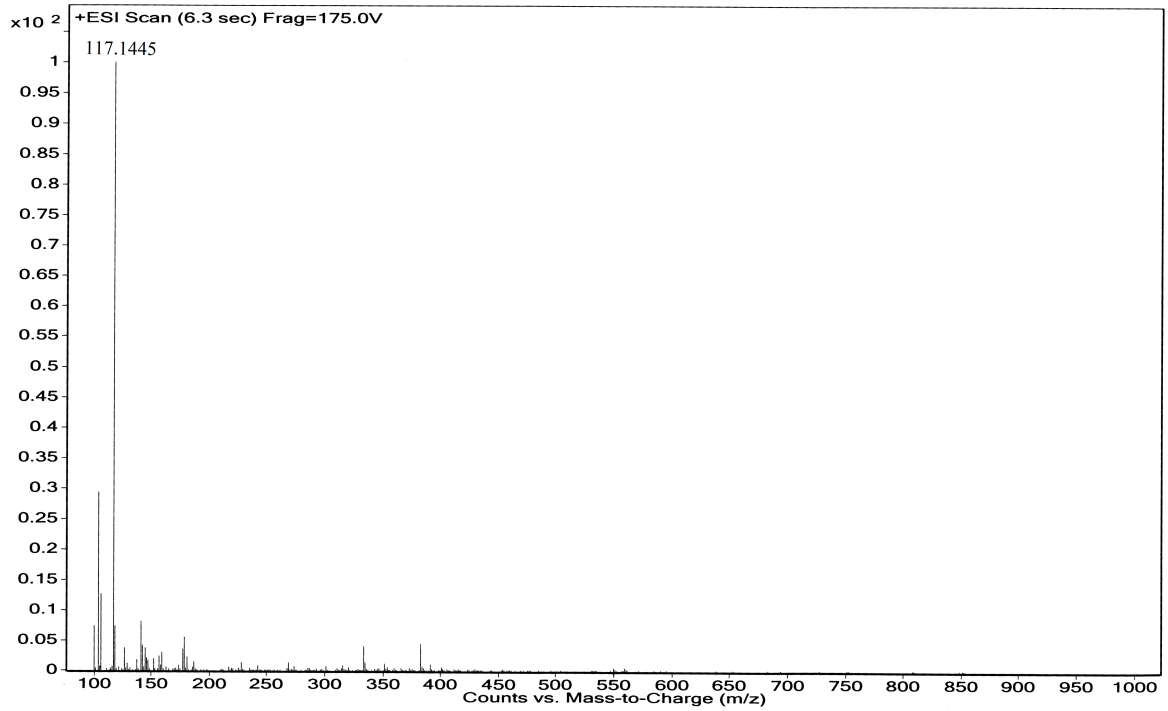

Figure A1.12 ESI mass spectrum of ligand $\mathbf{L_2}$ in acetonitrile.

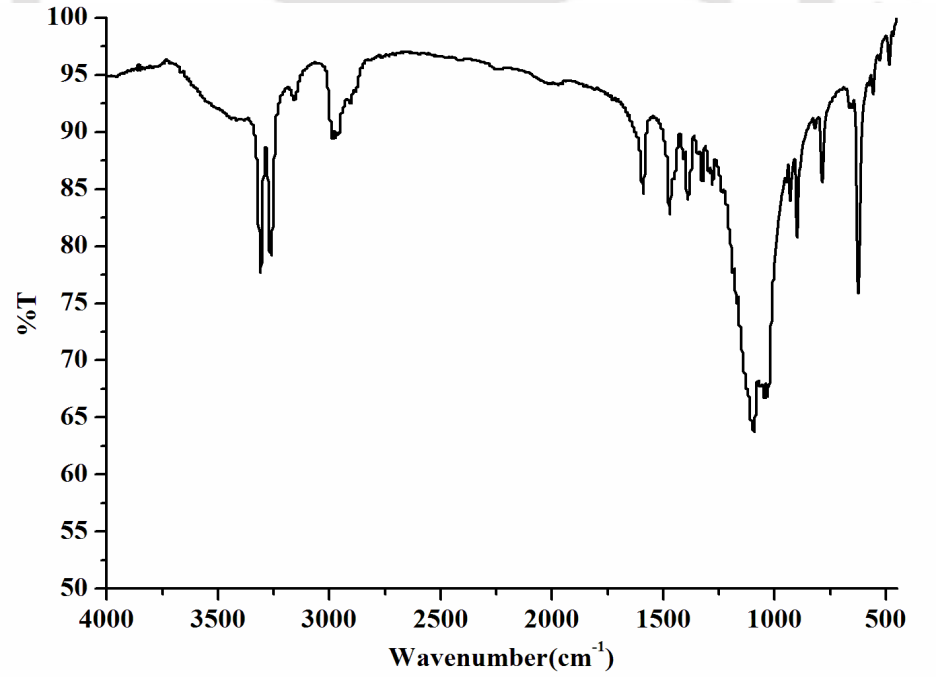

Figure A1.13 FT-IR spectrum of complex **2.2** in KBr pellet.

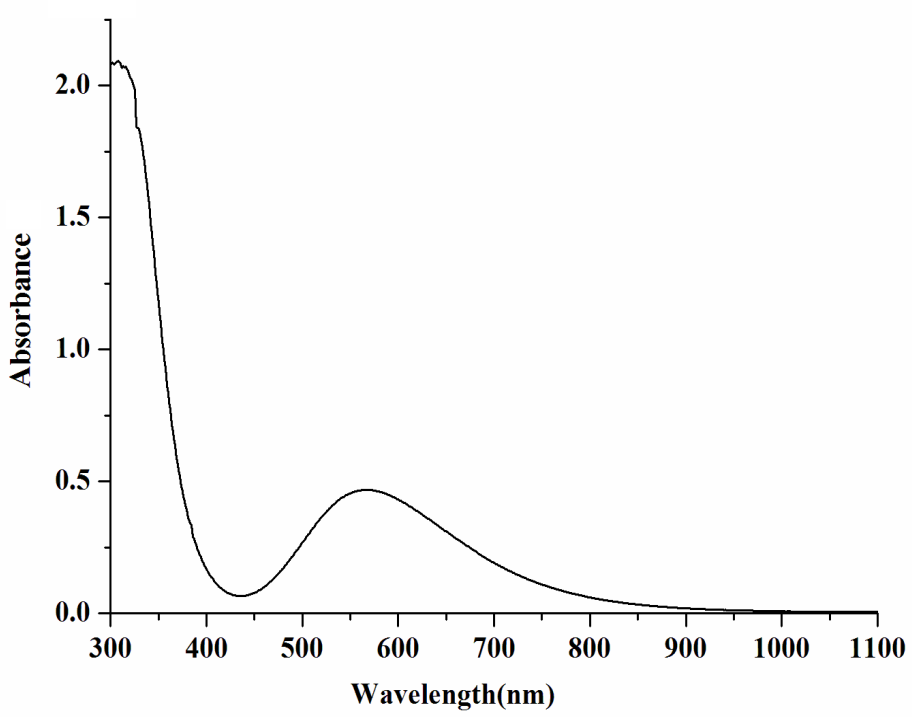

Figure A1.14 UV-visible spectrum of complex **2.2** in acetonitrile.

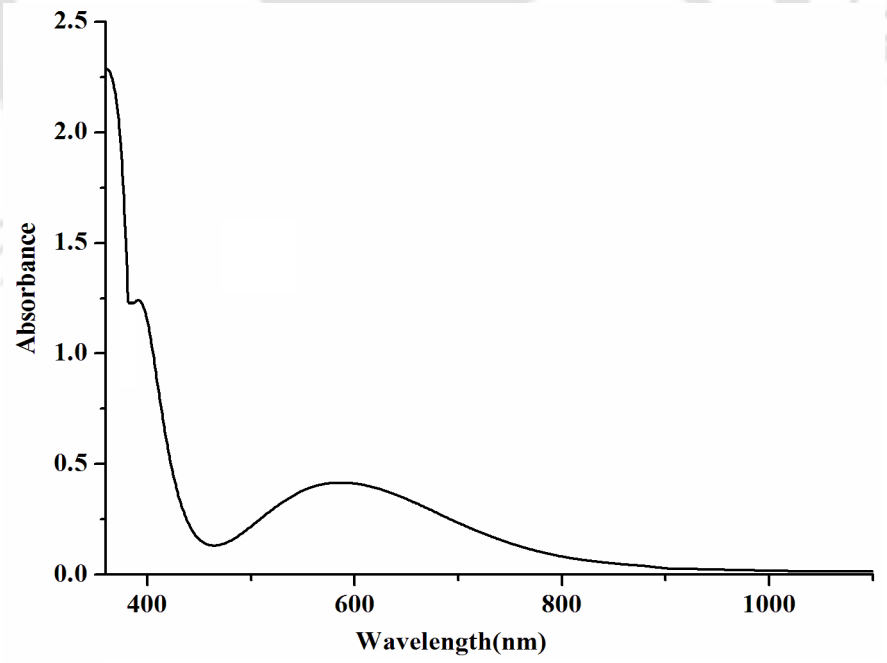

Figure A1.15 UV-visible spectrum of complex **2.2** in methanol.

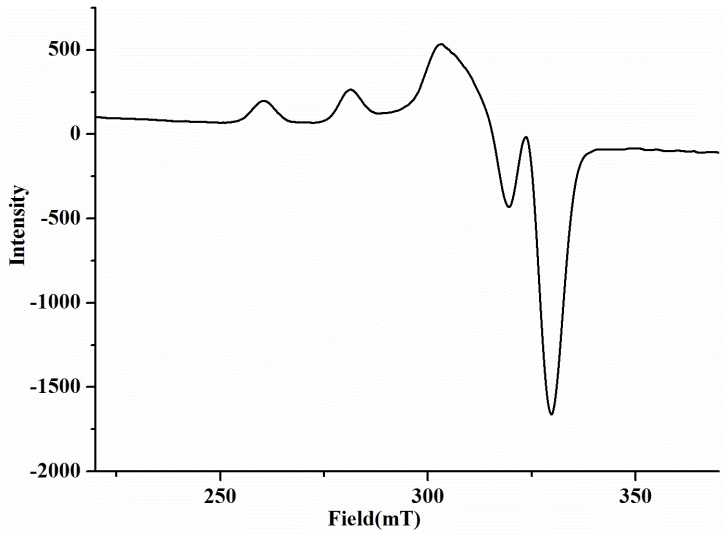

Figure A1.16 X-Band EPR spectrum of complex **2.2** in acetonitrile at 77 K.

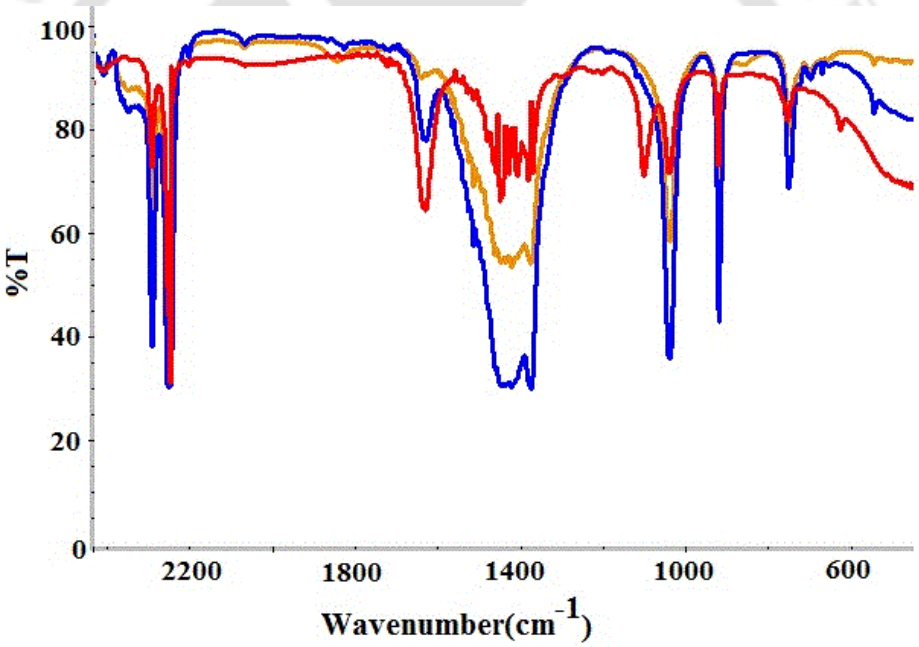

Figure A1.17 Solution FT-IR spectra of complex **2.2** after purging NO (red trace) and gradual decay of intensity of the peak at 1634 cm^{-1} in acetonitrile.

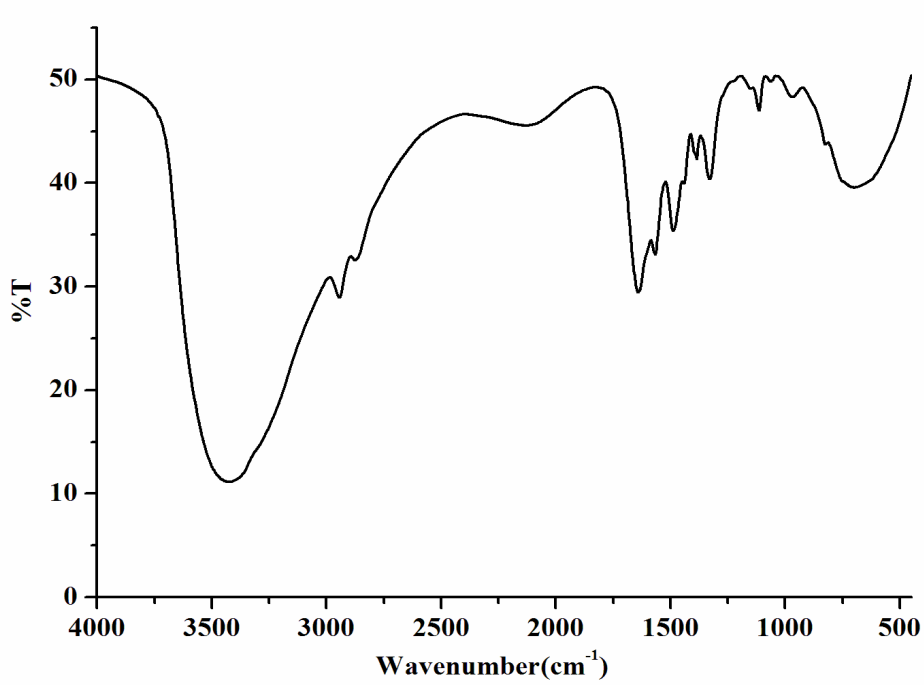

Figure A1.18 FT-IR spectrum of modified ligand $\mathbf{L_1}'$ in KBr pellet.

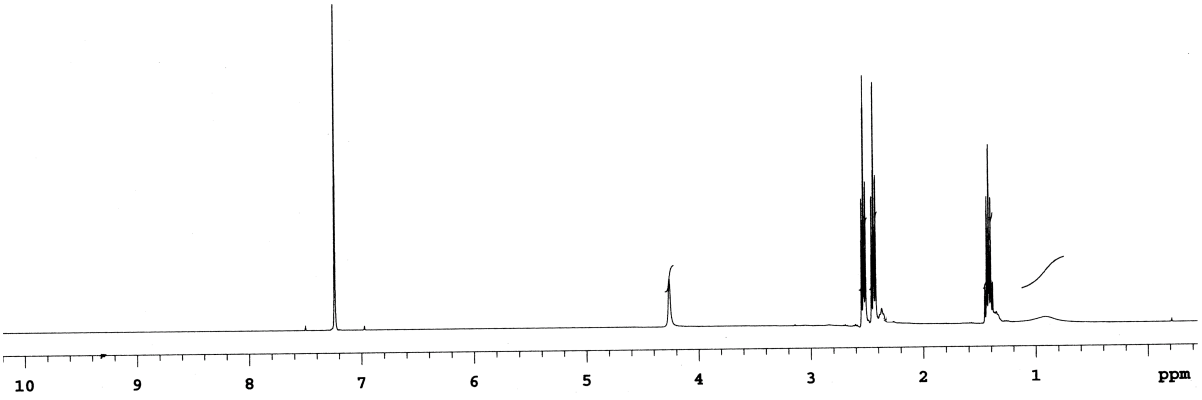

Figure A1.19 ^{1}H-NMR spectrum of modified ligand $\mathbf{L_1}'$ in $CDCl_3$.

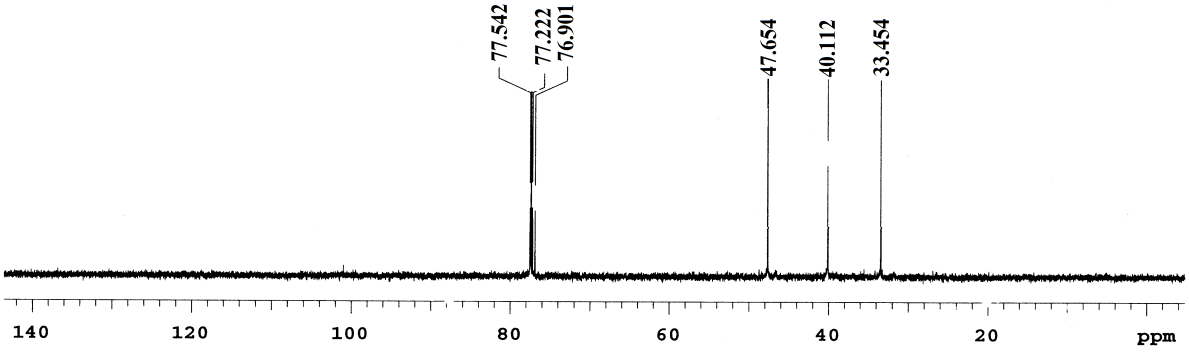

Figure A1.20 ^{13}C-NMR spectrum of modified ligand $\mathbf{L_1}'$ in $CDCl_3$.

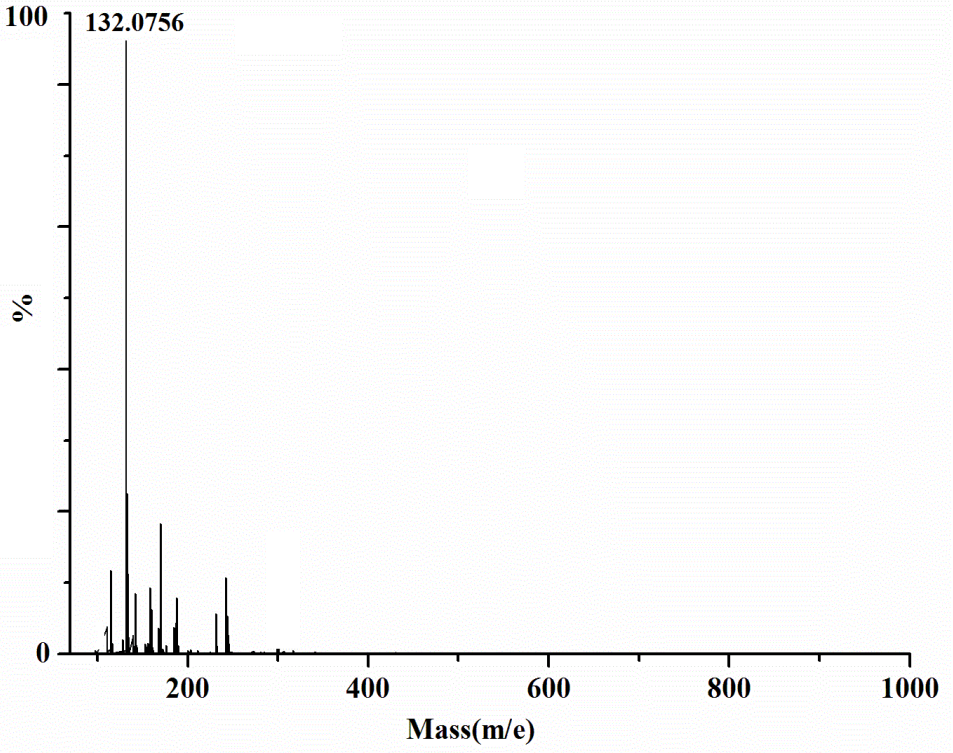

Figure A1.21 ESI mass spectrum of modified ligand $\mathbf{L_1}'$ in acetonitrile.

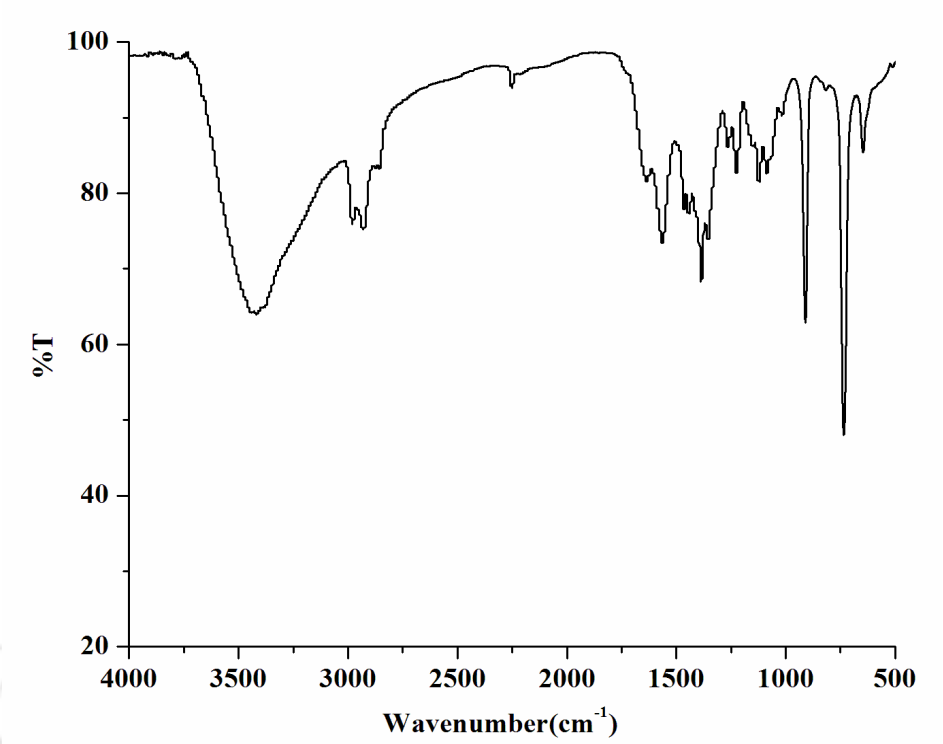

Figure A1.22 FT-IR spectrum of modified ligand $\mathbf{L_2'}$ in KBr pellet.

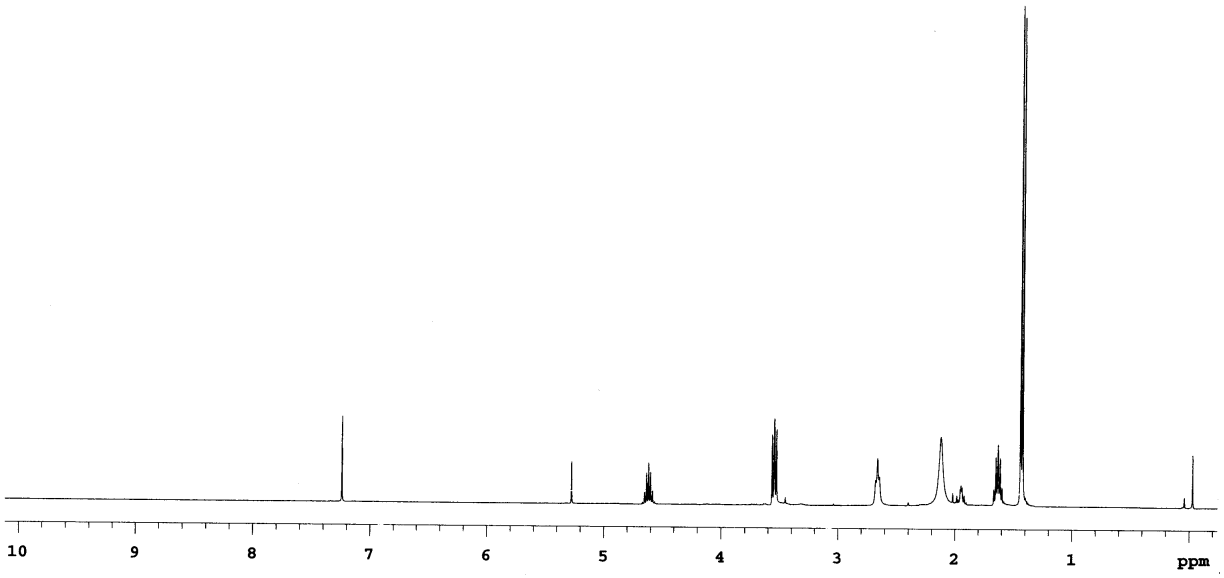

Figure A1.23 ^{1}H-NMR spectrum of modified ligand $\mathbf{L_2'}$ in $CDCl_3$.

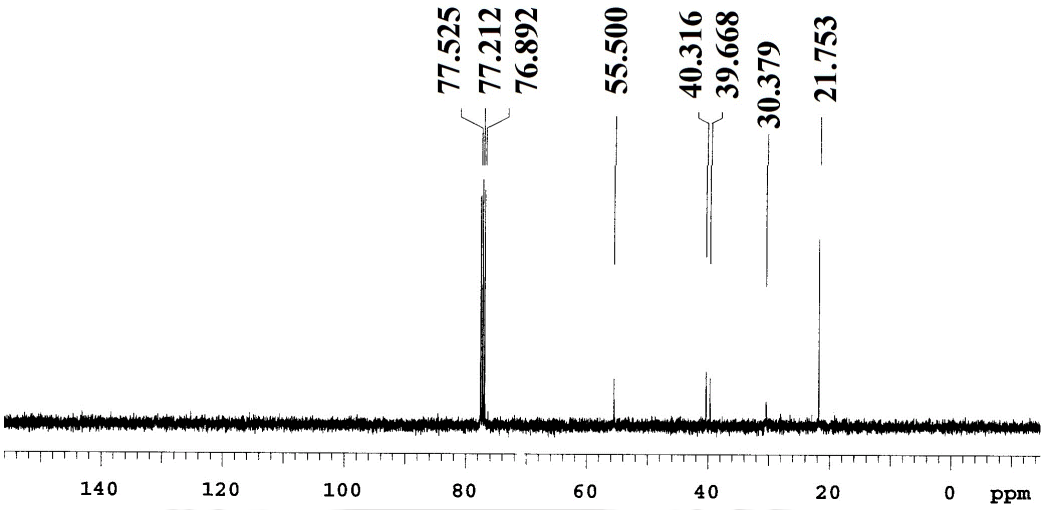

Figure A1.24 ^{13}C-NMR spectrum of modified ligand $\mathbf{L_2'}$ in $CDCl_3$.

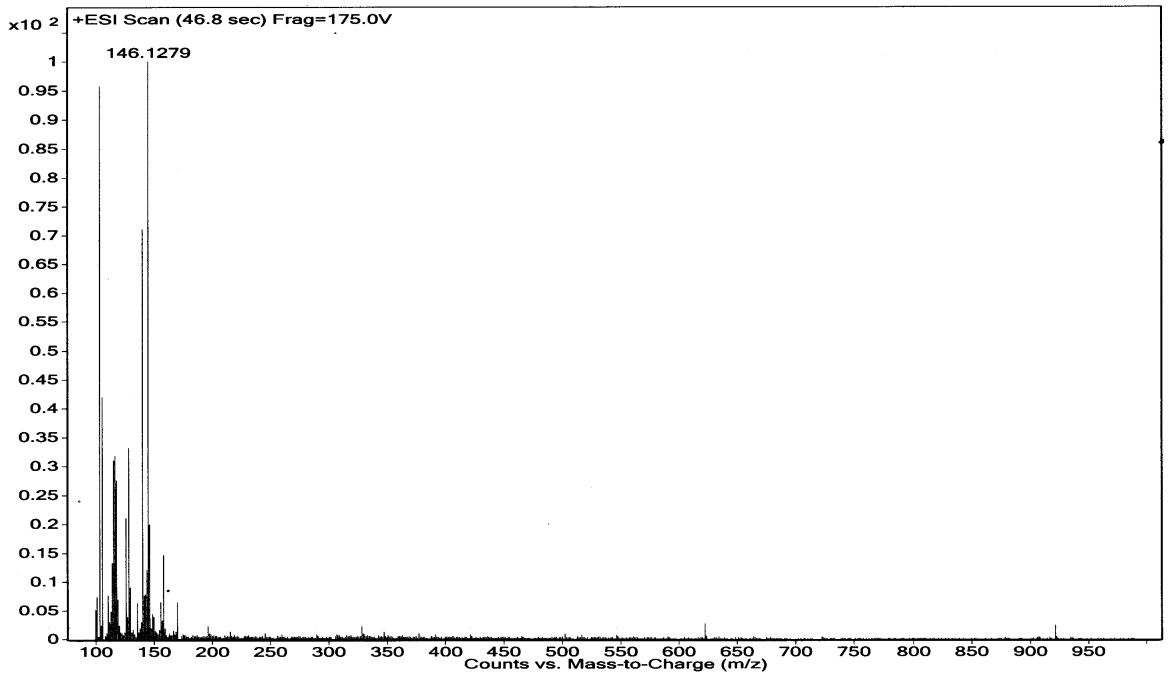

Figure A1.25 ESI mass spectrum of modified ligand $\mathbf{L_2'}$ in acetonitrile.

Appendix II

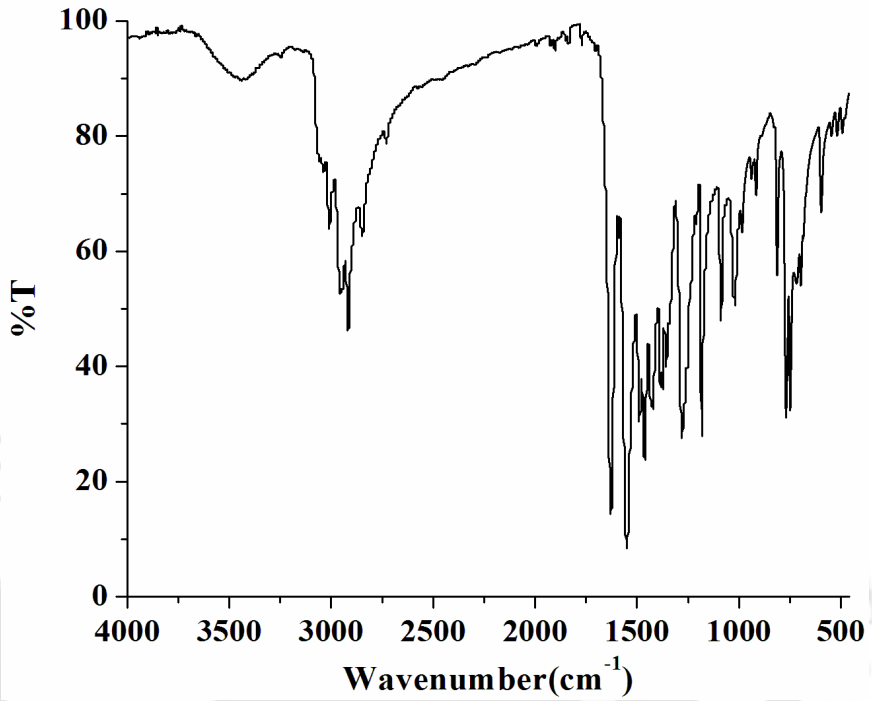

Figure A2.1 FT-IR spectrum of ligand $\mathbf{L_3}$ in KBr pellet.

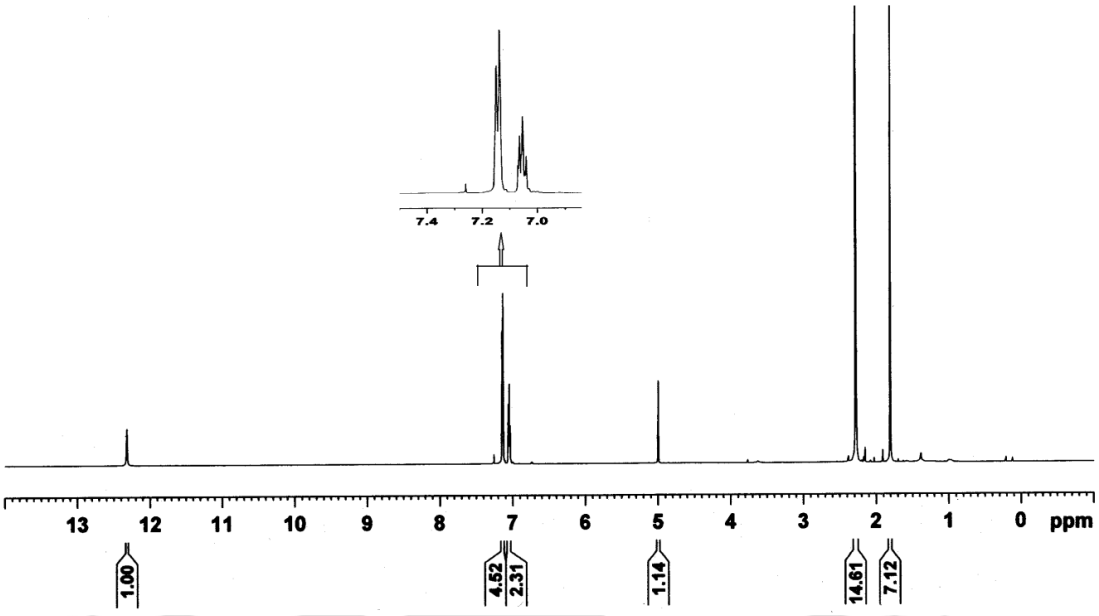

Figure A2.2 ^{1}H-NMR spectrum of ligand **L_3** in $CDCl_3$.

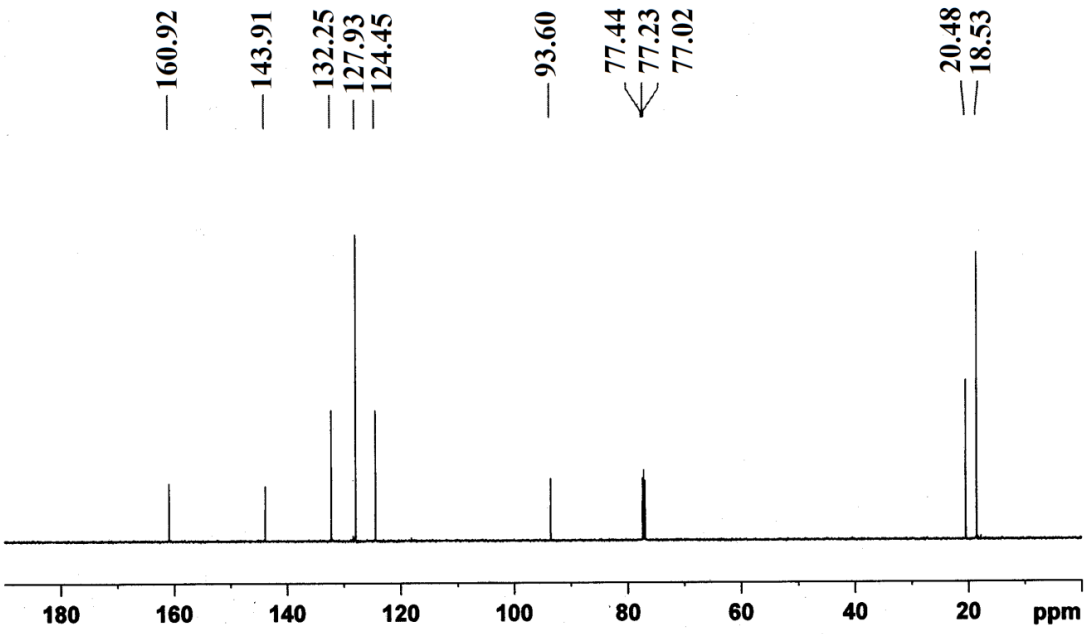

Figure A2.3 ^{13}C-NMR spectrum of ligand **L_3** in $CDCl_3$.

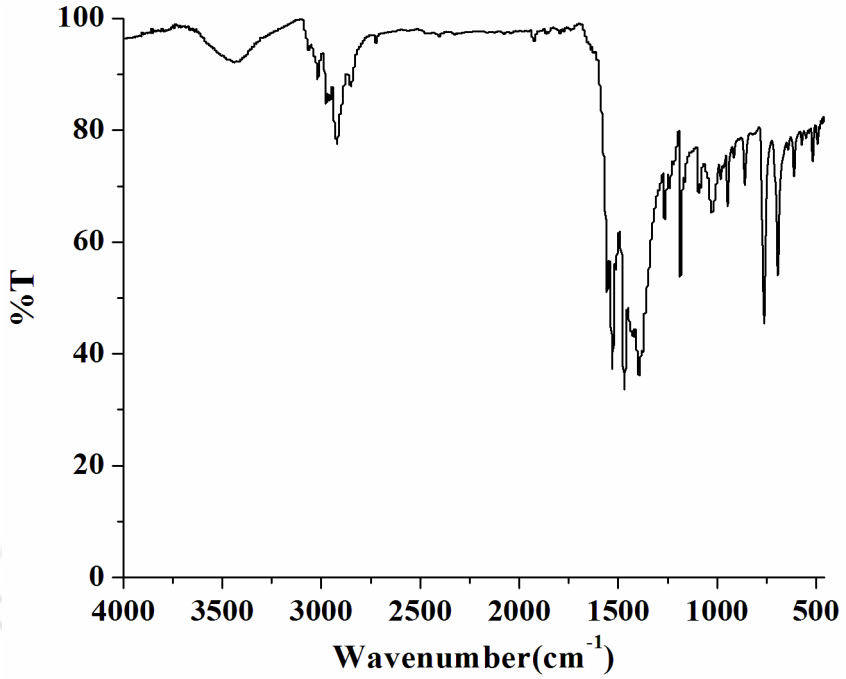

Figure A2.4 FT-IR spectrum of complex **3.1** in KBr pellet.

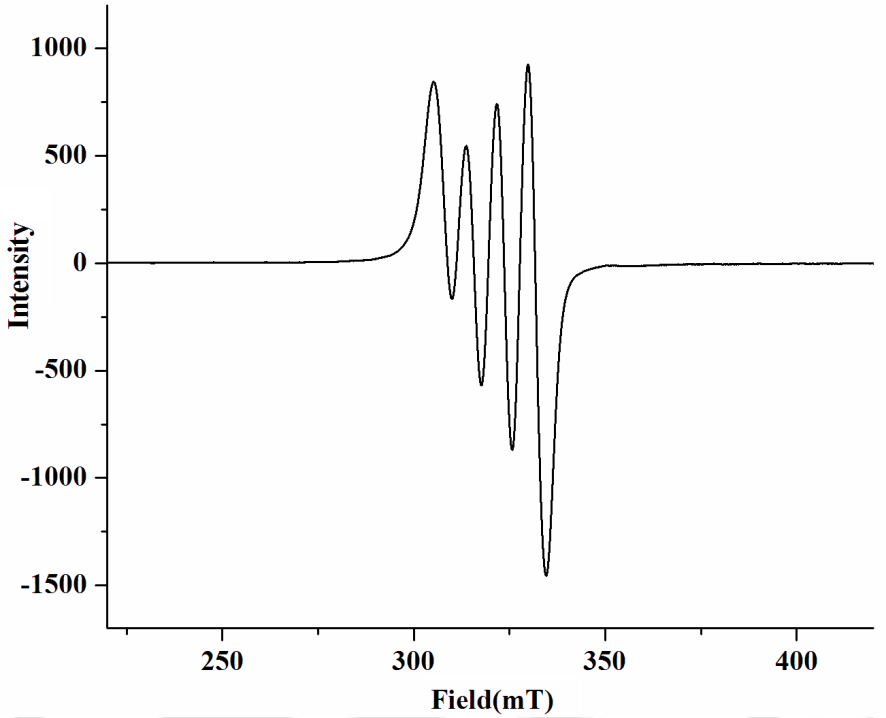

Figure A2.5 X-band EPR spectrum of complex **3.1** in acetonitrile.

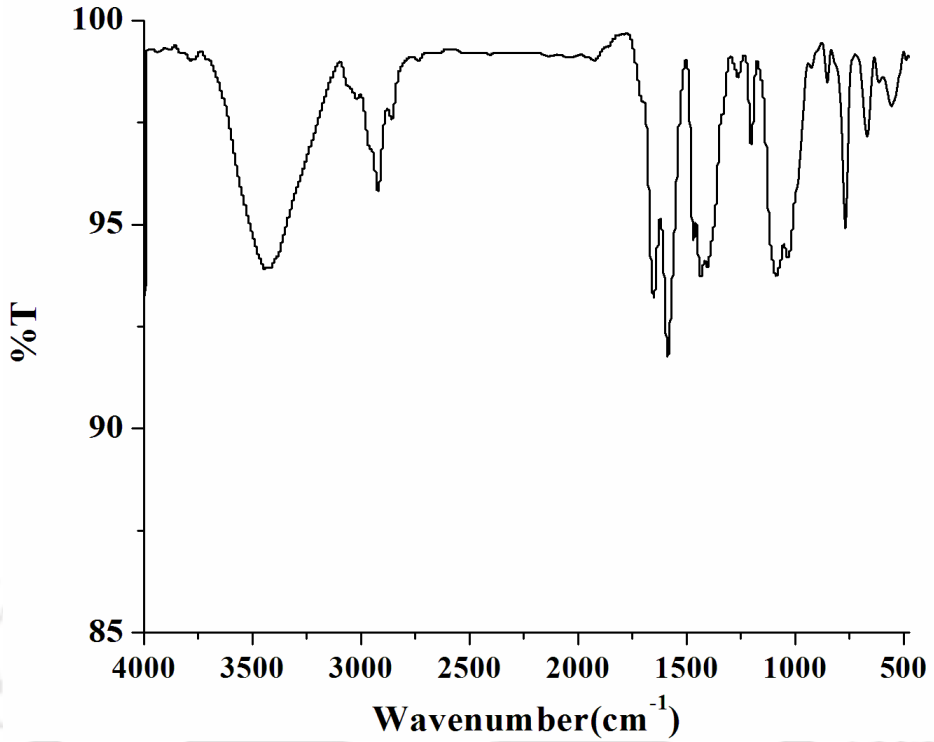

Figure A2.6 FT-IR spectrum of complex **3.2** in KBr pellet.

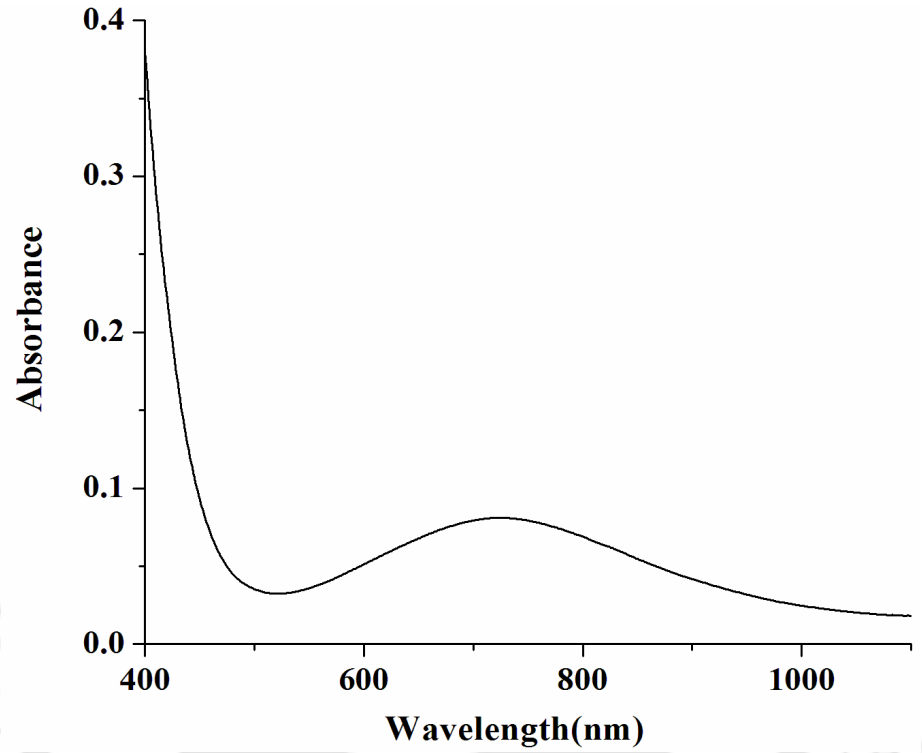

Figure A2.7 UV-visible spectrum of complex **3.2** in acetonitrile.

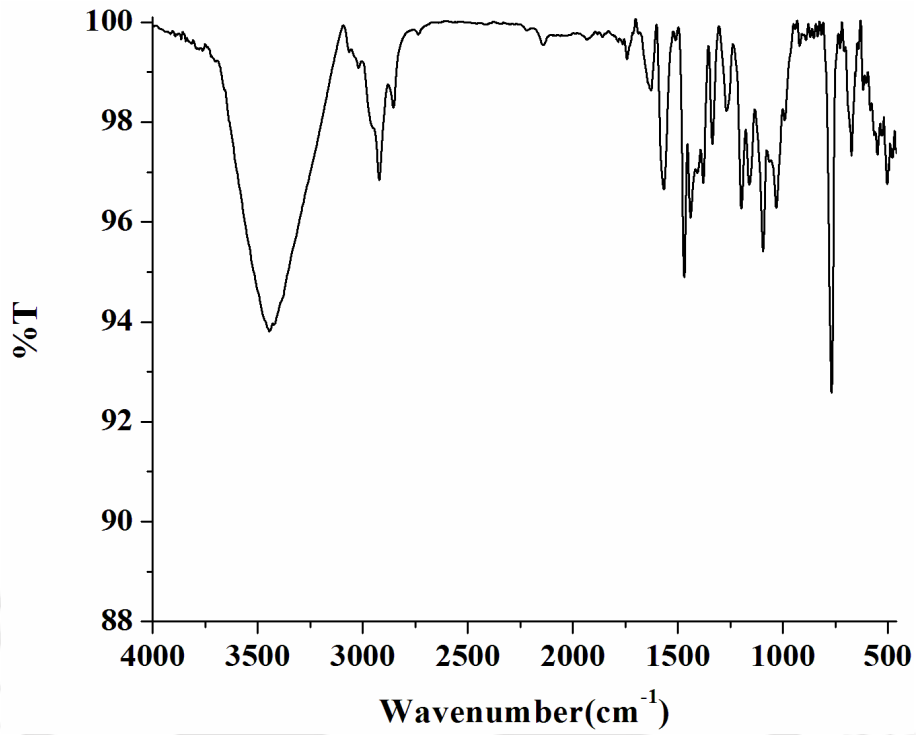

Figure A2.8 FT-IR spectrum of complex **3.3** in KBr pellet.

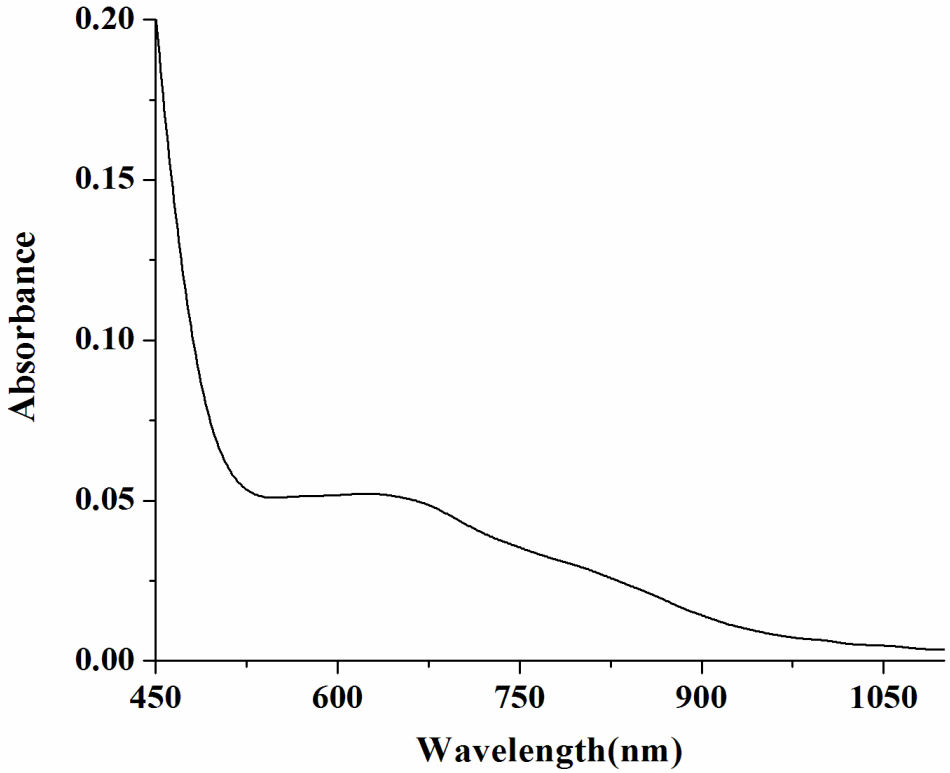

Figure A2.9 UV-visible spectrum of complex **3.3** in acetonitrile.

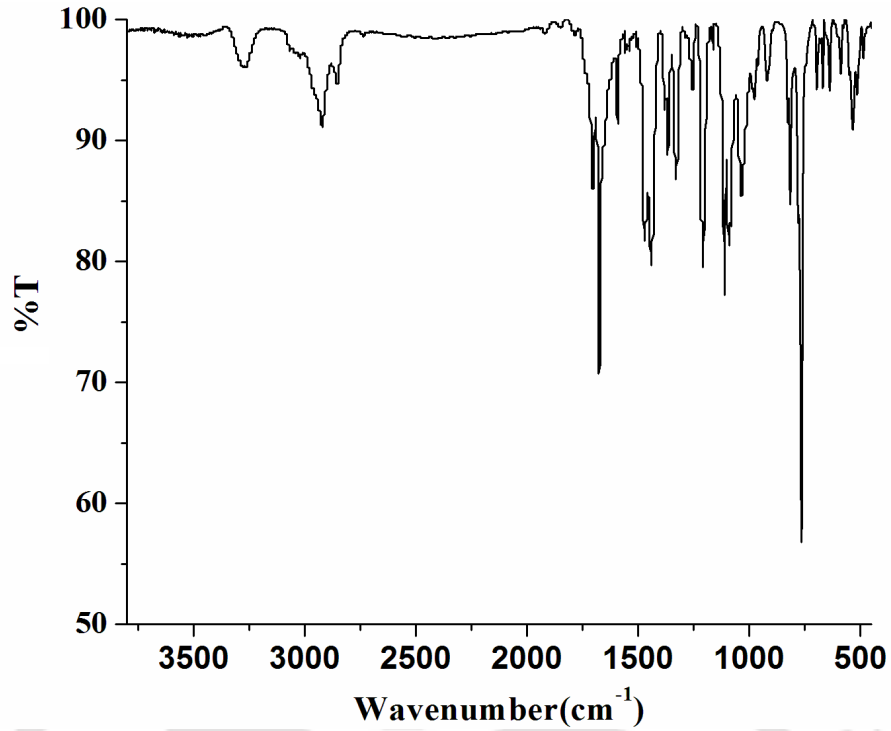

Figure A2.10 FT-IR spectrum of L_3' in KBr pellet.

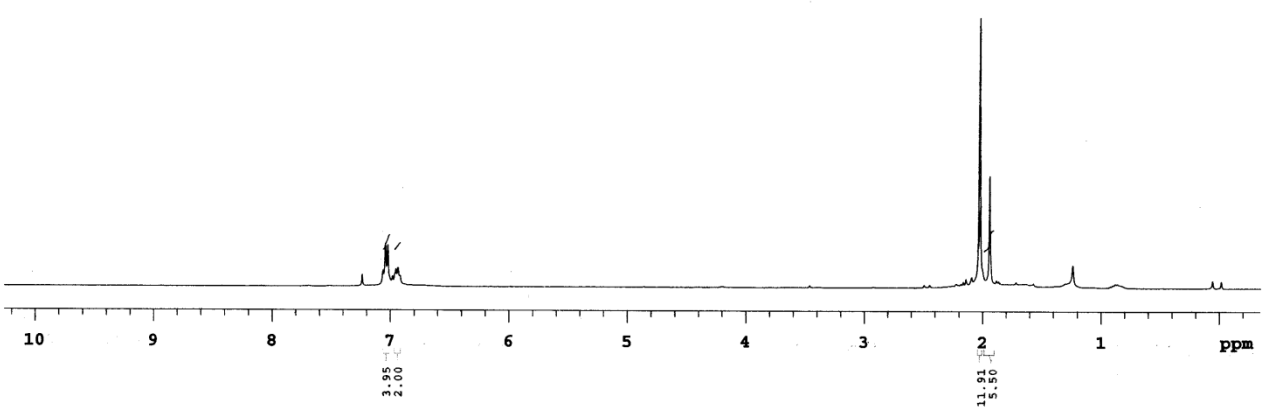

Figure A2.11 ^{1}H-NMR spectrum of $\mathbf{L_3'}$ in $CDCl_3$.

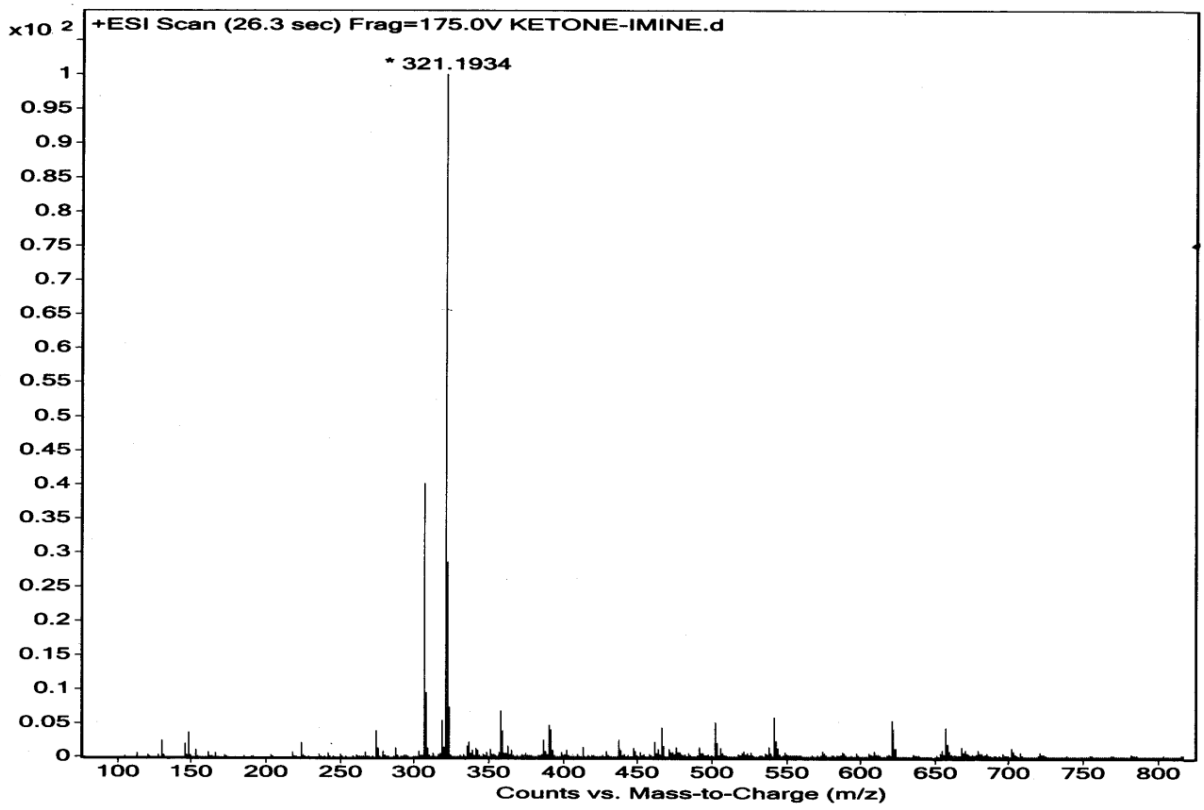

Figure A2.12 ESI-mass spectrum of $L_3^{/}$ in acetonitrile.

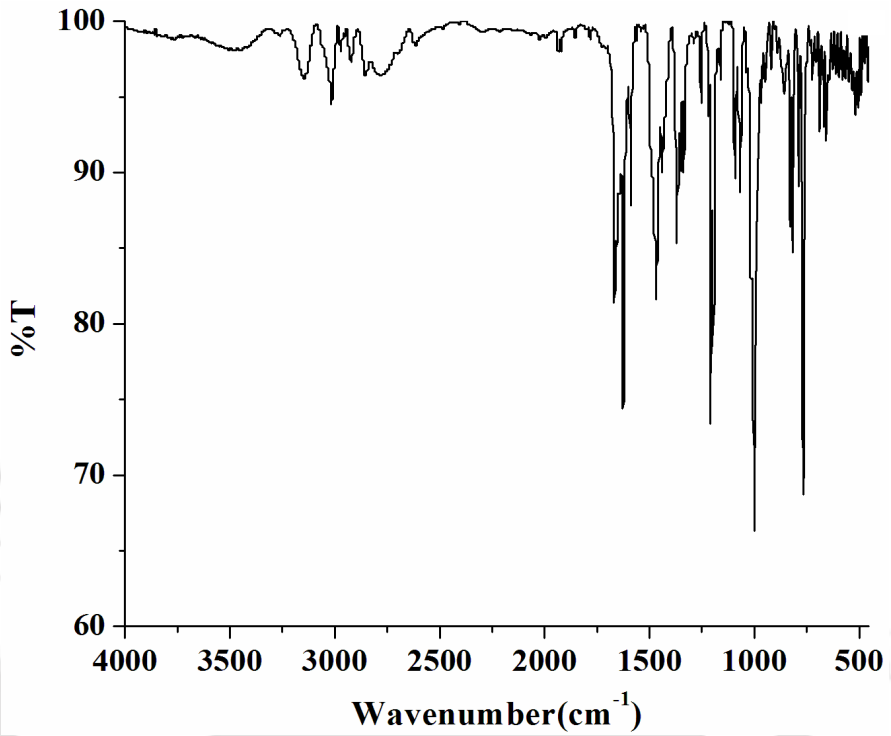

Figure A2.13 FT-IR spectrum of $L_3^{//}$ in KBr pellet.

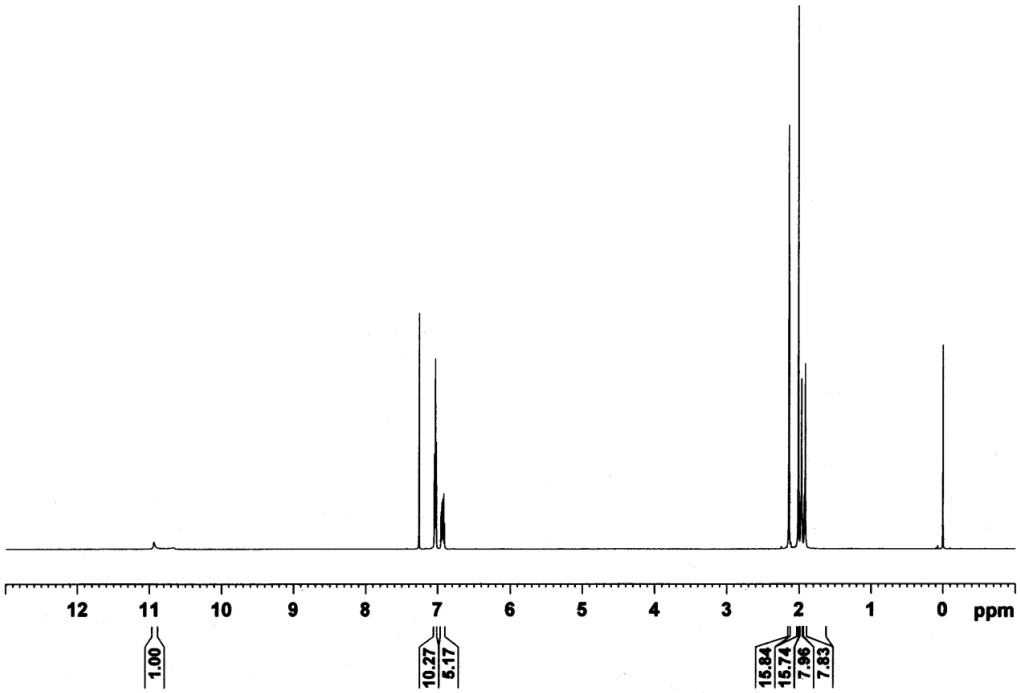

Figure A2.14 ^{1}H-NMR spectrum of $\mathbf{L_3}^{//}$ in $CDCl_3$.

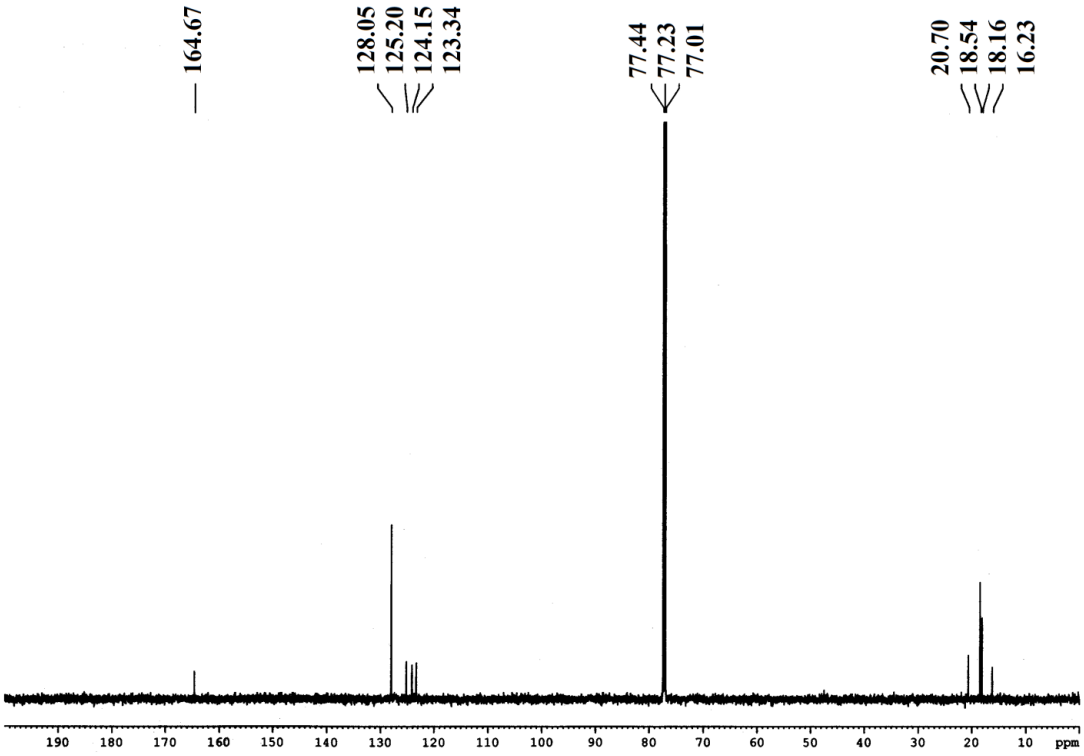

Figure A2.15 ^{13}C-NMR spectrum of $\mathbf{L_3}^{//}$ in $CDCl_3$.

Appendix III

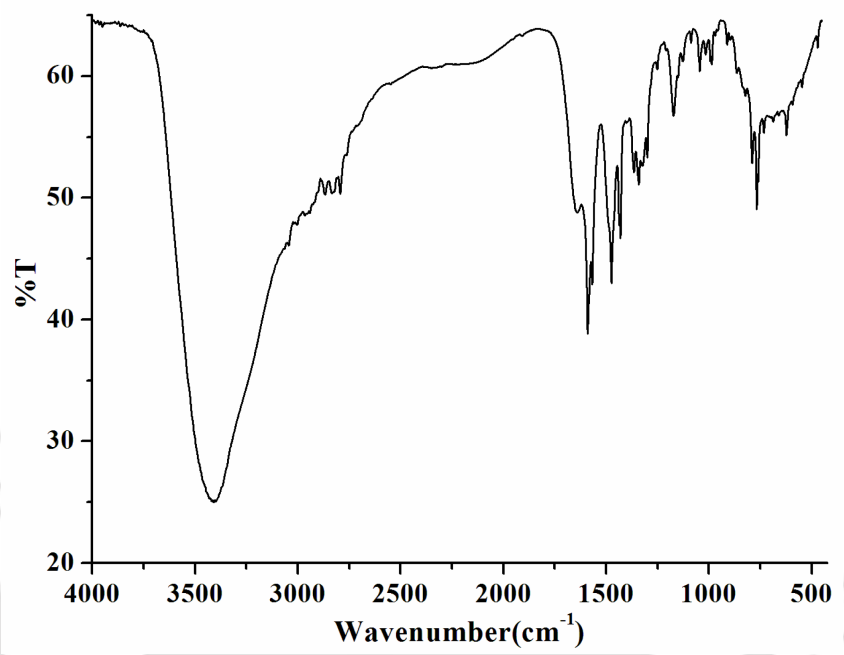

Figure A3.1 FT-IR spectrum of $\mathbf{L_4}$ in KBr pellet.

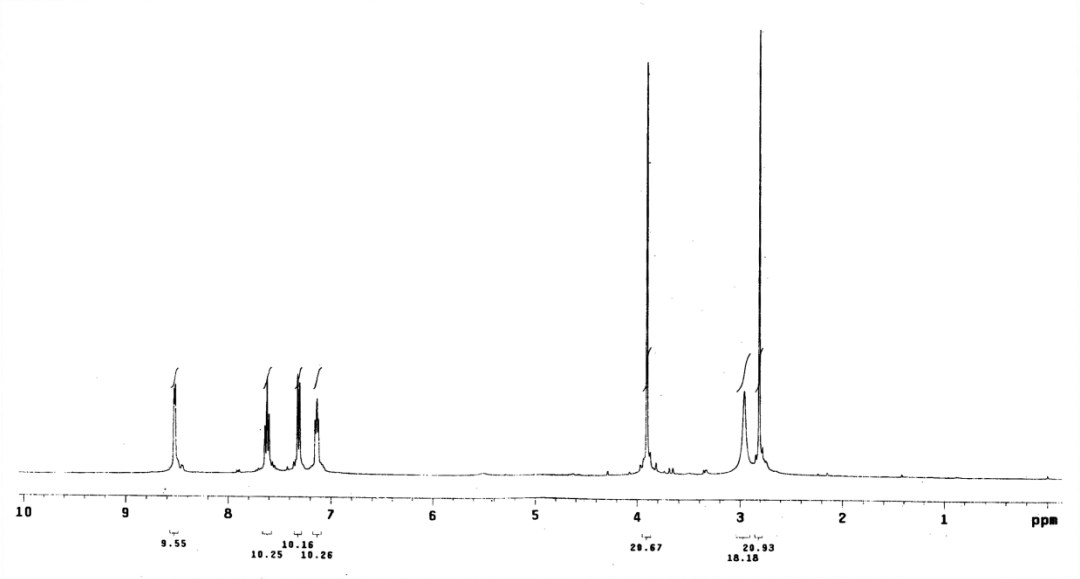

Figure A3.2 ^{1}H-NMR spectrum of $\mathbf{L_4}$ in $CDCl_3$.

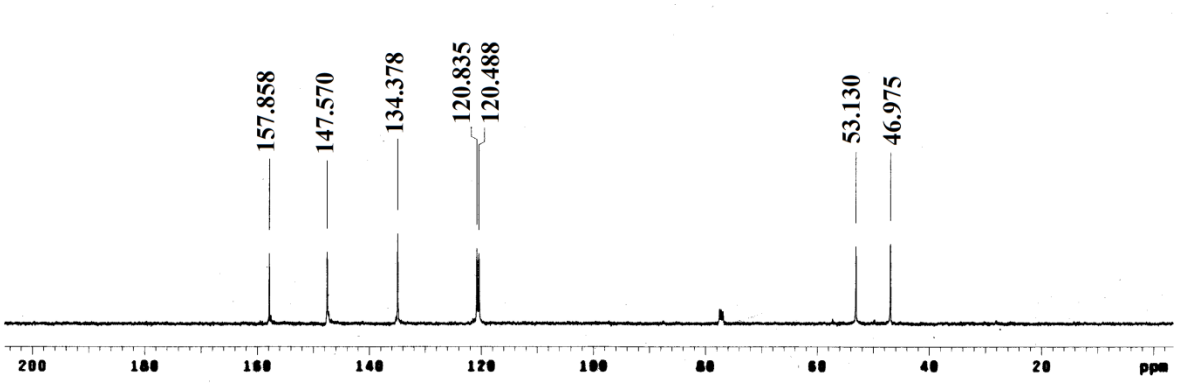

Figure A3.3 ^{13}C-NMR spectrum of $\mathbf{L_4}$ in $CDCl_3$.

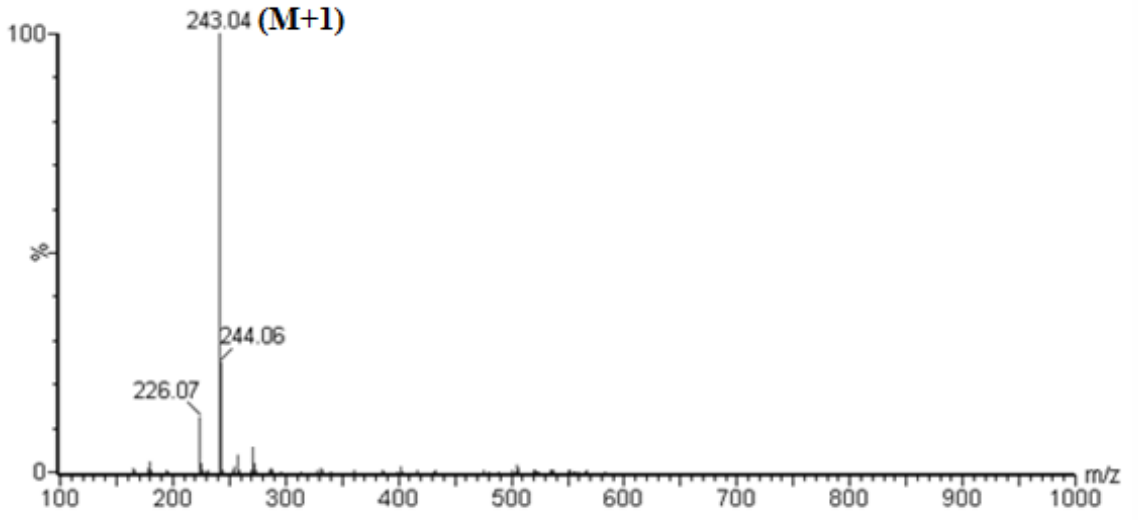

Figure A3.4 ESI-Mass spectrum of $\mathbf{L_4}$ in acetonitrile.

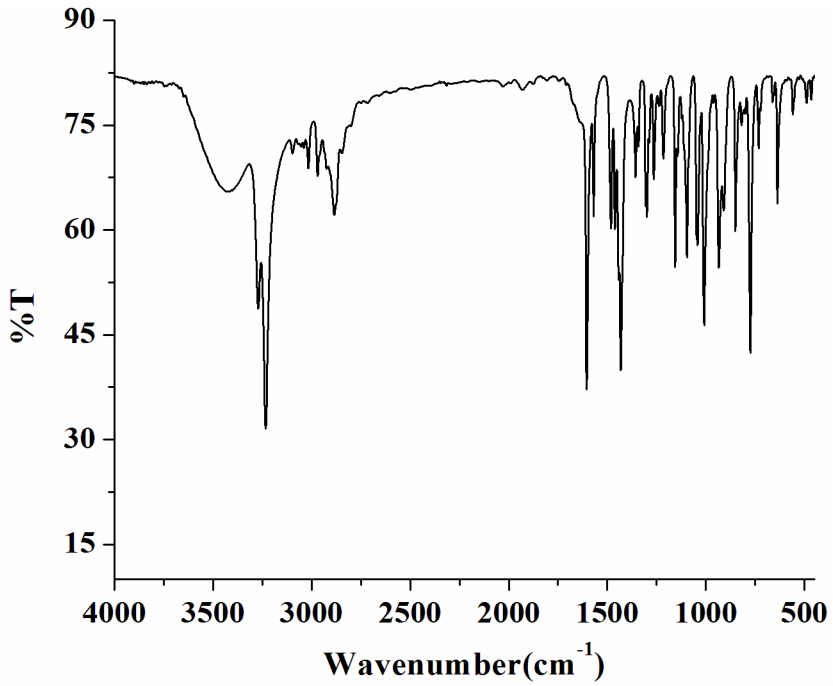

Figure A3.5 FT-IR spectrum of complex **4.1** in KBr pellet.

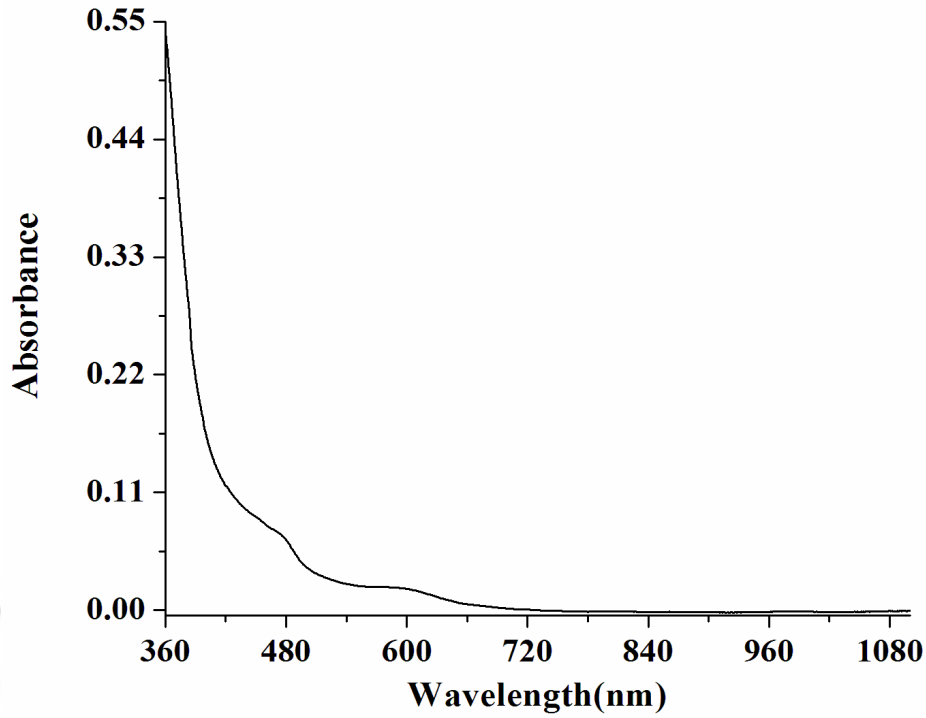

Figure A3.6 UV-visible spectrum of complex **4.1** in acetonitrile.

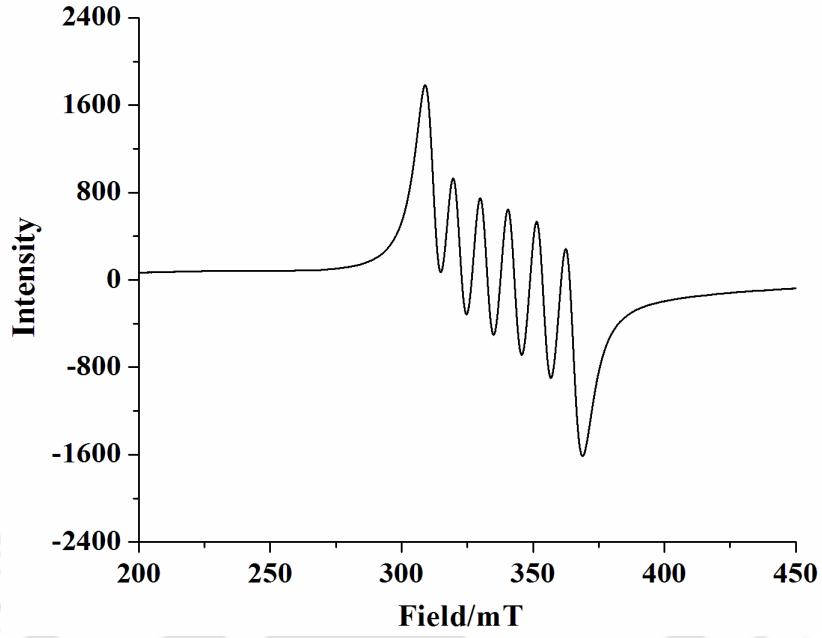

Figure A3.7 X-band EPR spectrum of complex **4.1** in acetonitrile.

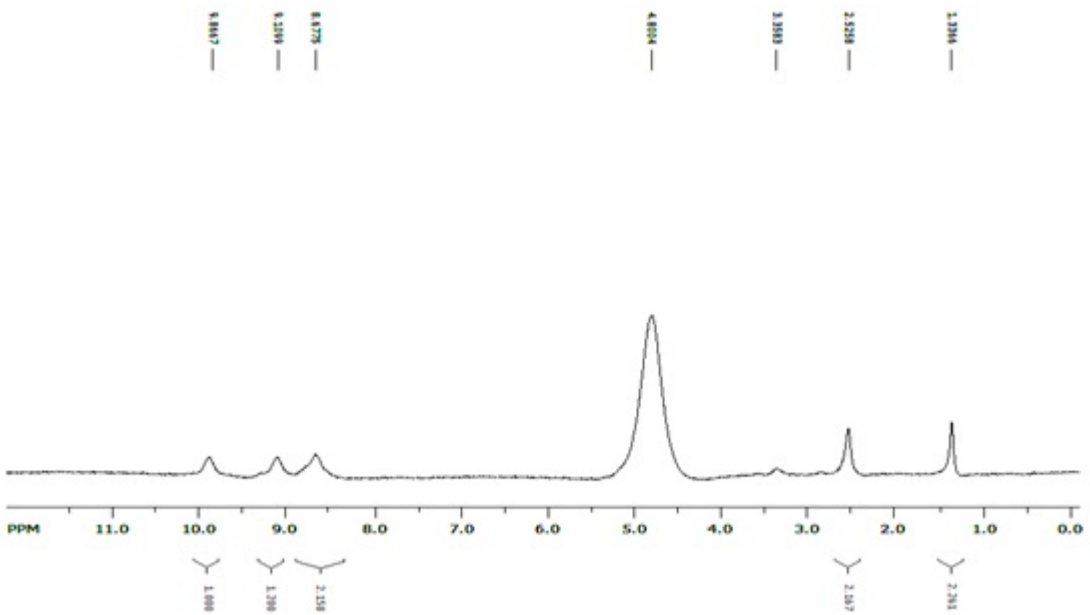

Figure A3.8 ^{1}H-NMR spectrum of complex **4.1** in CD_3OD.

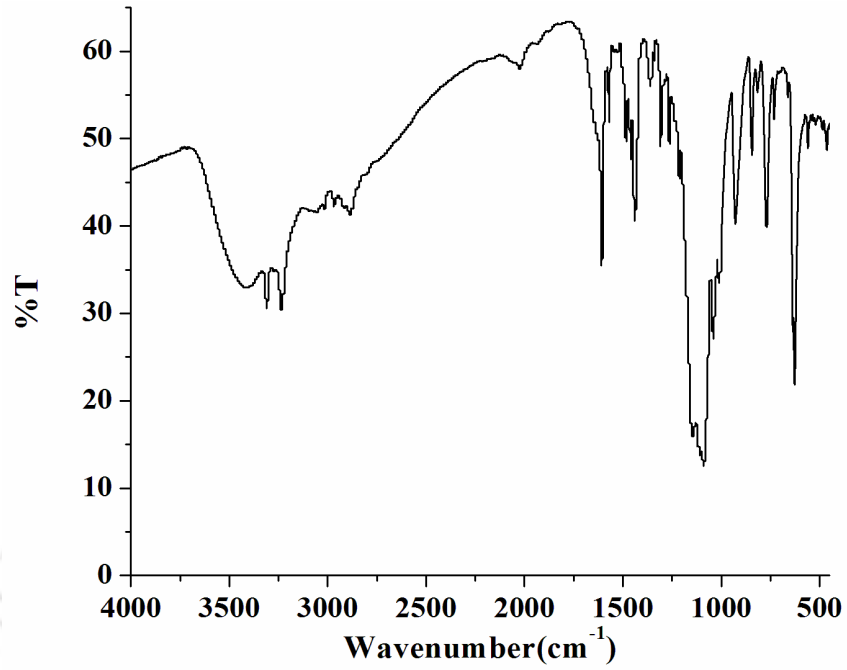

Figure A3.9 FT-IR spectrum of complex **4.2** in KBr pellet.

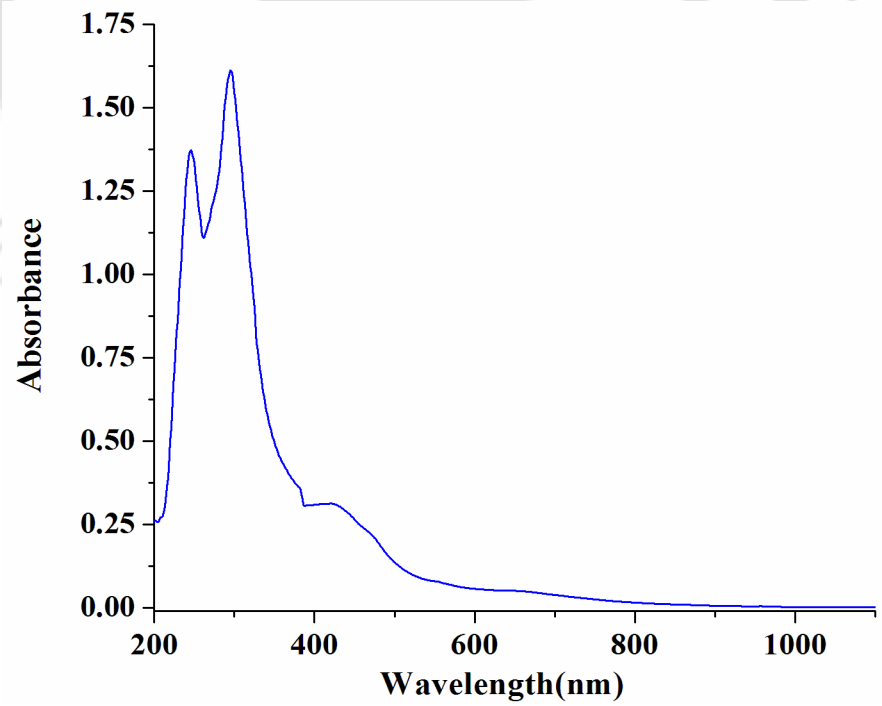

Figure A3.10 UV-visible spectrum of complex **4.2** in acetonitrile.

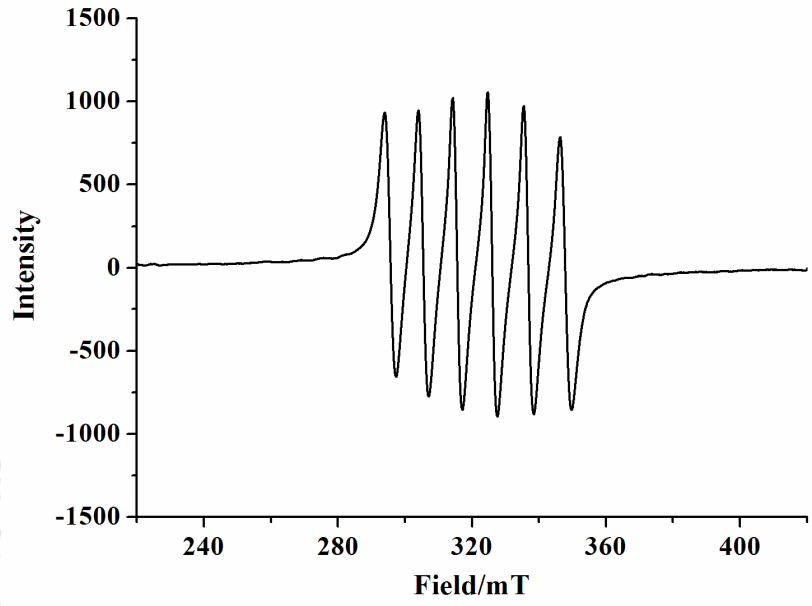

Figure A3.11 X-band EPR spectrum of complex **4.2** in acetonitrile.

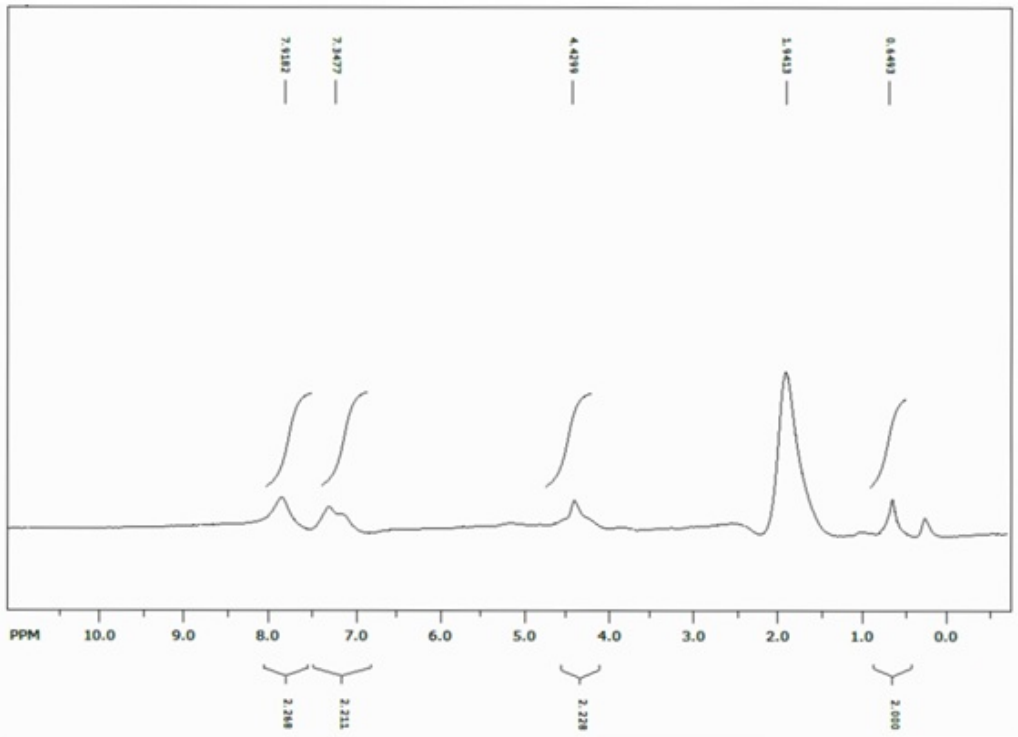

Figure A3.12 ^{1}H-NMR spectrum of complex **4.2** in CD_3CN.

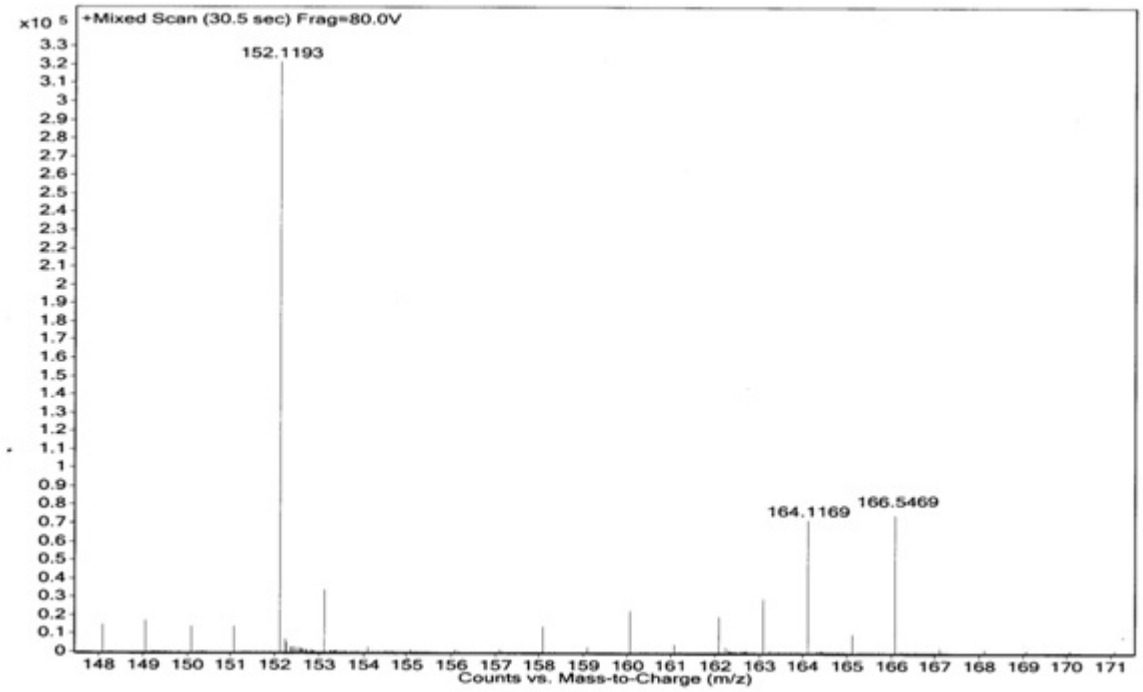

Figure A3.13 HRMS spectrum of complex **4.2** in acetonitrile.

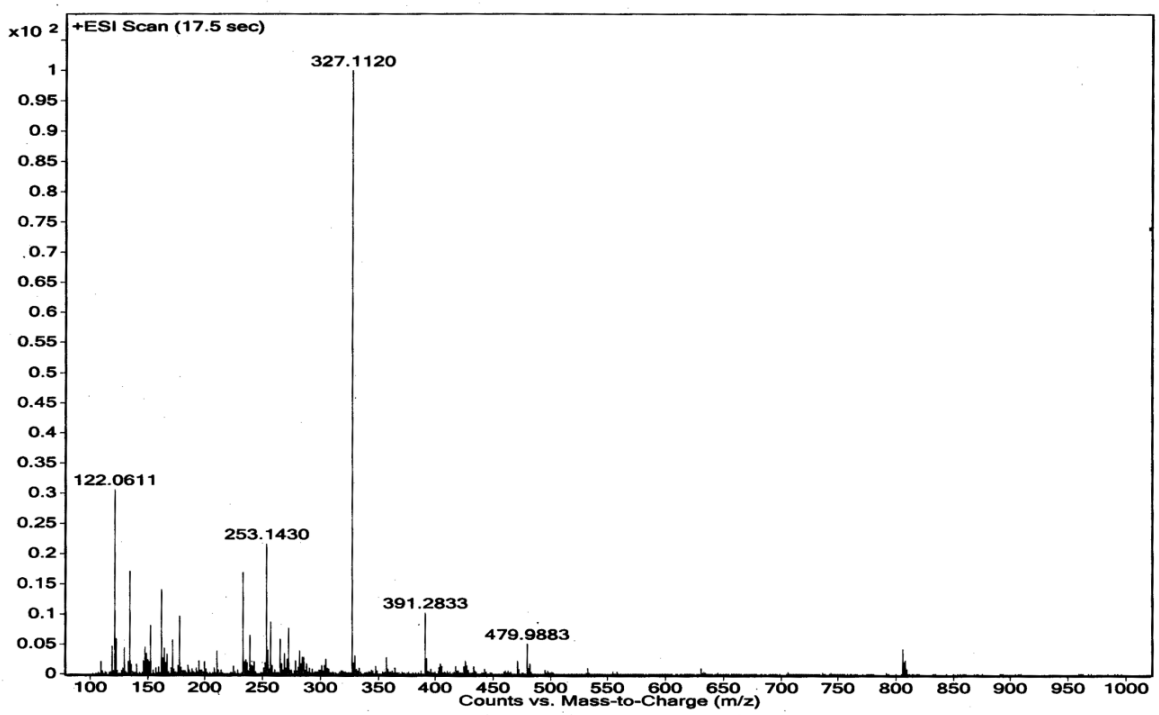

Figure A3.14 HRMS spectrum of complex **4.1** after purging NO(g) in argon atmosphere in acetonitrile.

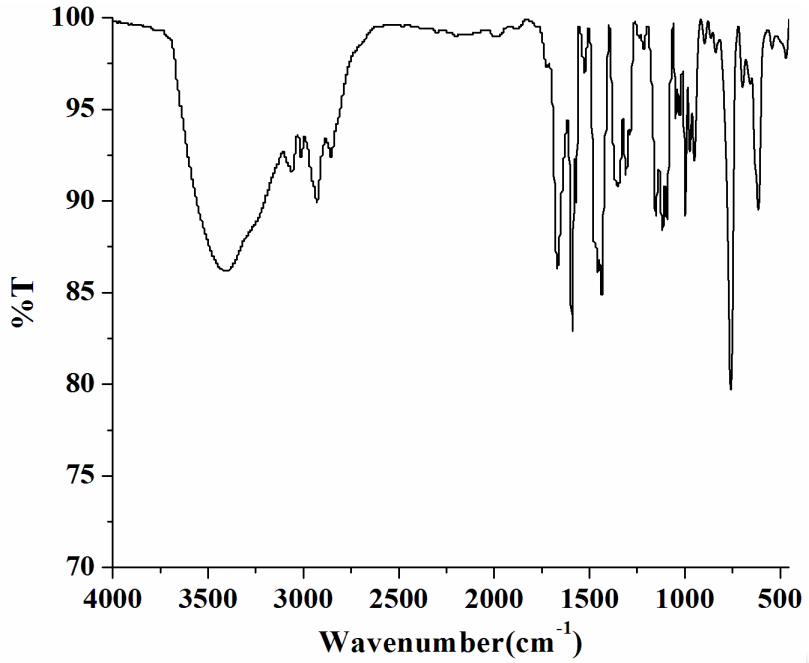

Figure A3.15 FT-IR spectrum of $\mathbf{L_4'(ClO_4)_2}$ in KBr pellet.

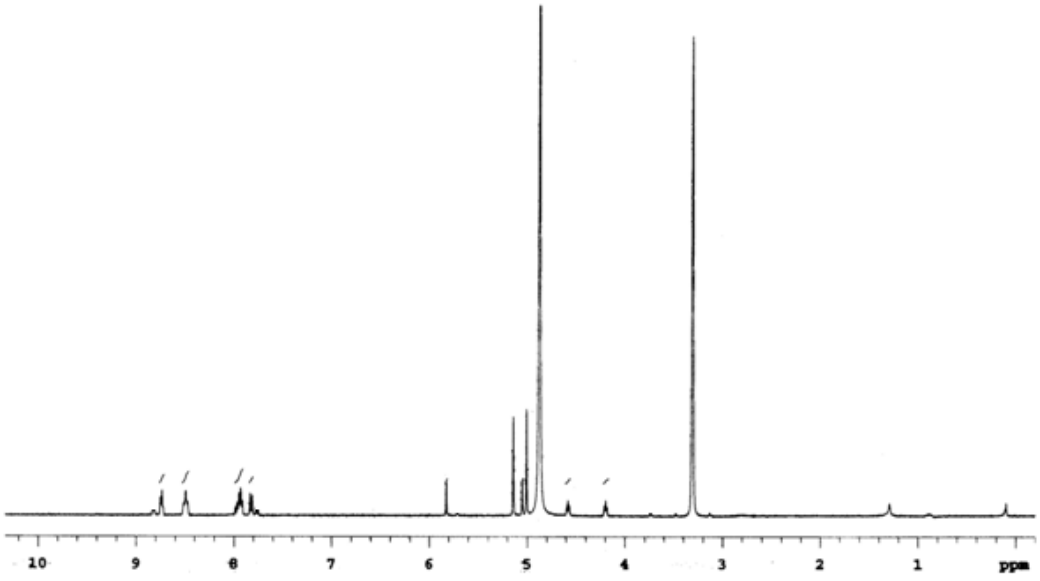

Figure A3.16 ^{1}H-NMR spectrum of $\mathbf{L_4'(ClO_4)_2}$ in CD_3OD

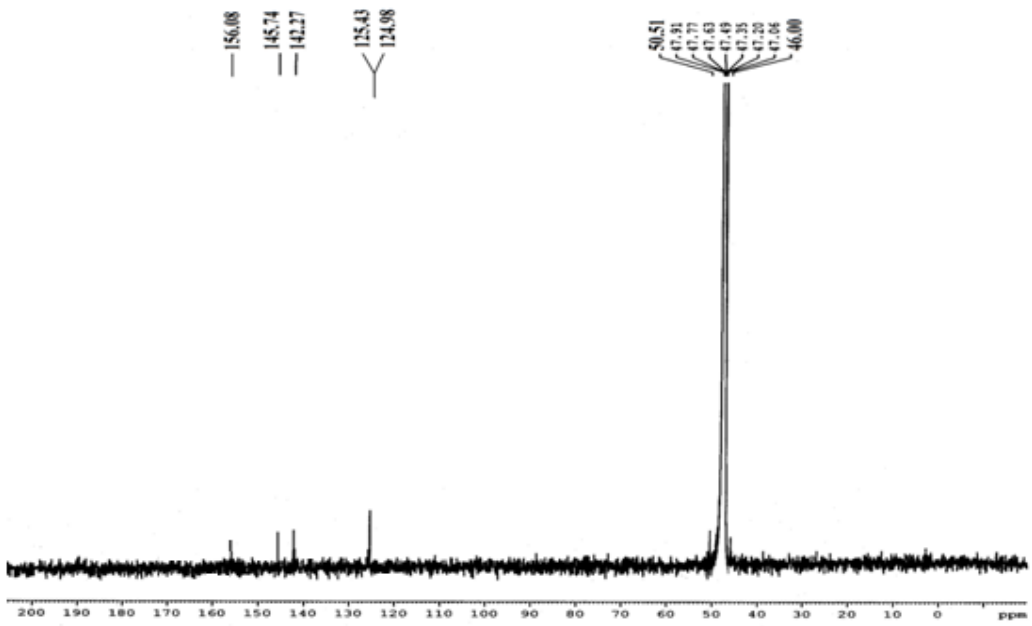

Figure A3.17 ^{13}C-NMR spectrum of $\mathbf{L_4'(ClO_4)_2}$ in CD_3OD.

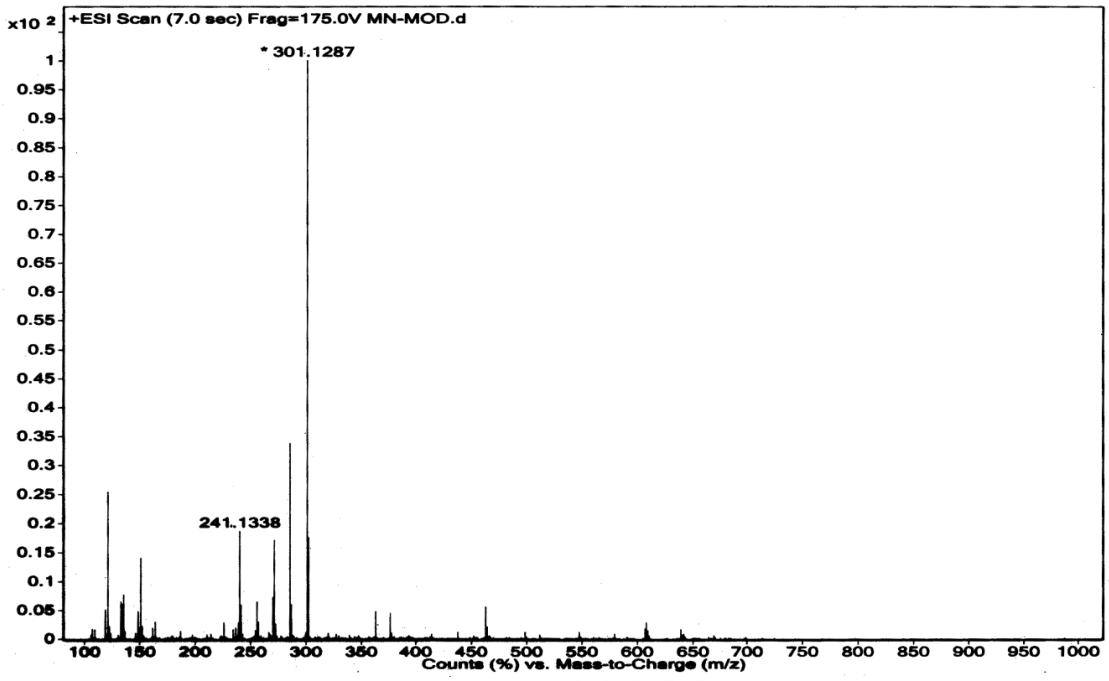

Figure A3.18 ESI-Mass spectrum of $\mathbf{L_4'(ClO_4)_2}$ in methanol.

Appendix IV

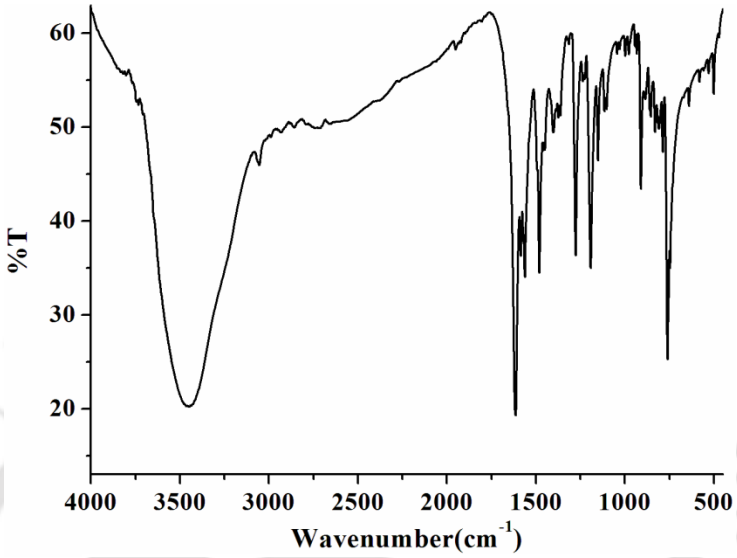

Figure A4.1 FT-IR spectrum of $\mathbf{L_{5a}}$ in KBr pellet.

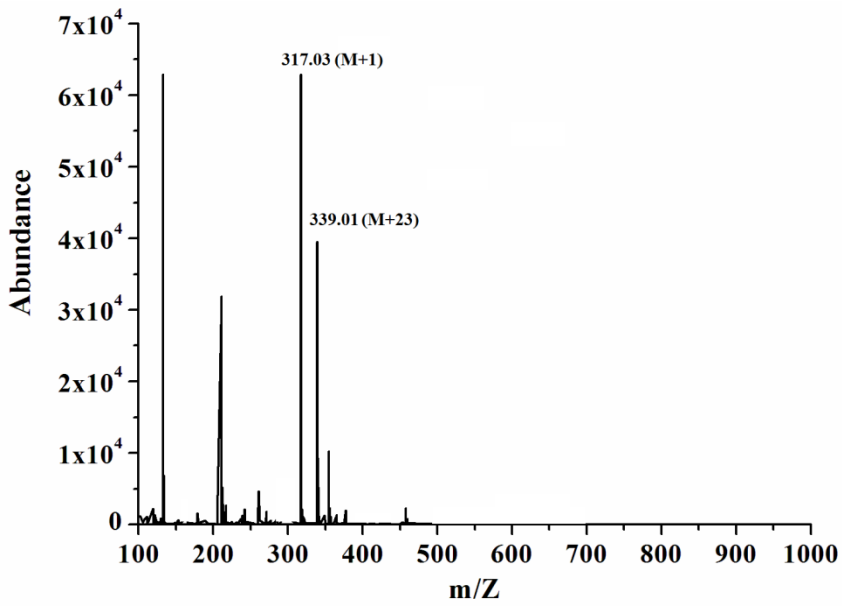

Figure A4.2 ESI-mass spectrum of $\mathbf{L_{5a}}$ in methanol.

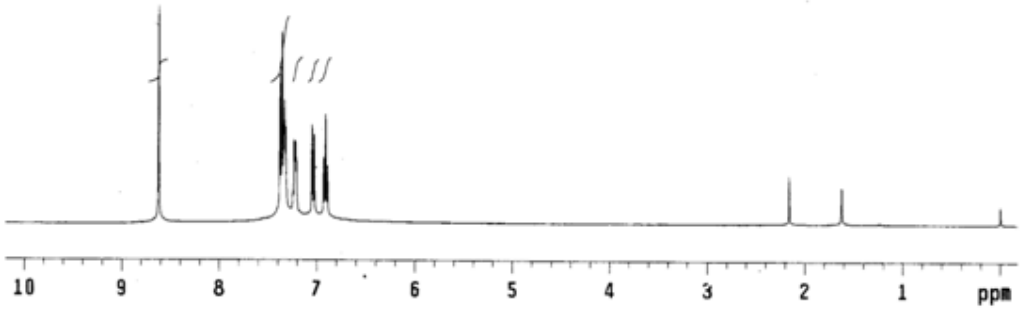

Figure A4.3 ^{1}H-NMR spectrum of $\mathbf{L_{5a}}$ in $CDCl_3$.

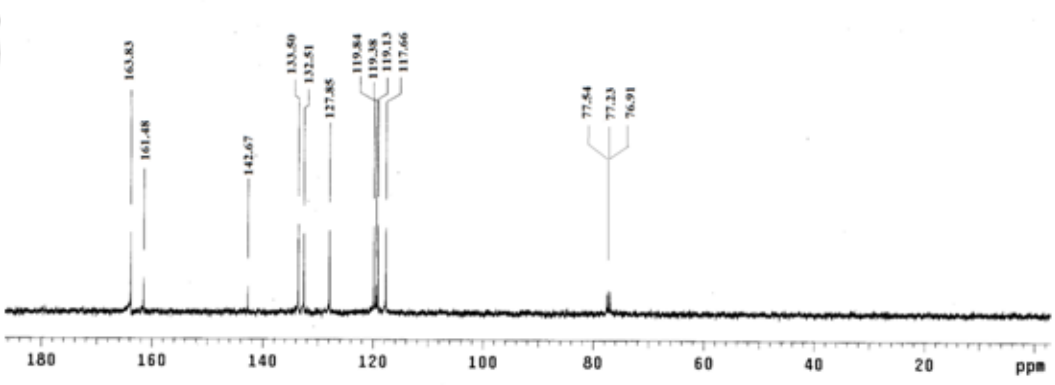

Figure A4.4 ^{13}C-NMR spectrum of $\mathbf{L_{5a}}$ in $CDCl_3$

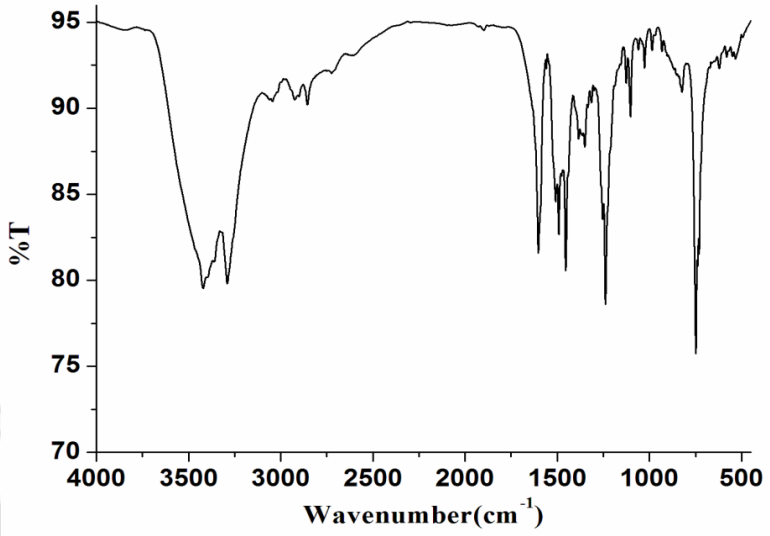

Figure A4.5 FT-IR spectrum of $\mathbf{L_5}$ in KBr pellet.

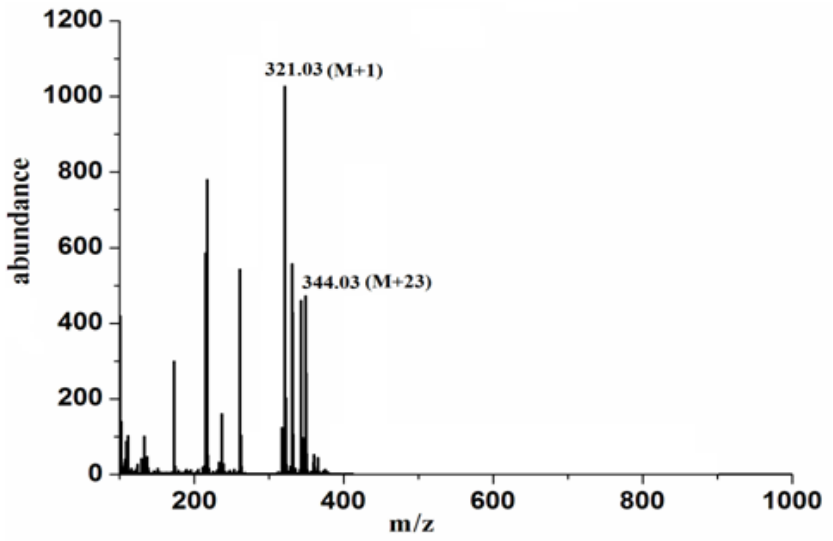

Figure A4.6 ESI-mass spectrum of **L_5** in methanol.

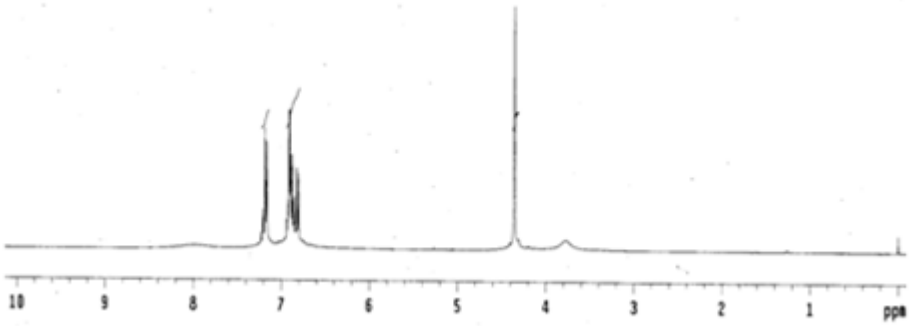

Figure A4.7 ^{1}H-NMR spectrum of **L5** in $CDCl_3$.

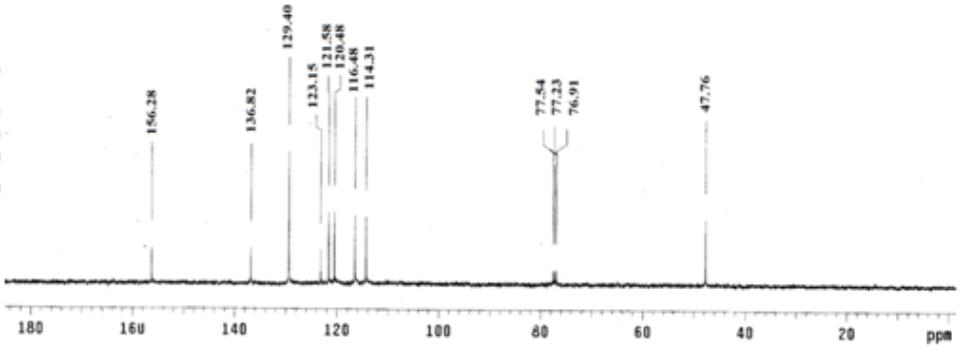

Figure A4.8 ^{13}C-NMR spectrum of $\mathbf{L_5}$ in $CDCl_3$

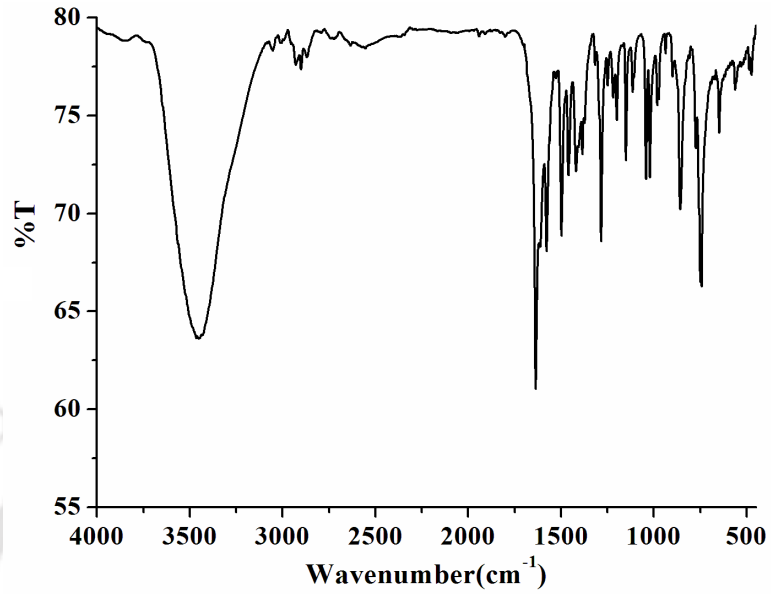

Figure A4.9 FT-IR spectrum of $\mathbf{L_{6a}}$ in KBr pellet.

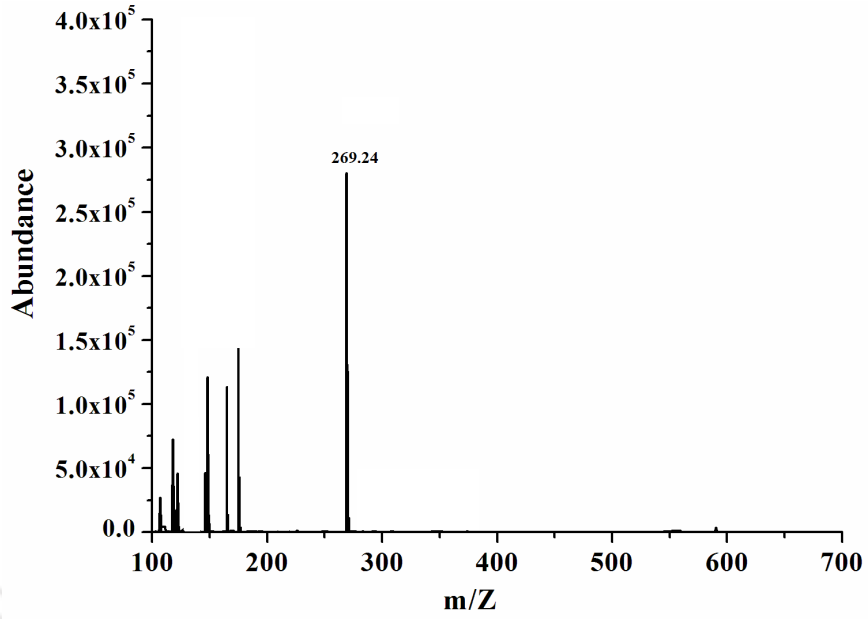

Figure A4.10 ESI-mass spectrum of $\mathbf{L_{6a}}$ in methanol.

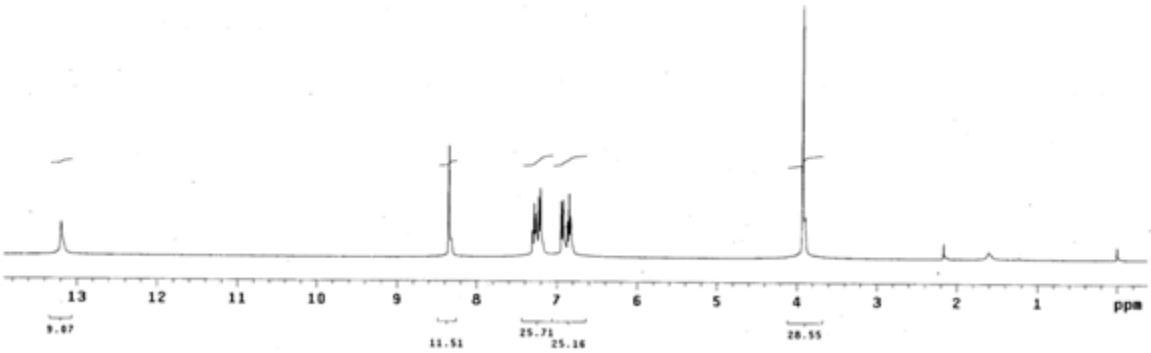

Figure A4.11 ^{1}H-NMR spectrum of $\mathbf{L_{6a}}$ in $CDCl_3$.

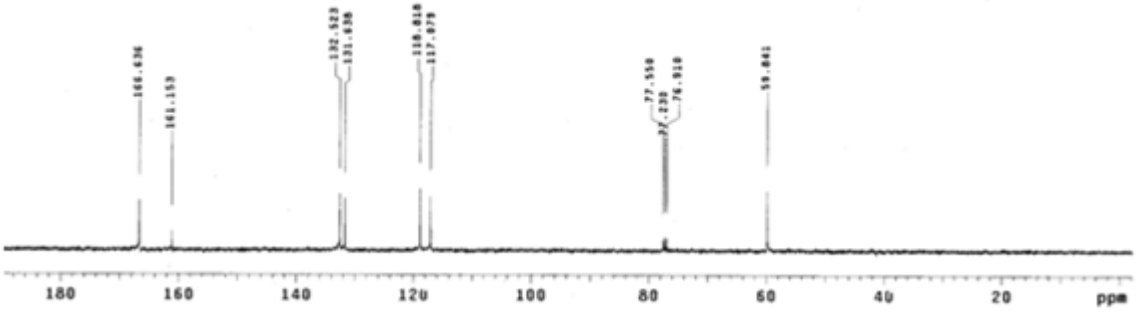

Figure A4.12 ^{13}C-NMR spectrum of $\mathbf{L_{6a}}$ in $CDCl_3$.

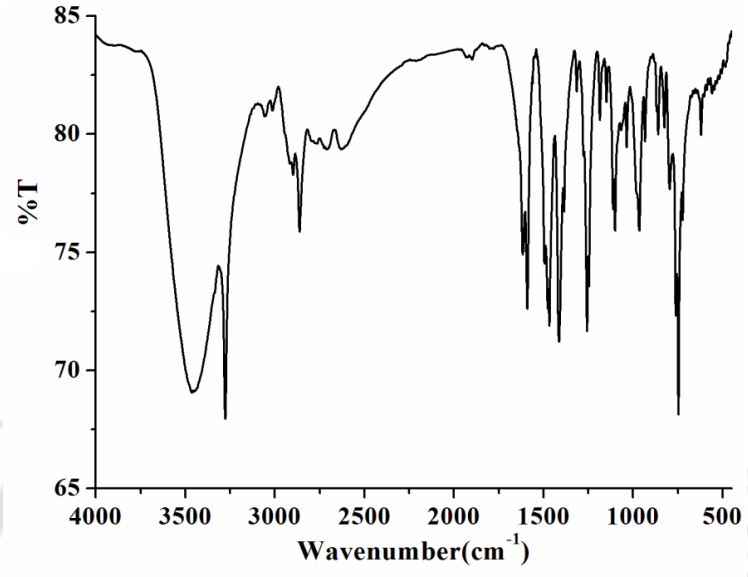

Figure A4.13 FT-IR spectrum of $\mathbf{L_6}$ in KBr pellet.

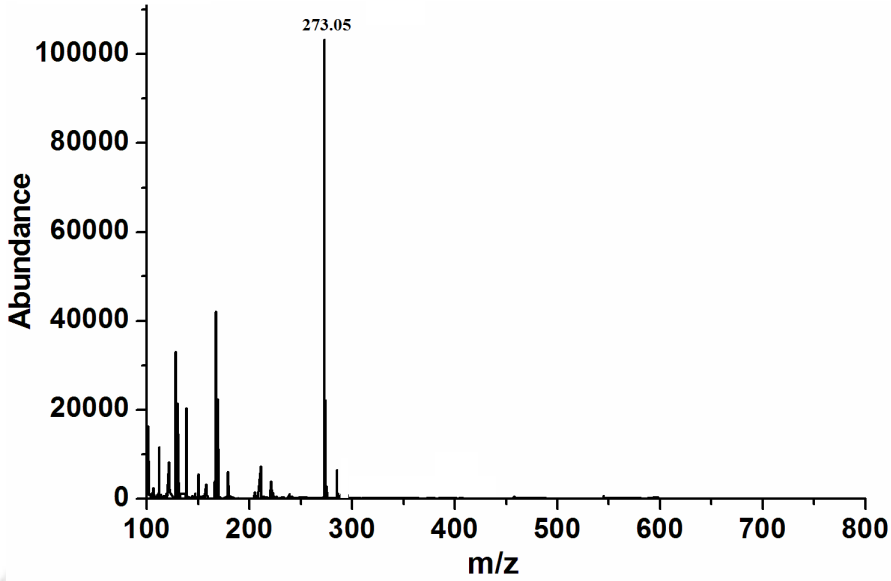

Figure A4.14 ESI-mass spectrum of $\mathbf{L_6}$ in methanol.

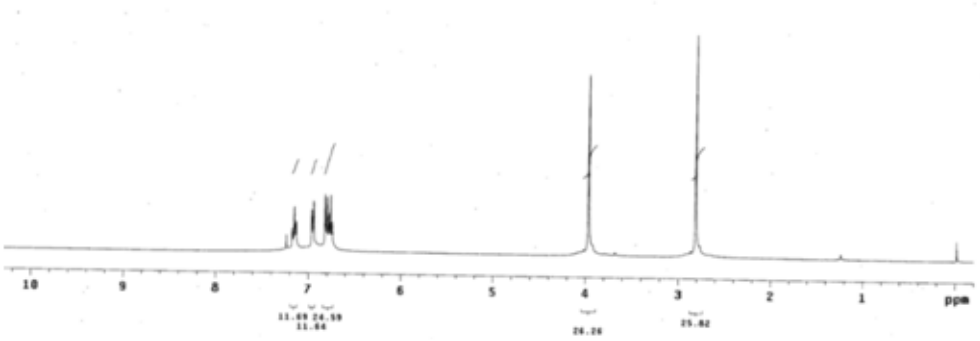

Figure A4.15 ^{1}H-NMR spectrum of **L_6** in $CDCl_3$.

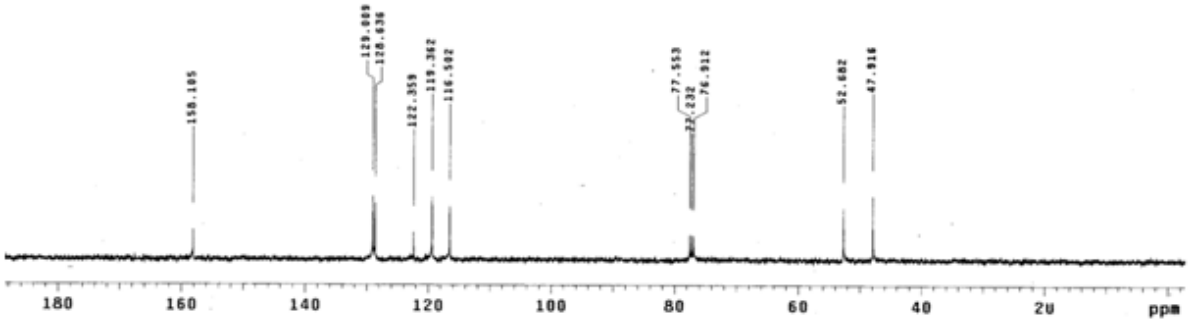

Figure A4.16 ^{13}C-NMR spectrum of $\mathbf{L_6}$ in $CDCl_3$.

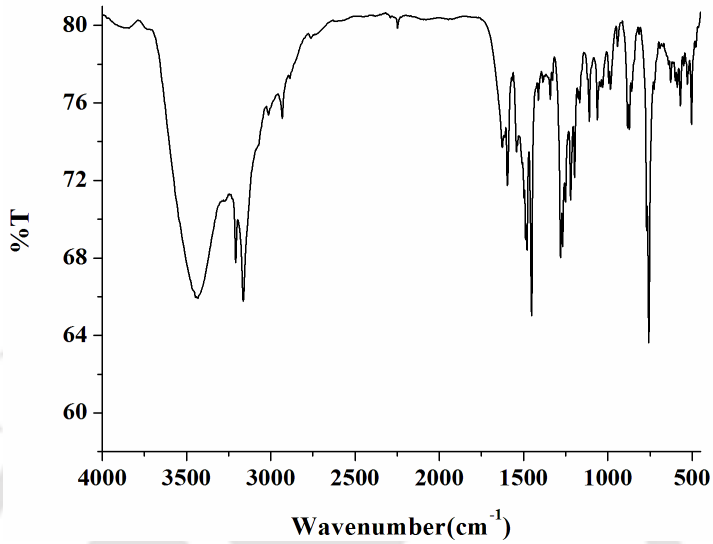

Figure A4.17 FT-IR spectrum of complex **5.1** in KBr pellet.

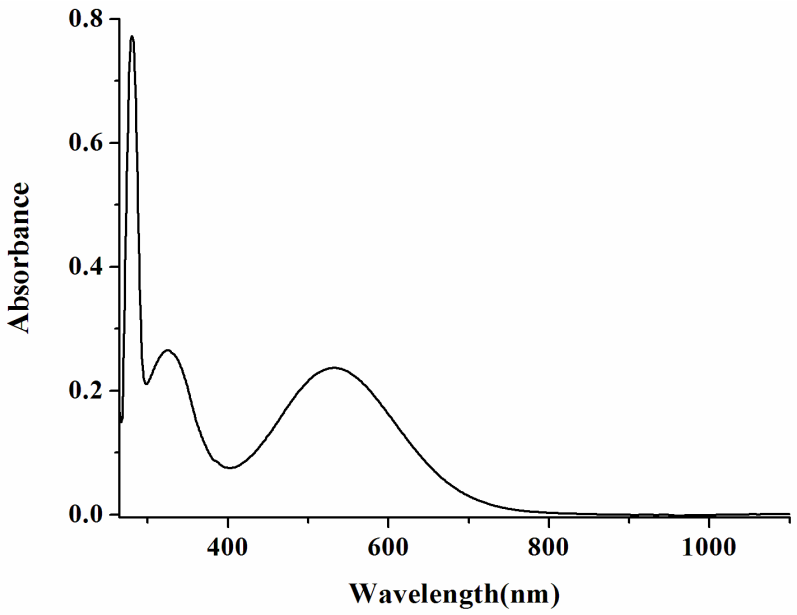

Figure A4.18 UV-visible spectrum of complex **5.1** in methanol.

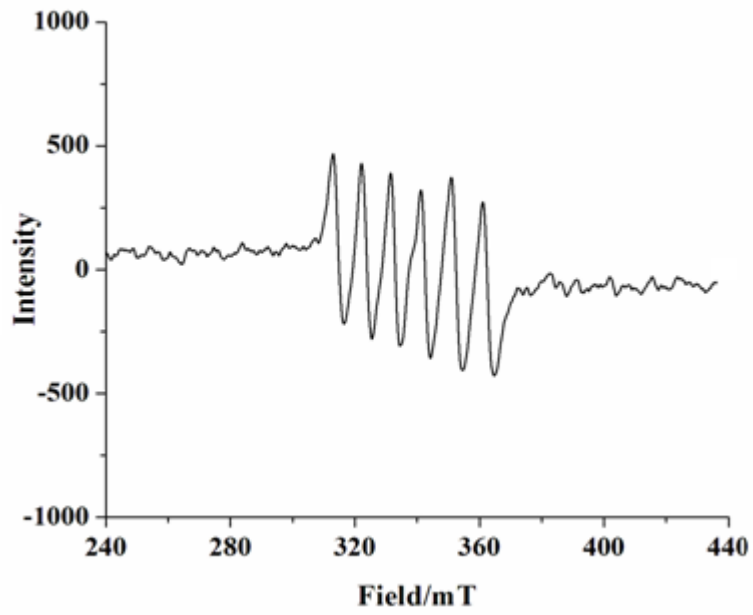

Figure A4.19 X-band EPR spectrum of complex **5.1** in methanol.

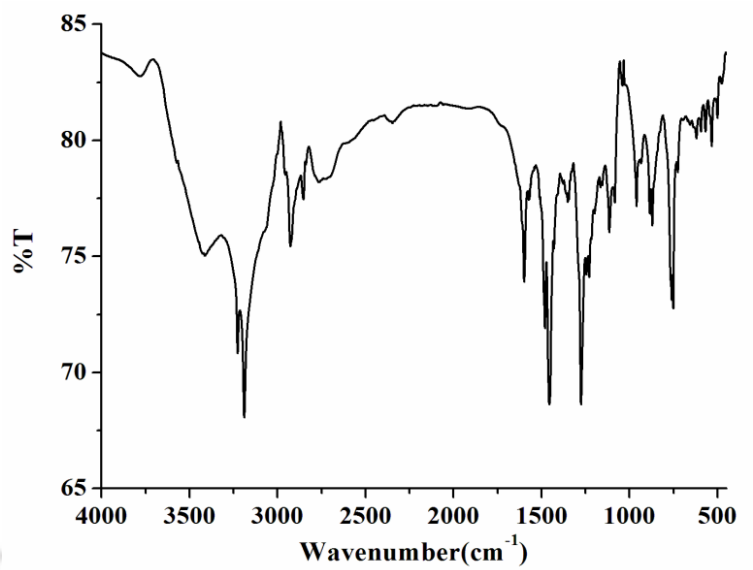

Figure A4.20 FT-IR spectrum of complex **5.2** in KBr pellet.

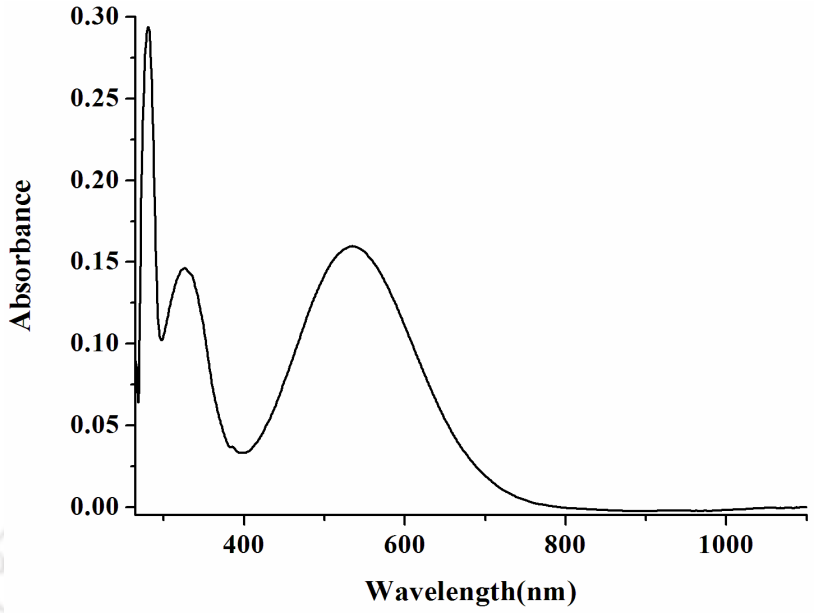

Figure A4.21 UV-visible spectrum of complex **5.2** in methanol.

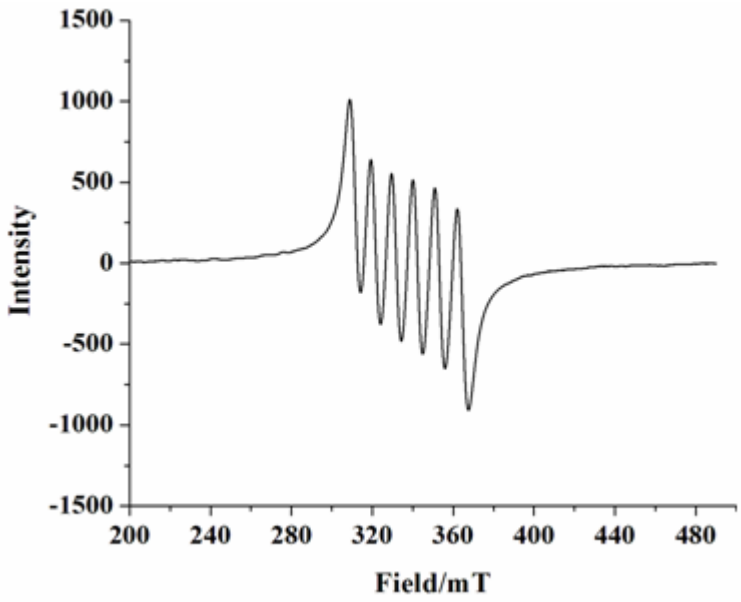

Figure A4.22 X-band EPR spectrum of complex **5.2** in methanol

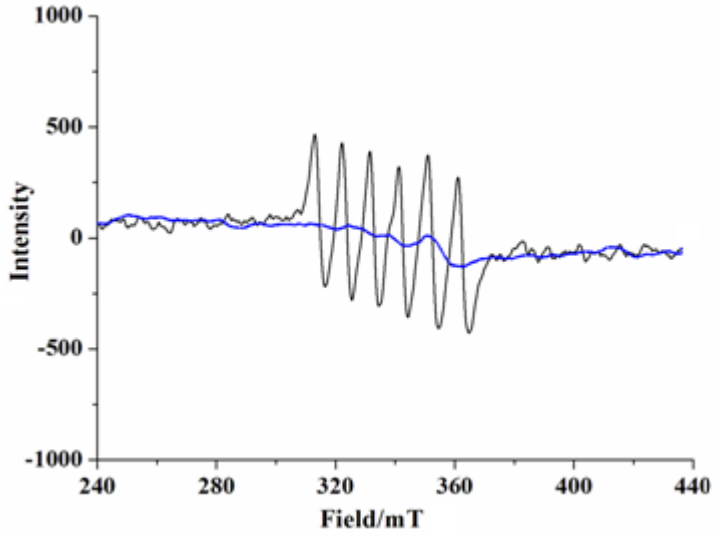

Figure A4.23 X-band EPR spectrum of complex **5.1** (black trace) after purging NO (blue trace) in methanol.

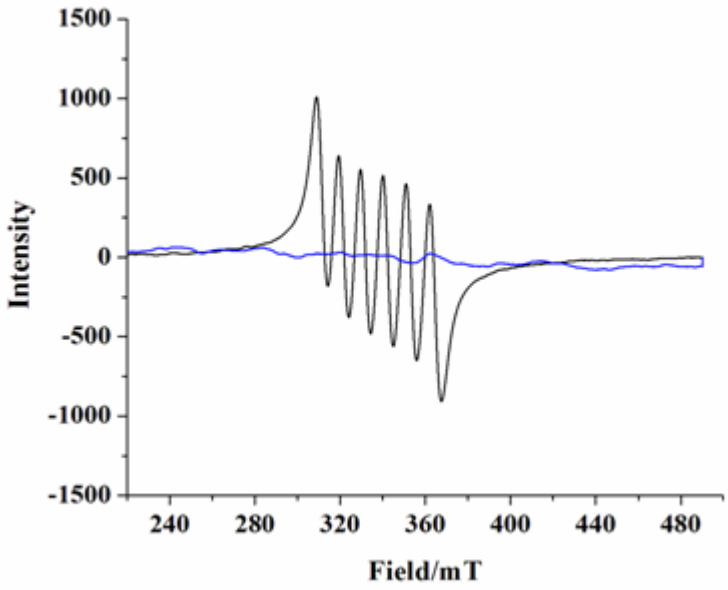

Figure A4.24 X-band EPR spectrum of complex **5.2** (black trace) and after purging NO (blue trace) in methanol.

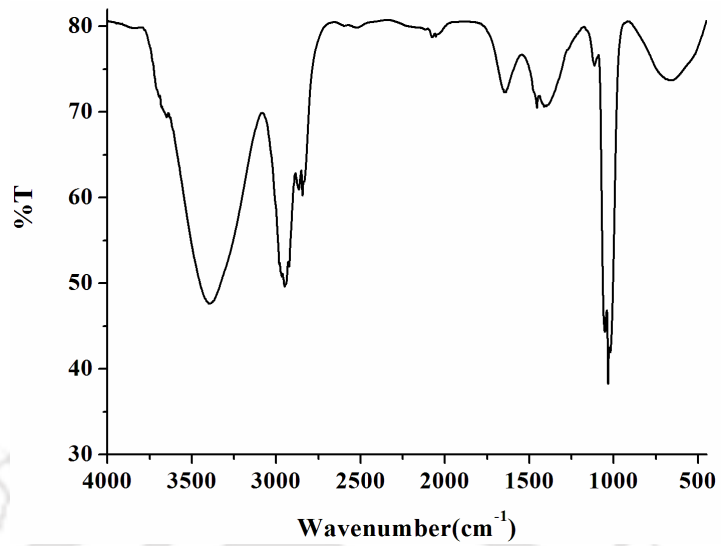

Figure A4.25 FT-IR spectrum of complex **5.3** in KBr pellet.

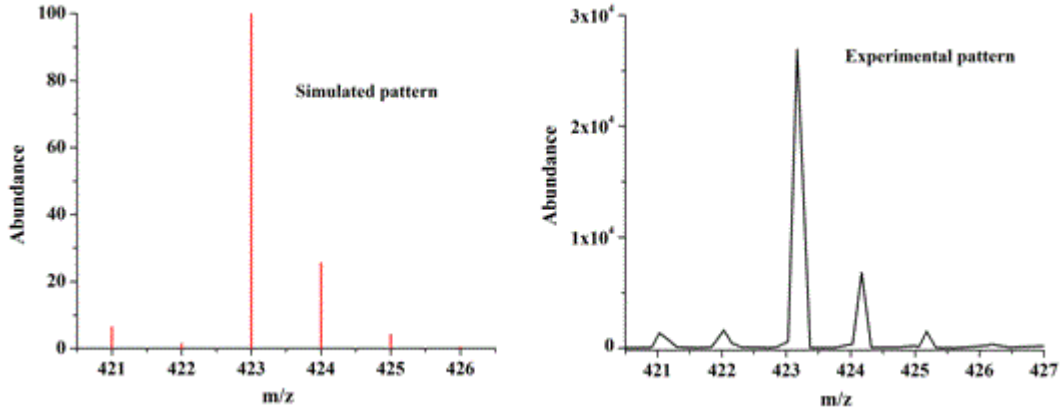

Figure A4.26 Simulated and experimental ESI-mass patterns of complex **5.3** in methanol.

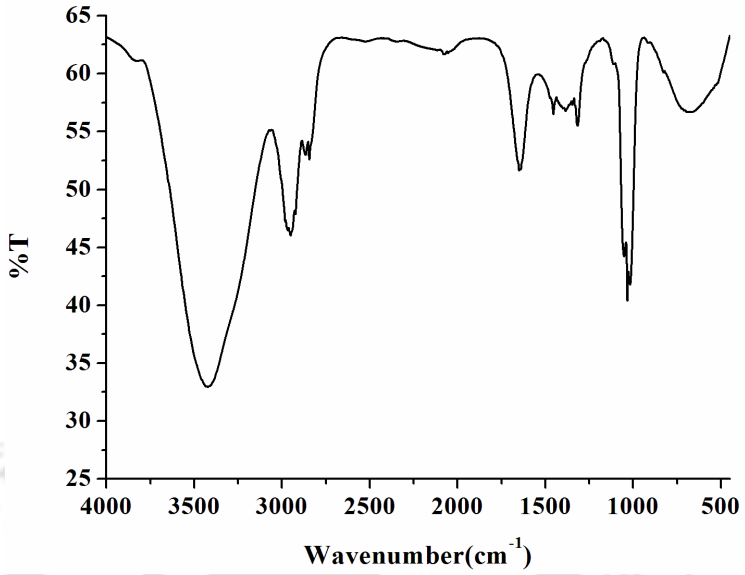

Figure A4.27 FT-IR spectrum of complex **5.4** in KBr pellet.

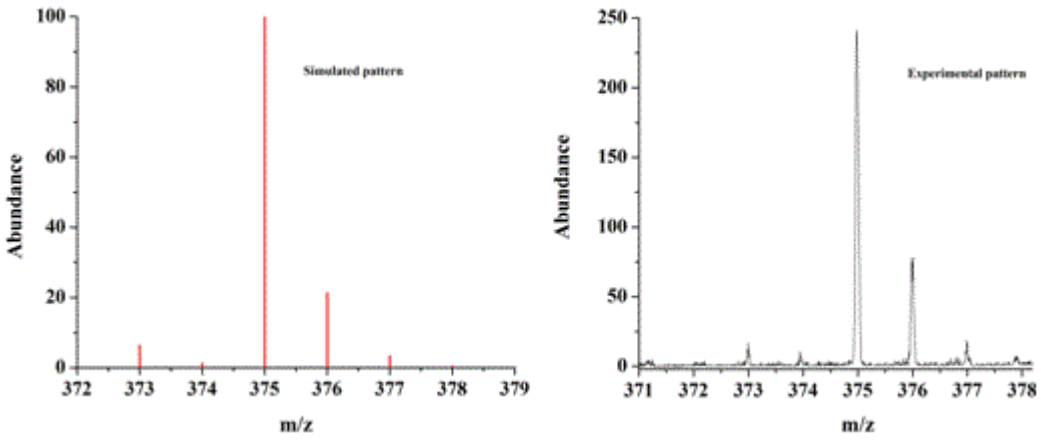

Figure A4.28 Simulated and experimental ESI-mass patterns of complex **5.4** in methanol.

List of Publications

1. **Reductive nitrosylation of iron(III) complexes of tetradentate ligands**

   Kalita, A.; Mondal, B.

   (Communicated)

2. **Nitric oxide reactivity of copper(II) complexes of bidentate amine ligands**

   Kalita, A.; Mondal, B. *Inorg. Chim. Acta.* **2015**, *430,* 55.

3. **C-nitrosation of a β-diketiminate ligand in copper(II)complex**

   Kalita, A.; Kumar, V.; Mondal, B. *Rsc. Adv.* **2015**, *5*, 643.

4. **Nitric oxide reactivity of a manganese(II) complex leading to nitrosation of the ligand**

   Kalita, A.; Ghosh, S.; Mondal, B. *Inorg. Chim. Acta.* **2015**, *429,* 183.

5. **Phenol ring nitration induced by the unprecedented reduction of the Cu(II) centre by nitrogen dioxide**

   Kumar, V.; **Kalita, A**.; Mondal, B. *Dalton Trans*., **2013**, *42*, 16264.

6. **Nitric oxide reactivity of copper(II) complexes of bidentate amine ligands: Effect of chelate ring size on the stability of [Cu^{II}-NO] intermediate**

   Sarma, M.; Kumar, V.; **Kalita, A**.; Deka, R. C.; Mondal, B. *Dalton Trans*., **2012**, *41*, 9543.

7. **Synthesis and supramolecular structures of iso- and heteropolymetallate sassisted by organoamino phosphonium cations**

   Gupta, A.K.; **Kalita, A**.; Shankar, R.B. *Inorg. Chim. Acta.* **2011**, *372*, 152.